

STATUS OF THESIS

Title of thesis

DESIGN AND IMPLEMENTATION OF INTELLIGENT
MONITORING SYSTEMS FOR THERMAL POWER PLANT
BOILER TRIPS

I FIRAS BASIM ISMAIL ALNAIMI

hereby allow my thesis to be placed at the Information Resource Center (IRC) of Universiti Teknologi PETRONAS (UTP) with the following conditions:

1. The thesis becomes the property of UTP.
2. The IRC of UTP may make copies of the thesis for academic purposes only.
3. This thesis is classified as

Confidential

Non-confidential

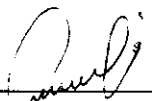
If this thesis is confidential, please state the reason:

As per requested by the source of real data, meaning JANAMANJUNG power plant management.

The contents of the thesis will remain confidential for five years.

Remarks on disclosure:

According to the agreement with the station management, the researchers can publish with the condition of not mentioning the name of the plant.



Signature of Author

Permanent Address:

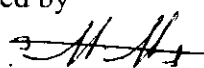
University of Technology

Faculty of engineering

Baghdad, Iraq

Date: 17 Dec, 2010

Endorsed by



Signature of Supervisor

Name of Supervisor

AP. Dr. Hussain H. Al Kayiem

Date: 15 Dec. 2010

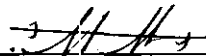
UNIVERSITI TEKNOLOGI PETRONAS
DESIGN AND IMPLEMENTATION OF INTELLIGENT MONITORING
SYSTEMS FOR THERMAL POWER PLANT BOILER TRIPS

by

FIRAS BASIM ISMAIL ALNAIMI

The undersigned certify that they have read, and recommend to the Postgraduate Studies Programme for acceptance this thesis for the fulfillment of the requirements for the degree stated.

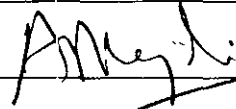
Signature:



Main Supervisor:

AP. Dr. Hussain H. Al Kayiem

Signature:



Head of Department:

Date:

Dr Ahmad Majdi Abdul Rani
Head of Department/Senior Lecturer
Mechanical Engineering Department
Universiti Teknologi PETRONAS
Bandar Seri Iskandar 31750 Tronok,
Perak Darul Ridzuan, Malaysia

17/12/2010

DESIGN AND IMPLEMENTATION OF INTELLIGENT MONITORING
SYSTEMS FOR THERMAL POWER PLANT BOILER TRIPS

by

FIRAS BASIM ISMAIL ALNAIMI

A Thesis

Submitted to the Postgraduate Studies Programme
as a Requirement for the Degree of

DOCTOR OF PHILOSOPHY

MECHANICAL ENGINEERING DEPARTMENT

UNIVERSITI TEKNOLOGI PETRONAS

BANDAR SRI ISKANDAR

PERAK

DECEMBER 2010

DECLARATION OF THESIS

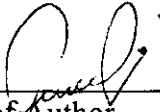
Title of thesis

DESIGN AND IMPLEMENTATION OF INTELLIGENT
MONITORING SYSTEMS FOR THERMAL POWER
PLANT BOILER TRIPS

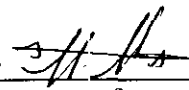
I FIRAS BASIM ISMAIL ALNAIMI

hereby declare that the thesis is based on my original work except for quotations and citations which have been duly acknowledged. I also declare that it has not been previously or concurrently submitted for any other degree at UTP or other institutions.

Witnessed by



Signature of Author



Signature of supervisor

Permanent Address: University of Technology
Faculty of engineering
Baghdad, Iraq

Name of Supervisor
AP. Dr. Hussain H. Al Kayiem

Date: 17 Dec. 2010

Date: 15 Dec. 2010

ACKNOWLEDGEMENTS

I would like to place on record my deep gratitude to:

Assoc. Prof. Dr. Hussain H. Ja'afar Al-Kayiem for his invaluable support, encouragement and technical advice throughout the entire period of this research, as my major advisor.

Prof. Ir. Dr. Hj. Kamsani Abdul Majid, Lead Researcher of generation unit, TNB Research Center, for his helpful advice and exceptional guidance, as my field advisor.

Eng. Mat Isa Bin Osman, Performance Manger of TNB JANAMANJUNG coal-fired power plant, Perak, Malaysia, for his precious help during the plant data capturing period.

Assoc. Prof. Dr. Mohd Noh Karsiti, The Director for Postgraduate Studies, Universiti Teknologi PETRONAS, for his support and help.

Dr. Ahmad Majdi Bin Abdul Rani, The head of Mechanical Engineering Department, Universiti Teknologi PETRONAS, for his contribution to my education.

Dr. Vijanth S. Asirvadam, Prof. Dr.Siddeeq Amin, Dr. Mazin Othman, Dr. Ahmed M. Zeki, Dr. Konstantions Ferentinos, for their time, suggestions and comments.

Fellow Iraqis and Graduate Students in UTP, for their friendship, help and discussion.

My beloved parents, brothers and sisters, for their care, patience, love, encouragement and support.

Everyone who has supported this work.

DEDICATION

To Creator of earth and heaven

To Soul of the Mohammed

(God blessing and peace upon him)

To the candle that highlighted my way,

My great ... Father

To the spring of kindness,

My dearest ... Mother

To my dearest brother

... Dr. Sinan

To the jasmine flowers

My dearest Brothers and Sisters...Sala, Al-Hassan, Shaddan

To the special person in my life

...Dr.Nadia Ezdianie

ABSTRACT

Steam boilers represent the main equipment in the power plant. Some boiler trips may lead to an entire shutdown of the plant, which is economically burdensome. An early detection and diagnosis of the boiler trips is crucial to maintain normal and safe operational conditions of the plant. Numbers of methodologies have been proposed in the literature for fault diagnosis of power plants. However, rapid deployment of these methodologies is difficult to be achieved due to certain inherent limitations such as system inability to learn or a dynamically improve the system performance and the brittleness of the system beyond its domain of expertise. As a potential solution to these problems, two artificial intelligent monitoring systems specialized in boiler trips have been proposed and coded within the MATLAB environment in the present work. The training and validation of the two systems have been performed using real operational data which was captured from the plant integrated acquisition system of JANAMANJUNG coal-fired power plant. An integrated plant data preparation framework for seven boiler trips with related operational variables, has been proposed for the training and validation of the proposed artificial intelligent systems. The feed-forward neural network methodology has been adopted as a major computational intelligent tool in both systems. The root mean square error has been widely used as a performance indicator of the proposed systems. The first intelligent monitoring system represents the use of the pure artificial neural network system for boiler trip detection. The final architecture for this system has been explored after investigation of various main neural network topology combinations which include one and two hidden layers, one to ten neurons for each hidden layer, three types of activation function, and four types of multidimensional minimization training algorithms. It has been found that there was no general neural network topology combination that can be applied for all boiler trips. All seven boiler trips under consideration had been detected by the proposed systems before or at the same time as the plant control

system. The second intelligent monitoring system represents merging of genetic algorithms and artificial neural networks as a hybrid intelligent system. For this hybrid intelligent system, the selection of appropriate variables from hundreds of boiler operation variables with optimal neural network topology combinations to monitor boiler trips was a major concern. The encoding and optimization process using genetic algorithms has been applied successfully. A slightly lower root mean square error was observed in the second system which reveals that the hybrid intelligent system performed better than the pure neural network system. Also, the optimal selection of the most influencing variables was performed successfully by the hybrid intelligent system. The proposed artificial intelligent systems could be adopted on-line as a reliable controller of the thermal power plant boiler.

ABSTRAK

Dandang stim merupakan peralatan utama di dalam loji kuasa. Sesetengah gangguan dandang akan menyebabkan keseluruhan loji tidak berfungsi di mana mempengaruhi pengurusan penjana. Pengenalpastian dan pengesanan awal gangguan dandang adalah sangat penting untuk mengekalkan keadaan yang normal dan juga keadaan yang selamat semasi operasi penjana. Beberapa metodologi telah dicadangkan di dalam tesis ini untuk pengesanan di loji kuasa. Walaubagaimanapun, pembahagian yang cepat adalah sukar untuk dicapai disebabkan oleh sesetengah unsur yang terhad seperti ketidakupayaan sistem untuk dipelajari ataupun membaikinya dengan dinamik, sistem pelaksanaan dan kerapuhan di dalam sistem tersebut disebalik kepakaran. Sebagai jalan penyelesaian yang berpontensi bagi masalah ini, dua sistem mengawalan iaitu “artificial intelligent monitoring system” dikhususkan di dalam gangguan dandang telah dibangunkan dengan bantuan kod MATLAB. Latihan dan pengesanan dua sistem ini dilaksanakan dengan menggunakan data sebenar dari sistem kontrol di loji tenaga. Pengumpulan data loji bagi persediaan rangka kerja untuk tujuh gangguan dandang dengan fungsi berubah yang berhubung telah dicadangkan untuk analisis data untuk intelligent monitoring sistem. Metodologi NN telah diadaptasikan sebagai peralatan pengiraan majoriti di dalam kedua-dua sistem ini. Formula matematik “root mean square error” telah digunakan secara meluas sebagai intelligent monitoring sistem indicator. intelligent monitoring sistem yang pertama diwakili dengan penggunaan sistem rangkaian saraf sebagai “pure artificial neural sytem” untuk pengesanan gangguan dandang. Seni bina untuk sistem ini telah diterokai selepas penyelidikan berbagai-bagai gabungan saraf sebagai topologi yang utama dimana termasuk satu dan dua lapisan yang terselindung, satu sehingga sepuluh neuron untuk setiap lapisan yang tersembunyi, tiga jenis pula untuk fungsi pengaktifan dan terdapat empat jenis untuk pelbagai dimensi meminimumkan algoritma. Tiada gabungan saraf sebagai topologi umum yang dapat diaplikasikan untuk kesemua gangguan dandang.

Dapat dipertimbangkan tujuh gangguan dandang telah dikesan melalui IMSs sebelum atau pada masa yang sama dengan sistem kontrol di loji. intelligent monitoring sistem yang kedua diwakili oleh algoritma genetic dan rangkaian saraf sebagai sistem hybrid kepakaran "hybrid intelligent system". Untuk sistem ini pemilihan anu yang tepat daripada seratus operasi dandang dengan optimum gabungan saraf sebagai topologi untuk mengawal gangguan dandang amat dititikberatkan. Proses mengekod dan optimize dengan menggunakan algoritma genetic telah diaplikasikan dengan jayanya. Di dalam sistem intelligent monitoring sistem yang kedua root mean square error sedikit rendah telah diperhatikan di mana menunjukkan sistem hybrid intelligent melakukan dengan lebih baik daripada pure intelligent monitoring sistem. Selain daripada itu, pemilihan yng optimum dari anu-anu yang dipengaruhi dilakukan dengan jayanya oleh sistem hybrid intelligent. Pembangunan sistem artificial intelligent sepatutnya diaplikasikan sebagai pengawalan kuasa terma di loji dandang.

In compliance with the terms of the Copyright Act 1987 and the IP Policy of the university, the copyright of this thesis has been reassigned by the author to the legal entity of the university,

Institute of Technology PETRONAS Sdn Bhd.

Due acknowledgement shall always be made of the use of any material contained in, or derived from, this thesis.

© Firas Basim Ismail Alnaimi, 2010
Institute of Technology PETRONAS Sdn Bhd
All right reserved.

TABLE OF CONTENTS

DECLARATION OF THESIS.....	iv
ACKNOWLEDGEMENTS.....	v
DEDICATION.....	vi
ABSTRACT.....	vii
ABSTRAK.....	ix
TABLE OF CONTENTS.....	xii
LIST OF TABLES.....	xvii
LIST OF FIGURES.....	xxi
ABBREVIATION.....	xxiv
SYMBOLS.....	xxvii

Chapter

1. INTRODUCTION.....	1
1.1 Overview of Fault Detection System.....	1
1.2 Intelligent Monitoring Systems in Power Plant.....	2
1.3 Artificial Intelligent Systems in Power Plants.....	4
1.3.1 Artificial Neural Network.....	5
1.3.2 Genetic Algorithms.....	6
1.4 Research Problem Statement.....	7
1.5 Motivations.....	7
1.6 Research Objectives.....	8
1.7 Thesis Organization.....	9

2.	SURVERY OF PAST WORKS ON INTELLIGENT FAULT DIAGNOSIS	11
2.1	Introduction.....	11
2.2	Fault Detection and Diagnosis.....	12
2.3	Techniques of Fault Detection and Diagnosis.....	13
2.3.1	Estimation Technique.....	13
2.3.2	Pattern Recognition Techniques.....	15
2.4	Brief Comparison between Estimation and Pattern Recognition Techniques.....	16
2.5	Intelligent Systems as Candidates for Cognition in Thermal Power Plant Monitoring.....	17
2.5.1	Knowledge Based systems.....	18
2.5.2	Soft Computing Methods.....	22
2.6	Application of Neural Network System for Fault Detection and Diagnosis.....	23
2.7	A Hybrid Intelligent System Strategy for the Thermal Power Plant.....	28
2.7.1	Application of Hybrid Intelligent Systems.....	28
2.8	Summary.....	35
3.	THEORY OF INTELLIGENT SYSTEMS	36
3.1	Introduction.....	36
3.2	Artificial Neural Networks (ANNs).....	36
3.3	Why Use Neural Networks.....	40
3.4	ANN Taxonomies.....	41
3.4.1	ANN Models.....	42
3.4.2	ANN Learning Algorithms.....	42
3.4.3	ANN Performance Indicator.....	43
3.4.4	The Application Type Categories of ANNs Models.....	44
3.4.5	Neural Network Architectures.....	45
3.5	Genetic Algorithms (GAs).....	46
3.5.1	GA Components.....	47
3.5.2	GA System Operations.....	47
3.6	Summary.....	50

4.	DATA ACQUISITION AND PREPARATION	51
4.1	Introduction.....	51
4.2	Thermal Power Plant (TPP).....	51
4.3	MNJTPP Boiler Description and Characteristics.....	53
4.4	Boiler Trips Identification.....	55
4.4.1	Boiler Tube Wall Trip.....	55
4.4.2	Superheater Trips.....	56
4.4.3	Boiler Drum Trip.....	57
4.4.4	Boiler Circulating Pump Trips.....	58
4.5	Data Preparation Framework.....	58
4.5.1	Data Pre-Analysis Stage.....	60
4.5.2	Data Pre-Processing Stage.....	64
4.5.3	Data Post Analysis Stage.....	68
4.6	Summary.....	88
5.	DESIGN AND IMPLEMENTATION OF IMSs	89
5.1	Introduction.....	89
5.2	Development of IMS-I (Pure ANN).....	89
5.2.1	Why Use Back-Propagation Neural Networks.....	90
5.2.2	Architecture of Back-Propagation Network.....	90
5.2.3	Back-Propagation Learning Method.....	91
5.2.4	The BBP Training Algorithm.....	92
5.2.5	Selection of ANN Topologies.....	93
5.3	Design of IMS-I.....	98
5.3.1	Training Processes of IMS-I.....	99
5.3.2	ANN Validation Phases.....	100
5.4	Development of IMS-II (Hybrid ANN+GA).....	102
5.4.1	GA Encoding.....	103
5.4.2	IMS-II Scheme.....	110
5.5	Summary.....	111

6.	ASSESSMENT OF RESULTS	113
6.1	Introduction.....	113
6.2	Results of IMS-I.....	113
6.2.1	IMS-I Training Process Results.....	114
6.2.2	IMS-I Validation Process Results.....	140
6.3	Application of IMS-II.....	148
6.3.1	Determination of Crossover Probability.....	149
6.3.2	Determination of Population Size.....	153
6.3.3	IMS-II Result Analysis.....	162
6.4	IMS-II Performance.....	170
6.4.1	IMS-II Validation Results of Trip 1.....	170
6.4.2	IMS-II Validation Results of Trip 2.....	171
6.4.3	IMS-II Validation Results of Trip 3.....	172
6.4.4	IMS-II Validation Results of Trip 4.....	173
6.4.5	IMS-II Validation Results of Trip 5.....	174
6.4.6	IMS-II Validation Results of Trip 6.....	175
6.4.7	IMS-II Validation Results of Trip 7.....	176
6.5	Comparison between IMS-I and IMS-II Performances.....	177
6.6	Actions on Detecting the MNJTTP Boilers Trips.....	180
6.7	Summary.....	189
7.	CONCLUSIONS AND FUTURE WORKS	190
7.1	Introduction.....	190
7.2	Contributions of the Research.....	191
7.3	Critique of the Work.....	192
7.4	Conclusions of IMSs.....	193
7.4.1	The IMS-I Conclusions.....	193
7.4.2	The IMS-II Conclusions.....	194
7.5	Recommendations And Future Works.....	195

REFERENCES..... 197
PUBLICATIONS..... 206
APPENDIX A 208
APPENDIX B 215

LIST OF TABLES

Table 4.1 Influential boiler operation variables.....	62
Table 4.2 MNJTTP boilers outages	63
Table 4.3 Plant data acquisition grouping.....	64
Table 4.4 Normalized mean values for normal and faulty boiler operation	84
Table 4.5 High alarm occurrence of influencing variables corresponding to each trip	85
Table 4.6 Results from behavior analysis of the effective and the most effective variables.....	86
Table 5.1 Convergence time for back-propagation algorithms [91].....	94
Table 5.2 Binary representation of the training algorithms	105
Table 5.3 ANN structures binary representation	106
Table 5.4 Activation function binary representation for 1HL	107
Table 5.5 Activation function binary representation for 2HL	107
Table 5.6 Boiler operation variables binary representation	109
Table 6.1 Description of training data set.....	114
Table 6.2 Trip (1) Scaled RMSE of 1-HL with NHLN nodes in the hidden layer for all activation functions probability combinations with all four training algorithms	116
Table 6.3 Trip (2) Scaled RMSE of 1-HL with NHLN nodes in the hidden layer for all activation functions probability combinations with all four training algorithms	117
Table 6.4 Trip (3) Scaled RMSE of 1-HL with NHLN nodes in the hidden layer for all activation functions probability combinations with all four training algorithms	118
Table 6.5 Trip (4) Scaled RMSE of 1-HL with NHLN nodes in the hidden layer for all activation functions probability combinations with all four training algorithms	119
Table 6.6 Trip (5) Scaled RMSE of 1-HL with NHLN nodes in the hidden layer for all activation functions probability combinations with all four training algorithms	120

Table 6.7 Trip (6) Scaled RMSE of 1-HL with NHLN nodes in the hidden layer for all activation functions probability combinations with all four training algorithms	121
Table 6.8 Trip (7) Scaled RMSE of 1-HL with NHLN nodes in the hidden layer for all activation functions probability combinations with all four training algorithms	122
Table 6.9 The best ANN topologies combination of 1HL for all boiler operation trips	123
Table 6.10 Scaled RMSE of 2-HL structure (with N1and N2 in each layer) using Levenberg-Marquardt and Resilient Back-Propagation training algorithms for trip (1).....	125
Table 6.11 Scaled RMSE of 2-HL structure (with N1and N2 in each layer) using Scaled Conjugate Gradient and BFGS Quasi Newton training algorithms for trip (1).....	126
Table 6.12 Scaled RMSE of 2-HL structure (with N1and N2 in each layer) using Levenberg-Marquardt and Resilient Back-Propagation training algorithms for trip (2).....	127
Table 6.13 Scaled RMSE of 2-HL structure (with N1and N2 in each layer) using Scaled Conjugate Gradient and BFGS Quasi Newton training algorithms for trip (2).....	128
Table 6.14 Scaled RMSE of 2-HL structure (with N1and N2 in each layer) using Levenberg-Marquardt and Resilient Back-Propagation training algorithms for trip (3).....	129
Table 6.15 Scaled RMSE of 2-HL structure (with N1and N2 in each layer) using Scaled Conjugate Gradient and BFGS Quasi Newton training algorithms for trip (3).....	130
Table 6.16 Scaled RMSE of 2-HL structure (with N1and N2 in each layer) using Levenberg-Marquardt and Resilient Back-Propagation training algorithms for trip (4).....	131
Table 6.17 Scaled RMSE of 2-HL structure (with N1and N2 in each layer) using Scaled Conjugate Gradient and BFGS Quasi Newton training algorithms for trip (4).....	132
Table 6.18 Scaled RMSE of 2-HL structure (with N1and N2 in each layer) using Levenberg-Marquardt and Resilient Back-Propagation training algorithms for trip (5).....	133
Table 6.19 Scaled RMSE of 2-HL structure (with N1and N2 in each layer) using Scaled Conjugate Gradient and BFGS Quasi Newton training algorithms for trip (5).....	134

Table 6.20 Scaled RMSE of 2-HL structure (with N1 and N2 in each layer) using Levenberg-Marquardt and Resilient Back-Propagation training algorithms for trip (6).....	135
Table 6.21 Scaled RMSE of 2-HL structure (with N1 and N2 in each layer) using Scaled Conjugate Gradient and BFGS Quasi Newton training algorithms for trip (6).....	136
Table 6.22 Scaled RMSE of 2-HL structure (with N1 and N2 in each layer) using Levenberg-Marquardt and Resilient Back-Propagation training algorithms for trip (7).....	137
Table 6.23 Scaled RMSE of 2-HL structure (with N1 and N2 in each layer) using Scaled Conjugate Gradient and BFGS Quasi Newton training algorithms for trip (7).....	138
Table 6.24 The best ANN topology combination of a 2HL for all boiler operation trips	139
Table 6.25 The best ANN topology combination for both the 1HL and the 2HL for all boiler operation trips.....	139
Table 6.26 Description of basic validation data sets for IMS-I.....	140
Table 6.27 Several probabilities of crossover and mutation for GA System for seven trips	153
Table 6.28 Several population sizes for two values generations	157
Table 6.29 Best RMSE found during the best GA run for seven boiler trips	161
Table 6.30 Best GA selection interpretations for trip (1)	163
Table 6.31 Best GA selection interpretations for trip (2)	164
Table 6.32 Best GA selection interpretations for trip (3)	165
Table 6.33 Best GA selection interpretations for trip (4)	166
Table 6.34 Best GA selection interpretations for trip (5)	167
Table 6.35 Best GA selection interpretations for trip (6)	168
Table 6.36 Best GA selection interpretations for trip (7)	169
Table 6.37 Best GA selection interpretations for all boiler operation trips.....	170
Table 6.38 Optimal solution given by the IMS-I and IMS-II.....	178
Table 6.39 The most effective boiler variables by plant control system and IMS-II	179
Table 6.40 Necessary actions for trip (1).....	182
Table 6.41 Necessary actions for trip (2).....	183
Table 6.42 Necessary actions for trip (3).....	184
Table 6.43 Necessary actions for trip (4).....	185

Table 6.44 Necessary actions for trip (5).....	186
Table 6.45 Necessary actions for trip (6).....	187
Table 6.46 Necessary actions for trip (7).....	188

LIST OF FIGURES

Figure 1.1 Method of prescribing the range of acceptable performance [2]	1
Figure 1.2 Fault detection system for automatic diagnosis [2].....	4
Figure 1.3 Typical ANN learning methods for basic learning strategies [11].....	6
Figure 2.1 Classifications of methods for fault detection and diagnosis [2]	14
Figure 2.2 Complete structure of a rule-based expert system [25].....	20
Figure 2.3 Power plant control system interface	23
Figure 3.1 Input layer of the typical neural network [62].....	37
Figure 3.2 Conceptual structure of the classical neuron [63]	37
Figure 3.3 Artificial neuron with activation function [64]	38
Figure 3.4 Activation signal function [65].....	40
Figure 3.5 Categories of ANN steps by application type [70].....	45
Figure 3.6 GA System Operations [75]	49
Figure 4.1 Data processing sequences adopted in the present work.....	52
Figure 4.2 Schematic diagram of MNJ TPP Boiler	54
Figure 4.3 Execution phases	59
Figure 4.4 Plant data preparation framework	60
Figure 4.5 Plant data reduction stages of the observations to variables	61
Figure 4.6 Boiler operation variables (from V_1 to V_{16}) behavior for trip 1	69
Figure 4.7 Boiler operation variables (from V_{17} to V_{32}) behavior for trip 1.....	70
Figure 4.8 Boiler operation variables (from V_1 to V_{16}) behavior for trip 2.....	71
Figure 4.9 Boiler operation variables (from V_{17} to V_{32}) behavior for trip 2.....	72
Figure 4.10 Boiler operation variables (from V_1 to V_{16}) behavior for trip 3	73
Figure 4.11 Boiler operation variables (from V_{17} to V_{32}) behavior for trip 3.....	74
Figure 4.12 Boiler operation variables (from V_1 to V_{16}) behavior for trip 4.....	75
Figure 4.13 Boiler operation variables (from V_{17} to V_{32}) behavior for trip 4.....	76
Figure 4.14 Boiler operation variables (from V_1 to V_{16}) behavior for trip 5	77
Figure 4.15 Boiler operation variables (from V_{17} to V_{32}) behavior for trip 5	78

Figure 4.16 Boiler operation variables (from V_1 to V_{16}) behavior for trip 6	79
Figure 4.17 Boiler Operation variables (from V_{17} to V_{32}) behavior for trip 6	80
Figure 4.18 Boiler Operation variables (from V_1 to V_{16}) behavior for trip 7	81
Figure 4.19 Boiler operation variables (from V_{17} to V_{32}) behavior for trip 7	82
Figure 4.20 Data segmentation sub groups for training and validation	87
Figure 5.1 Weight matrices of a three layered back-propagation system [88]	91
Figure 5.2 Back-Propagation NN training steps [63]	93
Figure 5.3 IMS-I structure	98
Figure 5.4 Execution flow chart of the proposed IMS-I code	102
Figure 5.5 GA binary representation	104
Figure 5.6 Schematic representation of proposed IMS-II	112
Figure 6.1 IMS-I outputs for trip (1)	141
Figure 6.2 IMS-I outputs for trip (2)	142
Figure 6.3 IMS-I outputs for trip (3)	143
Figure 6.4 IMS-I outputs for trip (4)	144
Figure 6.5 IMS-I outputs for trip (5)	145
Figure 6.6 IMS-I outputs for trip (6)	146
Figure 6.7 IMS-I outputs for trip (7)	147
Figure 6.8 IMS-I outputs for Normal operation	147
Figure 6.9 Performance of the IMS-II using several probabilities of crossover and mutation for trip (1)	149
Figure 6.10 Performance of the IMS-II using several probabilities of crossover and mutation for trip (2)	150
Figure 6.11 Performance of the IMS-II using several probabilities of crossover and mutation for trip (3)	150
Figure 6.12 Performance of the IMS-II using several probabilities of crossover and mutation for trip (4)	151
Figure 6.13 Performance of the IMS-II using several probabilities of crossover and mutation for trip (5)	151
Figure 6.14 Performance of the IMS-II using several probabilities of crossover and mutation for trip (6)	152
Figure 6.15 Performance of the IMS-II using several probabilities of crossover and mutation for trip (7)	152
Figure 6.16 Performance of the IMS-II using two population size candidates for	154

Figure 6.17 Performance of the IMS-II using two population size candidates for....	154
Figure 6.18 Performance of the IMS-II using two population size candidates for....	155
Figure 6.19 Performance of the IMS-II using two population size candidates for....	155
Figure 6.20 Performance of the IMS-II using two population size candidates for....	156
Figure 6.21 Performance of the IMS-II using two population size candidates for....	156
Figure 6.22 Performance of the IMS-II using two population size candidates for....	157
Figure 6.23 Best RMSE obtained during the best IMS-II run for trip (1)	158
Figure 6.24 Best RMSE obtained during the best IMS-II run for trip (2)	158
Figure 6.25 Best RMSE obtained during the best IMS-II run for trip (3)	159
Figure 6.26 Best RMSE obtained during the best IMS-II run for trip (4)	159
Figure 6.27 Best RMSE obtained during the best IMS-II run for trip (5)	160
Figure 6.28 Best RMSE obtained during the best IMS-II run for trip (6)	160
Figure 6.29 Best RMSE obtained during the best IMS-II run for trip (7)	161
Figure 6.30 IMS-I output during the first validation real data set (T1)	171
Figure 6.31 IMS-I output during the first validation real data set (T2)	172
Figure 6.32 IMS-I output during the first validation real data set (T3)	173
Figure 6.33 IMS-I output during the first validation real data set (T4)	174
Figure 6.34 IMS-I output during the first validation real data set (T5)	175
Figure 6.35 IMS-I output during the first validation real data set (T6)	176
Figure 6.36 IMS-I output during the first validation real data set (T7)	177

ABBREVIATION

AISs	Artificial Intelligent Systems
ABB	Asea Brown Boveri Ltd (Zurich)
ADALINE	ADaptive LINEar
AI	Artificial Intelligent
AM	Associative Memories
ANNs	Artificial Neural Networks
ART	Adaptive Resonant Theory
ATWS	Anticipated Transient Without Scram
BAM	Bi-directional Associative Memory
BFGS	BFGS Quasi-Newton
BMCR	Boiler Maximum Continuous Rate
BN	Bayesian Networks
BBP	Back-Propagation
BSB	Brain-State in-a-Box
BWR	Boiling Water Reactor
CCN	Cascade Correlation Network
CHP	Combined Heat and Power Plant
CIS	Computational Intelligence System
CISs	Computational Intelligence Systems
CPN	Counter Propagation Network
DAEC	Duane Arnold Energy Center
DMW	Dissimilar Metal Weld
EESA	Error Estimation by Series Association
ES	Expert System
ESP	Electro-Static Precipitator
FAM	Fuzzy Associative Memory

FDD	Fault Detection and Diagnosis
FFT	Fast Fourier Transform
FGD	Flue Gas Desulphurisation
FL	Fuzzy Logic
FNN	Fuzzy Neural Network
GA	Genetic Algorithm
GAs	Genetic Algorithms
GDR	Generalized Delta Rule
GRNN	Generalized Regression Neural Network
HP	High Pressure
HRSG	Heat Recovery System Generator
HTR	High Temperature Reheater
HTS	High Temperature Superheater
IMS	Intelligent Monitoring System
IMs	Intelligent Monitoring Systems
ITS	Intermediate Temperature Superheater
KBS	Knowledge Based System
LM	Levenberg-Marquardt
LTR	Low Temperature Reheater
LTS	Low Temperature Superheater
LVQ	Learning Vector Quantization
MADALINE	Many ADALINE
MB	Model Based
MLFF	Multi-Layer-Feed-Forward
MNJ	JANAMANJUNG
MP	Intermediate Pressure
NLNs	Neural Logic Networks
NN	Neural Network
NPP	Nuclear Power Plants
OFA	Over Fire Air
PNN	Probabilistic Neural Network
RB	Rule Based

RBFNN	Radial Basis Functions Neural Networks
RCE	Radial Counter Electronic
RNN	Recurrent Neural Network
RPROP	Resilient back-Propagation
SCC	Stress Corrosion Cracking
SCG	Scaled Conjugate Gradient
SN	Semantic Network
SOFM	Self-Organizing Feature Map
SSR	Strong Specification Representation
TPP	Thermal Power Plant
TPPB	Thermal Power Plant Boiler
WSR	Weak Specification Representation

SYMBOLS

1HL	One H idden L ayer
μ	Observation Mean
1HLN	First H idden L ayer N eurons
2HL	T wo H idden L ayers
α	Momentum C oefficient
AF	A ctivation F unction
A_k	Hussian Matrix
BBP _s	The Parameters Set For BBP Training Algorithms
d	D esired Output of Neural Network Node
δ	Learning Rate
F _{sum}	S um The F itness Of All Population Members
G	Number of G enetic Algorithm' Generation
G _n	Number of G enerations
HL1	H idden L ayer one
HL2	H idden L ayer Two
HSG	H ybrid S ystem G eneration
I/O	I nput- O utput
IMS-I	Pure Neural Networks M onitoring S ystem
IMS-II	Hybrid Neural Networks and Genetic algorithms M onitoring S ystem
J	J acobian Matrix
L	Sigmoid L ogistic Function
L	L ength of The Bit Strings
m	A Number of Randomly Selected Individuals
M _F	F aulty M ean
Min.	M inute
MMT _{algo}	M ultidimensional M inimization T raining A lgorithms

M_N	Normal Mean
N	Generation Number, The Number of Variables
N_1	Number of First Hidden Layer' Neurons
N_2	Number of Second Hidden Layer' Neurons
NHL	Number of H idden L ayer
$NHLN$	Number of H idden L ayer' N eurons
NO_x	Mono-Nitrogen O xides
o	Predicated O utput of Neural Network Node
P	Linear Summation Function
P_c	Probabilities of C rossover
P_m	M utation P robability
ps	Training Data Set
P_{vc}	Probability of V ariables C ombinations
P_z	S ize of P opulation
r	R andom Number
$RMSE$	R oot- M ean- S quare- E rror
SO_2	S ulfur D ioxide
$struct$	Network S tructure
T	T rip
T	H yperbolic T angent
TP	Neural Network T raining P arameters
T_s	Neural Network T raining S et
U	P lant U nit
V	V ariable
V_{ft}	F itness V ector
X_{int}	I nitial P opulation
X_{nw}	F inal P opulation
X_{par}	P arents
σ	O bservation S tandard D eviation

CHAPTER 1
INTRODUCTION

1.1 Overview of Fault Detection System

The terms fault, failure and malfunctions have many connotations in the literature as well as in general daily life usage. The words fault and malfunction can be defined as a departing from the normal operation range of observed operational variable or the measured parameter associated with process equipment [1]. These terms are used to show the interchangeability for the cause sequence of the abnormal signs in the plant data which is detected by sensors and actuators. Figure (1.1) shows the method of prescribing the range of acceptable performance which has a direct bearing on the definition of a fault.

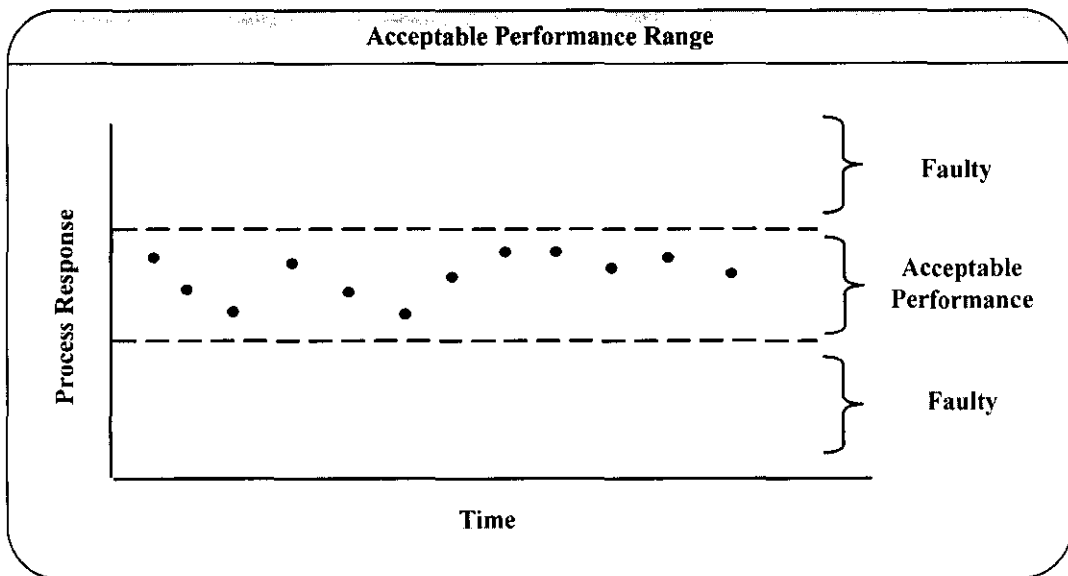


Figure 1.1 Method of prescribing the range of acceptable performance [2]

“...Clearly, the prescription of the boundaries to delineate a fault is a subjective task, and even after the boundaries are established, the classification of faulty versus non faulty is by no means clear-cut if the stochastic aspects of classification are taken into account...” [2].

Malfunction of plant equipment and instrumentation increase the operating costs of any plant. Even more serious are the consequences of a gross accident which lead to unit shutdown because of faulty design or faulty operation.

Considerable attention should be devoted to any system of fault detection that permits the use of less expensive equipment, increases the unit availability, and/or reduce maintenance costs. Therefore, the fault detection system of the process equipment is of definite economic significance in both the design and operation of the plant.

The main objectives of early fault detection in a plant are: to prevent the sudden failure of equipment (trip), to capture higher grade fault information, to improve the plan of the plant maintenance, and to achieve a highly automated plant. In many cases, failures of instruments and key auxiliary equipment can be prevented if early signs of an impending unit trip are recognized. However, computation becomes meaningless if an instrument incurs a fault which is allowed to go on undetected for a long period of time and that situation can easily lead to a plant shutdown [3].

Sudden failure (trip) detection should initiate action to improve instrumentation and instrument maintenance as well as organize the plant control system so that they can make use of substitute measurements in the event of a partial failure being detected [4]. An on-line intelligent plant monitoring system is considered equivalent to providing a redundant control system without incurring any further costs.

1.2 Intelligent Monitoring Systems in Power Plant

Two issues should be taken into account in the design of intelligent monitoring systems (IMSs). The first is, the rapid response of the IMS when a fault occurs and the second is the system sensitivity to noise which consequently generates too many

alarms. The trade-off between these two issues is best investigated in the context of a specific plant in which the cost issue of the various trade-offs could be estimated. Another trade-off involves the IMS complexity, in the other words, its expense relative to its performance.

The complexity vice versa performance trade off is vitally important in the design of IMS. It goes without mention that the first step in setting up an IMS is to get to know the process of the plant. All kinds of special indicators that influence the IMS design such as the layout and environment of the process are associated with a specific process [5].

The establishment of subsystem boundaries is more useful for the IMS. The term subsystem refers to the smallest part of the process for which malfunction is to be diagnosed. The designer should examine the hardware which is required for IMS and perform some modification on the process design to include the IMS capability to detect the faults, compensating for them by control algorithms, introducing short-term storage, activating a backup tool, rerouting flows, and so on [6]. Figure (1.2) illustrates the outlines of an intelligent monitoring system in a power plant [2].

Presently, power plant operations and its advanced machines becomes very complex and are based on an automatic monitoring system for tolerable operation. These features lead to a high cost of downtime. For the purpose of achieving and monitoring dynamic system reliability and assure satisfactory operation, there's a highly increased demand for a power plant to continue a tolerable operation before failures.

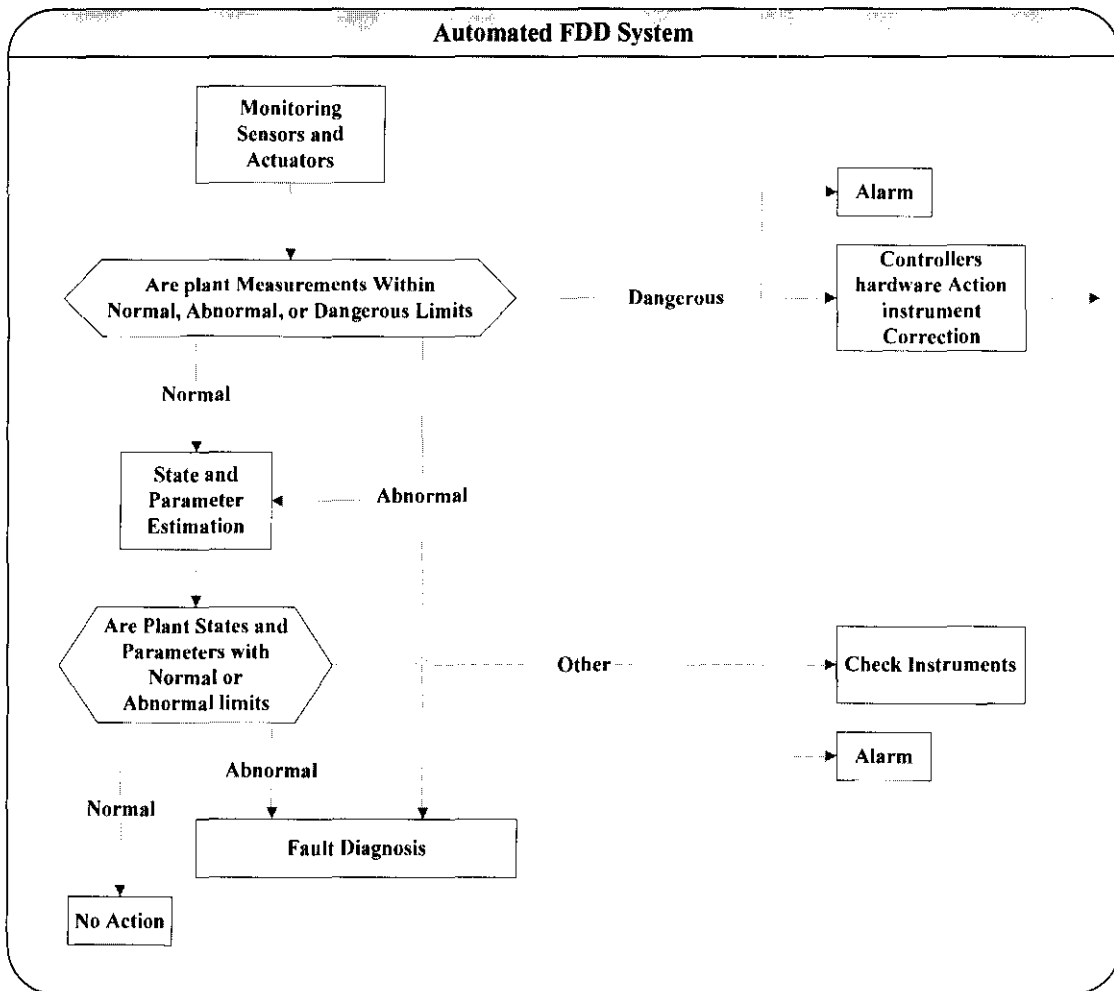


Figure 1.2 Fault detection system for automatic diagnosis [2]

1.3 Artificial Intelligent Systems in Power Plants

The adoption of advanced technologies has increased the complexity of power plants operations and led to a transition from supervision by plant operator expert to supervision by artificial intelligent systems (AISs). AISs have been proposed to such a degree that they can lead to an intelligent system (AI) which has self-examination capability. The most important aspect in these AISs is the quality of plant information provided by the sensors, as well as, the quality of important plant process decisions to be passed to actuators [7].

AISs have been defined as the simulating human intelligence on a machine, which makes the intelligent machine able to identify and use the right piece of knowledge at a given short frame of time to solve a problem [8]. The most commonly used

computational tools of AISs in research fields are Artificial Neural Networks (ANNs), fuzzy logic, expert systems and Genetic Algorithms (GAs). In this work, two computational tools were used for the development of intelligent monitoring systems, which are namely ANNs and GAs. The motivations for studying and understanding these systems are inspired by the studies in the neuro-science and mechanics of natural selection and natural genetics in many different fields.

1.3.1 Artificial Neural Network

Classification of isolated plant information derived from specific sensors or actuators could be achieved by ANNs methodology. ANNs topologies are based on our present full understanding of the biological nervous system. An accurate design for ANNs topologies to solve real problems may also change the way of our thinking about real problems and can lead to new understanding and algorithmic strategy improvements [9]. ANNs are essentially inter-connected groups of artificial neurodes or artificial neurons that use computational models for information processing which are non-algorithmic, non-digital and intensely parallel. The artificial neurons are connected by a large number of weight connections and noticed by a form of layers arrangement. The activation function and learning rate of neurons determine the adaptive coefficients way of adjusting in order to match the neural network with the actual dynamic system [10].

As shown in Figure (1.3), ANNs can be categorized into two learning groups; the first group is recognized by their learning algorithms which comprise of two forms: a supervised learning Neural Network (NN) form and an unsupervised learning NN. The second group is recognized by their recall structures which comprise of two forms: a feed-forward neural network recall form and a feed-back neural network recall form [11].

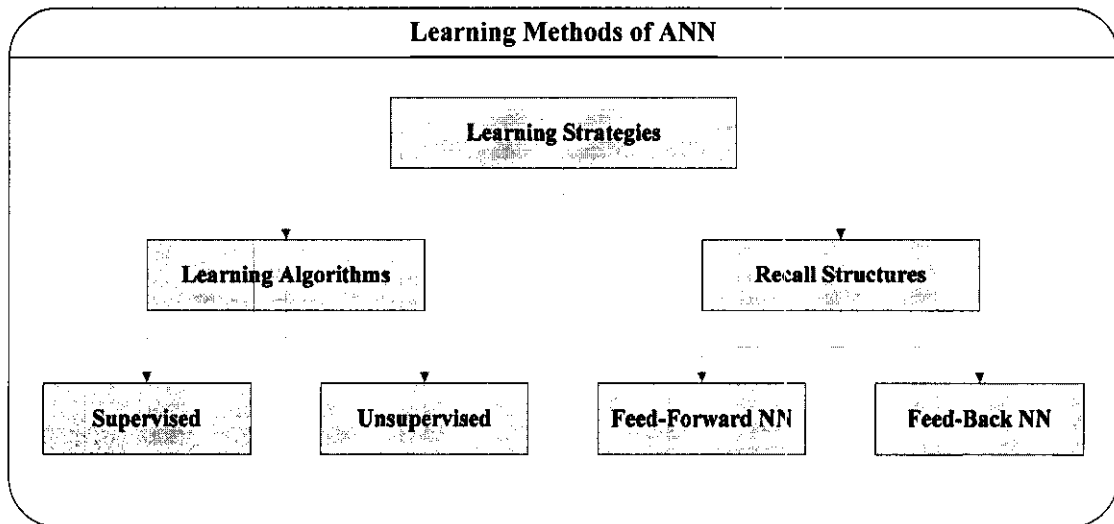


Figure 1.3 Typical ANN learning methods for basic learning strategies [11]

ANNs have many exceptional characteristics such as the capability to process noisy, sparse and incomplete data, the ability to operate the NN properly due to their high fault tolerance even with few damaged neurons or weighted links in the network, and its response ability in real time due to their inherent parallelism. ANNs have gained very remarkable applications with their characteristics in pattern recognition, image processing, speech recognition and adaptive control [11].

1.3.2 Genetic Algorithms

The basic fundamentals of GAs were found by John Holland [12] in 1975. GAs are search algorithms based on the evolutionary optimization mechanics of natural selection and natural genetics. The GAs breeding procedure has three major operations, namely, reproduction, crossover and mutation, which form the main body of the GAs. GAs have the ability of a very simple coding representation (bit string) to encode complicated architecture and the power capability of simple transformation to improve such architecture. Theoretically and empirically, the GA has been proven to supply the complex search scope with a robust search. The basic differences between the GA and the most common used optimization methods, such as a calculus-based search method and a hill climbing method is outlined by [13].

The GA codes the set of parameters, not the parameters themselves. The GA searches from a population of points, not a single point. The GA uses the information

of function objective, not derivatives or other auxiliary knowledge; and uses the probabilistic transition rules, not deterministic rules. These differences contribute to the robustness of a GA and result in pros over other more commonly adopted techniques.

GAs have been established as a valid heuristic approach for solving real problems which require more effective and efficient search. Nowadays, it has become a more widespread application in business, scientific and engineering studies.

1.4 Research Problem Statement

Steam boilers are very important equipment in the power plant. Some boiler trips may lead to an entire shutdown of the plant, which causes a high cost of downtime. An early detection and diagnosis of the boiler trips is crucial to maintain normal and safe operational conditions [14-16]. Numbers of artificial methodologies have been proposed in the literature for fault detection of power plants. However, rapid deployment of these methodologies was difficult to be achieved due to certain inherent limitations such as system inability to learn or dynamically improve the system performance and the brittleness of the system beyond its domain of expertise [17-19]. As a potential solution to these problems, two IMSs specialize in boiler trips have been proposed with the help of MATLAB codes in the present work.

1.5 Motivations

A few questions need to be addressed as research motivations:

- i. Are IMSs capable of detecting and isolating, in real time, trips of a thermal plant boiler?
- ii. What is the degree of success of the IMSs in achieving this task?
- iii. Can an IMS typical to a thermal power plant (TPP) boiler be handled using a pure IMS and/or a hybrid IMS?

- iv. Can the pure system handle the boiler trip detection or would support by another AIS technique enhance its capability?

These questions were answered by the analysis of the results of this work.

In the present work, since it has been not been recorded in the literature, the pure ANN and the ANN supported with GA have been proposed to perform the boiler trip detection. They both performed successfully. The selection of input data to the IMS is commonly based on the plant experience, as noticed from the literature. To support the ANN, the capabilities of the GA in the present work were investigated as a replacement for plant experience. One more issue on the selection of the best NN topology combination is usually achieved by a trial and error approach of an ANN. The hybrid of the GA with an ANN was found to be a powerful tool in selecting the optimum combination of ANN topologies for the recent application of boiler trip detection.

1.6 Research Objectives

The following could be addressed as objectives of this work:

- i. To develop an IMS for boiler trip detection by the adoption of a pure artificial neural network system.
- ii. To develop a hybrid IMS specialize in boiler trips by the adoption both genetic algorithms and artificial neural networks to form a hybrid intelligent system.
- iii. To establish an integrated data preparation framework for specified boiler trips.
- iv. To perform the training and validation of the proposed IMSs using real operational data captured from the plant control system of an MNJ coal-fired power plant.

1.7 Thesis Organization

The introductory remarks of the fault detection, artificial intelligent systems, and intelligent monitoring systems in power plants are given in chapter (1). The problem statement, research objectives, motivations of developing plant IMSs are also highlighted.

Chapter (2) presents a literature review, which provides a background of artificial development of fault detection systems, the fault detection and diagnosis using NN systems, and the hybrid intelligent monitoring systems. A justification for choosing the ANN methodology for trip detection is presented. Following this, related issues in the application of hybrid intelligent systems based on evolutionary optimization techniques of genetic algorithms are summarized.

The theory of the two proposed IMSs and feed forward ANN methodology is presented in chapter (3). The first intelligent monitoring system (IMS-I) represented the use of pure ANN for boiler trip detection. The second intelligent monitoring system (IMS-II) presented the use of GA and ANN as a hybrid intelligent system.

The main focus of chapter (4) is on the plant data acquisition and preparation adopted in the construction of the IMSs, which consists of two major parts. The first part describes the data source which is the selected thermal power plant, and focus on a boiler with its common trips. The second part presents the transformation of raw data to data that is useful for intelligent monitoring system training and validation.

The development of the IMS-I is presented in chapter (5). The investigation of various main NN topology combinations and the IMS-I capabilities to detect all seven boiler trips is discussed. Moreover, the development of the IMS-II to select appropriate boiler operation variables with optimal NN topology combinations to monitor boiler trips, and the application of encoding and optimization process using genetic algorithms are presented in this chapter.

Chapter (6) summarizes the training and validation results obtained from proposed IMSs. Conclusions are presented on the strengths and weaknesses of the two IMSs. An overview of the NN topology combinations and optimal boiler operation

variables selection is provided. Actions to be taken by the plant specialist with correspondence to each trip are listed.

Chapter (7) concludes and discusses the contributions and critiques of the work. Detailed conclusions of the IMS-I and the IMS-II are presented. The chapter is ended by the suggesting for future works in this field and suggestions for the plant operators.

CHAPTER 2

SURVEY OF PAST WORKS ON INTELLIGENT FAULT DIAGNOSIS

2.1 Introduction

The core purpose of this chapter is to provide an overview of literature and reasoning employed in the development of an IMS as a guide for the most appropriate methodology for steam boiler trip monitoring so as to enhance the thermal power plant operational workability and reliability. Advanced technologies have usually been used at the design stage of power plants along with traditional computer programs. Furthermore, such technologies have come into play for monitoring of the operational variables in the power plant operations. It has also got benefits of avoiding plant outages. It is important for the trend of critical features to confirm the safe and dependable operations of the thermal power plants. There are already many such features that are monitored in the power plant and includes those elements from simple sensor/actuator features to more a complicated status to other plant elements. For real time fault detection and diagnosis, prediction and decision making, introduction of different advanced technologies is recently gaining attention as it brings significant operational improvements of the power plant. So as to promote the thermal power plant operational workability and reliability, the most relevant techniques of AI branch of computational science have been adopted with new strategies in place.

2.2 Fault Detection and Diagnosis

Fault detection and diagnosis (FDD) evidently are activities of pattern recognition. Sensors and actuators that carry no readily distinguishable message can possibly be transformed via pattern recognition into information usable for decision-making that accounts for factors of safety, energy conservation, and efficiency during operation [2].

Fault diagnosis is an essential task with immense significance and has been conducted in different perspectives. Factors that reduce process performance can be diagnosed by three mechanisms [2]:

- i. Alarm (the binary decision either that something has gone wrong or that everything is satisfactory).
- ii. Isolation (determination of the source of the faulty performance).
- iii. Estimation (determination of the extent of the fault).

Certain controlled variables have specifications that have to be fulfilled with regard to the needs of the operator who supervises the performance of the equipment against time. The process is said to be operating normally if the factors under consideration are at or around the desired set values. A fault happens when one or more of the states suffer from deterioration of states and subsequent temporary or permanent physical changes such as scaling, tube plugging, sensor and actuators deterioration, leaks, etc.

As an extension of the deterioration process above, failure may happen and it is complete performance decadence. A fault may not only lead to poor economy but also result in horrible outcomes where by people get injured or equipment is damaged.

2.3 Techniques of Fault Detection and Diagnosis

Fault detection and diagnosis has become a very essential feature in a number of processes. Most complex systems comprise many interdependent working segments and their normal operation relies on early detection and diagnosis of any faults or failure.

Normal operation of a process is achieved if a process operates with its controlled variables changing in the acceptable range of the desired values. By definition, a fault is an unacceptable deviation in one of the system variables or parameters that might hamper normal operation. Early detection of a fault in a process is greatly required and therefore this is considered as a target [20].

There are many techniques used in fault detection and diagnosis. Some of the techniques are relatively well-known, while others are more speculative. Broadly, the techniques of fault detection and diagnosis can be classified into two general categories: namely, the estimation technique, and the pattern recognition technique [2, 7]. Figure (2.1) displays the relationship between several fault detection methods and these two techniques.

2.3.1 Estimation Technique

The estimation technique has as usual the existence of a mathematical model that describes the process satisfactorily. In practice, a mathematical model cannot accurately represent complex processes, hence fault detection can be quite difficult because some errors in the model may be interpreted as a fault, or some faults may be undetected when they occur. In this regard, the model should not be too complicated as it makes the model far too tedious and time-consuming [21].

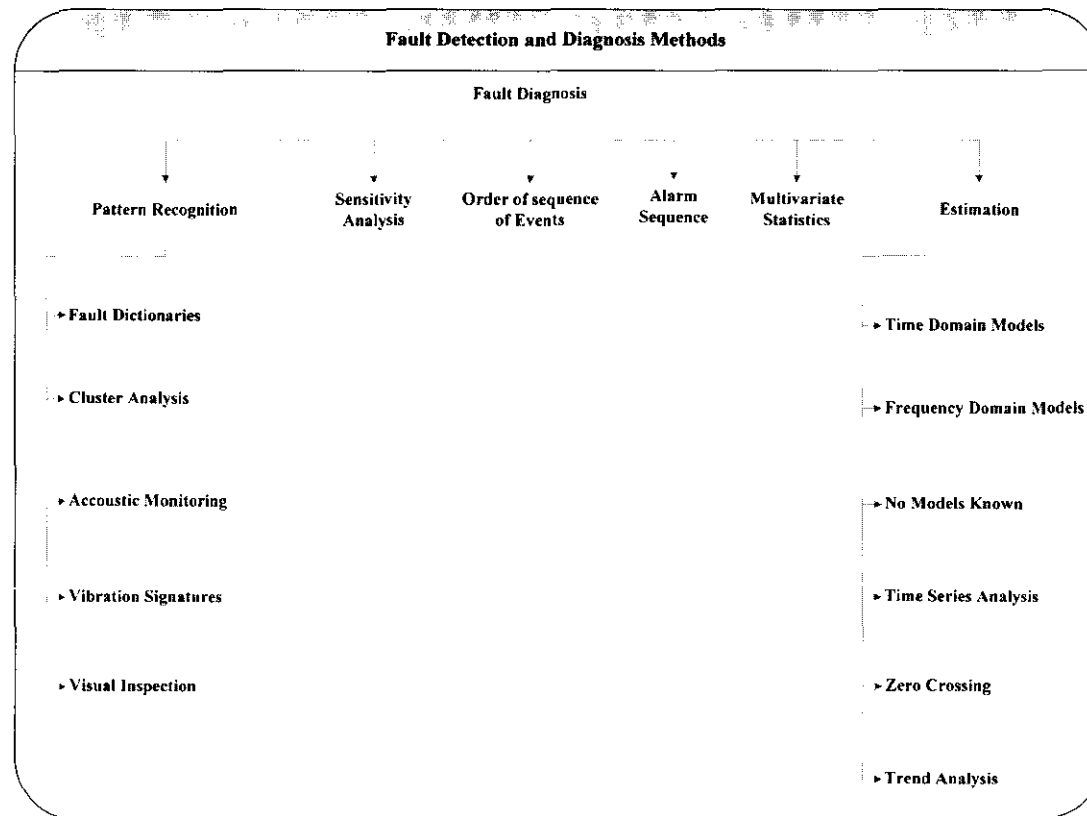


Figure 2.1 Classifications of methods for fault detection and diagnosis [2]

Estimation techniques are generally classified into two categories according to what is to be estimated:

2.3.1.1 State Variable Estimation

In complex systems, there are probably some non-measurable state variables. These state variables are estimated using a dynamic process model, which is linearized about an operating point. Later, the residuals are generated and some statistical methods have been employed in order to achieve the fault detection. Two points are really important here, the presence of a relatively accurate understanding of the parameters of the linearized model and the operation of the process near the point of the linearization of the model.

2.3.1.2 Process Parameters Estimation

In a number of dynamical systems there is a complex relationship between the process model parameters and the physical process coefficients. Faults mostly influence the physical coefficients and the consequence can also be felt in the process parameters. If the above functionality is unique and well understood, we can compute the shift of some physical process parameters that cannot be directly measured by using the estimated process model parameters. Unfortunately, the above mentioned unique relationship is rarely adequately understood.

2.3.2 Pattern Recognition Techniques

A mathematical model of the process is not required in applying pattern recognition techniques for fault detection and diagnosis. The operation of the process and the categorization is dictated by measured data. So, pattern recognition is the process of assigning a category to a pattern according to some features in the pattern. There are two techniques of pattern recognition:

2.3.2.1 Template Matching

Template matching is similar to the procedure involved in the human mind to recognize several patterns. When a pattern recognition puzzle is given to a human being, he/she unknowingly compares the pattern with other similar works of his/her knowledge. In other words, the human's pattern recognition is the result of experience or learning. So, template matching is a comparison of a sample with a stored set of prototypes.

2.3.2.2 Feature Extraction and Classification

This second technique of pattern recognition can be divided into three stages: measurement, feature extraction and classification. First, the appropriate data are measured from the measurement space, which is in vector form. Then, in the extraction stage, selected features of the measurements are separated and combined to form a new vector called the feature space. Lastly, several decision making rules are applied to the feature space vector so that this vector is categorized into one or more classes. In fault detection and diagnosis, these classes are normal operation classes and are comprised of several types of faults. Pattern recognition mainly concentrates on the stage of the classification of features. The main problem though is the extraction of the features. It is quite difficult to know which features are essential and which are irrelevant. If a good selection of features is undertaken, then simple decision rules are able to perform the classification in stage three. On the other hand, if the feature extraction is not so efficient then the decision rules have to be quite complex.

2.4 Brief Comparison between Estimation and Pattern Recognition

Techniques

The major drawback of the estimation techniques for fault detection and diagnosis is the sensitivity to a modeling error. The mathematical model of the process must involve every situation under consideration and should enable one to describe any changes in the operation point. If the model fails to describe the variations in the

process to a satisfactory degree, the whole diagnostic system fails. On the other hand, pattern recognition techniques do not need an analytical model of the process. They get all the information from some representative training data of the process, so they are sensitive to the quality of that training data [7].

When the analytical model of the process gets very complex as in the case of nonlinear models, the estimation technique becomes very computationally demanding. Pattern recognition techniques are less computationally demanding, depending on the data and actual problem, hence they are preferable for a nonlinear process.

Another disadvantage of estimation techniques is that they are not flexible. If one equation is changed in a diagnostic system, many changes have to be made. On the other hand, pattern recognition techniques are more flexible, because a change in the system can be taken into consideration with just some changes in the training data.

2.5 Intelligent Systems as Candidates for Cognition in Thermal Power Plant Monitoring

Intelligent system is a broad term which encompasses a variety of computing techniques that have emerged from researches into AI. Symbolic and numerical approaches and their hybrids make parts of the AI system. The very purpose of AI is to construct a machine that mimics or exceeds human mental capabilities including reasoning, understanding, recognition, creation and emotion. Nevertheless, intelligent systems have not managed to reach to a level of an artificial human brain. However, they are playing a crucial role in terms of enabling one to tackle a range of problems that were considered to be very difficult earlier by eliminating the tediousness of operations through proper monitoring and decision making [22].

The techniques in AI, which can be candidates for accomplishing the task of TPPB trips detection, are evaluated in the following sections:

2.5.1 Knowledge Based Systems

A Knowledge Based System (KBS) is a symbolic representation of a system where domain knowledge is markedly separated from the software controlling the application of that knowledge. In a KBS, there are normally two modules; the knowledge base and the inference engine. For many applications, components of real-time data acquisition should be included. The knowledge base is represented in words and symbols that are joined to form a logical ground which may comprise rules, facts and casual relations.

The explicit detachment of knowledge from control facilitates the addition of new knowledge to the system during the development of the program or during its later use. Another essential aspect of a KBS is its capability to generate an explanation for its conclusions and reasonings. With a KBS it is possible to give a description of how a result comes out and why a specific way of reasoning is followed which, in turn, is very important for understanding human user's.

There are a variety of knowledge based systems which can be used for the purposes of fault diagnosis, prediction and support to decision making in thermal power plants. There are as listed below [23] :

2.5.1.1 Rule Based Systems

A Rule Based (RB) system is a knowledge based system where a set or sets of rules are used to represent the knowledge base. The simplest kind of rule is a production rule, which appears as in the form shown below:

IF <Condition> THEN <Conclusion>

The inference engine in RB systems involves a strategy so as to decide which rules to apply and when to apply them. An RB system is the most traditional and

initial application of a KBS which resembles natural language that is easy to understand.

However, the amount of knowledge that can be presented in rules alone for a fairly complex device is limited. There are four major deficiencies of a purely rule based diagnostic system as illustrated here:

- i. The relationships between individual operations in many real applications are not as sharp as rules. Therefore, to draw direct conclusions by production rules is very likely to produce misleading results.
- ii. To build a complete rule set that is economically affordable and technically achievable is a huge task. It may probably be possible to overcome this obstacle by deliberately enforcing the fault in a component and observe the outcomes. But this is still economically unviable.
- iii. A large number of rules are required to verify the sensor data for consistency before diagnosing a failure.
- iv. Obsolescence is the other challenge of building a complete rule set.

In order to alleviate the shortcomings of RB systems other diagnostic techniques of KBSs have been proposed [24]. The complete structure of a rule-based expert system is shown in Figure (2.2).

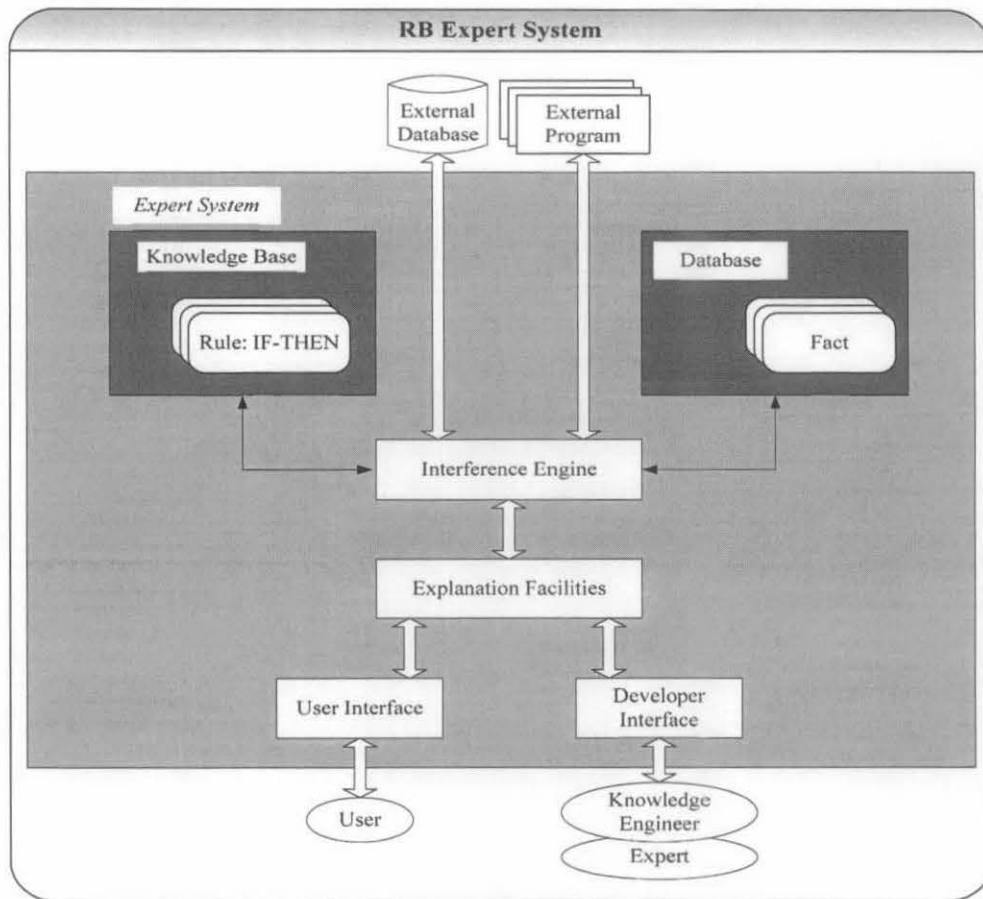


Figure 2.2 Complete structure of a rule-based expert system [25]

2.5.1.2 Model-Based Systems

Physical principles are applied to generate a symptom cause pair that must be considered in the diagnosis. This is a foundation of all MB (Model-Based) systems. The common representation in a model based system is object oriented. The device is made up of components where the function of each individual component is identified within a class definition and the structure of the device is defined by the connection between the instances of components that build the device. Ultimately, the device would be in one of the several possible operational states. Important advantages of MB systems include:

- i. The model is less cumbersome to manipulate or to use than a rule base.
- ii. The model does not require sensor verification as the sensor is handled the same way as other components and a faulty sensor can be detected as with other faults.

- iii. The separation of the function structure and state may help a diagnostic system to go beyond its area of expertise and provide a reason for a problem.
- iv. The model can be used to simulate a physical system in order to monitor or verify a hypothesis.

Nevertheless, model based systems suffer from the disadvantage of not being able to model complex physical systems [24].

2.5.1.3 Semantic Networks

A Semantic Network (SN) [26], is a labeled directed graph in which individual nodes represent concepts, objects, properties and relationships. An SN is intuitive and easy to comprehend. This allows it to represent relationships between concepts and taxonomic knowledge and solve classification problems in which reasoning is based on taxonomies.

2.5.1.4 Fuzzy Sets and Fuzzy Logic Systems

The possibility theory or Fuzzy Logic (FL), builds upon the theory of fuzzy sets where uncertainties due to vagueness in language are handled. Fuzzy sets are means of smoothing out the boundaries of the observations that contain some vague language [27].

2.5.1.5 Bayesian Networks

Bayesian Networks (BN) comprise directed acyclic graphs and the condition probability tables. They involve rigorous probability terms to handle uncertainties in the graphs in BN systems which are proposed from variable nodes and represent the causality between the variables [28].

2.5.1.6 Decision Trees and Influence Diagrams

Decision trees have graphical representation of event variables and decision variables. The quantitative aspect of the decision tree is composed of probabilities and utilities. Every event has a probability fitted to itself and each decision variable has a utility attached to it. The order of decisions and the set of observations between the decisions are the two most important factors involved in decision scenarios which are represented in a BN [28].

2.5.2 Soft Computing Methods

The numerical technique in Computational Intelligence Systems (CISs) is different from symbolic techniques involved in knowledge based systems. The CIS knowledge is not explicitly stated as in the case of a KBS but, it is represented by numbers that are adjustable according to the improvement in the accuracy of the system. These techniques are broadly classified as *soft computing methods* [28].

A CIS includes neural networks, genetic algorithms and other optimization techniques. Fuzzy logic and bayesian systems used for accommodating uncertainties can comply with CIS categories. Where as GAs and other related optimization techniques are not in conformity with the purpose of fault diagnosis and prediction in the complex operational domains. ANNs techniques are used for classification, non-linear estimation, etc. Consequently, these two intelligent systems are used in sequence to model and optimize the thermal power plant considered in this research.

2.5.2.1 Neural Networks

ANNs are a body of techniques used for numerical learning. They are composed of many non-linear computational elements which make the network's nodes or neurons linked by weighted interconnections. Each node in ANN may have several inputs with specific weighting. The node does a simple computation on its input values to generate a single numerical output. The output from a node can either form an input to either nodes or contribute to the whole output of the network. ANNs can be applied

for *classification* and *non-linear estimation* of a fault diagnosis and prediction systems in a thermal power plant [29].

The application of intelligent system technology for diagnosis is a function of several factors. First, diagnostic systems must utilize plant quantitative data. Second, it may be impossible to anticipate or predict every possible cause of malfunction as the field of search is not entirely known. Third, the end users are plant operators instead of managers. Fourth, the advice drawn from such systems is expected to be non trivial and dependable [25].

Intelligent systems for plant status monitoring are anticipatory synthesis of signal validation, diagnostics and alarm filtering techniques. In brief the aim of these systems is to provide the operator with an assessment of the status of the plant as a whole with strong supporting justifications for conclusions made [29, 30]. Figure (2.3) shows the power plant control system interface.

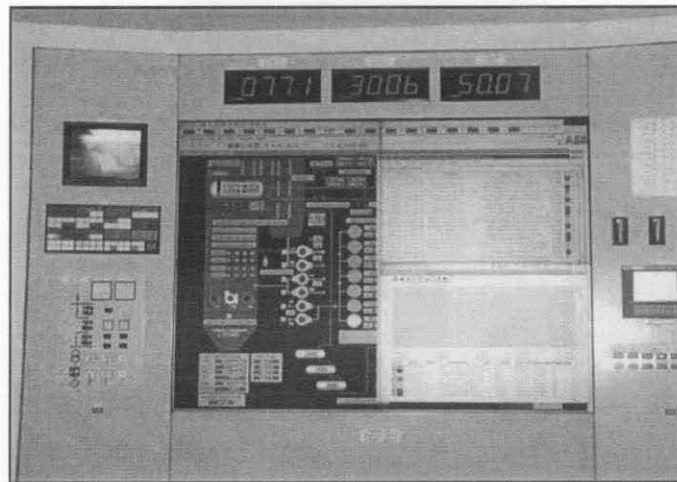


Figure 2.3 Power plant control system interface¹

2.6 Application of Neural Network System for Fault Detection and Diagnosis

This subsection summarizes the studies dealing with artificial intelligent systems particularly a neural network technique in power plants.

¹ From the operation and maintenance instruction manual for the MNJTTP

Kim *et al.* [31] demonstrated the feasibility of a multi layer NN model coupled with a stacked generalization technique to the early recognition of San Onofre nuclear station operational transients. They used the data of ten scenarios obtained from the plant training simulator and investigated the ability of the NN to provide a measure of the diagnosis confidence level. The proposed model responds very rapidly to the variation of the plant conditions. They have concluded that the NN adviser model required further development and working on an integrated ANN advisor which is capable of classifying more transients and providing a prediction of error in these results. Furthermore, it needs to be faster and requires a reliable diagnostic system to enhance the safety of the nuclear power plant.

Guglielmi *et al.* [32] have adopted a multilayer feed forward and Radial Basis Function Neural Network (RBFNN) tool to solve real system diagnostic problems. The ANN testing process has been applied to four heaters of a feed water high-pressure line of a 320 MW power plant. A different ANN classifier has been employed to solve the power plant fault detection and diagnosis as a one pattern-recognition problem. NN classifier data have been captured via the simulation of a complex nonlinear model (71 state variables and 29 sensor variables). However, various types of real system faults have been assumed for different important operating conditions. They have validated the model with respect to the real plant performances. From neural classifier results, it is obvious that such a diagnostic system has the ability to decide correctly in terms of generalization capabilities even under different plant conditions. They have commented that further work is required for a detailed analysis of noise effects on the performances of the fault diagnostic system, the possibility of on-line real process parameters training and the consequent adaptability of the method. Also, they recommended more investigation of unsupervised learning algorithms and rule-base NN methodologies integration.

Simani and Fantuzzi [33] designed a two-stage fault detection and diagnostic system for input-output industrial gas turbine process sensors. In the first stage, fault detection is performed by residuals generated from a bank of kalman filters, while, in the second stage, fault diagnosis is achieved by experimenting with supervised NN pattern recognition techniques (multilayer perceptron networks and RBF). Their simulation results showed the reliability of a multilayer perceptron network to classify

training patterns with satisfactory performance. On the other hand, the RBFNN training process experienced severe limits with noisy data.

Babar and Kushwaha [34] proposed operator support system software based on the ANN as a means to identify the undesired plant condition (initiating event). Event identification was carried out by a resilient back-propagation NN training algorithm for different combination of neurons and number of hidden layers. Simulated data was obtained from eight initiating events for the atomic plant considered in the study. The implementation of such an expert system was reasonably good. The system helped to minimize the operator error and assisted operators in minimizing the occurrence of abnormal situations during reactor operations. They concluded that the development of the tool reliability can be further improved by directly utilizing the real plant data, in the sense that the diagnostic system will perform better if the real data is provided.

Bae *et al.* [35] designed a fault diagnostic system using an NN based on the pattern of principle variables which could represent the type and severity of failures. Two-steps NN for FDD were constructed; the first step was to classify the fault type and the second was to detect the fault severity. The results deteriorated; therefore, it was necessary to adopt other supplementary techniques in order to increase the NN model accuracy.

Romeo and Garetta [36] designed a set of NN monitoring methodologies to analyze the influence of fouling and slagging for a biomass boiler. The NN models can predict a set of operational parameters and the fouling state of the boiler. As a result, diagnostic model outputs were validated with real and traditional equation-based monitoring data. They have concluded that the ANN is a stronger tool for monitoring than equation-based monitoring. However, few ANN sets such as a fouling prediction set, boiler behavior evolution set and fuzzy logic rules based on the real data set are needed. The results from these ANN sets with knowledge could optimize boiler cleaning cycles and fouling evolution. In addition, NN proposed sets can serve as the ground work for the future development and validation of (NN + Fuzzy Logic) software to minimize the effect of fouling in biomass boilers.

Due to the complexity in analytical modeling and its long computation time, Rusinowski and Stanek [37] have presented an NN estimation model for a steam boiler. The proposed estimation NN model has the capability of mapping the influence of flue gas losses and energy losses due to unburned combustibles on the main operational parameters of the boiler with a short computation time and a high accuracy of calculations. It has been proven that the model was a suitable tool to the influence of the operational parameters upon the energy losses and energy efficiency of the boiler. The model results have confirmed that the air excess ratio and flue gas temperature exert a dominant influence upon the flue gas losses as a result, as a future extension to the work, the proposed estimation NN model would be applied in the control system of a power unit for the optimization of the boiler operation parameters.

De *et al.* [38] proposed two NN sub-modules for real time monitoring of the plant for the biomass and coal-fired plants. On-line plant data was used to train a feed-forward back-propagation NN model. The first sub-module was designed to predict the boiler exhaust and emission characteristics, and the second sub-module was designed to estimate the power output. While it was desired to observe the effects of the parameters of Heat Recovery System Generator HRSG, district heat and input parameters of the boiler such as fuel and air flow rates and air temperature on the power output, these parameters were included as input parameters for this ANN sub-model. With good accuracy and a quickly online monitoring system aided by two ANN prediction sub-modules of the power output, the assessment of degradation of the plant performance could be implemented. It was obvious that retraining of the ANN modules were required for any changes occurring in the system.

Mo *et al.* [39] proposed a two level classifier architecture with a dynamic NN for detection of transients; classification and prediction in nuclear power plants (NPP). Transient type, severity and location were individually obtained by assigning that model for different purposes. Large amounts of simulated transients have been used as inputs for model training and testing; the dynamic NN model results were compared with widely used general purpose NNs. Transient types have been recognized quickly only in several seconds after transient began not after. Low bias is comparatively recognized between the results and qualitative predication. From the comparison, the model performance was better in the system sets.

Zhang *et al.* [40] proposed a combination of integrated NN for fault diagnosis in a steam turbine generator. They have suggested the combination of an NN method to reduce the amount of information needed to train an ANN system to diagnosis different types of faults. Instead, a combination of many sub-NNs could reduce the training effort and be able to diagnosis different types of faults.

Santosh *et al.* [41] proposed a symptom based diagnostic system based on an ANN for the identification of reactor process accident scenarios in 220 MW power plants. Several large break loss of coolant accident scenarios have been considered and analyzed. Time dependent simulated transient data have been generated using specialized codes. The NN diagnostic results have been incorporated in a symptom based diagnostic system software for operator assistance.

Fast *et al.* [42] have constructed an ANN model with multi-layer which has been trained using commercial software NeuroSolution. Back-propagation was the basis to train and supervise the ANN. They have used real plant data for the training of the ANN to predict the performance of the gas turbine. The main aim of a unified ANN was to identify anti-icing or normal mode of operation with input local ambient conditions (temperature, pressure, and relative humidity) and then to predict the different operating and performance parameters of the gas turbine. They found that using an initial NN to decide the switching on or off of the anti-icing system and providing information to a second ANN about the mode of operation, the prediction accuracy was increased considerably.

Fast and Palme [43] have applied an ANN system for condition monitoring and diagnosis of a Combined Heat and Power plant (CHP) in Sweden. The system consisted of ANN models which represented each component in the plant. They are connected to a graphical user interface and were integrated on the power generation information manger (control system) in the computer system of the plant. They have trained the ANN Models using a back-propagation algorithm. They concluded that the established ANN models are plant specific but the method is general and it is applicable to other power plants.

Smrekar *et al.* [44] proposed two artificial neural network models using real plant data to predict fresh steam properties and to examine the feasibility of ANN modeling for coal-based power or combined heat and power (CHP) plants. Real data were selected from a brown coal-fired boiler of a Slovenian power plant and used to train the model using NeuroSolution commercial software. Initial NN input parameters selection was made on the basis of expert knowledge and previous experience. On the other hand, the final NN input parameters set were optimized with a compromise between a smaller number of parameters and a higher level of accuracy through sensitivity analysis. The first proposed model included mass flow rate of coal, while the second one included belt conveyor speed as one of the NN input parameters. They concluded that both of the NN models may be used, either for on-line or off-line applications as well as ANN models which can take into account everything known and unknown for some processes for which it's difficult to develop a physical model.

2.7 A Hybrid Intelligent System Strategy for the Thermal Power Plant

It is evident that no single technique can solve the variety of complex tasks in the thermal power plant domain. Thus, this work takes appropriate AI techniques as complementary tools that can be integrated into a hybrid system for boiler trips detection of the thermal power plant. In this respect, hybrid systems have the purpose of dealing with multifaceted systems, enhancing the capabilities of individual techniques or setting the parameters of a constituent technique.

Hence, practical intelligent systems in thermal power plant operations should be designed in a way that they comprise several modules where each one uses the most appropriate tool for its specific task. These modules will then interact with each other both at the design and at the operational stage to handle different tasks and ameliorate the capabilities of each other and that of the overall system.

2.7.1 Application of Hybrid Intelligent Systems

Selection of the proper input variables of an NN from thousands of process variables for a nuclear power plant control room is crucially important and is a very challenging

task to successes in. Guo and Uhrig [45] investigated a special fault diagnostic method based on a genetic algorithm search to guide the search for an optimal combination of neural network inputs to achieve the criteria of fewer inputs, faster training and a more accurate recall. Simulation data obtained from a nuclear power plant was used to reveal the potential applications of ANNs and GAs in nuclear power plants. They showed that the GA could be adopted to search for optimal NN input variables to achieve higher performance in different diagnostic tasks. The main disadvantage of using evolutionary optimization based on a GA to select NN inputs was cost in the sense of computer processing time as each individual string in a population represents a selection of NN inputs that needs to be checked and tested through a training process and error recall. To overcome this drawback, training process time for each test should be reduced in order to speed up the search process by using different NN structures and learning algorithms. Therefore, the training process and error recall are only required for newly created off springs which are only a portion of the whole generation. Hybrid fault diagnosis NN-GA can be used in cases where the influential parameters need to be distinguished from other parameters but no prior knowledge is available to guide the selection.

Hines *et al.* [46] have reported a hybrid approach for detecting and isolating faults in nuclear power plant interfacing systems. They have combined two tools: observation based residual generation and NN pattern matching to produce a hybrid diagnostic system. The NN training was conducted using boiling water reactor simulation (BWR) data. The simulation was carried out by simulink. Back-propagation with momentum and adaptive learning rate, Moller's Scaled Conjugate Gradient method and Levenberg-Marquardt training algorithms were implemented in a MATLAB NN toolbox and compared to determine the most efficient method. They have selected Levenberg-Marquardt for NN training. Besides that they have demonstrated that the hybrid method has significant advantages over the conventional NN diagnostic methods.

Kim and Bartlett [47] performed a new error estimation scheme associated with a nuclear power plant diagnostic neural network advisor. The proposed error estimation technique has been addressed to provide bounds on the output obtained from the neural network fault diagnostic advisor in order to obtain more accurate reliable

information with considerably reduced computational requirements. Data from twenty-five distinct simulated transients were obtained from the Duane Arnold Energy Center (DAEC) nuclear power plant for (33) transient scenarios ranging from a main stream line break to anticipated transient without scram (ATWS) conditions. The new method called Error Estimation by Series Association (EESA) used simulated data were only from DAEC to solve the complexity and difficulty of previous error estimation procedures and validate the advisor's diagnostic output.

Several aggregation methods were recommended for different modelling approaches as useful methods in model design for the complicated plants with immeasurable or hard measurable variables. Mincho B. *et al.* [48] proposed a new aggregation combinational approach based on the First Principles, fuzzy logic, ANN concepts and statistical models to design adequate models for a steam boiler mill-fan with large uncertainties. The proposed hybrid system was capable of successfully identifying a highly non-linear pulverising system and improving the current estimation of plant behavior.

To present the various applications of artificial neural networks in energy problems, Kalogirou [49] applied ANN models with multiple hidden layer architecture in the field of solar energy; for modeling and designing of a solar steam generating plant, the estimation of a parabolic-trough collector intercept factor, local concentration ratio and for the modeling and performance prediction of solar water-heating systems. He has demonstrated that a past history data, data of the real system performance and a suitable selection of NN models are required for all ANN models which result in acceptable error limits.

Volponi *et al.* [50] carried out a favorable comparison in terms of accuracy between two publicized diagnostic tools for single gas turbine fault isolation symptoms. The first diagnostic technique was a nonlinear-supervised back-propagation neural network which was trained by offline obtained data based on known relationships between the input-output. On the other hand, the training process for underlying faults using that tool with real data could be considered as drawbacks as precise disposition of the fault may or may not be known, as a result, they have decided that the NN should be re-trained. The second diagnostic tool used by them

was a hybrid NN utilizing the kalman filter approach. Based on the obtained results, the back-propagation NN, the hybrid NN, and the kalman filter method are highly accurate single gas turbine fault symptoms. They have recommended the kalman filter approach for better accuracy.

The fault confirmation process without expert knowledge can be prevented by illusive and real-time series signals for complex and high reliable nuclear power plants. Yangping *et al.* [51] proposed a hybrid fault diagnostic method to solve this problem by combining GAs and classical probability with an expert knowledge base. The hybrid model performed on the 950 MW full size simulators at the Beijing NPP simulation training center. The proposed hybrid model showed that this method has comparative adaptability to diagnose signals and faults changed in time, imperfect expert knowledge, illusive real-time series signals and other phenomena. On the other hand, they have mentioned, more work is needed to get effective fitness function.

During normal plant operation or emergency situations for complex system operation, plant operators and system managers have difficulty analyzing the great quantity of data captured to formalize correct and timely decisions. Yildiz et.al [52] introduces a hybrid intelligent system as a solution to solve nuclear power plant operation complexity which combines an Expert System (ES) module and the ANN module incorporated into the proposed complete system. The proposed hybrid system holds the desired properties of each individual technique. The ES module has been completed and validated on the bearing system of horizontal charging pumps in nuclear power plants; however, the artificial neural network module is in the development stage. As a future development of this research work, more efforts should be employed and greater focus should be drawn on completing the design of the NN module, integrating all the elements in the hybrid structure and validating the complete system.

Classification of accidents into groups of initiating events and identification of major severe accident scenarios after the initiating events is very difficult for nuclear power plants. Na et.al [53] applied two prediction systems: the Probabilistic Neural Network (PNN) system and hybrid Fuzzy Neural Network (FNN) system. The PNN system has been designed to classify the initiating events under severe accident

conditions by using one minute interval integrated values of 13 measured plant parameters. Moreover, the hybrid fuzzy neural network system has been designed to identify the important timings representing major severe accident scenarios by using the (two-three) minutes integrated values of three or four measured plant parameters after a reactor scram. Both estimation systems were trained by using the simulation data using specialized codes. It was shown that the PNN system could accurately classify a lot of the initiating events into five kinds of categorized events. In addition, the proposed hybrid fuzzy neural network could accurately estimate important timings which represent major severe accident scenarios.

Because of the good potential of ANNs and Fuzzy ARTMAP (FAM) for fault detection and diagnosis in complex processes, Tan and Lim [54] examined the applicability of pruned and ordinary FAM neural networks to fault diagnosis and condition monitoring problems of heat transfer and tube blockage of the circulating water system. The proposed hybrid model for two study cases has been adopted to investigate the effectiveness of FAM in fault detection and diagnosis, and to extract a set of domain rules from the trained FAM network. From the perspective of fault detection and diagnosis, both the pruned and ordinary FAM neural networks achieved very high performances with the accuracy rates of around 90% in both case studies. From the perspective of rule extraction, the rules reveal a high degree of accuracy, in which they could be used as a set of fault-diagnostic references. They recommended that further work should be focused on aspects of real implementation, accurate evaluation and validation of FAM as an intelligent fault diagnosis and condition monitoring tool in the real life power generation plant.

Mark and Benedek [55] presented a novel hybrid feed-forward neural network with global normalization methodology to classify the unlabeled transients correctly. Back-propagation training algorithms with a probabilistic method were adopted to identify the misleading recognition of unlabeled malfunctions. Many other types of networks and codes were successfully applied using simulated data to identify labeled and unlabeled malfunctions of the Hungarian Paks nuclear power plant. Several issues were important for proper analysis of the processes such as the drift of electronic elements of a simulator, the digitization of simulated actual plant signals and the accumulating error during numerical integration. The global normalization yields less

resolution and it's not sensitive to the presence of drift signals (effects) and the local normalization should be avoided at any cost to eliminate potentially harmful effects from drifts. Recognition was good only for a few transients using time-series data and Fast Fourier Transform (FFT) series among all plant transients. They have recommended that instead of training one network with 20 outputs, twenty different nets with one output could be trained.

In order to overcome the problem of the trial-and-error approach to network design and parameterization, Ferentinos [56] proposed, designed and parameterized an evolutionary approach to an automated two-feed forward neural network based on genetic algorithms of a real world biological engineering field. The two proposed systems are a fault detection NN model and a fault prediction NN model. An indirect representation of the genetic algorithm was used as an encoding means for training parameters and NN topologies such as: back-propagation multidimensional minimization training algorithms, number of neurons for each hidden layer and type of activation function. Both one-hidden-layer and two-hidden-layer network structures were investigated by the GA. The statistical comparison results demonstrate that the proposed models based on the GA system should be preferred over the most common used trial-and-error approach. It was clear that the proposed GA model is not fully automated and several GA parameters have to be tuned such as: probabilities of crossover and mutation, and population size. As a result, the influence of the GA model parameters variation is not as significant to the final performance of the system as that of the parameters of NN topologies design and training.

In order to overcome the back-propagation problems such as slow rate of convergence and falling easily into local minimum, Tian *et al.* [57] implemented a hybrid neural genetic algorithms model for steam turbine-generators fault diagnosis. The hybrid diagnostic model shows that the algorithm converges quickly and diagnoses faults efficiently. Theoretical analysis and an emulational experiment pointed out that the hybrid diagnostic model is an excellent approach. It can optimize not only the value of the NN weight, but also the architecture of the NN.

There was a strong need to develop an automatic fault detection and diagnostic system to avoid a possible nuclear power plant disaster which could be caused by an

inaccurate fault diagnosis by the plant operator. A hybrid fault diagnostic system was introduced by Cheng *et. al* [58] for the condensation and feed water system of a nuclear power plant. The hybrid genetic-radial basis function neural network model makes the neural network smaller in size and higher in generalization ability which led to the improvement in the accuracy and speed of the diagnostic process for non-typical systems.

To improve on the operation of the steam boiler, Rusinowski and Stanek [59] proposed a hybrid model for a steam boiler associated with the application of both analytical modelling and an artificial intelligence system. The proposed hybrid model for a steam boiler has been implemented for multi variant simulative calculations of the influence of the steam boiler operating parameters on the energy losses from the steam boiler and its energy efficiency. The proposed hybrid model for a steam boiler consisted of two parts; the first part is the analytical model part which includes the balance equations. The second part is based on empirical models which are carried out by means of an ANN and regression modelling to express the dependence of the flue gas temperature and the mass fraction of the unburnt combustibles in solid combustion products on the steam boiler operating parameters. Based on the results of the hybrid model, they have concluded that the decrease in feed water temperature leads to an increase in energy efficiency. The energy efficiency of the steam boiler for the proposed hybrid model can be applied in the operating control system.

An ANN design with lesser human dependence and a more powerful and sophisticated prediction and optimization is an extremely important task. Ahmed *et al.* [60] proposed a hybrid artificial neural network and genetic algorithm model for the determination of optimal operational parameter settings for three different cases: gas turbine, drilling process and debutanizer based on the proposed approach. Different ANN predication procedures have been presented to solve the time-consuming problem of the learning process, enhance the generalizing ability, achieve a robust and accurate model, and reduce the computational complexity. The preliminary hybrid model results have indicated that the proposed hybrid model can optimize operational parameters precisely and quickly; subsequently, a satisfactory performance can be achieved. As a future work for this research, they recommended that a GA should be applied to find other optimal ANN designing parameters.

2.8 Summary

Deep functional observation into the afore discussed published works enables the one to conclude that many researchers used a one-hidden layer (IHL) ANN structure for fault detection and diagnosis. Furthermore, intelligent system training was based mostly on simulation data, except in the cases of a few researchers, where real data had been used, and few works focused on the neural network inputs parameterization depending on plant operator experience. On the other hand, no general hybrid intelligent system (NN-GA) framework was reported before for the thermal power plant steam boiler diagnosis for trip detection. Moreover, no standard real data preparation scheme for IMSs so far has been suggested and no attention has been given for NN topologies to IMSs.

On account of the above observations, this particular research is aimed at preparing of a real plant data framework with a related operational variables training and validation of the proposed Intelligent Monitoring System's (IMSs), representing pure ANNs (IMS-I). Later, it employs hybrid GAs and ANNs (IMS-II). Various main NN topology combinations were investigated to explore the final IMS structure.

CHAPTER 3

THEORY OF INTELLIGENT SYSTEMS

3.1 Introduction

The problem statement and the main objectives are discussed in chapter one. The related literature in the field of fault detection and diagnostic systems for power plants are reviewed in chapter two. Some further artificial computational tools adopted in this work are discussed in this chapter.

The following represents the computational tools used in designing and implementing the steam boiler trip monitoring systems:

3.2 Artificial Neural Networks (ANNs)

The ANN is a system loosely modeled and based on the human brain. This field is known by many names, such as connectionism, parallel distributed processing, neuro-computing, natural intelligent system, machine learning algorithms and artificial neural networks. The aim is to simulate the system within specialized sophisticated hardware. The multiple layers of simple processing elements are called neurons and connected to certain neighbors with a variety of coefficients of connectivity that represent the strength of these connections. Learning is accomplished by adjusting these coefficients to result in appropriate results from the overall network [61].

Figure (3.1) is a typical neural network; the circular nodes represent neurons in three layers: input layer, hidden layer and output layer. The directed graph mentioned shows the connections from layer to layer or connection weight [62].

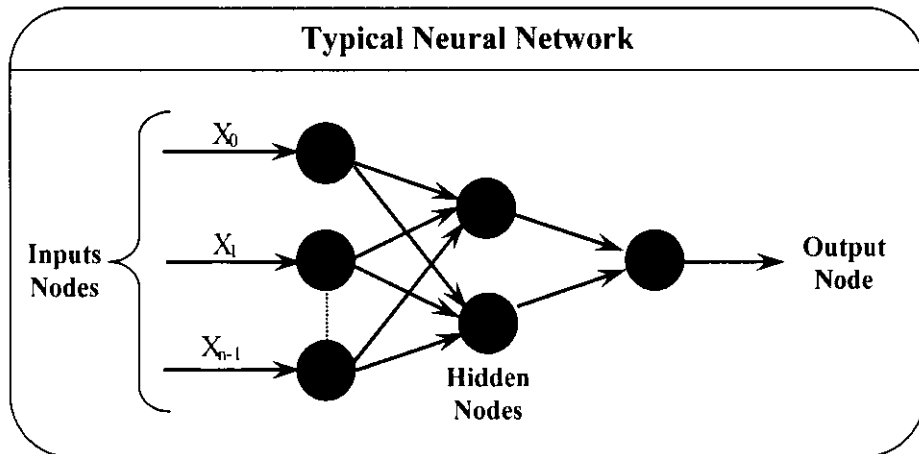


Figure 3.1 Input layer of the typical neural network [62]

A human brain contains over one hundred billion computing elements called neurons. The neurons communicate throughout the body by ways of nerve fibers that makes perhaps one hundred trillion connections called synapses. The neuron system contains two classes of cells; nerve cells and glial cells, the nerve cell is a special biological cell that processes information and the nerve cells are the building – blocks of the brain [62].

There are many types of neurons in the nervous system but they all share the following: the biological neurons are built up of three parts: the cell body, dendrites and axon [63] as shown in Figure (3.2): cell body, dendrites and finally the axon.

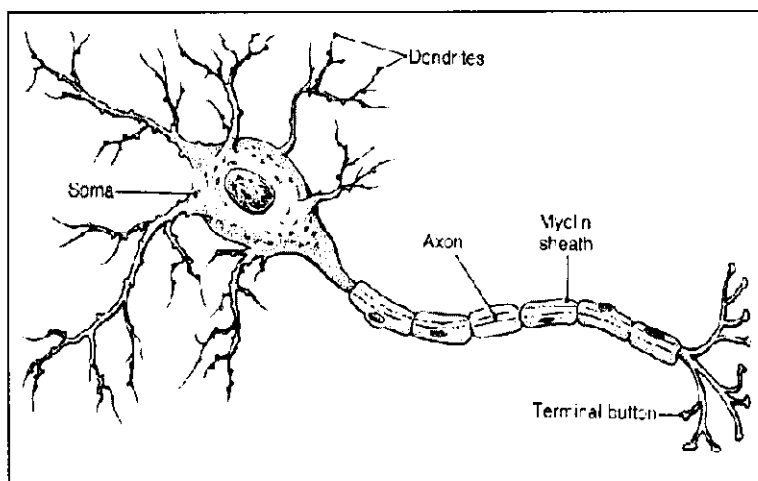


Figure 3.2 Conceptual structure of the classical neuron [63]

In the artificial neuron, each input is represented as the output of another neuron. Each input is multiplied by a corresponding weight and all the weighted inputs are then summed to determine the activation level of the neuron. Figure (3.3) shows a model that implements this idea where a set of inputs (x_1, x_2, \dots, x_n) are applied to the artificial neuron. These inputs are collectively referred to as vector x . Each signal is multiplied by an associated weight (w_1, w_2, \dots, w_n) before applying it to the summation block. If the summation exceeds a certain threshold, the neuron responds by issuing a new pulse which is propagated along its axon; otherwise the neurons remain inactive.

Each weight corresponds to the strength of single biological synaptic connections; the set of weights is collectively referred to as the vector w , the summation block, corresponding roughly to a biological cell body. Adding all of the weighted inputs algebraically x , producing an output (s) in vector notation [64].

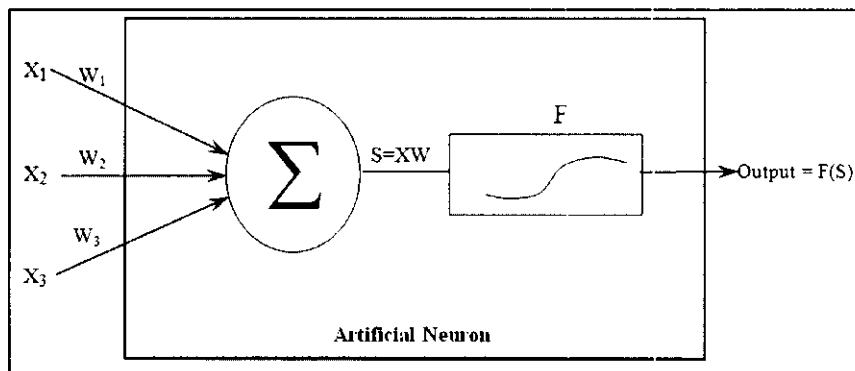


Figure 3.3 Artificial neuron with activation function [64]

A general neuron model may be defined by the following five elements [64]:

- i. The nature of its input.
- ii. The input function.
- iii. The activation function of the neuron.
- iv. The output function.
- v. The nature of the output of its neuron.

The neuron input may be binary, with a value of (-1,+1) or (0,1), it may be continuous, or a real number.

Several common types of activation signal functions (Figure 3.4) are defined as the following [65]:

- i. Linear function.
- ii. Threshold linear function (saturation function).
- iii. Unit step function (threshold function).
- iv. Hard limit function (sign function).
- v. Sigmoid logistic function.
- vi. Hyperbolic tangent function.

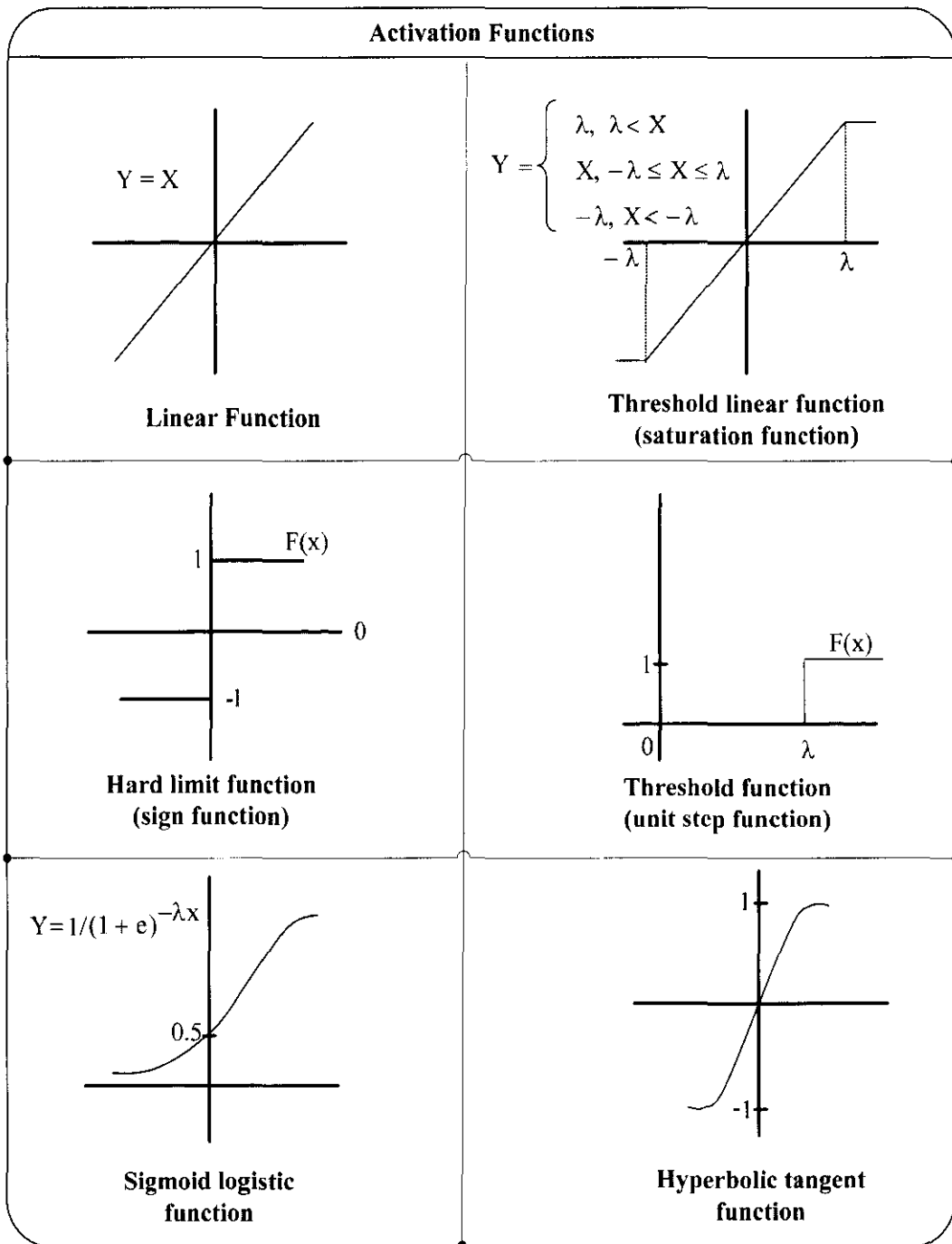


Figure 3.4 Activation signal function [65]

3.3 Why Use Neural Networks

With their remarkable ability to derive mean from complicated and imprecise data, neural networks can be used to extract patterns and detect trends that are too complex to be noticed by either humans or other computer techniques. A trained neural network can be thought of as an “expert” in the category of information it has been

given to analyze. This expert can then be used to provide projections to give new situations of interest.

Other advantages include [66, 67]:

- i. Adaptive learning: the ability to learn how to do tasks based on the data given for training or initial experience.
- ii. Self-organization: an ANN can create its own organization or order of the information it receives during learning time.
- iii. Real time operation: ANN computation may be carried out in parallel. Currently, special hardware devices are being designed and manufactured which take advantage of this capability.
- iv. Fault tolerance via redundant information coding: partial destruction of a network leads to degradation of performance. However some network capabilities may be retrained even with major network damage.
- v. Generalization: the process of describing the whole from parts, reasoning from the specific to the general case, or defining a class of objects from one or more known instances.
- vi. Parallelism: This is fundamental in the architecture of neural networks when the neurons are considered as sets of elementary units. Operating simultaneously results in a great efficiency of calculation.

3.4 ANN Taxonomies

In this section five different ANN taxonomies are presented. Each gives a different perspective of ANNs in terms of network models, learning algorithms, performance indicators, architectures and general areas of application.

3.4.1 ANN Models

There are more than 30 different types of neural networks currently being used in research and applications [68]. 22 types of common ones are listed below:

- i. **ADALINE (Adaptive Linear Neural Element).**
- ii. **ART (Adaptive Resonant Theory).**
- iii. **AM (Associative Memories).**
- iv. **BAM (Bi-Directional Associative Memory).**
- v. **BOLTZMANN MACHINE.**
- vi. **BSB (Brain-State-In-A-Box).**
- vii. **CCN (Cascade Correlation Network).**
- viii. **CAUCHY MACHINE.**
- ix. **CPN (Counter Propagation Network).**
- x. **GRNN (Generalized Regression Neural Network).**
- xi. **HAMMING MODEL.**
- xii. **HOPFIELD MODEL.**
- xiii. **LVQ (Learning Vector Quantization).**
- xiv. **MADALINE (Many Adalne).**
- xv. **MLFF WITH BBP (Multi-Layer Feed-Forward Back-Propagation).**
- xvi. **NEOCOGNITRON.**
- xvii. **NLNs (Neural Logis Networks).**
- xviii. **PERCEPTRON.**
- xix. **PNN (Probabilistic Neural Network).**
- xx. **RBF (Radial Basis Function).**
- xxi. **RNN (Recurrent Neural Network).**
- xxii. **SOFM (Self-Organizing Feature Map).**

3.4.2 ANN Learning Algorithms

The application of an ANN is to approximate a specific function which is attained after a correct selection of the connection weights. This process is called the training or learning of the ANN. The correct selection is made by adjusting the weight in order

to have an NN predicated output “closer” to the actual system outputs. The adjustment of the weights is performed by the training algorithm that tries to minimize the error indicator between the NN predicated outputs and actual system outputs [69]. The classification by learning strategy includes the following broad classes:

- i. Supervised training: is a process of adjusting the weights in a neural net using a learning algorithm; the desired output for each set of training input vectors is presented to the net. Excessive iteration through the training data is required.
- ii. Unsupervised training: can be accomplished by modifying the weights of a neural net without specifying the desired output for any input of patterns. It is used in self-organizing neural nets for clustering data, extracting principal components or curve fitting.
- iii. Reinforced training: when a pattern actually belongs to any class but is not selected, then the weight vector should be reinforced by adding to it a proportion of that training pattern.

For each of these categories an ANN will fall into one of four sub-categories [70]:

- i. Error correction: This includes algorithms such as perceptron learning, the Delta rule and Back-propagation.
- ii. Hebbian learning: includes variants of hebbian learning.
- iii. Competitive learning: it can be considered as unsupervised learning in which a competitive neural net (or subnet) adjusts its weight after the winning node has been chosen.
- iv. Stochastic learning: is a probabilistic learning algorithm, which includes Boltzmann Machine and Cauchy Machine.

3.4.3 ANN Performance Indicator

The total performance error of the network with a particular set of weights can be computed by comparing the actual and the desired output patterns for every case.

The most commonly used error metric is the Root-Mean-Square-Error, RMSE, defined as [71]:

$$(\text{RMSE})_{ps} = \sqrt{\sum_i^n \frac{(d_i - o_i)^2}{n}} \quad (3.1)$$

Where,

$i = 1, 2, 3, \dots, n$

RMSE: is the root-mean-square error for training data set p .

ps : is the number of training data sets.

d_i and o_i : are the desired and predicated outputs of node i .

3.4.4 The Application Type Categories of ANNs Models

The ANNs demonstrate a capability for a very broad spectrum of applications that includes but is not exclusive to: image classification, speech synthesis, sonar return classifications, knowledge base sensing, robotics processing, industrial inspection and scientific exploration. Areas of applications for neural nets can be grouped into six groups: associative memories, classification, pattern recognition, prediction, optimization and general mapping. The taxonomy of ANNs by application is illustrated in Figure (3.5) [70].

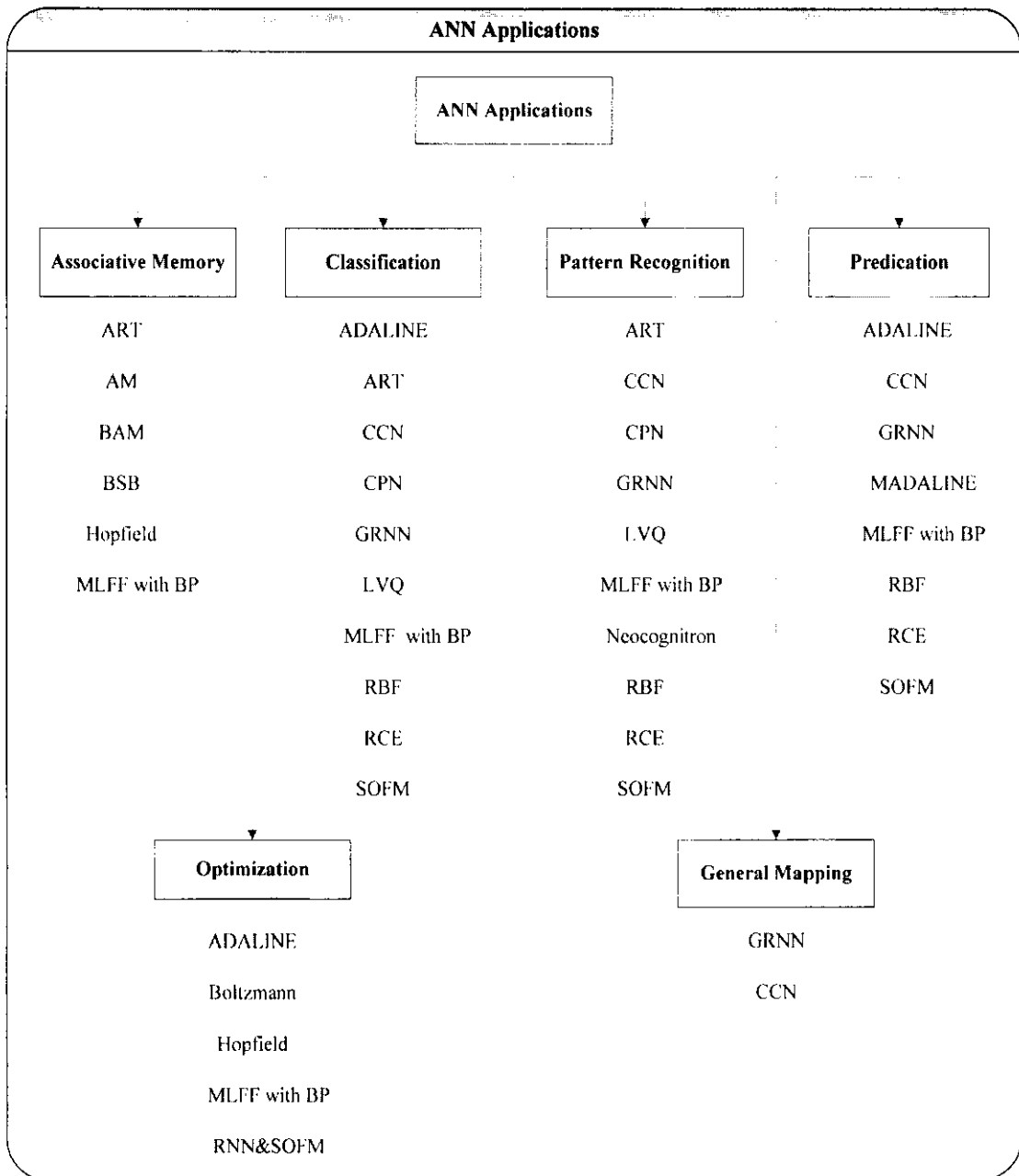


Figure 3.5 Categories of ANN steps by application type [70]

3.4.5 Neural Network Architectures

ANNs can be represented as weighted directed graphs in which artificial neurons are nodes and direct edges (with weights) are connections between neuron inputs.

Based on the connection pattern (architecture), ANNs can be grouped into three categories:

- i. **Feed-Back**, feed-back network are the type of neural networks that contain feedback connections, another name for them is “**recurrent**” nets [72]. Recurrent networks recalculate previous outputs back to inputs hence, their outputs are determined both by their current inputs and their previous outputs. For this reason recurrent networks can exhibit similarities to short-term memory in humans in that the state of the network outputs depends in part upon their previous inputs. The hopfield model is the simplest and most widely used feedback neural architecture; another example of a feedback network is the boltzmann machine which is close to the hopfield model architecture.
- ii. **Feed-Forward**, which is also called “Non-Recurrent” is a type of neural network that has no feedback connection that connects through weights expended from the output of a layer to the input of the same or previous layer.
- iii. **Self-Organization**, a self-forward network such as kohonen feature map, monitors itself and corrects errors without receiving any additional information.

3.5 Genetic Algorithms (GAs)

GAs are optimization tools. GAs are inspired by the mechanism of natural selection where stronger individuals are likely the winner in a competing environment.

GAs have been applied with success to domains such as: optimization, automatic programming, machine learning, economics, immune systems, ecology, population genetics, evolution and learning, and in social systems [73].

3.5.1 GA Components

A GA has three major components [73]:

i. GA Component One:

The first GA component represents the creation of an *initial population*. The created population consists of a number of randomly selected individuals (m) that shape the first GA generation.

ii. GA Component Two:

The second GA component represents the evaluation process for each one of the inputs (m) based on an objective function which is called *fitness function*.

iii. GA Component Three:

The third GA component represents the formulation of the Next GA generation based on the fitness value of the previous one. The evaluation process of generation N (component 2) and the production of generation N+1 (component 3) are repeated until a performance criterion is met.

3.5.2 GA System Operations

The GA breeding process is defined as the creation of offspring based on the fitness function value of the previous individuals of the generation. The main GA breeding procedure includes three basic genetic operations [74]:

i. Reproduction: it begins with a probabilistical selection process that selects one of the fittest individuals of generation N and then, passes it to generation N+1 without applying any changes to it.

ii. Crossover: it begins with a probabilistical selection process that selects two of the fittest individuals of generation N; followed by a randomly chosen characteristic process in which a random way to choose a number of the fittest individuals characteristics and then exchanges the chosen characteristics in a

way that the first individual would be captured by the second and vice versa. Finally, two new offspring are created which belong to the new generation.

- iii. Mutation: it begins with a probabilistical selection process that selects one of the fittest individuals of generation N and then in a random way, changes a number of its characteristics. The new offspring that results out of this transformation is passed to the next generation.

The definition of *genes* is adopted for the individual characteristics. Upon the biological paradigm the set off all genes of an individual form its *chromosome* and each generation can be described by a set of m *chromosomes*. Figure (3.6) describes the main GA system operation [75].

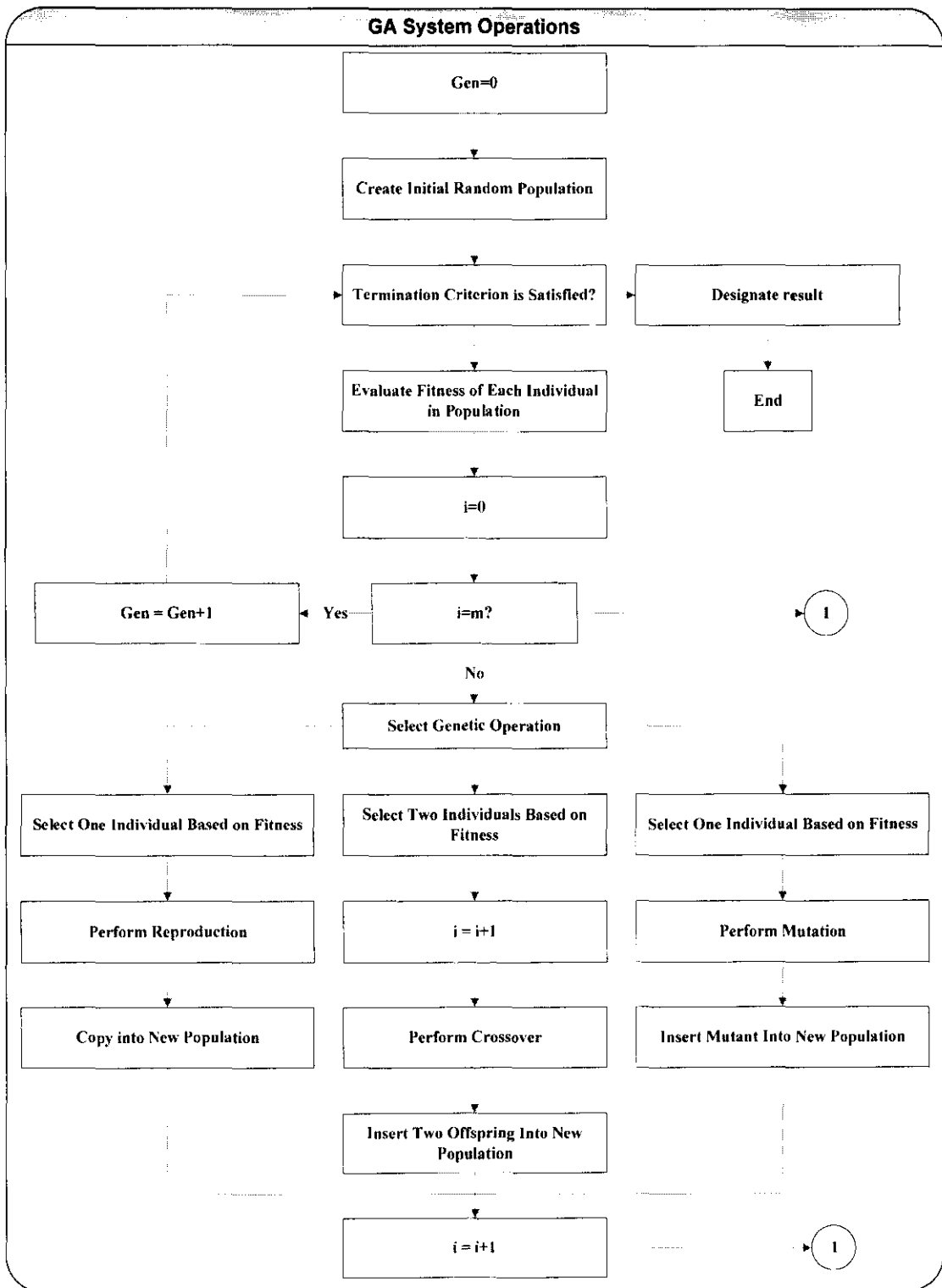


Figure 3.6 GA System Operations [75]

Based on the fitness function, the selection of an individual, i.e. two in the case of crossover, is implemented by a scheme known as *roulette wheel* [76-78].

Using the GAs fact “the higher fitness value of an individual, the better the individual is”, A *roulette wheel* is creating by the following steps:

- i. Place all population members in a specific sequence.
- ii. Sum the fitness of all population members F_{sum} .
- iii. Generate a random number (r) between zero and F_{sum} .
- iv. Return the first population members whose fitness value added to the fitness of the preceding population members, is greater than or equal to (r).

The GA termination criterion is a crucial issue. It can be either a number of generations or the amount of variation of individuals between two successive generations, or a pre-defined value of fitness [76, 77, 79].

3.6 Summary

Two artificial intelligent monitoring systems specialized in boiler trips were proposed. Feed forward ANN methodology was described in details as a major adopted computational intelligent tool in the proposed systems. The first intelligent monitoring system (IMS-I) represented the use of pure ANN for boiler trip detection. The second intelligent monitoring system (IMS-II) presented the use of GA and ANN as a hybrid intelligent system.

CHAPTER 4

DATA ACQUISITION AND PREPARATION

4.1 Introduction

Plant data preparation is a crucial issue and it has an immense impact on the success of the IMSs dealing with complex plant data. The quality of the prepared data to be used as input to the IMS may strongly influence the system performance.

In this chapter, the procedure of the raw plant data processing to be ready for IMS training and validation is presented. The structure of this chapter is based on the data processing sequence shown in Figure (4.1). The first part of this chapter describes an MNJ thermal power plant as the data source, specifically the boiler unit and its trips. The second part presents the manipulation of the raw data until it is ready for IMS training and validation. The various processing methods are discussed in detail.

4.2 Thermal Power Plant (TPP)

A major portion of the demand for electric power is met by TPPs. These plants can be operated safely, efficiently and economically. The TPP can be considered to have two major divisions, namely, the boiler unit and the turbine unit. The boiler unit converts the chemical energy of the fuel into heat energy, and the turbine unit converts the heat energy in the steam into electricity.

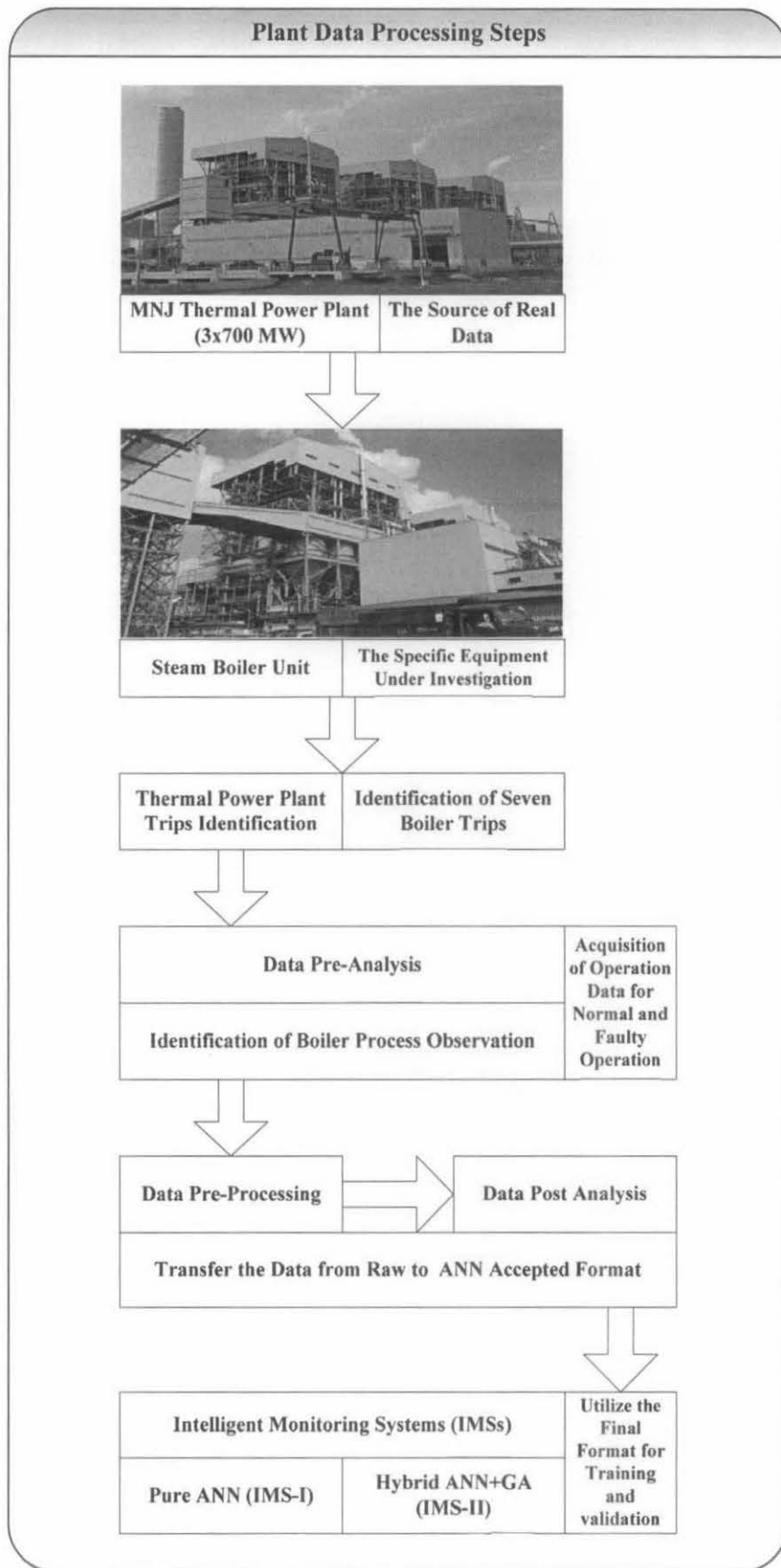


Figure 4.1 Data processing sequences adopted in the present work

In thermal power plants, fossil fuels such as coal, crude oil/furnace oil and natural gas are commonly used. The selection of the fuel is decided by availability and economic considerations [80].

In this study, the JANAMANJUNG coal-fired power plant (MNJTPP) has been selected as a real data source for the proposed intelligent monitoring systems.

Within the scope of this work, the intelligent monitoring systems were implemented in the boiler components, where the working fluid is circulated, which are the drum, superheater, boiler feed pump and water tube. The main reason behind choosing those components was the frequent occurrence of trips within the specific period of the plant operation time.

4.3 MNJTPP Boiler Description and Characteristics

MNJTPP (3*700MW) boilers are of a sub-critical pressure, single reheat and controlled circulation type. Each boiler is fired with pulverized coal to produce steam for the continuous generation of 700 MW(e).

The combustion circuit consists of a single furnace, with direct tangential firing and balanced draught. The coal milling plant consists of 7 vertical bowl mills. The maximum heat input that can be achieved when firing fuel oil is 40% of the Boiler Maximum Continuous Rate (BMCR). The boiler has been designed to comply with the Malaysian environmental requirements. NO_x control is achieved with a low NO_x combustion burner system including Over Fire Air (OFA) ports. An Electro-Static Precipitator (ESP) removes dust in the flue gas at the boiler outlet and Flue Gas Desulphurisation (FGD) plant, scrubs the flue gas and controls the SO₂ emission level at the stack.

The firing equipment consists of: four elevations; (16) of, remote controlled fuel oil burners equipped with high energy ignitrons. They are used to start-up the boiler and to support combustion of the pulverized coal at low firing rates. The capacity of oil burners is 40% of the BMCR. Seven elevations; (28) of, coal burners located just above or below a fuel oil burner. The capacity of coal burners is 100% BMCR when

firing coal within the design range. All the burners are located in the furnace corners (tangential firing).

The major auxiliary equipment consists of: three boiler circulating pumps, two forced draft fans, two primary air fans and two induced draft fans. All these fans are centrifugal fans with control vanes at the inlet to adjust the flow or the pressure. There are also two steam air preheaters, one piece of sootblowing equipment, two electrostatic precipitators, one coal milling plant consisting of 7 vertical bowl mills, type BCP2820 and one wet FGD. The schematic diagram of the steam boiler is shown in Figure (4.2).

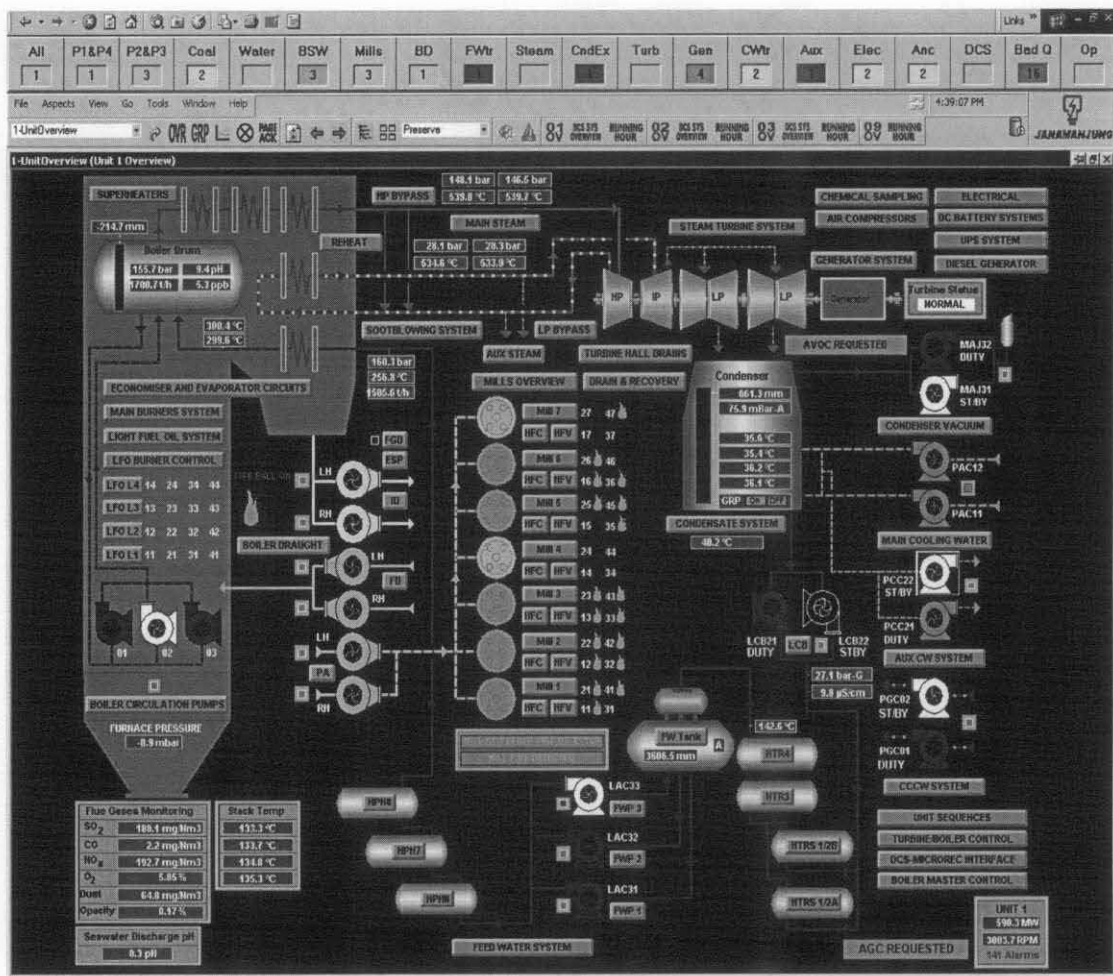


Figure 4.2 Schematic diagram of MNJ TPP Boiler²

² From the operation and maintenance instruction manual for the MNJTPP

4.4 Boiler Trips Identification

Boiler trips are the leading cause of forced outages in a thermal power plant boiler (TPPB). To get a TPPB back on line and reduce or eliminate future forced outages due to the trip, it is extremely important to determine and correct the root cause.

The experience of designing, fabricating, building and servicing of the boilers shows that the most effective method of determining the root cause of the trip is by a comprehensive assessment.

The full-scope investigation with the plant operator experience of all boiler operation aspects leading to the trip should be considered in order to fully understand the root cause and to isolate it. MNJTPP trips can be classified into four types based on the part of the boiler most frequently tripped as:

4.4.1 Boiler Tube Wall Trip

Water tube boilers were proposed to permit increases in boiler pressure and capacity with reasonable metal stress. In the water tube boiler, water flows through the tubes and flue gases flow outside them, putting the pressure in the tubes and the relatively small diameter drums, which are capable of withstanding the extreme pressures of the modern steam generator [81].

Boiler tube leaks are the single biggest cause of loss of thermal power plant availability. Detecting leaks by measuring the make up water or walking the boiler is very insensitive and usually gives information about the existence of leak only when that tube leak is already large and creating serious secondary damage. A boiler water wall leak can be caused by one of the following reasons: caustic attack, oxygen pitting, hydrogen damage, acid attack, Stress Corrosion Cracking (SCC), waterside corrosion fatigue, superheater fireside ash corrosion, water wall fireside corrosion, fireside corrosion fatigue, short-term overheating, long-term overheating, graphitization, Dissimilar Metal Weld (DMW) Failure, erosion, and mechanical fatigue. The benefits of the early detection of boiler water wall tube leaks are: to increase operating profit, to increase personal safety, to increase availability and tube life, avoid

unscheduled outages, reduce of outages, repair costs and secondary damage, and reduction of financial penalties and insurance costs [29].

4.4.2 Superheater Trips

The superheater consists of a Low Temperature Superheater (L.T.S), an Intermediate Temperature Superheater (I.T.S) and a High Temperature Superheater (H.T.S). The I.T.S is a horizontal exchanger located in the rear pass of the boiler. The L.T.S and H.T.S are pendant exchangers located above the furnace. The dry saturated steam flows from the drum via the furnace roof tubes, and the rear passwalls to the LTS inlet header for one part of the total flow or directly from the drum to the LTS for the other part. The LTS is a vertical exchanger consisting of 3 elements located at the furnace top against the front, right and of the left water walls. After crossing the LTS, the steam flows via the interconnecting pipes to the ITS. The first stage of desuperheaters is installed on the interconnection pipes. The first spray-water injection controls a differential steam temperature between the LTS outlet and the ITS inlet.

The outlet headers of the ITS are linked to the inlet header of the HTS. On these interconnection pipes, a second stage of desuperheaters is installed. The second spray water injection controls the steam at the HTS outlet. After the outlet header of the HTS, steam enters the turbine through the main steam piping.

The superheated steam temperature is adjusted by spray water injections for the LTS and the HTS. The LTS, HTS and the main steam lines are completely drained. Insufficient draining time may result in a trip due to equipment damage. LTS and HTS trips can be caused either by the in service spray water injection when the steam flow is below 20% of the maximum continuous rate, as it is difficult to obtain a regular spray water flow through the control valves slightly opened or that the spray water at low steam flow is not completely evaporated and it can be the source of considerable damage leading to a unit trip.

4.4.3 Boiler Drum Trip

The purpose of the boiler drum is to ensure a good separation of steam and water and to feed the superheaters with a perfectly dried steam at any boiler load. The boiler drum is fitted with the necessary instrumentation: three level transmitters at each drum end, one local level gauge at each drum end, one electric level transmitter (electrode type) at each drum end, three pressure transmitters on the upper part of the drum for pressure monitoring and level compensation, and eight pairs of metal thermocouples four on drum water side (lower part) and four on the steam drum side (upper part) [29, 81].

These measures are used to monitor the differential temperature to assure that it stays under allowable limits of thermal stress. They are also used for fatigue monitoring. Four simple metal thermocouples, two at each drum end, one on the lower water part, one on the upper steam part for drum end absolute metal temperature monitoring, and one drum steam pressure local regulation manometer.

The drum is fitted with four regulation relief safety valves (4 items) and their silencers. The drum is also equipped with tapings for: water sampling, steam sampling, continuous blow down, vents, nitrogen injection points and exhaust to pressure safety valves.

The steam boiler drum water level should be maintained for all plant operation time as a critically important issue. Too low a level for the boiler drum can lead to boiler water tube damage. On the other hand, too high a water level for the boiler drum can result in damage in the steam separator or steam turbine from water carry over.

The main reasons behind a boiler drum level fluctuating are: the feed water circuits problem which may be caused by the trip of the three circulating pumps, a problem on the drum level start-up feed water control, and the water level indicator.

4.4.4 Boiler Circulating Pump Trips

In a controlled circulation boiler, circulating pumps placed in the downcomer circuits insure a proper circulation of water through the water walls. The feed water enters the unit through the economiser and is mixed in the drum with the boiler water/steam mixture from the risers. The water flows from the drum through the down comers to the circulation pumps suction manifold [29].

The economiser re-circulation line and the water-cooled spacer tubes are also supplied from the lower wall headers. The water rises through furnace wall tubes where heat from the combustion is absorbed.

The boiling process takes place and the resulting mixture of water and steam is collected in the water wall outlet headers. The mixture is discharged into the boiler drum through the riser tubes. The drum internal equipment separates the steam and the water. The steam flows to the superheater circuit and water returns to the lower part of the drum.

The boiler circulating pumps must be in good running condition and the alarm devices and interlocks, provided for protection of both the boiler and pumps, should be tested before the unit start up. The boiler feed pumps are tripped either due to lose suction, as indicated by a very low differential pressure and unstable motor current, or pumps not properly filled with water due to a problem with the condensate pumps.

4.5 Data Preparation Framework

The present work could be divided into four execution phases as shown in Figure (4.3). The integrated data preparation scheme represents the first phase among the four identified phases to execute the entire study.

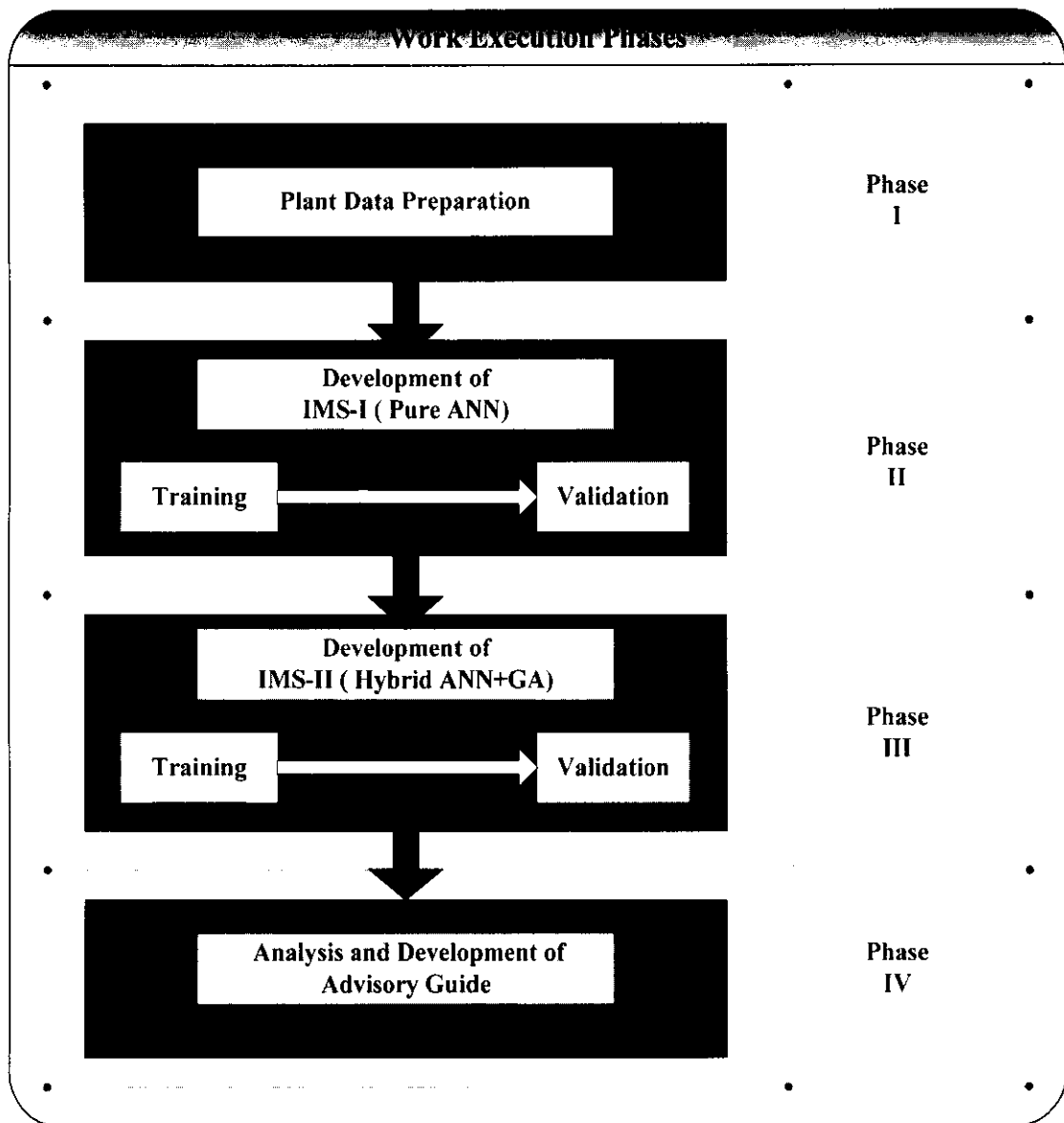


Figure 4.3 Execution phases

This phase is sub-divided into three stages as shown in Figure (4.4). Each stage consists of mathematical and statistical processes, each process represents a step.

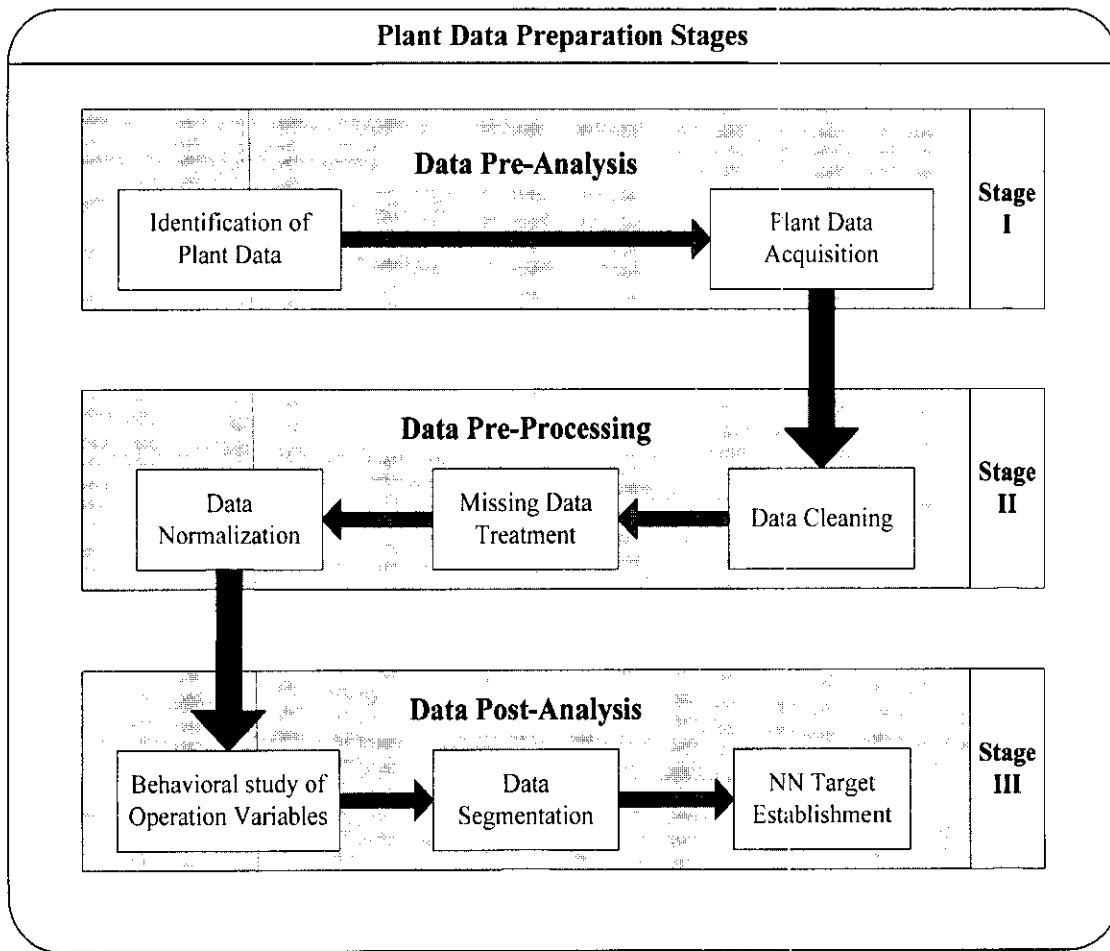


Figure 4.4 Plant data preparation framework

4.5.1 Data Pre-Analysis Stage

The data pre-analysis stage consists of two main steps, in which boiler operational variables were identified and collected for each specific boiler trip.

4.5.1.1 Plant Data Identification Step

Initially, 1800 observations (actuator and sensor signals) are identified as the boiler process observations through the on-line plant control system (ABB). The identified observations are passed through a reduction process which involves three stages as shown in Figure (4.5). Since the work scope focuses on the diagnosis of working fluid components in the boiler, the number of the observations is reduced from 1800 to 177 by excluding the observations of the furnace items, the induce fans and mills .

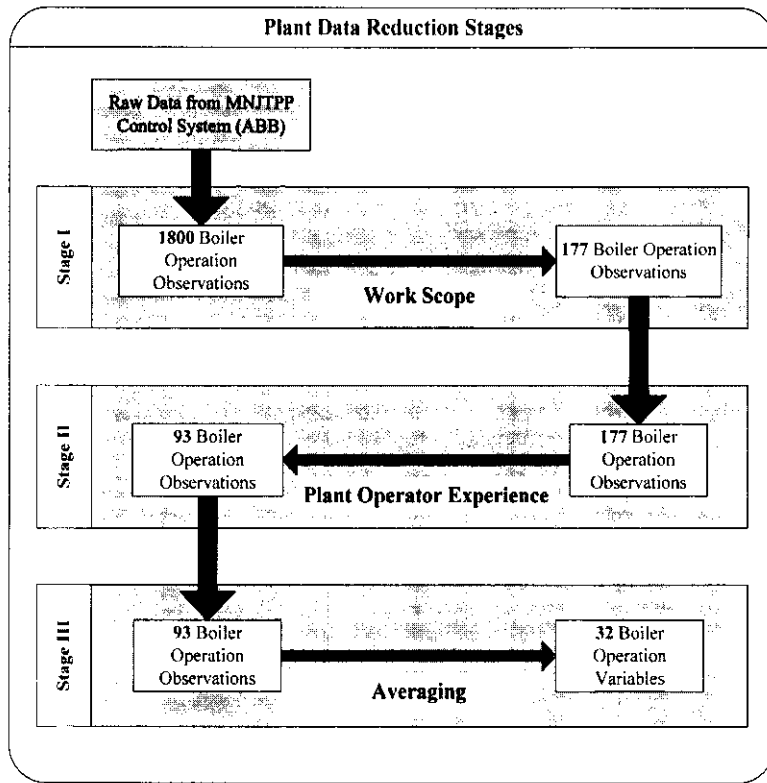


Figure 4.5 Plant data reduction stages of the observations to variables

The new sets of observations represent the relevant measurement values of the operational variables related to the economizers, drums, headers, circulating water pumps, risers and superheaters. The resulted 177 observations from the first stage are reduced again to 93 based on the plant operator experience.

The eighty-four neglected observations were considered as non-effective factors on the trip scenarios of the boiler. Many observations were measured by multi sensors. Finally, thirty-two influential operation boiler variables, as listed in Table (4.1) formed the final set by adopting the average criteria of various observations. The “criteria” column in Table (4.1) represents the average number of averaged signals acquired for each variable. E.g.; for a feed water valve station, V_{12} , there are eight actuators to measure and send signals of the same variable, hence:

$$V_{12} = \frac{1}{8} \sum_{i=1}^{i=8} V_{12,i} \quad (4.1)$$

Table 4.1 Influential boiler operation variables

Code	Variables	Unit	Criteria
V ₁	Total combined Steam flow	t/h	$= 1/1 \sum_{i=1}^1 v_{1i}$
V ₂	Feed water flow	t/h	$= 1/1 \sum_{i=1}^1 v_{2i}$
V ₃	Boiler drum pressure	Barg	$= 1/4 \sum_{i=1}^4 v_{3i}$
V ₄	Superheater steam pressure	Barg	$= 1/1 \sum_{i=1}^1 v_{4i}$
V ₅	Superheater steam temperature	°C	$= 1/1 \sum_{i=1}^1 v_{5i}$
V ₆	High temperature Re-heater outlet temperature	°C	$= 1/4 \sum_{i=1}^4 v_{6i}$
V ₇	High temperature superheater exchange metal temperature	°C	$= 1/4 \sum_{i=1}^4 v_{7i}$
V ₈	Intermediate temperature (A) superheater exchange metal temperature	°C	$= 1/4 \sum_{i=1}^4 v_{8i}$
V ₉	High temperature superheater inlet header metal temperature	°C	$= 1/4 \sum_{i=1}^4 v_{9i}$
V ₁₀	Final superheater outlet temperature	°C	$= 1/6 \sum_{i=1}^6 v_{10i}$
V ₁₁	Superheater steam pressure transmitter (control)	bar	$= 1/7 \sum_{i=1}^7 v_{11i}$
V ₁₂	Feed water valve station	t/h	$= 1/8 \sum_{i=1}^8 v_{12i}$
V ₁₃	Feed water control valve position	%	$= 1/4 \sum_{i=1}^4 v_{13i}$
V ₁₄	Drum level corrected (control)	mm	$= 1/1 \sum_{i=1}^1 v_{14i}$
V ₁₅	Drum level compensated (from protection)	mm	$= 1/1 \sum_{i=1}^1 v_{15i}$
V ₁₆	Feed water flow transmitter	%	$= 1/1 \sum_{i=1}^1 v_{16i}$
V ₁₇	Boiler circulation pump 1 pressure	bar	$= 1/1 \sum_{i=1}^1 v_{17i}$
V ₁₈	Boiler circulation pump 2 pressure	bar	$= 1/2 \sum_{i=1}^2 v_{18i}$
V ₁₉	Low temperature superheater left wall outlet before superheater dryer	°C	$= 1/4 \sum_{i=1}^4 v_{19i}$
V ₂₀	Low temperature superheater right wall outlet before superheater dryer	°C	$= 1/2 \sum_{i=1}^2 v_{20i}$
V ₂₁	Low temperature superheater left wall after superheater dryer	°C	$= 1/2 \sum_{i=1}^2 v_{21i}$
V ₂₂	Low temperature superheater right wall exchange metal temperature	°C	$= 1/1 \sum_{i=1}^1 v_{22i}$
V ₂₃	Intermediate temperature (B) superheater exchange metal temperature	°C	$= 1/1 \sum_{i=1}^1 v_{23i}$
V ₂₄	Intermediate temperature superheater outlet before superheater dryer	°C	$= 1/1 \sum_{i=1}^1 v_{24i}$
V ₂₅	Intermediate temperature superheater outlet header metal temperature	°C	$= 1/2 \sum_{i=1}^2 v_{25i}$
V ₂₆	High temperature superheater outlet header metal temperature	°C	$= 1/6 \sum_{i=1}^6 v_{26i}$
V ₂₇	High temperature Re-heater outlet steam pressure	bar	$= 1/2 \sum_{i=1}^2 v_{27i}$
V ₂₈	Superheated steam from intermediate temperatures outlet pressure	bar	$= 1/11 \sum_{i=1}^{11} v_{28i}$
V ₂₉	Superheater water injection compensated flow	ton/hr	$= 1/10 \sum_{i=1}^{10} v_{29i}$
V ₃₀	Economizer inlet Pressure	bar	$= 1/6 \sum_{i=1}^6 v_{30i}$
V ₃₁	Economizer inlet temperature	°C	$= 1/1 \sum_{i=1}^1 v_{31i}$
V ₃₂	Economizer outlet temperature	°C	$= 1/1 \sum_{i=1}^1 v_{32i}$

4.5.1.2 Plant Data Acquisition Step

Three different groups of boiler data were captured with different frequency sampling times, named as: Group (A) obtained based on a thirty minute time interval to form boiler data group (A) and group (B) formed with a one minute sampling time based on the outage period for each specified trip. Table (4.2) summarizes the MNJTPP boilers outages. Finally, a one minute sample time was used to form group (C) which consists of a normal boiler operation mode.

Table 4.2 MNJTPP boilers outages

Trip No.	Trip	Unit	Date out	Date in	Duration (Days)
1	Boiler Water Wall Tube Leak	U1	25.04.2008 19:24	30.04.2008 23:30	5.17
2	Low Temperature Superheater	U3	05.06.2008 06:30	05.06.2008 08:26	0.08
3	Boiler Drum Level Low	U3	06.06.2008 12:57	06.06.2008 21:54	0.37
4	Boiler Drum Level Low	U2	20.12.2008 12:17	21.12.2008 01:31	0.55
5	Boiler Feed Pump	U2	30.01.2009 20:48	31.01.2009 02:53	0.25
6	Boiler Drum Level High	U2	05.05.2009 16:23	05.05.2009 20:52	0.19
7	High Temperature Superheater	U1	01.06.2009 00:00	02.06.2009 02:00	1.08

The details of the groups acquisition process is shown in Table (4.3). The selection of the time interval for each trip is decided based on the plant operator experience. The trip data interval is chosen upon the shutdown duration. If the shutdown period is longer than 24 hours, then, the trip data interval is ± 48 hours; while, if the shutdown was less than 24 hours, the trip data interval is ± 24 hours.

The decision was made to consider data group (B) as a source data to generalize the new (IMSs) due to the short sampling interval, which indeed, means more precise training and validation of the pure IMS.

Table 4.3 Plant data acquisition grouping

Groups	Sets	Data Type	Date/ Time		Duration	Sampling Rate
			From	to		
A	U1 set	Normal / Faulty	01.06.2008 8:00:00	31.12.2008 8:00:00	6 Months	Thirty Minutes
	U2 set					
	U3 set					
B	T1/ U1	Faulty	20.04.2008 8:00:00	25.04.2008 19:23:00	5 days	One Minute
	T2/ U3		04.06.2008 8:00:00	05.05.2008 6:29:00	1 day	
	T3/ U3		05.06.2008 8:00:00	06.06.2008 12:56:00	1 day	
	T4/ U2		19.12.2008 8:00:00	20.12.2008 12:16:00	1 day	
	T5/ U2		29.01.2009 8:00:00	30.01.2009 20:47:00	1 day	
	T6/ U2		04.05.2009 8:00:00	05.05.2009 16:22:00	1 day	
	T7/ U1		31.05.2009 8:00:00	01.06.2009 23:59:00	2 days	
C	Set 1	Normal	01.05.2008 8:00:00	31.05.2008 8:00:00	1 Month	One Minute
	Set 2		01.11.2008 8:00:00	30.11.2008 8:00:00	1 Month	
	Set 3		01.07.2009 8:00:00	31.07.2009 8:00:00	1 Month	

4.5.2 Data Pre-Processing Stage

The data pre-processing stage consists of three main steps, in which noisy and non-number data were filtered and normalized between one and zero.

4.5.2.1 Data cleaning Process Step

The data cleaning process dealt with noise values in the information matrix of the data. In practice, the majority of the data pre-processing process takes place before storing the data. It can be considered as a data storehouse [82-84].

Noise represents a random error in the observed values. For the discussed plant, noise can come in a variety of shapes and forms. The common concerns about the noise in data can be listed as follows:

i. Locating Duplicate Records

Assume that a certain identified variable for example feed water flow has 2000 data points and 0.1% of the listed entries have a duplication erroneous listing under the variation of the same name, therefore, 200 extra data points will be processed. And therefore, errors such as these which were considered as data will be moved from an operational environment to a data storehouse facility. Automated graphical tools can be used to help with data cleaning.

ii. Locating Invalid Observation Values

Error detection in categorical data presents a difficulty in large plant datasets. Collected observation values with the zero scores or non-numeric are elected as error candidates.

A numeric or non numeric value for an occurrence such as boiler drum pressure is recorded as a certain error. Such an error often occurs when data is missed and the default value is assigned to fill in for missed items. In order to pass the difficulty of using mean and standard deviation scores testing methods for large datasets like the one discussed, a MATLAB code is devised as a data analysis tool to allow the user to input a valid range of values for numerical data (see Appendix B2-1).

iii. Data Smoothing

Data smoothing represents data cleaning and data transformation processes. Several techniques were used to reduce the number of values for a numeric record. Two well known smoothing techniques were used: rounding and computing mean values. Mean value smoothing is applicable when we wish to use a classifier that does not support numerical data and would like to train coarse information about numerical observation values. In this case, all numerical occurrence values are placed by a corresponding class mean.

Another known data smoothing technique is called outliers removal. Outlier's removal is used to find and possibly remove a typical data point from the dataset by

examining a data point typically representing those data points with the lowest typical scores. It is always useful to identify outliers in data, but it could result in a counterproductive removal of outliers from the database. For this propose a MATLAB Code is written as a removal tool for outliers with a confident level of 95% (see Appendix B2-1).

4.5.2.2 Missing Data Treatment Step

Missing data represents a problem that can be solved in several ways. In common cases, missed observation values are the lost information. The following are applicable options for dealing with missed observation values before the data is prepared for another process.

- i. Discard the records with the missing value: which is most applicable when a small percent of the total number of occurrences contain missing data, which indeed represent lost information.
- ii. Replace real data with missed values with the class mean: in many cases, this is considered a reasonable approach for numerical occurrences. It is generally considered a poor approach to replace numeric missed data with a zero or some arbitrary large or small value.
- iii. Replace real data with missed values with mathematical forecasting methods: the most common mathematical forecasting methods are: extrapolation and interpolation which are most suitable for a limited occurrence of missed values.
- iv. Replace missed data occurrences with the value found within other highly similar instances and fit it with MNJTPP boiler observation missing values.

4.5.2.3 Data Normalization Step

Data transformation can be represented in many forms and it is necessary for different reasons. The most known data transformation technique is data normalization. A common data transformation involves changing numeric values so that they relate to a specified range. Data normalization is important for treating multi-scale data. Non

scaled data could bias or interfere with the training process and lead to an instable operation of the IMS. The IMS performs better with numerical data scaled between 0 and 1. Data normalization is particularly appealing with a distance-based classifier, because by normalizing the occurrences, observations with a wide range of values are less likely to outweigh observations with a less initial range.

Four normalization techniques in common use, include [83]:

- i. Decimal scaling: decimal scaling separates each numerical value to the power of ten. E.g. if the values for an occurrence range between -1000 and 1000, then the range -1 and 1 can be counted by dividing each value by 1000.
- ii. Min-Max normalization: Min-Max is an applicable technique when minimum and maximum values for an occurrence are known. The Min-Max formula is [83]:

$$\text{New value} = \frac{\text{original value} - \text{oldMin}(\text{newMax} - \text{newMin}) + \text{newMin}}{\text{oldMax} - \text{oldMin}} \quad (4.2)$$

Where:

oldMax and oldMin: represent the original maximum and minimum observations values.

newMax and newMin: specify the new maximum and minimum values.

New value: represents the transformation of the original value.

Since the newMax equal is to one and the newMin is equal to zero, the formula simplifies to [83]:

$$\text{New value} = \frac{\text{original value} - \text{oldMin}}{\text{oldMax} - \text{oldMin}} \quad (4.3)$$

- iii. Normalization using Z-Scores: Z-Score normalization converts a value to a standard score by subtracting the observation mean (μ) from the value and dividing by the observation standard deviation (σ). Specifically [83],

$$\text{New value} = \frac{\text{original value} - \mu}{\sigma} \quad (4.4)$$

- iv. Logarithmic normalization: the best b logarithm of a number n is the exponent to b must be raised to equal n. e.g. the base 2 logarithm of 64 is 6 because $2^6 = 64$. Replacing a set of values with their algorithms have an effect on scaling the range of values without loss of information.

4.5.3 Data Post Analysis Stage

The data post analysis stage consists of three main steps, in which data were segmented into two sets for each trip: sub group data (A) and sub group data (B), NN targets were established, the behavior of influencing boiler operation variables were analyzed.

4.5.3.1 Behavioral Study of Boiler Operation Variables Step

The behaviors of the thirty-two boiler operation variables were studied carefully. The mean value for each variable is predicated from data group C classified in Table (4.3). This mean represents the normal operation value with no trip occurrence, i.e. non-faulty data. Then, the behavior of each one of the thirty-two variables is investigated during the seven specified trips in data group B, meaning, during the trip data period. The results are shown in Figures (4.6 through 4.19) for trips T1, T2 ...T7, respectively.

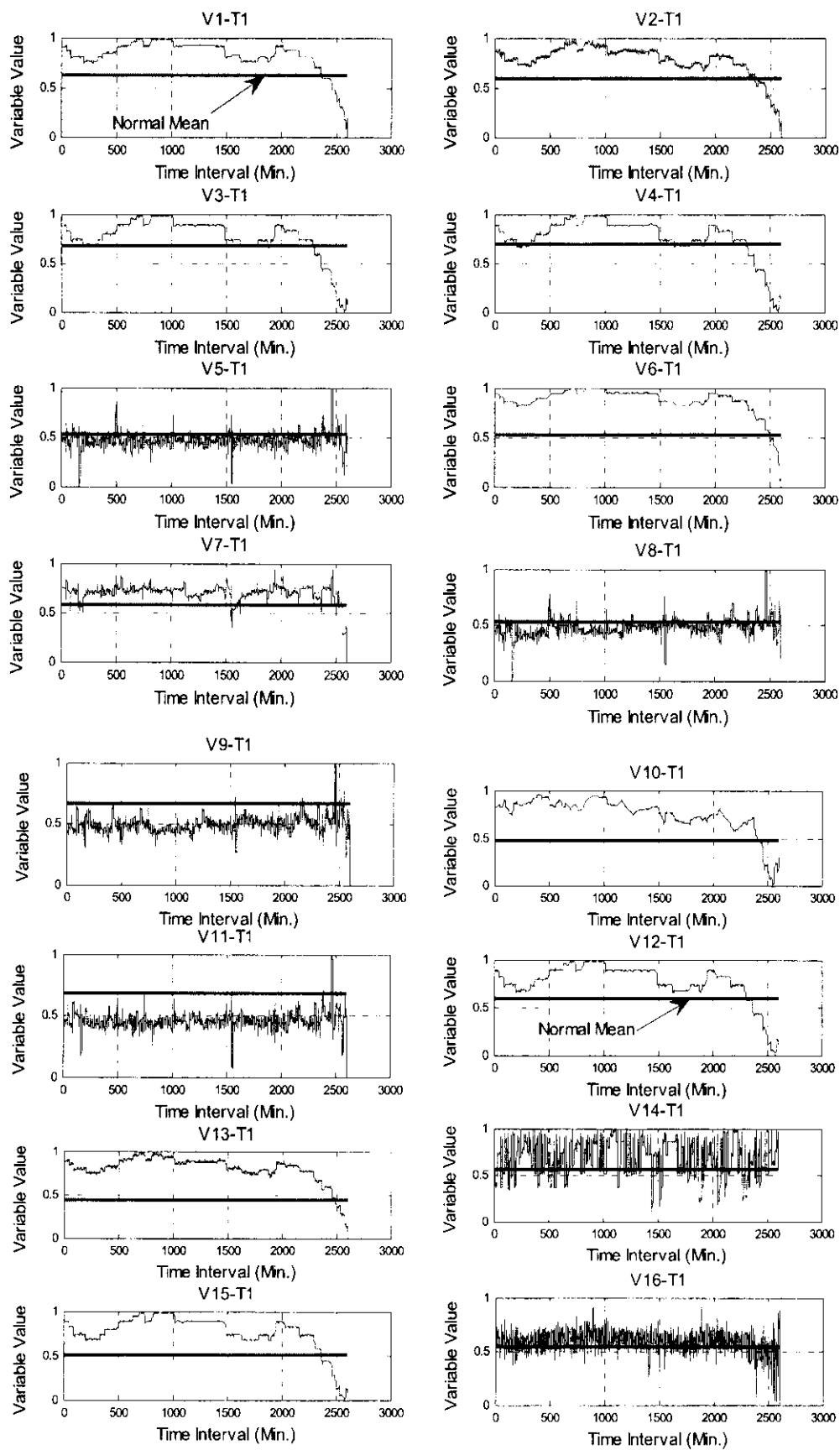


Figure 4.6 Boiler operation variables (from V_1 to V_{16}) behavior for trip 1

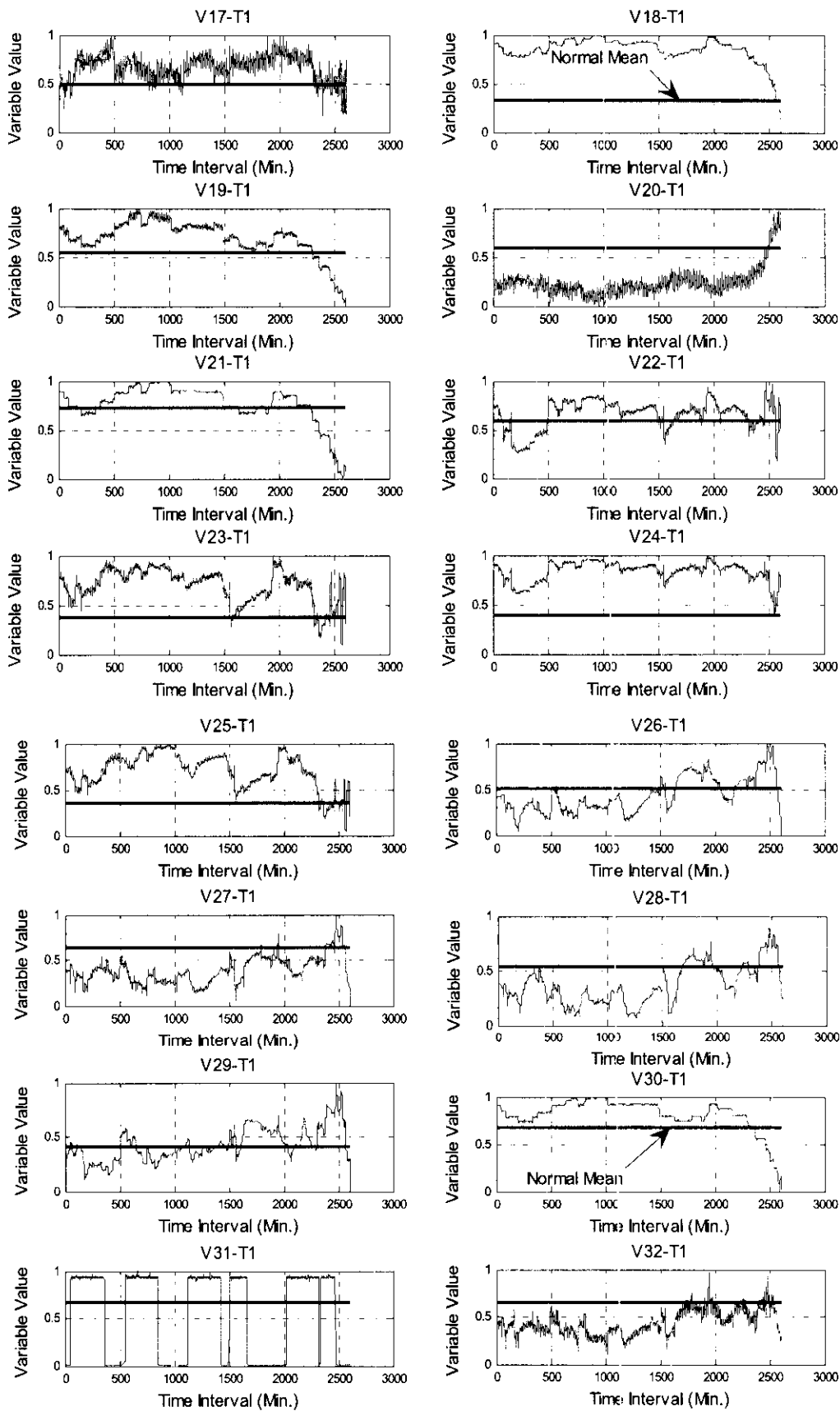


Figure 4.7 Boiler operation variables (from V₁₇ to V₃₂) behavior for trip 1

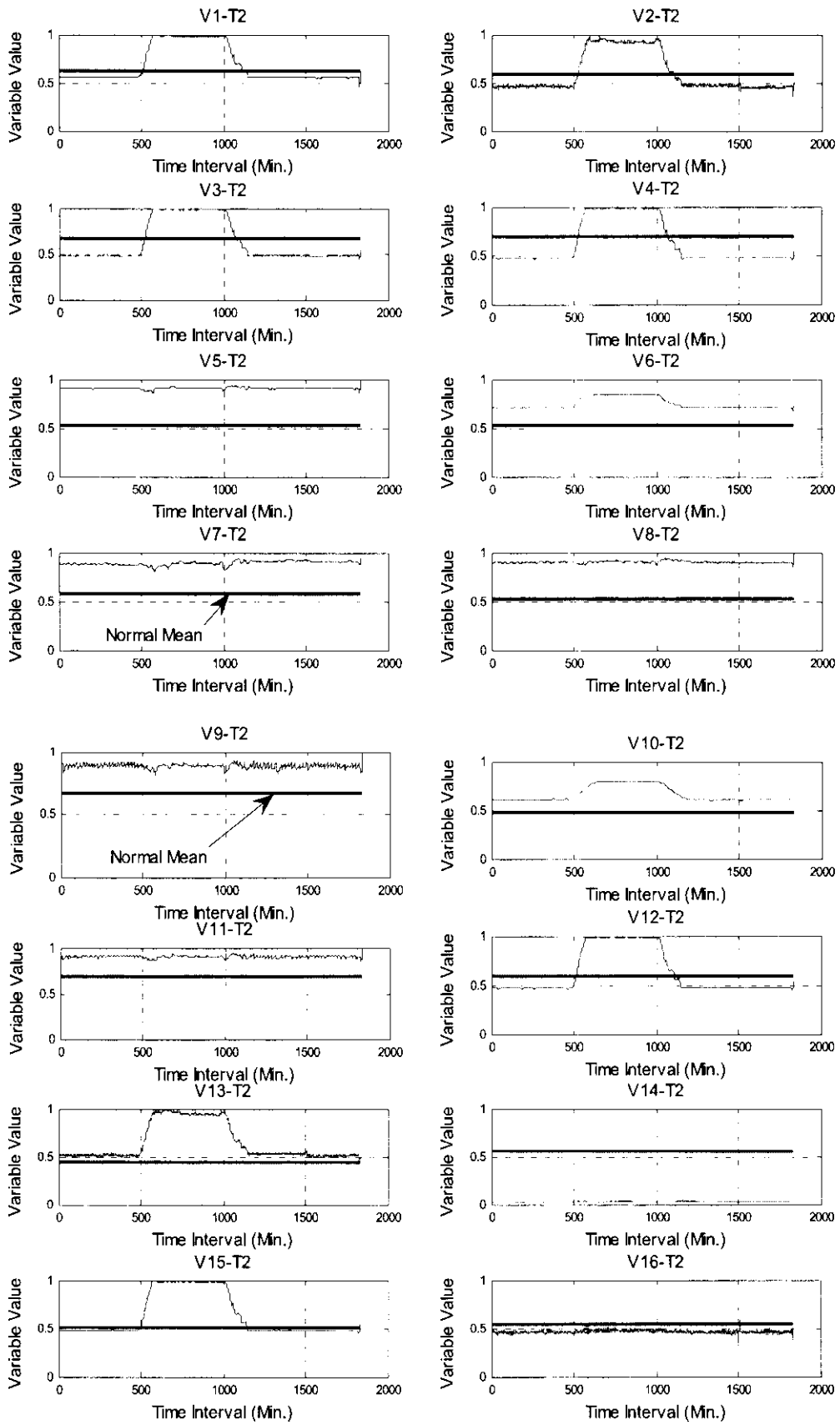


Figure 4.8 Boiler operation variables (from V₁ to V₁₆) behavior for trip 2

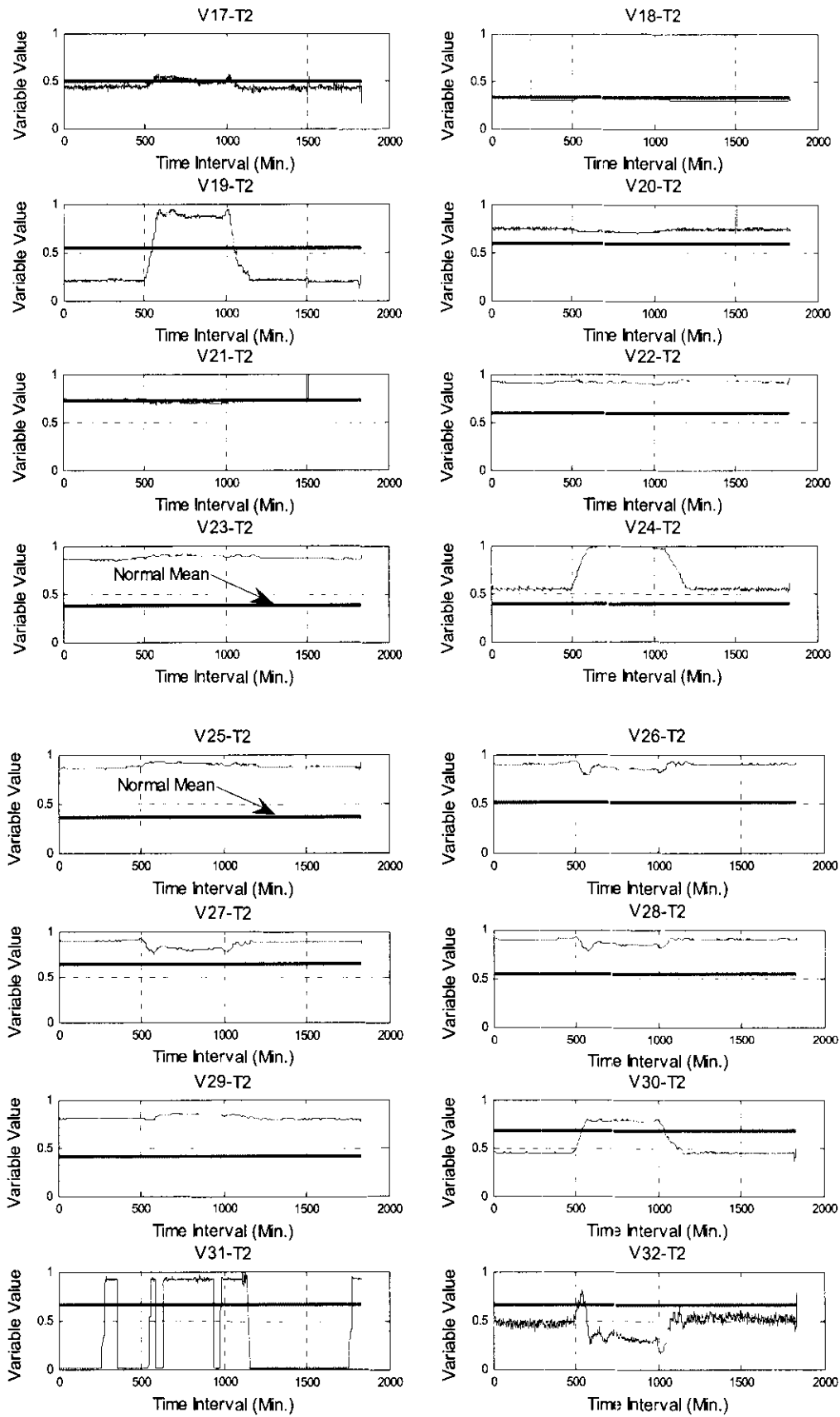


Figure 4.9 Boiler operation variables (from V₁₇ to V₃₂) behavior for trip 2

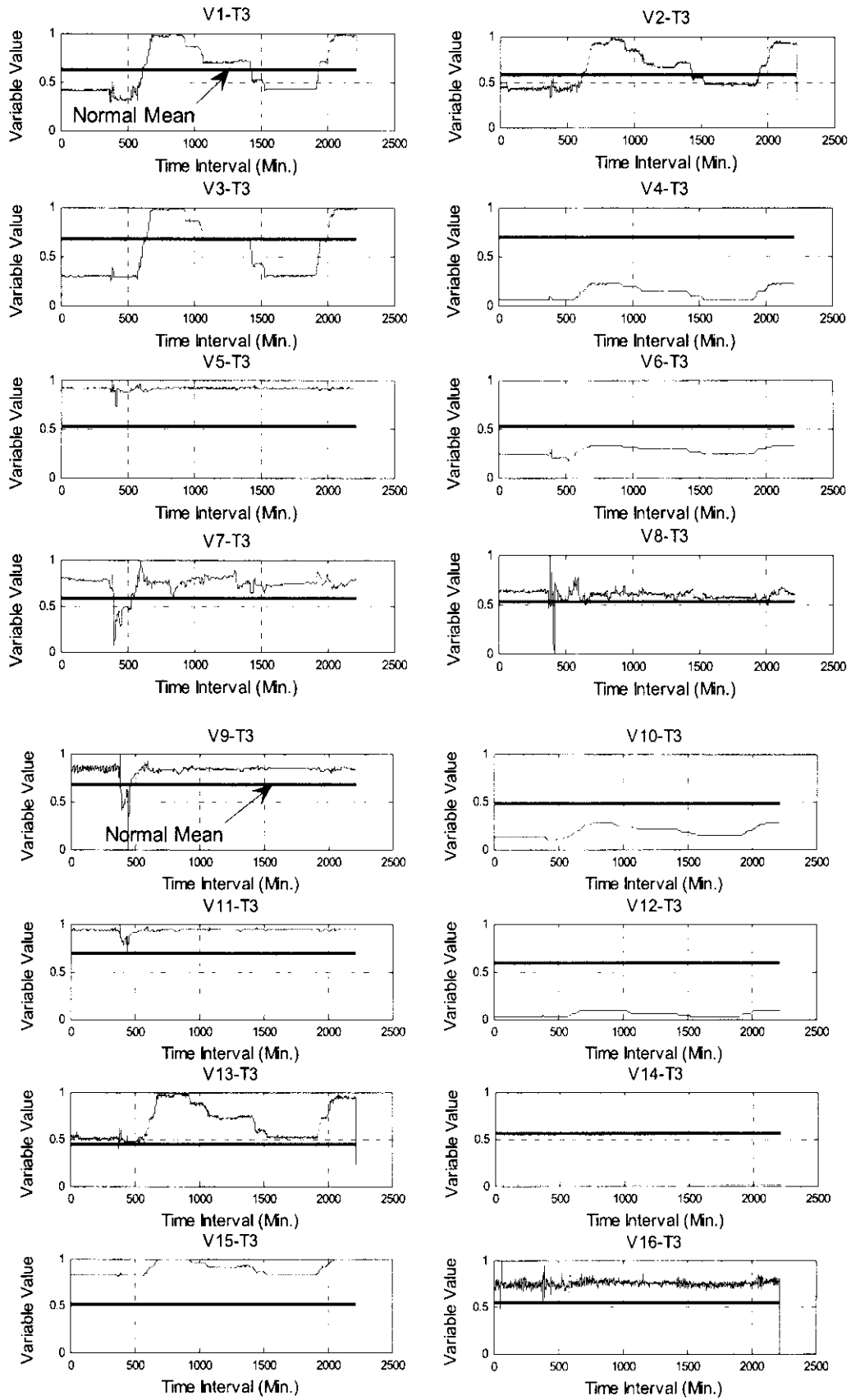


Figure 4.10 Boiler operation variables (from V₁ to V₁₆) behavior for trip 3

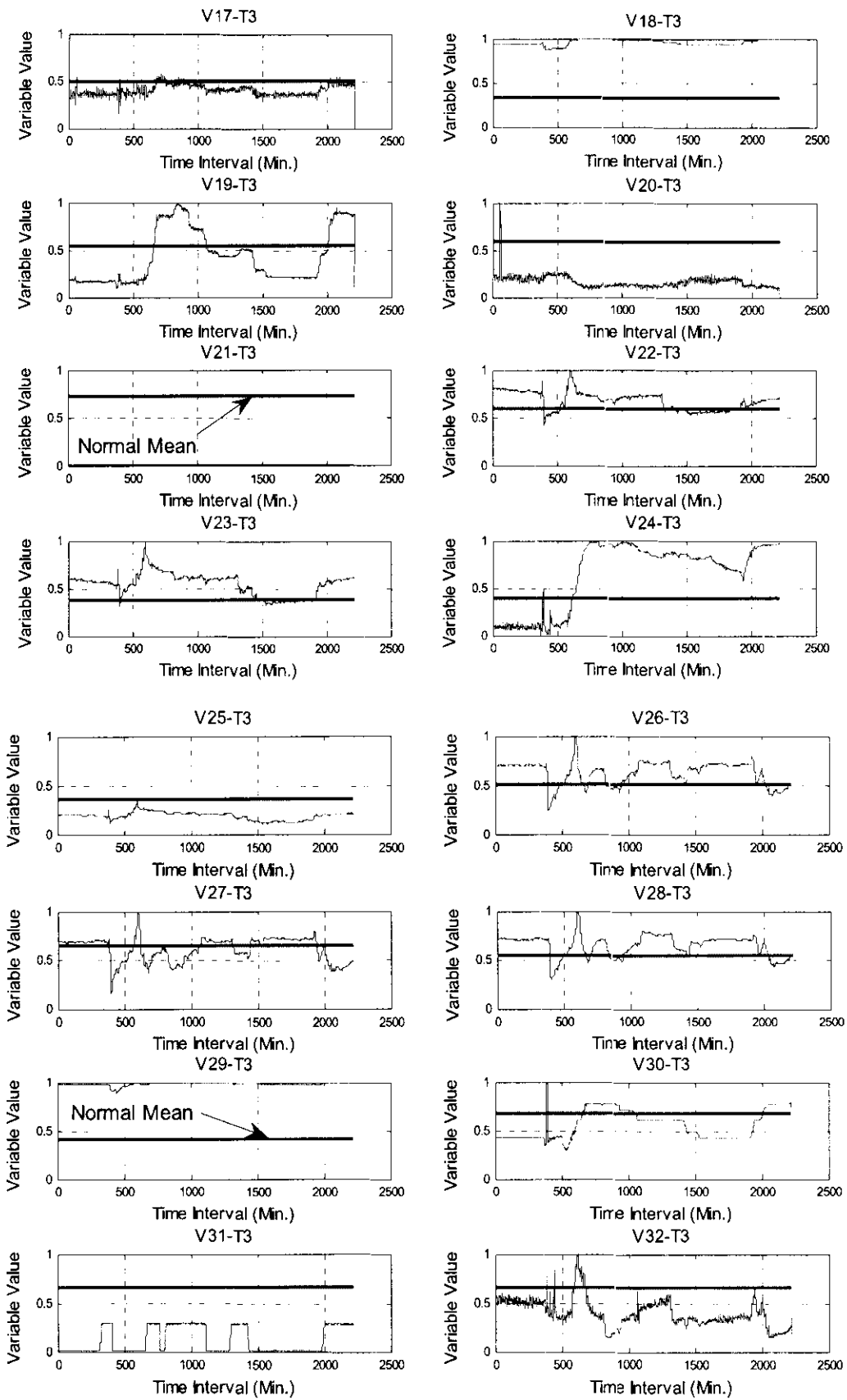


Figure 4.11 Boiler operation variables (from V₁₇ to V₃₂) behavior for trip 3

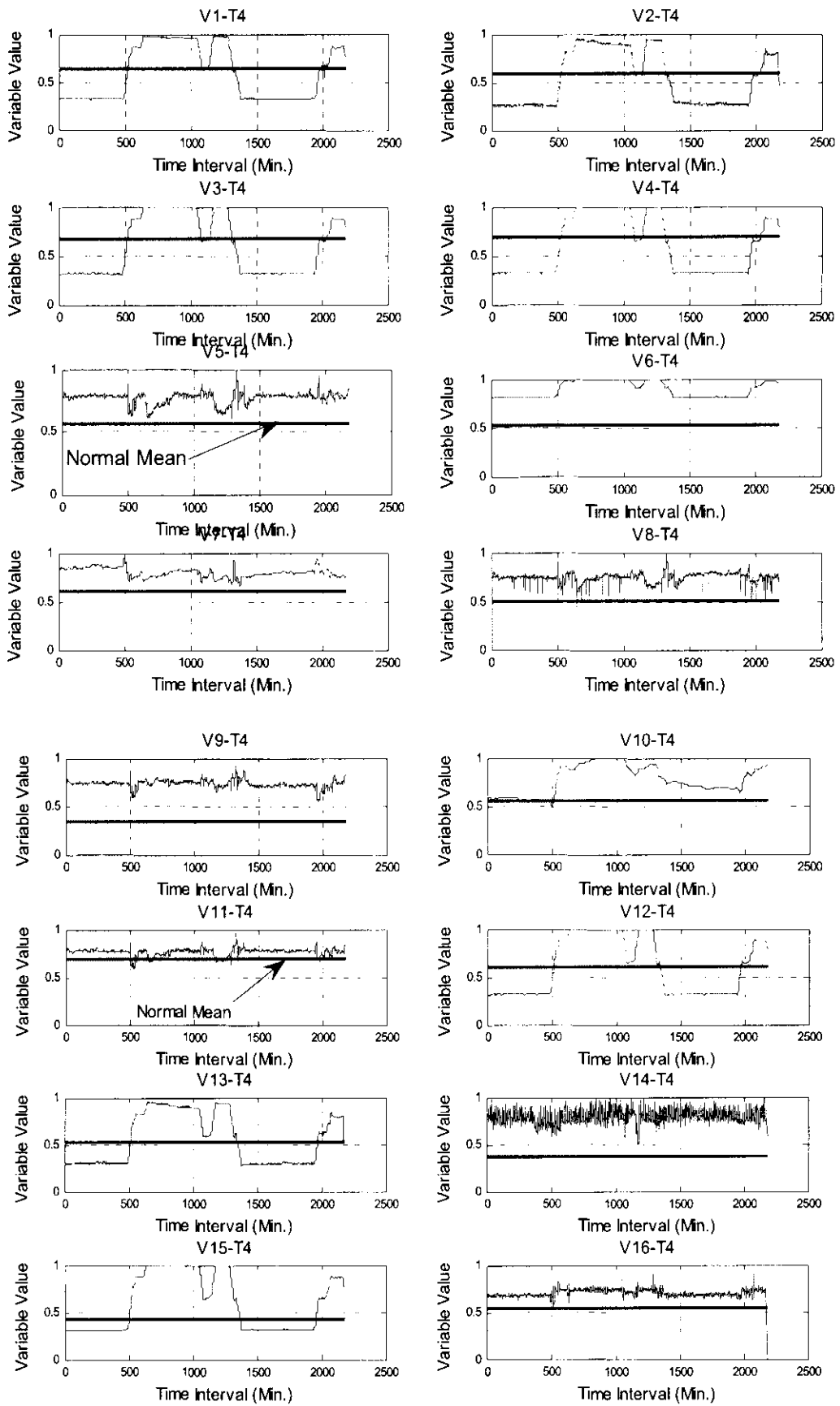


Figure 4.12 Boiler operation variables (from V₁ to V₁₆) behavior for trip 4

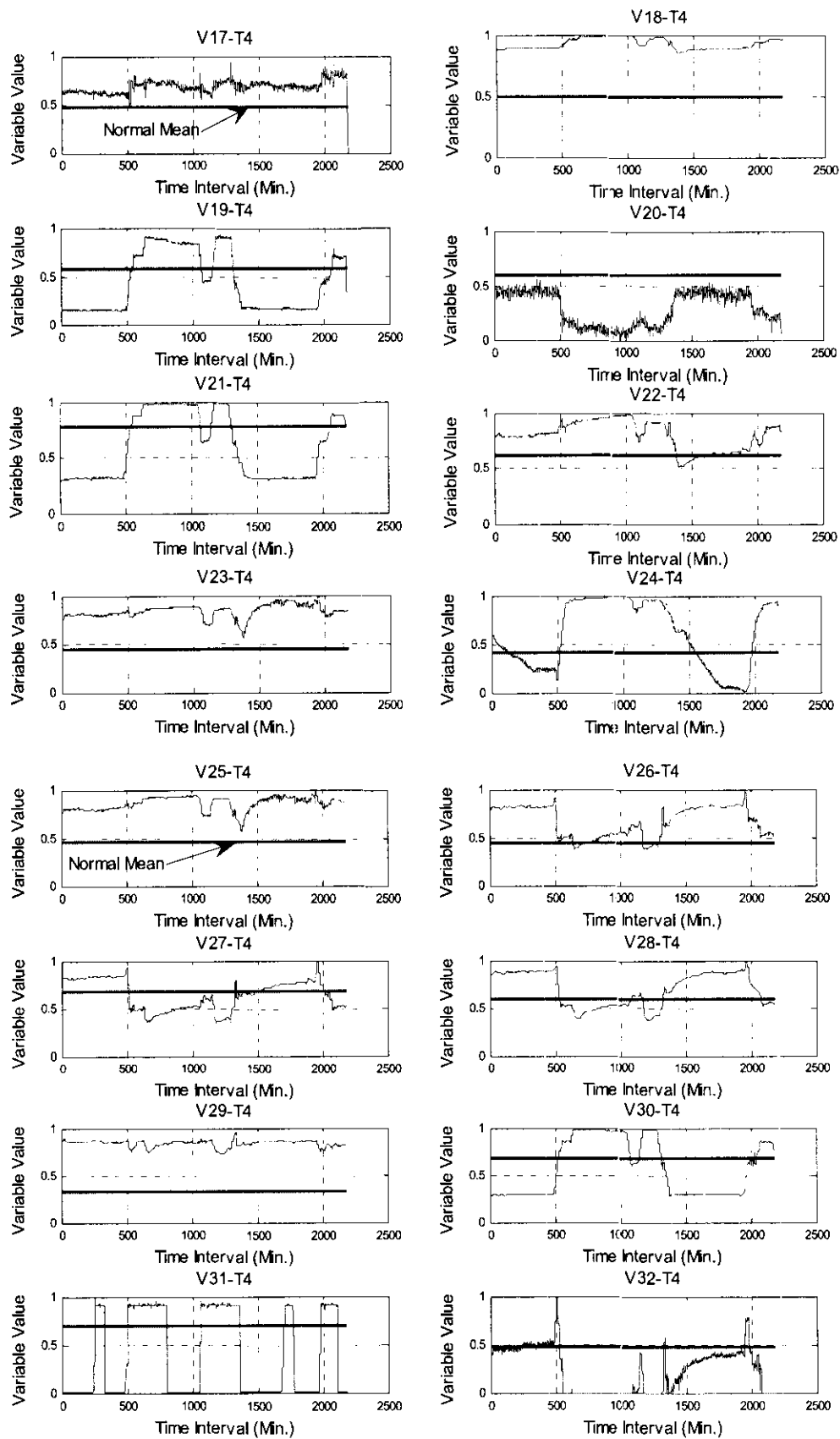


Figure 4.13 Boiler operation variables (from V₁₇ to V₃₂) behavior for trip 4

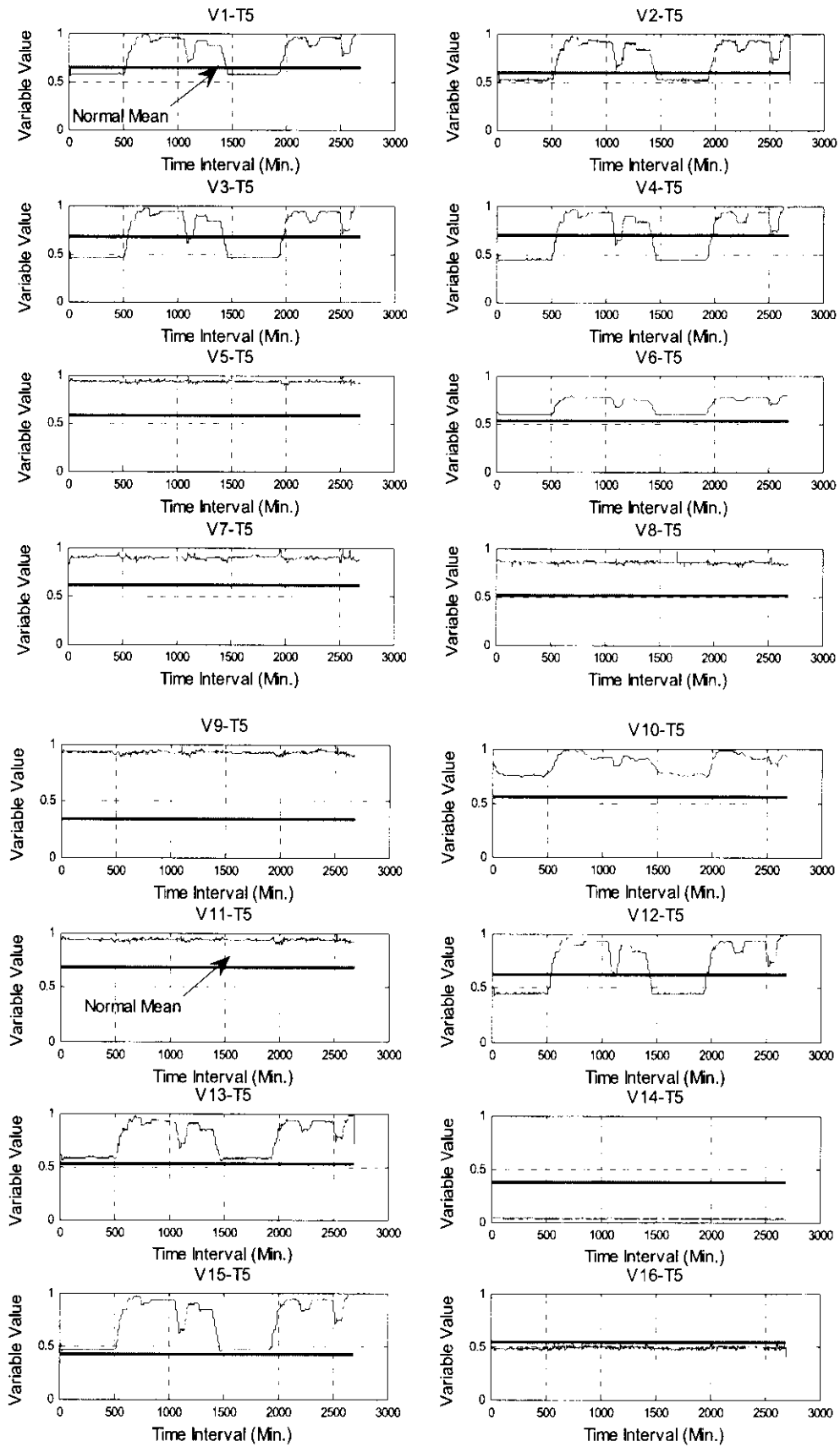


Figure 4.14 Boiler operation variables (from V₁ to V₁₆) behavior for trip 5

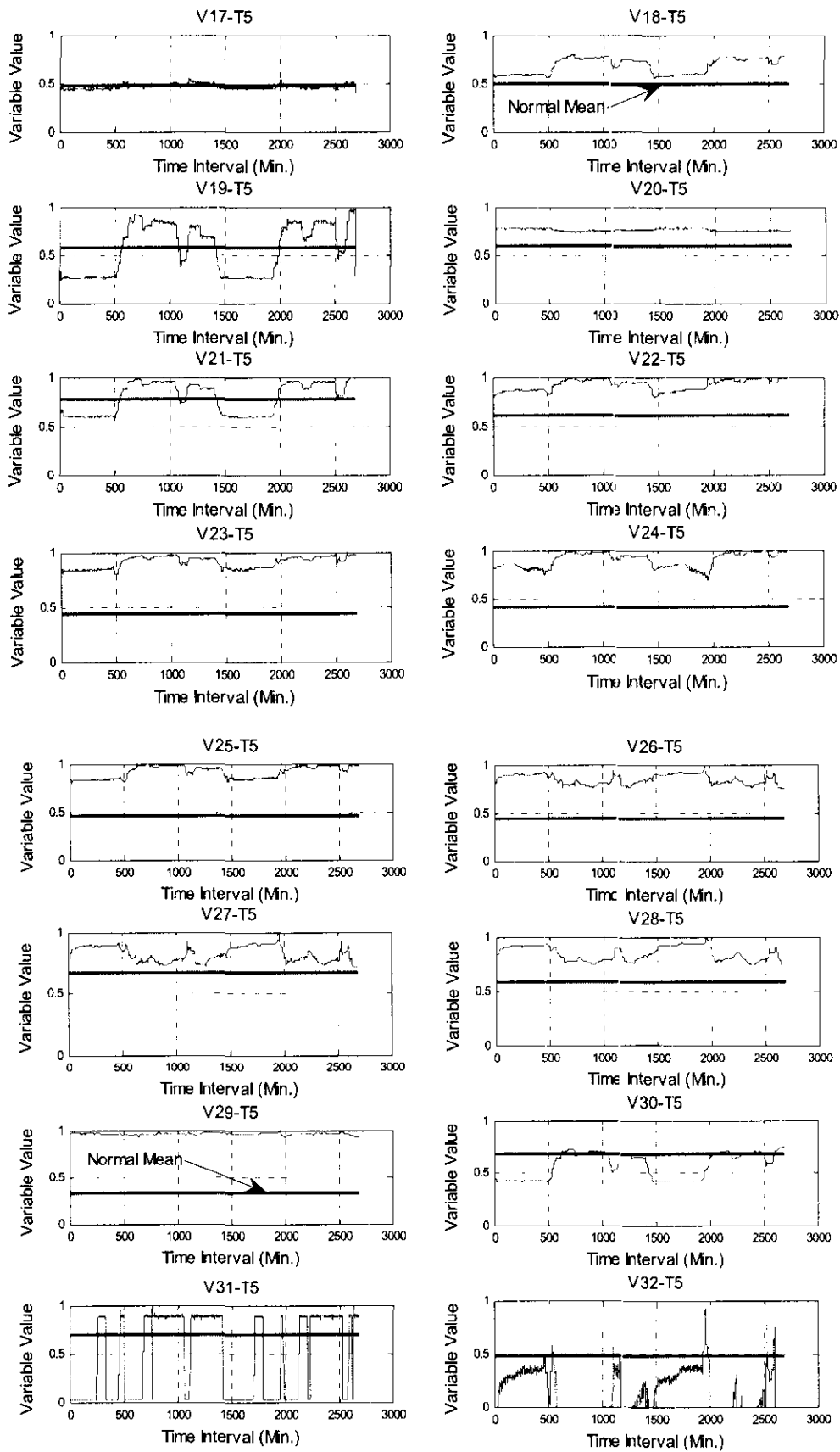


Figure 4.15 Boiler operation variables (from V₁₇ to V₃₂) behavior for trip 5

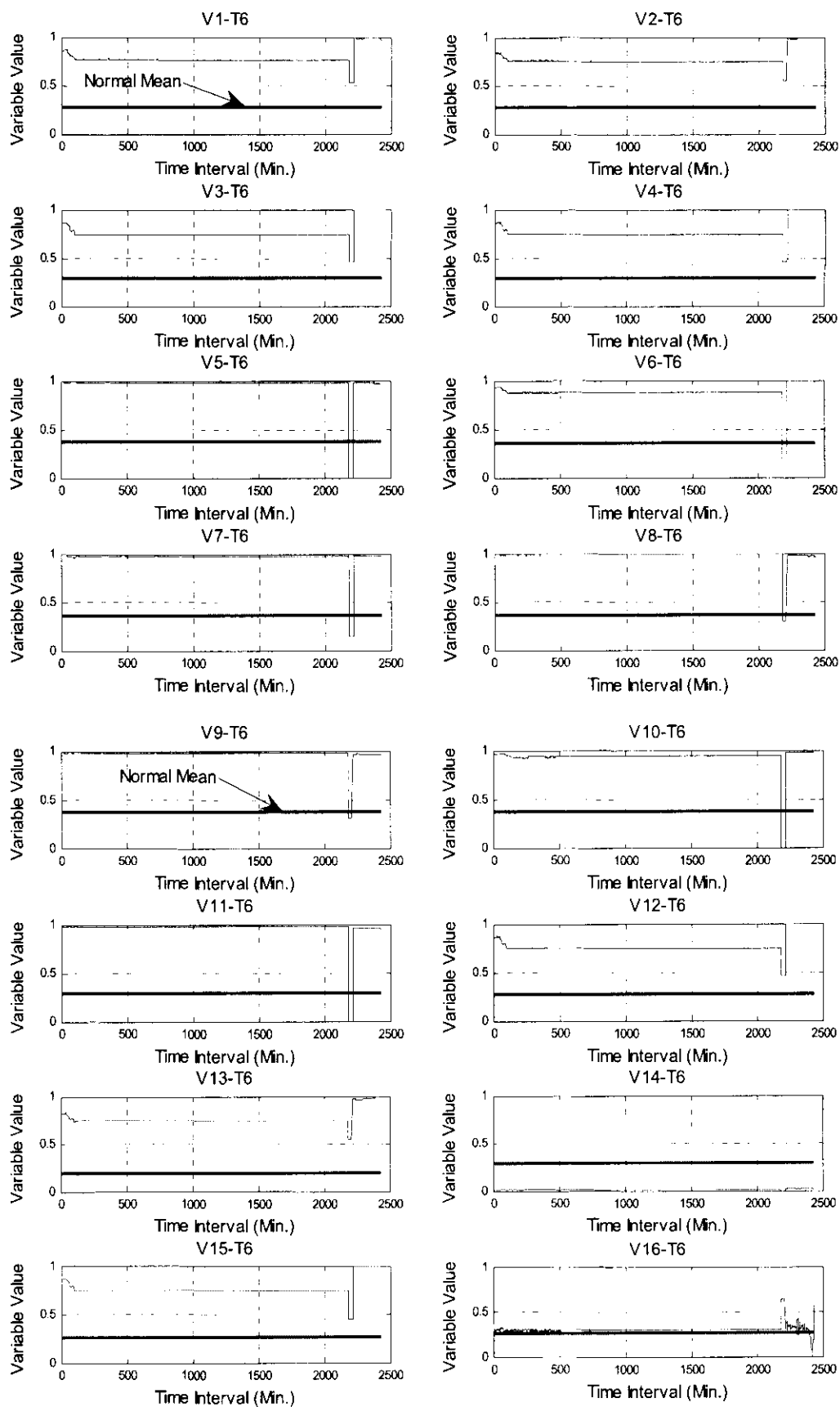


Figure 4.16 Boiler operation variables (from V₁ to V₁₆) behavior for trip 6

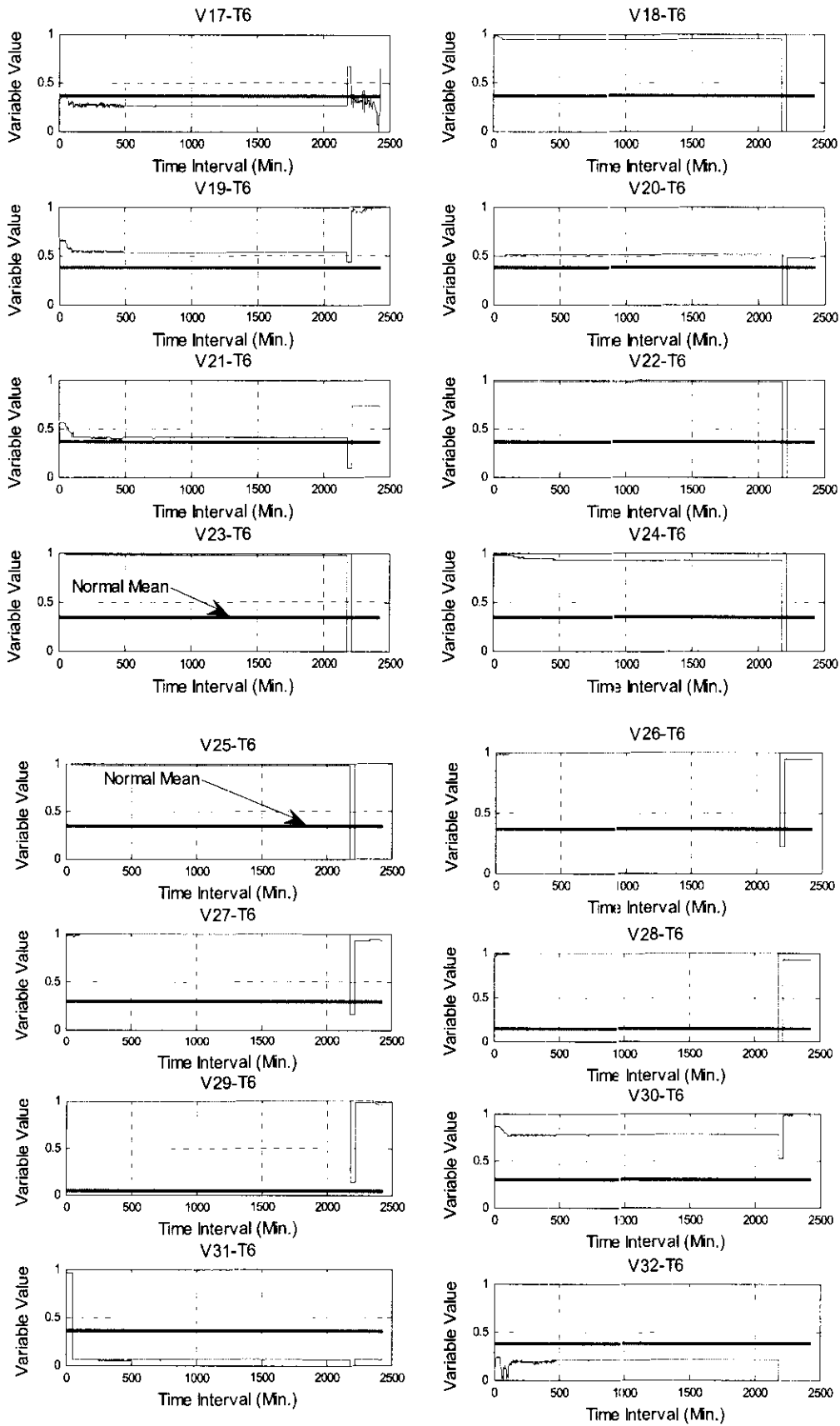


Figure 4.17 Boiler Operation variables (from V₁₇ to V₃₂) behavior for trip 6

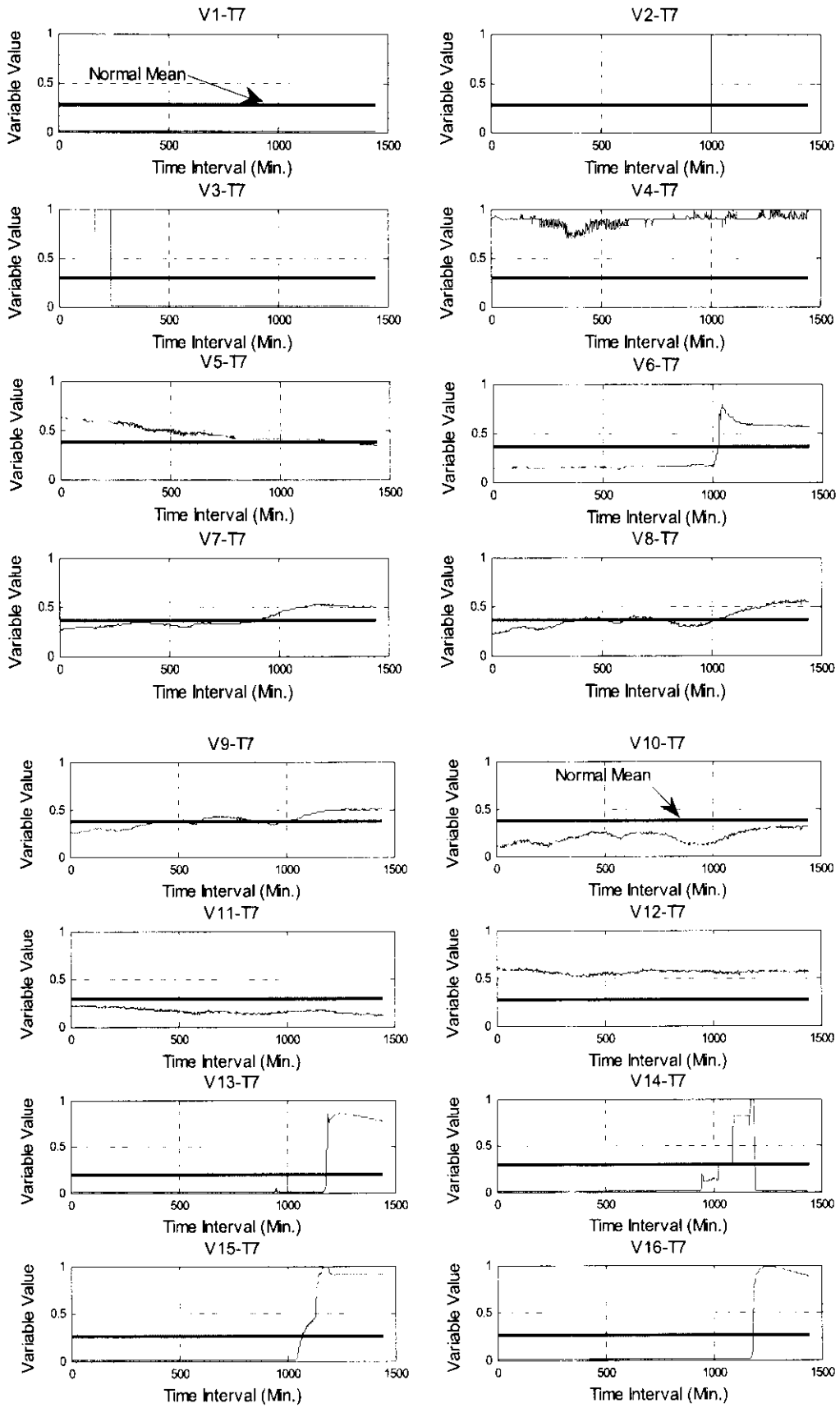


Figure 4.18 Boiler Operation variables (from V₁ to V₁₆) behavior for trip 7

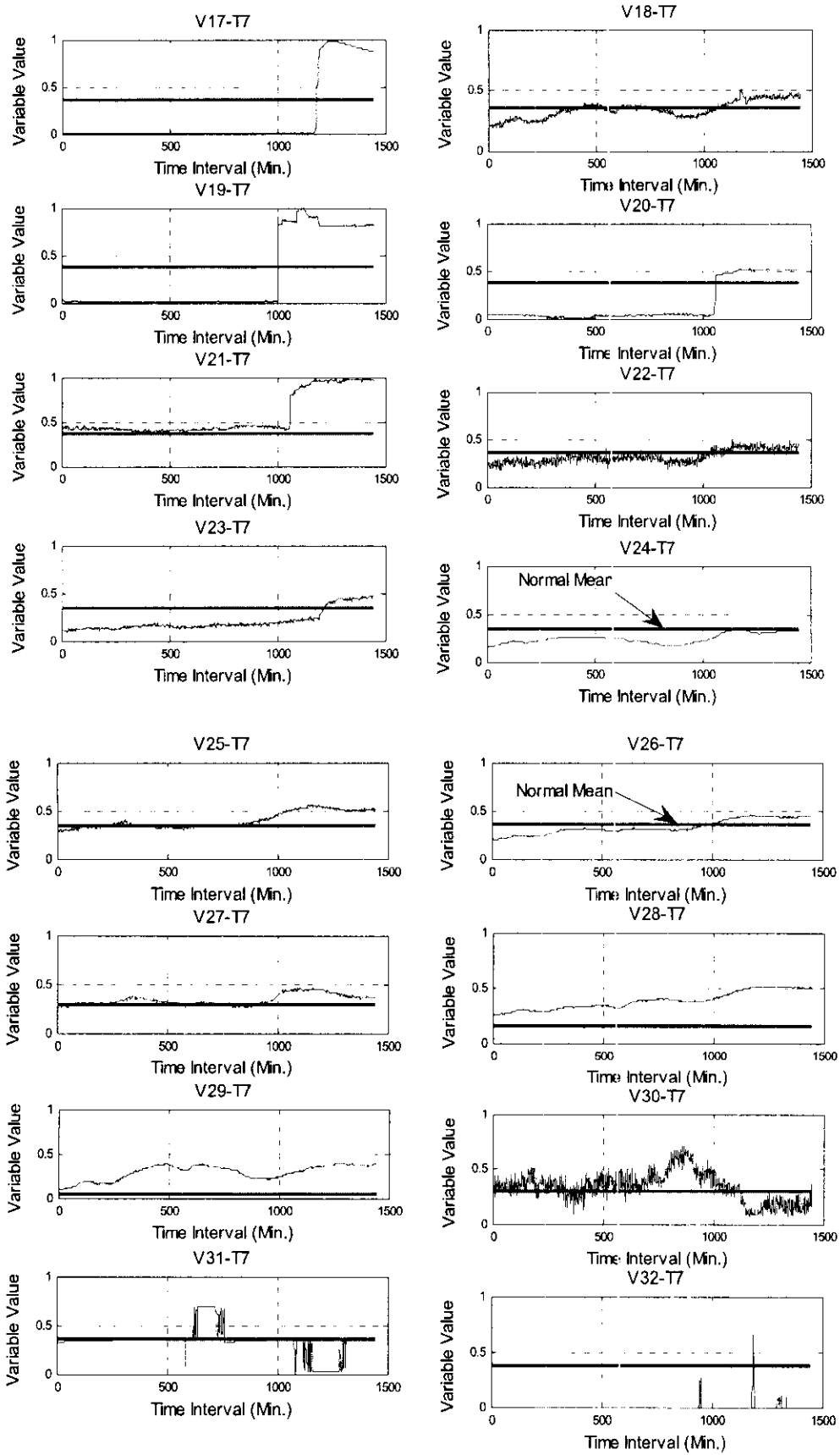


Figure 4.19 Boiler operation variables (from V₁₇ to V₃₂) behavior for trip 7

Those figures declare the behavior of each variable during the duration of the trip occurrence until the shutdown. The behavior of those variables is included in the investigation. The figures show the normalized data values during the trip as extracted from data group B and compared with the respective normalized mean of the variable which is extracted from data group C.

Following the desired ANN input range [0,1], the Min-Max data normalization transformation method is used as the transformation method for the plant data. A normalized mean value for normal and faulty boiler operation is show in Table (4.4).The tracking and study of the variables behavior is very important in the analysis of the IMS-I results.

From the variable behavior analysis, an important conclusion was gained as illustrated in Table (4.5). The table shows the time interval for each variable to reach the high alarm indicator “1”. Based on the results shown in this table, the IMS target for each trip is decided. From the high alarm occurrence table, the effective variables for each trip are decided and listed in Table (4.6).

Table 4.4 Normalized mean values for normal and faulty boiler operation

Normal Mean (M_N) and Faulty Mean (M_F) Values														
Trips	T1		T2		T3		T4		T5		T6		T7	
Sets	Set 1						Set 2				Set 3			
Variables	M_N	M_F	M_N	M_F	M_N	M_F	M_N	M_F	M_N	M_F	M_N	M_F	M_N	M_F
V ₁	0.623	0.825	0.623	0.633	0.623	0.607	0.642	0.618	0.642	0.683	0.281	0.832	0.281	0.039
V ₂	0.586	0.775	0.586	0.576	0.586	0.580	0.597	0.574	0.597	0.643	0.272	0.820	0.272	0.000
V ₃	0.678	0.764	0.678	0.612	0.678	0.542	0.682	0.608	0.682	0.607	0.291	0.829	0.291	0.057
V ₄	0.686	0.764	0.686	0.608	0.686	0.176	0.686	0.608	0.686	0.595	0.291	0.831	0.291	0.705
V ₅	0.520	0.463	0.520	0.846	0.520	0.855	0.569	0.764	0.569	0.892	0.368	0.954	0.368	0.447
V ₆	0.521	0.868	0.521	0.713	0.521	0.314	0.532	0.894	0.532	0.651	0.364	0.888	0.364	0.326
V ₇	0.577	0.697	0.577	0.813	0.577	0.724	0.613	0.788	0.613	0.856	0.356	0.957	0.356	0.441
V ₈	0.521	0.470	0.521	0.824	0.521	0.613	0.506	0.735	0.506	0.816	0.352	0.962	0.352	0.430
V ₉	0.672	0.497	0.672	0.812	0.672	0.778	0.337	0.727	0.337	0.891	0.367	0.957	0.367	0.428
V ₁₀	0.480	0.752	0.480	0.629	0.480	0.232	0.559	0.786	0.559	0.803	0.368	0.932	0.368	0.341
V ₁₁	0.684	0.459	0.684	0.843	0.684	0.878	0.685	0.758	0.685	0.899	0.291	0.946	0.291	0.205
V ₁₂	0.603	0.763	0.603	0.608	0.603	0.108	0.616	0.607	0.616	0.596	0.273	0.831	0.273	0.455
V ₁₃	0.434	0.797	0.434	0.611	0.434	0.624	0.522	0.596	0.522	0.680	0.185	0.811	0.185	0.222
V ₁₄	0.553	0.656	0.553	0.043	0.553	0.063	0.370	0.592	0.370	0.045	0.294	0.114	0.294	0.034
V ₁₅	0.501	0.761	0.501	0.609	0.501	0.836	0.421	0.605	0.421	0.607	0.257	0.829	0.257	0.363
V ₁₆	0.541	0.587	0.541	0.475	0.541	0.753	0.542	0.708	0.542	0.480	0.257	0.318	0.257	0.252
V ₁₇	0.492	0.670	0.492	0.457	0.492	0.438	0.478	0.696	0.478	0.452	0.360	0.277	0.360	0.252
V ₁₈	0.323	0.850	0.323	0.328	0.323	0.890	0.496	0.915	0.496	0.647	0.356	0.936	0.356	0.390
V ₁₉	0.537	0.694	0.537	0.396	0.537	0.378	0.578	0.474	0.578	0.447	0.369	0.667	0.369	0.356
V ₂₀	0.586	0.245	0.586	0.741	0.586	0.163	0.595	0.324	0.595	0.758	0.367	0.488	0.367	0.219
V ₂₁	0.722	0.767	0.722	0.728	0.722	0.063	0.780	0.604	0.780	0.712	0.366	0.515	0.366	0.506
V ₂₂	0.596	0.654	0.596	0.831	0.596	0.647	0.614	0.750	0.614	0.847	0.365	0.957	0.365	0.403
V ₂₃	0.372	0.694	0.372	0.808	0.372	0.531	0.440	0.780	0.440	0.848	0.340	0.959	0.340	0.362
V ₂₄	0.394	0.834	0.394	0.730	0.394	0.665	0.409	0.694	0.409	0.828	0.350	0.936	0.350	0.403
V ₂₅	0.354	0.701	0.354	0.816	0.354	0.241	0.459	0.812	0.459	0.847	0.341	0.955	0.341	0.441
V ₂₆	0.515	0.437	0.515	0.806	0.515	0.654	0.441	0.655	0.441	0.816	0.358	0.951	0.358	0.406
V ₂₇	0.641	0.390	0.641	0.786	0.641	0.601	0.673	0.634	0.673	0.798	0.294	0.946	0.294	0.428
V ₂₈	0.534	0.369	0.534	0.807	0.534	0.667	0.586	0.679	0.586	0.816	0.154	0.941	0.154	0.416
V ₂₉	0.406	0.429	0.406	0.757	0.406	0.923	0.328	0.822	0.328	0.918	0.039	0.962	0.039	0.430
V ₃₀	0.679	0.813	0.679	0.526	0.679	0.551	0.678	0.596	0.678	0.515	0.299	0.833	0.299	0.351
V ₃₁	0.662	0.544	0.662	0.313	0.662	0.161	0.695	0.423	0.695	0.308	0.366	0.148	0.366	0.352
V ₃₂	0.655	0.438	0.655	0.356	0.655	0.363	0.472	0.213	0.472	0.153	0.378	0.118	0.378	0.011

Table 4.5 High alarm occurrence of influencing variables corresponding to each trip

Code	Variable	Unit	High Alarm (Time/Minute)						
			T1	T2	T3	T4	T5	T6	T7
V ₁	Total Combined Steam Flow	t/h	705	582	825	—	2650	2420	—
V ₂	Feed Water Flow	t/h	704	—	848	—	2676	—	1005
V ₃	Boiler Drum Pressure	Barg	704	992	867	—	2650	2329	212
V ₄	Superheater Steam Pressure	Barg	704	992	—	805	—	2329	1288
V ₅	Superheater Steam Temperature	C	2471	1835	389	1329	1102	10	—
V ₆	High Temperature Re-Heater Outlet Temperature	°C	963	—	—	—	—	2332	—
V ₇	High Temperature Superheater Exchange Metal Temperature	°C	—	—	600	504	1959	20	—
V ₈	Intermediate Temperature (A) Superheater Exchange Metal Temperature	°C	2472	1835	389	1329	—	10	—
V ₉	High Temperature Superheater Inlet Header Metal Temperature	°C	2471	1835	389	—	—	11	—
V ₁₀	Final Superheater Outlet Temperature	°C	—	—	—	880	757	—	—
V ₁₁	Superheater Steam Pressure Transmitter (Control)	bar	2471	1835	389	—	1102	10	—
V ₁₂	Feed Water Valve Station	t/h	704	992	—	805	—	2329	—
V ₁₃	Feed Water Control Valve Position	%	704	—	852	—	2675	2410	—
V ₁₄	Drum Level Corrected (Control)	mm	2214	—	—	958	—	—	1180
V ₁₅	Drum Level Compensated (From Protection)	mm	704	—	867	—	2650	2329	—
V ₁₆	Feed Water Flow Transmitter	%	—	—	61	—	—	—	—
V ₁₇	Boiler Circulation Pump1 Pressure	bar	2031	—	—	—	—	—	—
V ₁₈	Boiler Circulation Pump 2 Pressure	bar	1959	5	713	—	—	2369	—
V ₁₉	Low Temperature Superheater Left Wall Outlet Before Super Heater Dryer	°C	704	—	853	—	2676	2433	1095
V ₂₀	Low Temperature Superheater Right Wall Outlet Before Super Heater Dryer	°C	2612	1505	59	—	—	—	—
V ₂₁	Low Temperature Superheater Left Wall After Super Heater Dryer	°C	958	1503	—	—	2649	—	1377
V ₂₂	Low Temperature Superheater Right Wall Exchange Metal Temperature	°C	2474	—	612	503	2605	—	—
V ₂₃	Intermediate Temperature (B) Superheater Exchange Metal Temperature	°C	1948	—	599	1953	2603	—	—
V ₂₄	Intermediate Temperature Superheater Outlet Before Super Heater Dryer	°C	1944	829	817	1001	2602	—	—
V ₂₅	Intermediate Temperature Superheater Outlet Header Metal Temperature	°C	2007	—	—	1953	2603	—	—
V ₂₆	High Temperature Superheater Outlet Header Metal Temperature	°C	2480	—	608	1960	1959	358	—
V ₂₇	High Temperature Re-Heater Outlet Steam Pressure	bar	2477	—	602	1962	1959	477	—
V ₂₈	Superheated Steam Form Intermediate Temperatures Outlet Pressure	bar	—	—	611	1967	1962	490	—
V ₂₉	Superheater Water Injection Compensated Flow	ton/hr	2479	—	—	—	2535	128	—
V ₃₀	Economizer Inlet Pressure	bar	961	—	393	—	—	2329	—
V ₃₁	Economizer Inlet Temperature	°C	—	1113	—	—	2641	—	—
V ₃₂	Economizer Outlet Temperature	°C	—	—	620	509	—	—	—

Table 4.6 Results from behavior analysis of the effective and the most effective variables

Trip	Shutdown Time/Minute	Effective Variables	Most Effective Variables
1	2614	V[5,8,9,11,14,17,18,20,22,23,24,25,26,27,29]	V20
2	1837	V[3,4,5,9,11,12,20,21,31]	V[5,9,11,12]
3	2226	V[1,2,3,13,19,24]	V3
4	2179	V[5,8,23,25,26,27,28]	V28
5	2688	V[1,2,3,13,15,19,20,21,22,23,24,29,31]	V19
6	2433	V[1,3,4,6,12,13,15,18,19,30]	V19
7	1445	V[2,4,14,19,21]	V21

4.5.3.2 Data Segmentation Step

For each trip data, only the data before the unit shutdown is used for the training and validation. Since this work targets the establishment of the best ANN topology combinations for each individual trip, the ANN training is carried out in two stages: the preliminary training stage and the basic training stage. For that, the data interval before the trip was segmented as follows:

- i. Subdivide the trip data interval before the unit shutdown into two equal data sub groups A and B.
- ii. Data sub group A: 70% for preliminary training and 30% for preliminary validation.
- iii. Data sub group B: 70% for basic training and 30% for basic validation.

The segmentation criteria for preliminary and basic training/validation are shown in Figure (4.20).

4.5.3.3 ANN Target Matrix Establishment Step

The results from the high alarm occurrence table were used to establish the target matrix. There were a number of influencing variables for each one of the seven trips. The fault introduced matrix indicates the time at which each influencing variable

reached its maximum value. i.e. reaching “1”. The method of the target matrix establishment was repeated by assuming the faulty data with ± 5 , ± 10 , ± 15 , ± 20 and ± 25 minutes. The analysis has shown that the ± 20 minutes provided optimum training performance of the ANN system, where RMSE change compared to the ± 25 is negligible; i.e., the steady state convergence was achieved.

It has been decided that the fault target interval was within 20 minutes before and 20 minutes after reaching “1”. Hence all the other values are assumed non-faulty values and they are “0” in the normalization format. In such a manner, a new matrix assigning the target of each trip was established and used later for the ANN training process.

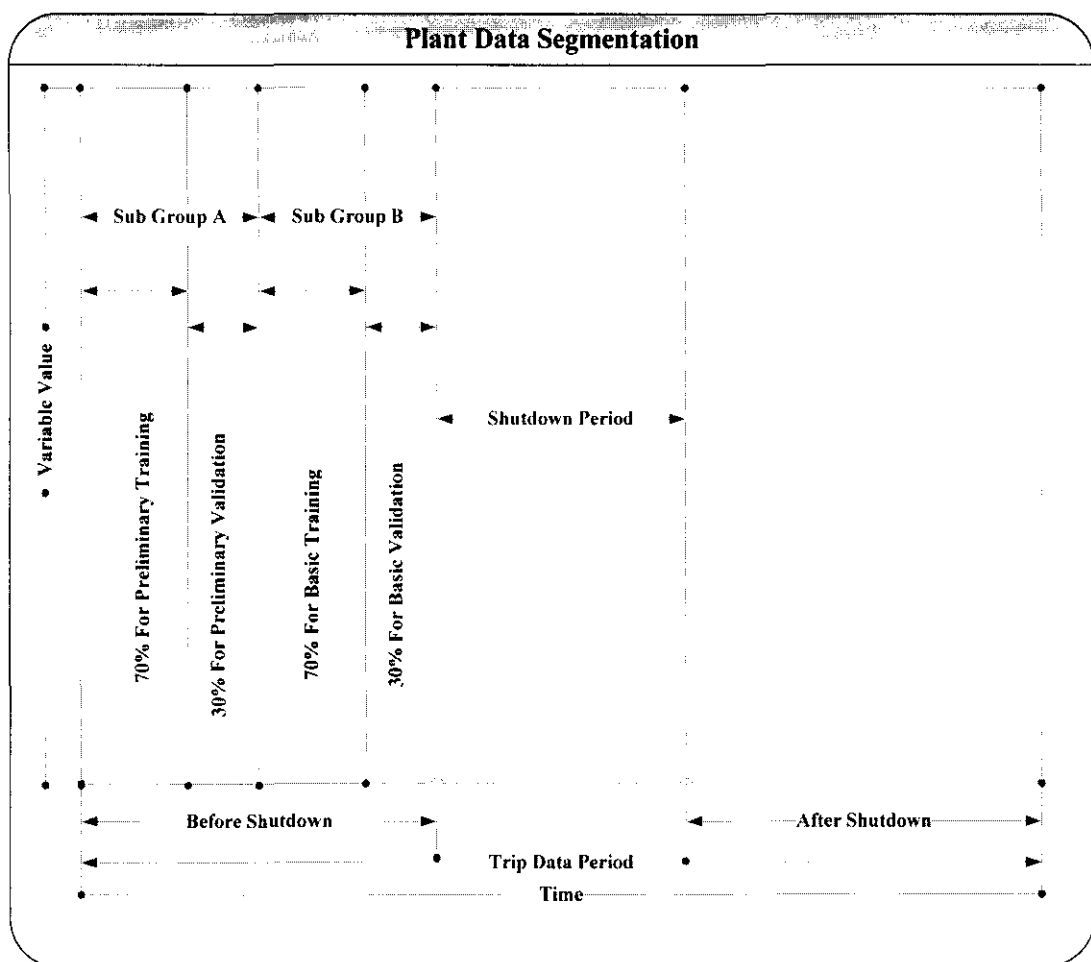


Figure 4.20 Data segmentation sub groups for training and validation

4.6 Summary

MNJTPP was described as the source of real data. The steam boiler unit was presented as the specific equipment under investigation. Seven TPP boiler trips were identified. An integrated plant data preparation framework has been proposed for the training and validation of the proposed artificial intelligent monitoring systems. The proposed integrated plant data scheme consisted of three phases: data pre-analysis phase, in which boiler operational variables were identified and collected for each specific boiler trip ; data pre-processing phase, in which noisy and non-number data were filtered and normalized between one and zero, and data post-analysis phase, in which data were segmented into two sets for each trip: sub group data (A): 70% for preliminary training and 30 % for preliminary validation and sub group data (B): 70% for basic training and 30% for basic validation, NN targets were established , the behavior of influencing boiler operation variables were analyzed.

CHAPTER 5

DESIGN AND IMPLEMENTATION OF IMSs

5.1 Introduction

In order to achieve the decided goals, two artificial intelligent monitoring systems (IMSs) specialized in boiler trips were proposed with the help of MATLAB codes. The development procedures are highlighted and discussed in this chapter. The adopted major computational intelligent tool in the proposed systems is represented by feed-forward ANN methodology which is described in details.

The first IMS represents the use of a pure ANN system for boiler trip detection. The second IMS represents the use of a GA and a ANN as a hybrid intelligent system. The NN learning/training phases and the main topologies are identified. The detailed design steps of both IMSs are discussed. The genetic algorithms operators and the encoding process are identified.

5.2 Development of IMS-I (Pure ANN)

The back-propagation neural network is considered a leap in the development of neuro computing systems. The powerful mapping of this scheme has been successfully applied to a wide range of problems from credit application scoring to pattern classification and recognition [85].

Back-propagation is a systematic method for training multilayer artificial neural networks [86]. Despite its limitations, a back-propagation can attack any problem that

concerns pattern mapping. Given an input pattern, the networks produce an associative output pattern.

5.2.1 Why Use Back-Propagation Neural Networks

Back-Propagation (BBP) offers several unique advantages over the conventional methods which can be illustrated as [9]:

- i. BBP training algorithm is a relatively simple implementation.
- ii. BBP is a standard method that leads to faster convergence.
- iii. BBP training algorithms are peculiar with the layer presentation for unknowns.
- iv. BBP ability to solve higher order systems of equations.

5.2.2 Architecture of Back-Propagation Network

The processing unit or the neuron used here is similar in nature to the perceptron cell. It applies an activation function to the weighted sum of its inputs; the activation function is a monotonic non-linear which is a smoothed form of the threshold function. BBP networks are usually layered, with each layer fully connected to the layers before and after. Neurons are not connected to other neurons in the same layer. Typically, BBP employs three or more layers of neurons (including an input layer) [87]. Figure (5.1) shows the matrix of weight values that correspond to each layer interconnections; units are indexed starting with (1) in each layer. Superscripts have been added to distinguish weights in different layers.

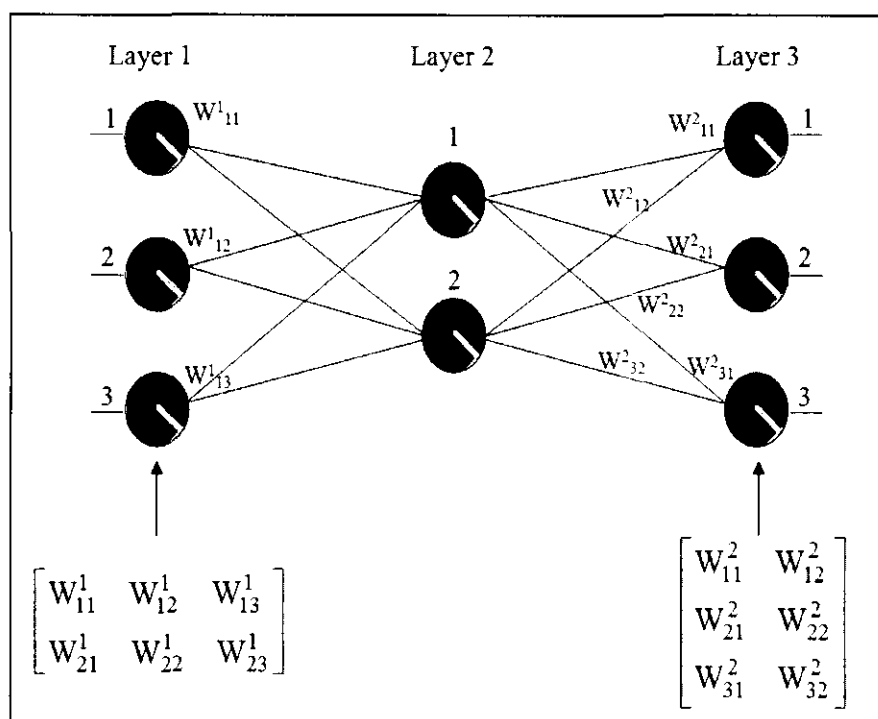


Figure 5.1 Weight matrices of a three layered back-propagation system [88]

5.2.3 Back-Propagation Learning Method

The BBP learning rule is generalized from the Widrow-Hoff rule for multilayer networks. A BBP is one of the easiest networks to understand and therefore, its learning and update procedure is intuitively appealing because it is based on a relatively simple concept. If the network results in an inappropriate output then, the weights are corrected so that the error is lessened and as a result responses of the network are more likely to be correct [89]. A BBP neural network is trained by supervised learning. The network is presented with pairs of patterns where an input pattern is paired with a target output pattern. Upon each presentation, weights are adjusted to decrease the differences between the network outputs and the target output. When the network corrects its internal parameters, the correction mechanism starts with the output unit and back-propagation backwards through each internal layer to the input layer, giving the method its name back-propagation.

A learning set (a set of inputs and target outputs) is used for training, and is presented to the network iteratively. Before starting the training process, all of the weights must be initialized to small random numbers. This ensures that the network is not saturated by large values of the weights, and prevents certain other training pathologies [90].

5.2.4 The BBP Training Algorithm

As shown in Figure (5.2), training the BBP requires the following steps [63]:

- i. Set the weights and thresholds to small random values for all the neurons.
- ii. Put the I/P vector into the I/P layer and specify the desired O/P layer.
- iii. Use the sigmoid non-linearity to calculate the O/P of the hidden and O/P layers.
- iv. Calculate the error ($Y_d - Y_0$).
- v. Calculate δ_k for the O/P layer and the changes in the weights Δw_{jk} .
- vi. Working back to the hidden layer, calculate δ_j for the hidden layer and Δw_{ij} .
- vii. Repeat by going to step 2.

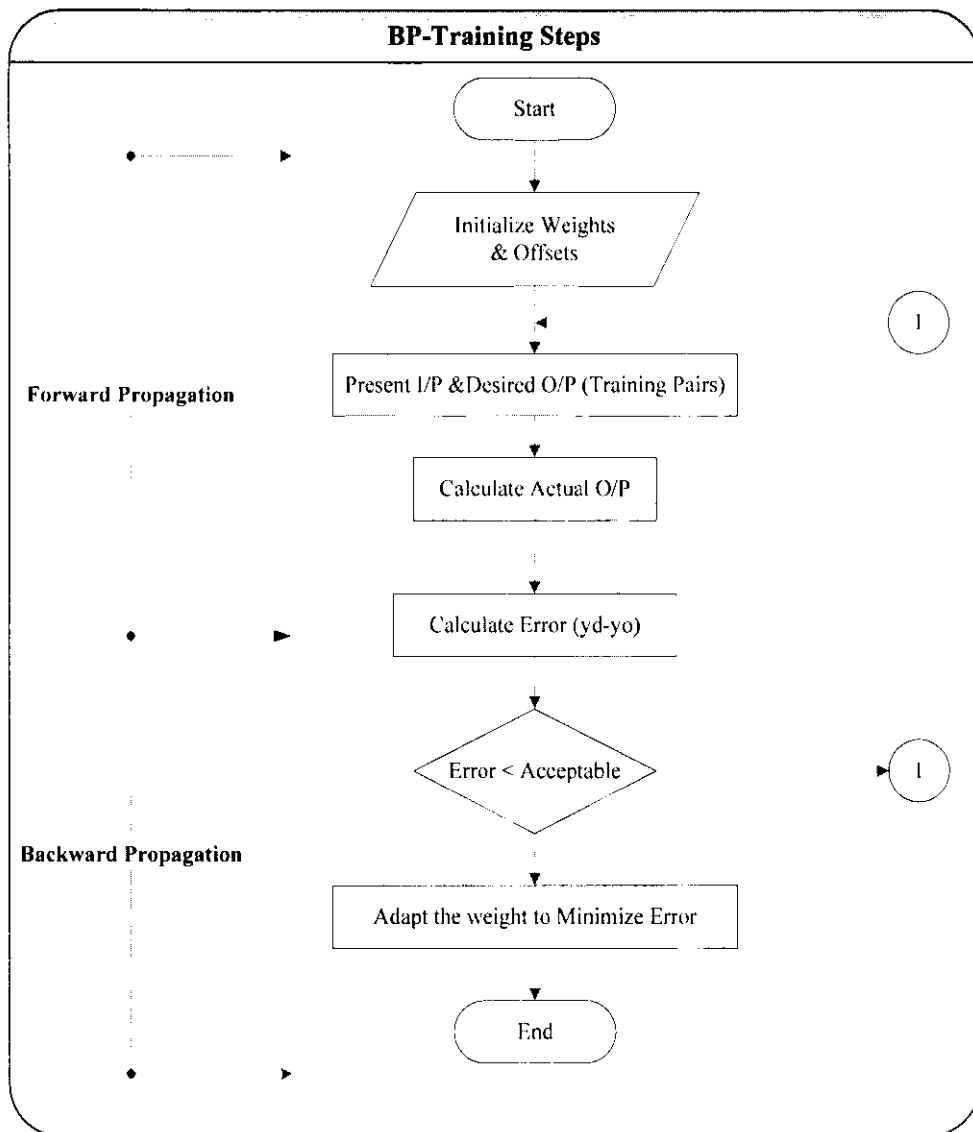


Figure 5.2 Back-Propagation NN training steps [63]

5.2.5 Selection of ANN Topologies

Choosing a good topology becomes a crucial task for the success of an ANN. Due to ANNs robustness, the topology selection influences the learning process time and classification. The selection criteria are based on the impact on the network performance. The main NN topologies include: training algorithms, learning rate, momentum coefficient, activation functions, the number of hidden layers and the number of hidden layer neurons.

5.2.5.1 Training Algorithms

A back-propagation training algorithm has several modifications according to the multidimensional minimization algorithms that is used to minimize the error estimator. Table (5.1) shows the convergence time for nine commonly known BBP faster training algorithms on one particular problem.

Table 5.1 Convergence time for back-propagation algorithms [91]

Function	Techniques	Time	Epochs	Mflops
traingdx	Variable Learning Rate	57.71	980	2.50
trainRprop	Rprop	12.95	185	0.56
trainscg	Scaled Conj. Grad.	16.06	106	0.70
traingcf	Fletcher-Powell CG	16.40	81	0.99
traingcp	Polak-Ribiere CG	19.16	89	0.75
taingcb	Powell-Beale CG	15.0.3	74	0.59
trainoss	One-Step-Secant	18.46	101	0.75
trainbfg	BFGS quasi-Newton	10.86	44	1.02
trainlm	Levenberg- Marquardt	1.87	6	0.46

Only four different types of minimization algorithms are considered in the present work. The selection was based on their computational times [91]. Namely, they are:

- i. Resilient back-propagation (Rprop)

Rprop is a high performance numerical optimization technique for ANN fast training. The main objective of the Rprop training algorithm is to eliminate the harmful effects by using the steepest descent algorithm to train multilayer networks with a sigmoid activation function which has a very small gradient magnitude that leads to small changes in weights and biases. Rprop is faster than the standard steepest descent optimization algorithm. Also, Rprop requires only a modest increase in memory requirements to store the updated values for each weight and bias, which is equivalent to the storage of the gradient and that is considered as a very nice property [91].

ii. Scaled Conjugate Gradient (SCG)

Each one of the conjugate gradient training algorithms requires a line search. This line is computationally expensive as it requires that the network response to all training must be computed many times for each search trial. The SCG was proposed by Moller to avoid the time consumption for a line search at each iteration. The basic idea of the SCG algorithm is to combine the model-trust region approach, which is used in the Levenberg-Maquardt training algorithm described later, with the conjugate gradient approach.

The SCG training algorithm routine may require more training iterations to converge than the other conjugate gradient algorithms; however, the total number of training iterations is significantly reduced as no line search is performed. The SCG memory storage requirements are about the same as those of Fletcher-Reeves [91].

iii. BFGS Quasi-Newton (BFGS)

The Quasi-Newton training algorithm which has been most successful in published studies is the Broyden, Fletcher, Goldfarb, and Shanno (BFGS) update. The BFGS is an alternative to the conjugate gradient methods as a fast optimization algorithm. The basic step of Quasi-Newton is:

$$x_{k+1} = x_k - A_k^{-1} g^k \quad (5.1)$$

Where: x_{k+1} is the update of the search iteration direction

A_k is the Hessian matrix

g^k is the gradient vector

BFGS updates an approximate Hessian matrix at each training iteration. The update is computed as a function of the gradient. The BFGS requires more computation in each training iteration and more memory storage than the conjugate gradient algorithms. It generally converges in fewer training iterations for a small network. However; BFGS can be considered as an efficient training algorithm [91].

iv. Levenberg-Marquardt (LM)

The Levenberg-Marquardt is a very efficient MATLAB implementation and it appears to be the fastest optimization algorithm for training a moderate-sized feed-forward NN. The Levenberg Marquardt was designed to approach the second order training speed without having to compute a Hessian matrix. Once the performance function has the form of square, Hessian matrix can be approximated as

$$H = J^T J \quad (5.2)$$

And the gradient can be computed as:

$$g = J^T e \quad (5.3)$$

Where: J is the Jacobian matrix, which contains first derivation of the network error with respect to the weights.

e is a vector of network error

The Levenberg-Marquardt Back-Propagation training algorithm uses this approximation to the Hessian matrix in the following Newton update:

$$x_{k+1} = x_k - [J^T J + \mu I]^{-1} J^T e \quad (5.4)$$

Where: μ is the network scalar

All four selected training algorithms calculate the search direction, x_k in many different ways. The first three are general optimization algorithms to minimize a quadratic error function. Certainly, most error surfaces are not quadratic but they will be so in a sufficiently small neighborhood of local minima. The Levenberg-Marquardt needs the Jacobian matrix to be calculated and is specifically used to minimize an error function that arises from quadratic criterion of the assuming form [91].

5.2.5.2 Learning Rate

The learning rate (δ) value (commonly between 0.1 and 0.9) is chosen by the neural network user and usually reflects the rate of learning of the network. Values that are very large might result in instability in the network and unsatisfactory learning. On the other hand, values that are too small might result in excessively slow learning.

In the present work, the learning rate is fixed at the value rate of 0.5.

5.2.5.3 Momentum Coefficient

The momentum coefficient (α) is in the range of 0.0 to 1.0. However, it is commonly set to around 0.9. With the adoption of the momentum method, the network tends to follow the bottom of narrow valleys in the error surface (if they exist) rather than cross rapidly. On the other hand, this method seems to work well on some problems, but it has little or negative effect on others. If (α) is 0.0, the smoothing is minimum, the entire weight adjustment comes from newly calculated change. If (α) is 1.0 the new adjustment is ignored and the previous one is repeated [92].

Here, the momentum coefficient is adjusted to the value of 0.8. Also, it should be mentioned that the size of epochs (number of iterations) for training and validation is adjusted to the value of 100.

5.2.5.4 Activation Functions

Several of the more common types of activation signal functions are defined in section 4.2. Only three different types of activation signal functions are considered and investigated in the present work. The selection was based on the normalized values of the plant captured data. Namely, they are:

- i. Linear summation function (P).
- ii. Sigmoid logistic function (L).

iii. Hyperbolic tangent (T).

5.2.5.5 Number of Hidden Layers and Number of Hidden Layer Neurons

In order to examine the NN performance, various numbers of the neural network hidden layers with various numbers of neurons in each layer should be investigated. In this work, one hidden layer (1HL) and two hidden layers (2HL) with one to ten neurons in each layer were considered.

5.3 Design of IMS-I

An IMS-I represents a pure ANN monitoring system. The feed-forward methodology was adopted to develop the IMS-I. The ANN inputs are listed in Table (4.1). The proposed IMS-I was formed to have two outputs for each trip: one for normal operation, one for tripped operation. Thus, the network had thirty-two inputs as shown in Figure (5.3).

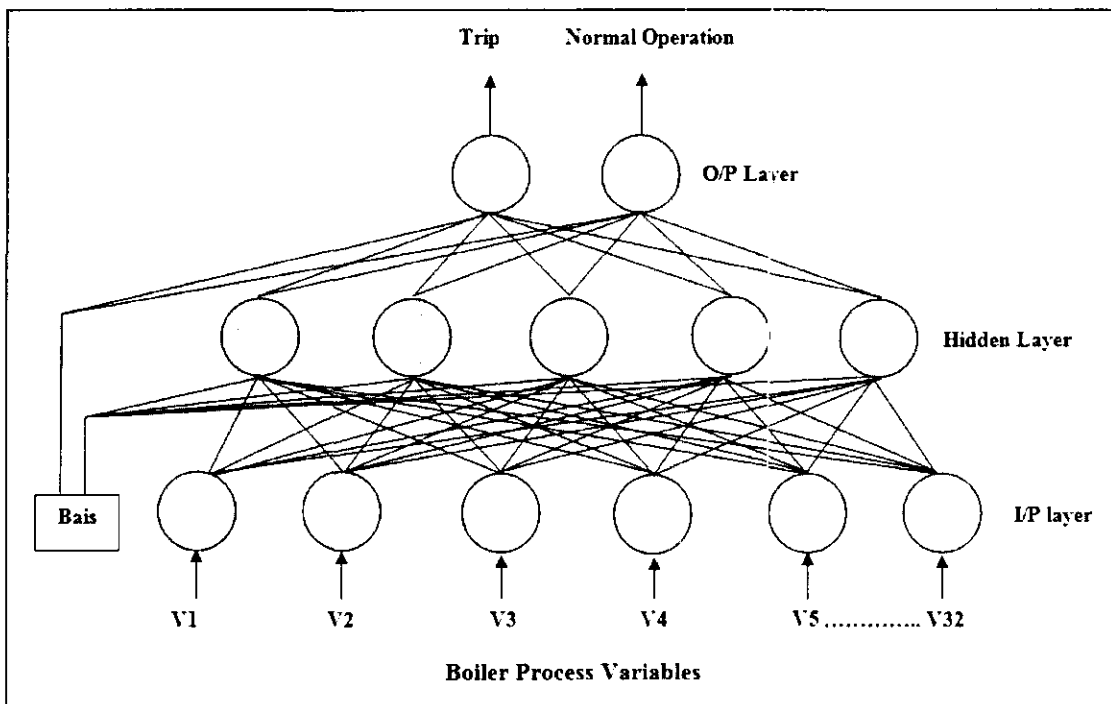


Figure 5.3 IMS-I structure

The ANNs training output values were binary. An output of unity for a specific NN output indicates the existence of the corresponding trip. The values of the other NN outputs were zero. The validation outputs of the IMS-I are, of course continuous, with values from zero to one. Thus, the crucial decision was formed to determine, above, which NN value output should be meaningful in terms of the existence of a critical fault.

The advantage of using a separate NN output for the normal boiler operation for each trip, instead of assuming normal boiler operation when critical fault output for each trip returns zero, is the growth of the ANN's generalization capability. In other words, with that additional NN output, the IMS-I is capable of detecting "unknown" critical faults. In the case of an unknown critical fault, output would be zero for each trip, but also for "normal boiler operation" output would be zero. This means that "normal boiler operation" would not be concluded. In this way, a general "faulty boiler operation" would be assumed. If the additional NN output of the normal boiler operation is not included in the proposed network, then, in the case of an "unknown" critical fault, normal boiler operation would be incorrectly-concluded [7].

5.3.1 Training Processes of IMS-I

In this section, the structured IMS-I performance was investigated based on an RMSE indicator. The best performance of the IMS-I would give an insight view into the capabilities of the fully structured IMS-I. Consequently, the IMS-I was trained and validated. This IMS-I had thirty two inputs as presented before with two outputs, either "0" or "1". These binary NN outputs, are corresponding to normal with the value of "0" and the other, "1" corresponding to an abnormal boiler situation.

The IMS-I training process included two processes:

5.3.1.1 Preliminary Training Process

The preliminary training took place in order to find out the optimal NN topology combination. Seven real boiler data sets (Faulty data) were input to the IMS-I as

preliminary training sets. Each set represents 70% of sub-group data (A). Various candidates of NN topologies were investigated for both one hidden layer (1HL) and two hidden layers (2HL). Several numbers of neurons for each hidden layer ranging from one to ten were tested. Thirty-two boiler operation variables were considered as network inputs. For each trip, the training results were compared based on the RMSE as a network performance indicator.

5.3.1.2 Basic Training Process

The preliminary training process of the ANN was followed by basic training using the optimal topology combination obtained from the preliminary training results. Another seven real boiler data sets (faulty data) were presented to the IMS-I as basic training sets. Each set represents 70% of sub-group data (B). Again, thirty-two boiler operation variables were considered as IMS-I inputs. For all investigated cases, the basic training results were analyzed from the point of view of the proposed system performance indicator. The main objective of NN basic training process is that the calculated RMSE values of the optimal NN topology combination should have equal or smaller values than the preliminary training process.

The sub grouping of the boiler data to sub group (A) and (B) is described and shown in Figure (3.20).

5.3.2 ANN Validation Processes

The IMS-I Validation process included two processes:

5.3.2.1 Preliminary Validation Process

The ANN basic training process was followed by the NN preliminary validation process by using eight validation real data sets. The first seven sets represent the last 30% of sub group data set (A). The last set contained only normal boiler operation real data. The preliminary validation process was carried out using the optimal NN

topology combinations obtained from preliminary training process. The validation real data sets were used to validate how rapidly the proposed IMS-I detects the specific trip, and validate the performance of the system during normal boiler operation.

5.3.2.2 Basic Validation Process

Based on the obtained optimal NN topology combinations from basic training, the basic NN validation was carried out also using eight validation data sets of the thirty-two boiler operation variables. The first seven sets represent the remaining 30% of sub group data set (B). The last set contained normal boiler operation real data.

Since our work deals with slowly developing faults, the time indicator becomes more important as these faults are more difficult to detect as they begin. Accordingly, in that phase, the rapid detection capability of the proposed IMS-I for the specific thermal power plant trip was explored. The proposed system performance was examined using the obtained results.

Training and validation of the IMS-I were executed using fourteen separate MATLAB codes which have been built (two codes for each specific boiler trip). Figure (5.4) shows the proposed IMS-I code execution flow chart. For more details about the proposed codes, refer back to (Appendix B2-1)

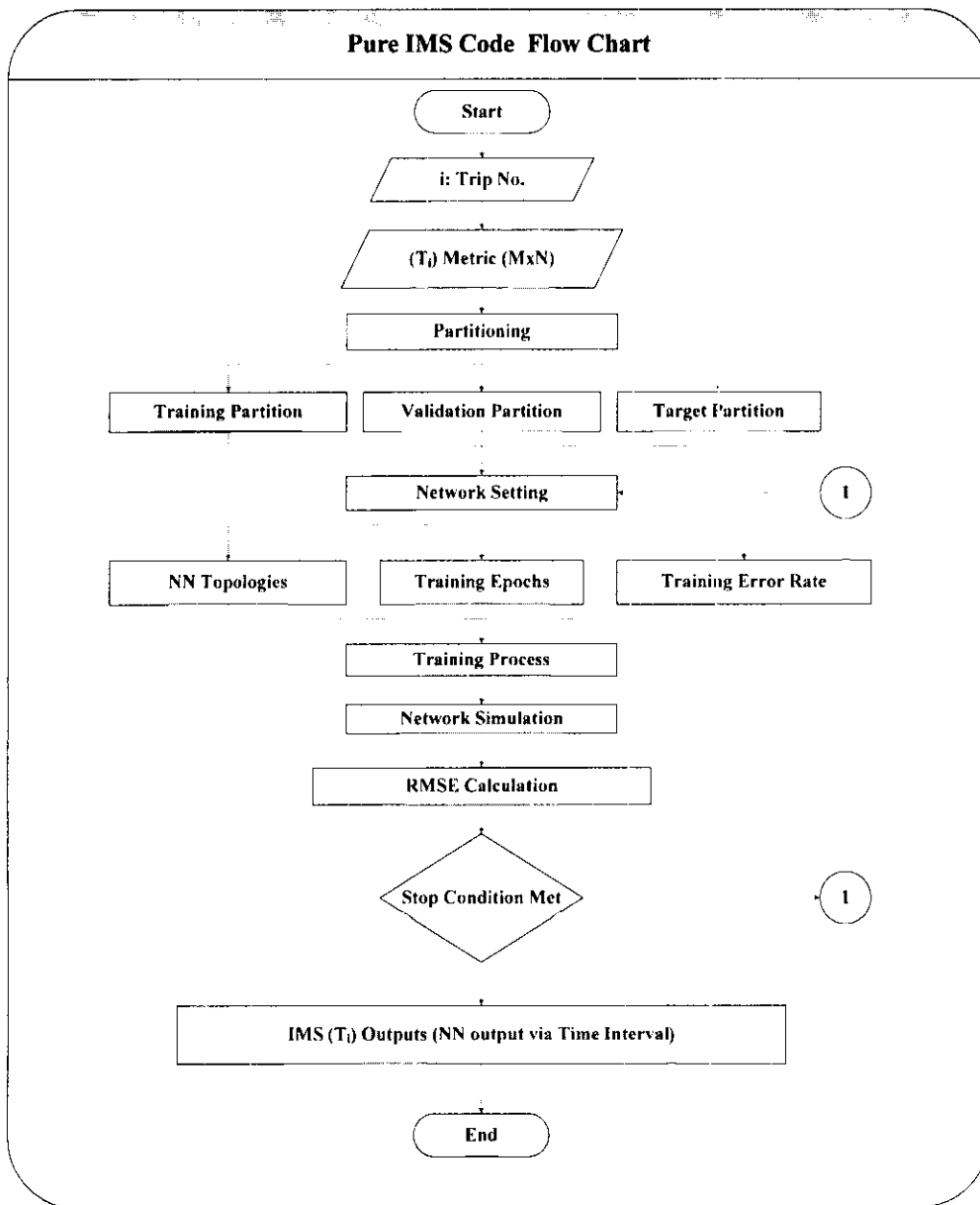


Figure 5.4 Execution flow chart of the proposed IMS-I code

5.4 Development of IMS-II (Hybrid ANN+GA)

The NN modeling application for a nonlinear system has central drawbacks: the lack of a precise method to choose the most appropriate NN topology and the most effective parameters for the training process. These two tasks are usually based on the trial and error approach of the ANN which is performed by the intelligent system developer. Due to the random search and the small portion of explored space of the whole search space, the optimality or even near-optimality is not guaranteed. In order

to overcome the human network design and parameters optimization problems, an evolutionary automated technique of the GA is proposed. The GA develops several network designs with different topologies in order that the best possible combination is finally chosen.

There have been several proposed artificial systems that merge (ANNs) with (GAs) in various ways. These generally fall into three categories [70]:

- i. Using a GA to determine the structure of ANNs.
- ii. Using a GA to calculate the weights of ANNs.
- iii. Using a GA to both determine the structure and the weights of ANNs.

In this work, a novel sophisticated combination strategy for automated design and NN parameter optimization was proposed.

5.4.1 GA Encoding

The main issue in a genetic system is the strategy of encoding the several possible phenotypes of the NN into specific genotypes. In this study, the phenotype consists of the NN topologies. A genotype is a sequence of bits (0/1) with a specific constant length. Each genotype corresponds to a unique phenotype. The phenotypes encoding representations are generally divided into two categories [7, 93]: the Strong Specification Representation (SSR) and the Weak Specification Representation (WSR). The (WSR) is used here to encode the NN topologies together with the NN training parameters into the genes of the GA. The WSR uses specific correspondences of specific binary strings with specific network architectures that are pre-defined by the user. For the present work, each binary string (genotype) of the proposed GA individual represents specific phenotype of ANN topologies together with training parameters. Figure (5.5) shows the proposed individual which consists of:

- i. Two bit strings for multi dimensional minimization back-propagation algorithms.
- ii. Seven bit strings for NN structure.
- iii. Five bit strings for activation functions.
- iv. Thirty-two bit strings for boiler operation variables.

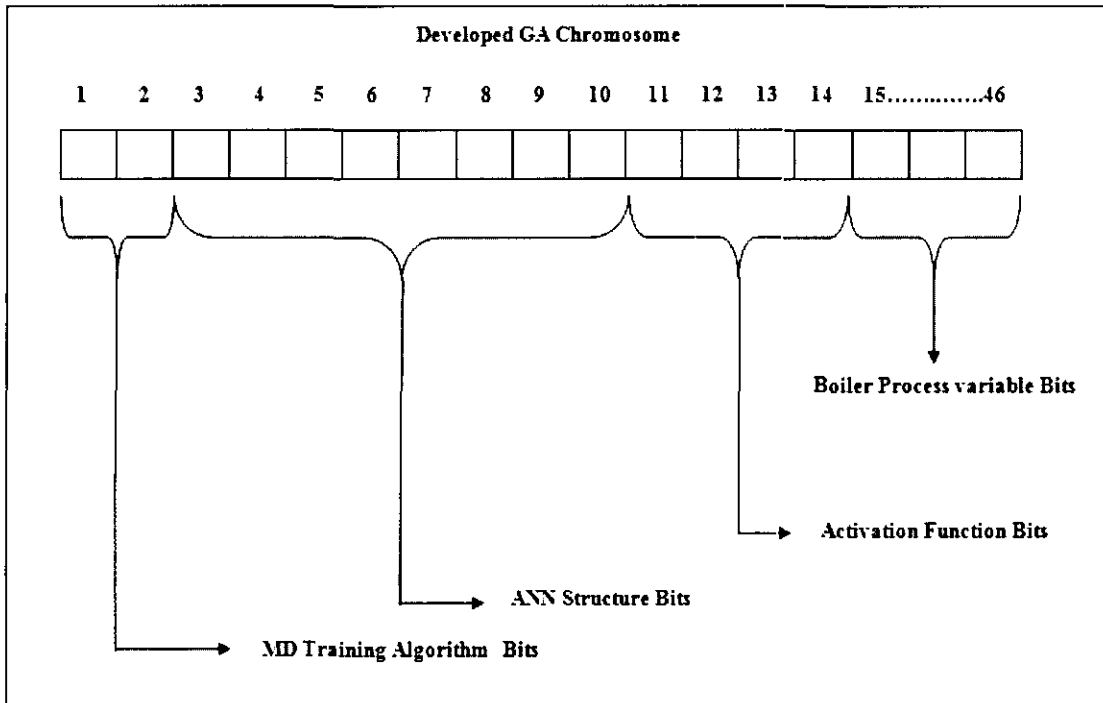


Figure 5.5 GA binary representation

A priori knowledge is considered for this study to reduce the search space drastically. The WSR scheme is proposed and used here for four tasks:

- i. Multidimensional minimization algorithm selection
- ii. Selection of activation function types of the hidden nodes and of the output nodes.
- iii. The ANN architecture.
- iv. Selection of optimal ANN input parameters (Boiler operation variables).

5.4.1.1 WSR of Multidimensional Minimization BBP Training Algorithms:

There are four different multidimensional minimization BBP training algorithms considered by the GA:

- i. Resilient Back-propagation (Rprop)
- ii. Scaled Conjugate Gradient (SCG)
- iii. BFGS Quasi Newton (BFGS)
- iv. Levenberg-Marquardt (LM)

These algorithms can be represented by two binary entries as shown in Table (5.2)

Table 5.2 Binary representation of the training algorithms

Training Algorithm	Rprop	SCG	BFGS	LM
Bit Sequence	00	01	10	11

And they form the first two bits of the binary string representation as shown in Figure (5.5).

5.4.1.2 WSR of ANN Structure

As shown in Figure (5.5), the next seven binary entries of the string represent 91 possible ANN structures of one hidden layer (1HL) and two hidden layers (2HL). The correspondences are shown in Table (5.3).

Table 5.3 ANN structures binary representation

Bit Sequence	Architecture	Bit Sequence	Architecture	Bit Sequence	Architecture
0000001	1HL-1	0100000	2HL-4/5	0111111	2HL-7/9
0000010	1HL-2	0100001	2HL-4/6	1000000	2HL-7/10
0000011	1HL-3	0100010	2HL-4/7	1000001	2HL-8/2
0000100	1HL-4	0100011	2HL-4/8	1000010	2HL-8/3
0000101	1HL-5	0100100	2HL-4/9	1000011	2HL-8/4
0000110	1HL-6	0100101	2HL-4/10	1000100	2HL-8/5
0000111	1HL-7	0100110	2HL-5/2	1000101	2HL-8/6
0001000	1HL-8	0100111	2HL-5/3	1000110	2HL-8/7
0001001	1HL-9	0101000	2HL-5/4	1000111	2HL-8/8
0001010	1HL-10	0101001	2HL-5/5	1001000	2HL-8/9
0001011	2HL-2/2	0101010	2HL-5/6	1001001	2HL-8/10
0001100	2HL-2/3	0101011	2HL-5/7	1001010	2HL-9/2
0001101	2HL-2/4	0101100	2HL-5/8	1001011	2HL-9/3
0001110	2HL-2/5	0101101	2HL-5/9	1001100	2HL-9/4
0001111	2HL-2/6	0101110	2HL-5/10	1001101	2HL-9/5
0010000	2HL-2/7	0101111	2HL-6/2	1001110	2HL-9/6
0010001	2HL-2/8	0110000	2HL-6/3	1001111	2HL-9/7
0010010	2HL-2/9	0110001	2HL-6/4	1010000	2HL-9/8
0010011	2HL-2/10	0110010	2HL-6/5	1010001	2HL-9/9
0010100	2HL-3/2	0110011	2HL-6/6	1010010	2HL-9/10
0010101	2HL-3/3	0110100	2HL-6/7	1010011	2HL-10/2
0010110	2HL-3/4	0110101	2HL-6/8	1010100	2HL-10/3
0010111	2HL-3/5	0110110	2HL-6/9	1010101	2HL-10/4
0011000	2HL-3/6	0110111	2HL-6/10	1010110	2HL-10/5
0011001	2HL-3/7	0111000	2HL-7/2	1010111	2HL-10/6
0011010	2HL-3/8	0111001	2HL-7/3	1011000	2HL-10/7
0011011	2HL-3/9	0111010	2HL-7/4	1011001	2HL-10/8
0011100	2HL-3/10	0111011	2HL-7/5	1011010	2HL-10/9
0011101	2HL-4/2	0111100	2HL-7/6	1011011	2HL-10/10
0011110	2HL-4/3	0111101	2HL-7/7		
0011111	2HL-4/4	0111110	2HL-7/8		

5.4.1.3 WSR of the Activation Function

Three activation functions were considered for the input nodes, hidden nodes and output nodes. Namely: Logistic (L), linear summation (P) and Tanh (T). Thus, for an NN with one-hidden layer, nine different combinations were included in the genetic

representations and were encoded with 5 final binary entries in the bit string, as shown in Table (5.4).

Table 5.4 Activation function binary representation for 1HL

No.	Bit Sequence	Hidden Layer 1 Nodes Activation Function	Output Layer Nodes Activation Function
1	00001	T	T
2	00010	T	L
3	00011	T	P
4	00100	L	L
5	00101	L	T
6	00110	L	P
7	00111	P	P
8	01000	P	L
9	01001	P	T

Table 5.5 Activation function binary representation for 2HL

No.	Bit Sequence	AF/HL1	AF/HL2	AF/Output
1	00001	T	T	T
2	00010	T	T	L
3	00011	T	T	P
4	00100	T	L	T
5	00101	T	L	P
6	00110	T	L	L
7	00111	T	P	T
8	01000	T	P	P
9	01001	T	P	L
10	01010	P	T	T
11	01011	P	T	L
12	01100	P	T	P
13	01101	P	L	T
14	01110	P	L	P
15	01111	P	L	L
16	10000	P	P	T
17	10001	P	P	P
18	10010	P	P	L
19	10011	L	T	T
20	10100	L	T	L
21	10101	L	T	P
22	10110	L	L	T
23	10111	L	L	P
24	11000	L	L	L
25	11001	L	P	T
26	11010	L	P	P
27	11011	L	P	L

And for an NN with two-hidden layers, 27 different combinations were included in the genetic representation and were encoded with 5 final binary entries in the bit string, as shown in Table (5.5).

5.4.1.4 WSR of Optimal NN Inputs

Thirty-two boiler process variables were encoded with binary entries in a binary string in order to form the last thirty-two bits of string as shown in Figure (5.5). The combinations probability for the thirty-two boiler process variables are computed with the formula:

$$P_{vc} = 2^n \quad (5.5)$$

Where:

P_{vc} : Probability of variables combinations.

n : The number of variables.

Base (2): Refer to the binary string (0 and 1).

N different combinations were included in the genetic representation and were encoded with thirty-two final binary entries in the bit string as shown in Table (5.6).

Table 5.6 Boiler operation variables binary representation

		Boiler Operation Variables																																
		1	2	3	4	5	6	7	8	9	10	11	12	13	14	15	16	17	18	19	20	21	22	23	24	25	26	27	28	29	30	31	32	
No.	P	Bit Sequence																																
1	P ₁	1	0	0	0	0	0	0	0	0	0	0	0	0	0	0	0	0	0	0	0	0	0	0	0	0	0	0	0	0	0	0	0	
2	P ₂	0	1	0	0	0	0	0	0	0	0	0	0	0	0	0	0	0	0	0	0	0	0	0	0	0	0	0	0	0	0	0	0	
3	P ₃	0	0	1	0	0	0	0	0	0	0	0	0	0	0	0	0	0	0	0	0	0	0	0	0	0	0	0	0	0	0	0	0	
4	P ₄	0	0	0	1	0	0	0	0	0	0	0	0	0	0	0	0	0	0	0	0	0	0	0	0	0	0	0	0	0	0	0	0	
5	P ₅	0	0	0	0	1	0	0	0	0	0	0	0	0	0	0	0	0	0	0	0	0	0	0	0	0	0	0	0	0	0	0	0	
6	P ₆	0	0	0	0	0	1	0	0	0	0	0	0	0	0	0	0	0	0	0	0	0	0	0	0	0	0	0	0	0	0	0	0	
7	P ₇	0	0	0	0	0	0	1	0	0	0	0	0	0	0	0	0	0	0	0	0	0	0	0	0	0	0	0	0	0	0	0	0	
8	P ₈	0	0	0	0	0	0	0	1	0	0	0	0	0	0	0	0	0	0	0	0	0	0	0	0	0	0	0	0	0	0	0	0	
9	P ₉	0	0	0	0	0	0	0	0	1	0	0	0	0	0	0	0	0	0	0	0	0	0	0	0	0	0	0	0	0	0	0	0	
10	P ₁₀	0	0	0	0	0	0	0	0	0	1	0	0	0	0	0	0	0	0	0	0	0	0	0	0	0	0	0	0	0	0	0	0	
⋮	⋮																																	
	P _i																																	
	⋮																																	
N	P _N	0	0	0	0	0	0	0	0	0	0	0	0	0	0	0	0	0	0	0	0	0	0	0	0	0	0	0	0	0	0	0	1	

5.4.2 IMS-II Scheme

The proposed IMS-II scheme for optimal NN topology combinations and boiler operation variables selection is shown in Figure (5.6). The scheme consists of three major elements: the user element, the genetic algorithm optimization element and the ANN training element. The user element deals with I/O processes, while the optimization part includes several sub-sections that interact with each other and with the user part in order to complete the desired procedure. It is obvious that each box in Figure (5.6) represents a separate internal function. Each box for the proposed scheme titled with the internal function name and the internal interaction between these functions are shown with proper arrows.

At the first element, the ANN training set (T_s), the parameters set for BP training algorithms (BP_s), the number of generations of the GA (G_n), the size of population of the GA (P_z), the probabilities of crossover of the GA (P_c), and the mutation probability of the GA (P_m) are provided by the user. The (X_{int}) stand for the initial population of several binary strings, each of which represents a specific network topology and the NN training parameters set. After that, all the user inputs are passed to the main optimization part.

The internal function namely the “GA decoding” receives the population of binary strings in order to decode each string of binary into explicit information about the four parts which are: Multidimensional Minimization Training algorithms (MMT_{algo}), the network structure (**struct**), the Activation Function type of the network (**AF**) and the NN Training Parameters (**TP**). All of the explicit information goes to the internal function namely “NN train”. Thus, the optimized parameters with specific topology are trained. The RMSE indicator for each individual is calculated after each training and is sent to the internal function namely the “GA fitness”. The fitness is simply the value that the GA tries to minimize. For this study, the fitness of each individual string is equal to the RMSE given by the equation:

$$\text{Fitness} = \text{RMSE} \quad (5.6)$$

To perform the GA “selection”, the internal function selects the new groups of strings based on this fitness which constitute the (\mathbf{X}_{par}) parents of the next generation of the GA. Each string is selected based on the probability of reproduction which is usually proportional to the fitness of each string. Then, these strings are subjected to crossover and mutation operations of the GA, followed by the formation of the final population (\mathbf{X}_{nw}). This process is repeated until the (\mathbf{G}_n) is reached to the maximum limit. The whole process is ended by returning the value that gave the minimum fitness (minimum RMSE) to the user as (Best RMSE).

More details about the application of the proposed hybrid IMS for the NN topology combination and boiler operation variable optimization that were considered, are presented in chapter five. Implementation of the proposed scheme is performed by devising a MATLAB code. This code is structured by sequential integration of eight sub-codes. The eight MATLAB codes are shown in (Appendix B).

5.5 Summary

The development procedures of the adopted IMSs were highlighted and discussed. The ANN learning/training processes and the main topologies were identified. The proposed intelligent system’s advantages were stated. The detailed design steps of both proposed IMSs were discussed. The GA operators and the encoding process were identified.

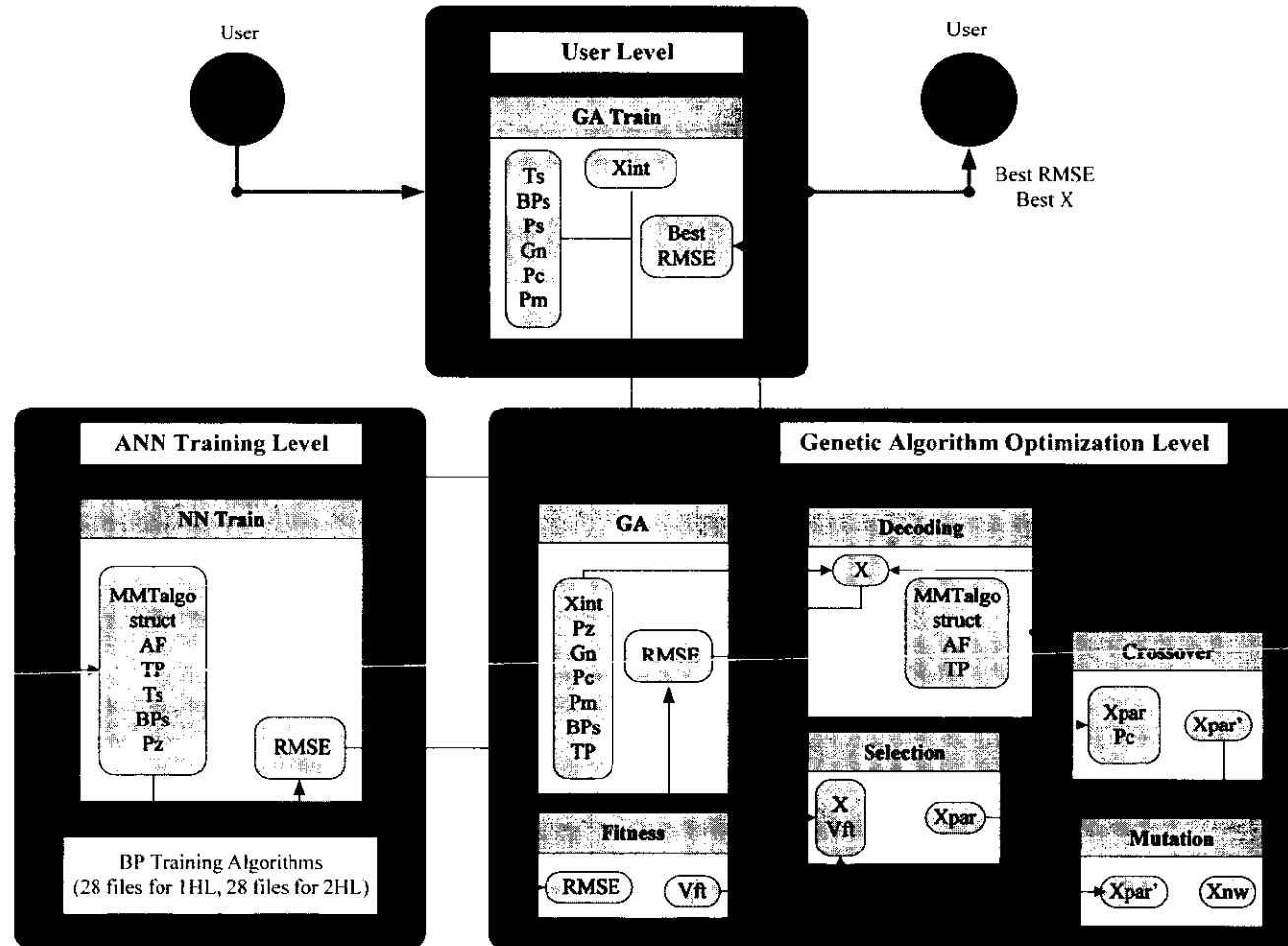


Figure 5.6 Schematic representation of proposed IMS-II

CHAPTER 6

ASSESSMENT OF RESULTS

6.1 Introduction

Two intelligent monitoring systems were proposed in chapter 3, to diagnosis the boiler trips. The Feed-forward ANN methodology was adopted for these two proposed intelligent systems. It was obvious that the construction of a boiler trip detection system should be based on the existence of a “faulty” operation by using data sets with fault existence only.

The two systems were coded in a MATLAB environment. The results of the proposed IMSs (training and validation) together with some additional information about the IMSs performance are presented in this chapter. The overall performance and adaptability of the proposed IMSs are discussed. The discussion is focused on determining the best NN topology combination together with the most influential boiler operation variables for each trip. Further more, ‘an action to be taken’ guide was proposed and presented to assist the plant operator in avoiding or reducing the trip occurrence.

This chapter is divided into three parts. The first deals with the results of the IMS-I. The second deals with the hybrid, IMS-II results. The third is the proposed ‘action to be taken’ guide.

6.2 Results of IMS-I

The training and validation results of the proposed IMS-I with some information about the IMS-I’ performance are discussed in the following sections:

6.2.1 IMS-I Training Process Results

The processes of the IMS-I training are described in section (5.3.1). A preliminary training process took place in order to find out the best NN topology combination. Several candidate NN topologies were trained for both a one hidden layer (1HL) case and a two hidden layers (2HL) case. Thirty-two boiler operation variables were considered as the number of NN inputs and the training results were compared based on the NN performance indicator (RMSE). Different numbers of neurons for each hidden layer cases ranging from one to ten neurons were tested. The conventional way of the NN was adopted for the training exploration. Seven real data sets were presented to IMS-I as training sets. These data sets are described in Table (6.1). The seven selected sets consisted of real data captured during faulty operation for seven boiler trips.

Table 6.1 Description of training data set

Data Set	Fault Status	Starting Date/Time	End Date/Time	No of Intervals	Interval that Fault Was Introduced
1	Trip 1	01.05.2008 21:41:00	02.05.2008 12:51:00	915	616
2	Trip 2	04.06.2008 15:15:00	05.06.2008 01:55:00	643	52
3	Trip 3	05.06.2008 18:29:00	06.06.2008 07:22:00	779	230
4	Trip 4	19.12.2008 12:33:00	19.12.2008 21:18:00	763	1
5	Trip 5	29.01.2009 16:16:00	30.01.2009 03:38:00	583	229
6	Trip 6	04.05.2009 20:12:00	05.05.2009 10:19:00	852	619
7	Trip 7	31.05.2009 12:01:00	31.05.2009 20:23:00	506	216

6.2.1.1 Training Results of 1HL

The results of the preliminary training process with the four multidimensional minimization back-propagation training algorithms for all boiler trips in the case of the one hidden layer NN showed that the logistic activation function for the input

node and the output node outperformed the other two activation function in most cases with exception of trip 3 and trip 6. More specifically, the performance achieved by all activation function probability combinations was proportional to the NN input value history. This can be noticed in Tables (6.2 through 6.8) , where the exact RMSE values achieved from all NN topology combinations for 1HL network are illustrated in detail.

Table 6.2 Trip (1) Scaled RMSE of 1-HL with NHLN nodes in the hidden layer for all activation functions probability combinations with all four training algorithms

IHLN	Levenberg-Marquardt									BFGS Quasi Newton								
	L+L	L+T	L+P	T+T	T+L	T+P	P+P	P+L	P+T	L+L	L+T	L+P	T+T	T+L	T+P	P+P	P+L	P+T
1	0.513	0.463	0.522	0.501	0.504	0.511	0.763	0.463	0.588	0.530	0.497	0.522	0.498	0.513	0.530	0.569	0.537	0.699
2	0.510	0.468	1.000	0.539	0.504	0.518	0.785	0.517	0.594	0.486	0.513	0.534	0.521	0.500	0.512	0.638	0.478	0.688
3	0.535	0.457	0.522	0.479	0.470	0.525	0.764	0.569	0.586	0.524	0.511	1.000	0.527	0.506	0.459	0.625	0.486	0.555
4	0.490	0.499	0.561	0.582	0.460	0.551	0.763	0.527	0.589	0.524	0.534	0.486	0.492	0.457	0.508	0.522	0.507	0.724
5	0.486	0.691	0.534	0.533	0.536	0.540	0.763	0.521	0.596	0.472	0.568	0.481	0.441	0.465	0.711	0.733	0.536	0.698
6	0.510	0.467	0.487	0.506	0.512	0.537	0.763	0.787	0.878	0.465	0.487	0.757	0.480	0.460	0.474	0.923	0.498	0.666
7	0.537	0.468	1.000	0.619	0.547	0.589	0.763	0.493	0.593	0.537	0.650	0.520	0.459	0.467	0.465	0.730	0.535	0.738
8	0.565	0.472	0.524	0.463	0.463	1.000	0.725	0.486	0.844	0.504	0.499	0.553	0.490	0.514	1.000	0.815	0.466	0.675
9	0.474	0.443	1.000	0.586	0.478	1.000	0.763	0.491	0.844	0.501	0.504	1.000	0.471	0.537	0.488	0.782	0.467	0.616
10	0.456	0.622	0.505	0.871	0.456	1.000	0.763	0.503	0.596	0.536	0.606	0.501	0.447	0.507	0.489	0.671	0.537	0.657
IHLN	Resilient Back-Propagation									Scaled Conjugate Gradient								
	L+L	L+T	L+P	T+T	T+L	T+P	P+P	P+L	P+T	L+L	L+T	L+P	T+T	T+L	T+P	P+P	P+L	P+T
1	0.513	0.583	0.541	0.526	0.536	0.669	0.580	0.534	0.585	0.449	0.513	0.542	0.500	0.517	0.515	0.562	0.450	0.562
2	0.537	0.560	0.842	0.637	0.507	0.546	0.558	0.535	0.511	0.462	0.507	0.538	0.613	0.518	0.528	0.579	0.472	0.523
3	0.537	0.554	0.582	0.532	0.525	0.514	0.529	0.535	0.570	0.536	0.536	0.576	0.632	0.464	0.661	0.564	0.536	0.561
4	0.518	0.533	0.530	0.543	0.536	0.522	0.539	0.536	0.638	0.524	0.607	0.521	0.724	0.520	0.520	0.587	0.498	0.590
5	0.537	0.585	0.539	0.522	0.536	0.746	0.594	0.536	0.568	0.499	0.603	0.529	0.586	0.464	0.645	0.509	0.470	0.569
6	0.537	0.495	0.538	0.523	0.535	0.508	0.570	0.536	0.563	0.433	0.559	0.593	0.584	0.460	0.619	0.550	0.482	0.578
7	0.536	0.624	0.585	0.545	0.536	0.605	0.468	0.524	0.606	0.535	0.539	0.525	0.734	0.526	0.501	0.520	0.536	0.544
8	0.536	0.679	0.524	0.581	0.500	0.522	0.536	0.534	0.601	0.481	0.497	0.539	0.585	0.521	0.525	0.535	0.537	0.545
9	0.536	0.508	0.623	0.505	0.525	0.516	0.534	0.536	0.612	0.537	0.511	0.500	0.549	0.511	0.604	0.503	0.531	0.592
10	0.536	0.483	0.582	0.509	0.522	0.542	0.559	0.537	0.509	0.474	0.596	0.589	0.579	0.529	0.518	0.537	0.473	0.606

Table 6.3 Trip (2) Scaled RMSE of 1-HL with NHLN nodes in the hidden layer for all activation functions probability combinations with all four training algorithms

1HLN	Levenberg-Marquardt									BFGS Quasi Newton								
	L+L	L+T	L+P	T+T	T+L	T+P	P+P	P+L	P+T	L+L	L+T	L+P	T+T	T+L	T+P	P+P	P+L	P+T
1	0.331	0.328	0.434	0.328	0.335	0.333	0.378	0.338	0.373	0.324	0.340	0.333	0.331	0.324	0.324	0.323	0.387	0.317
2	0.343	0.342	0.323	0.340	0.343	0.343	0.378	0.343	0.939	0.342	0.333	0.325	0.339	0.333	0.325	0.332	0.360	0.319
3	0.343	0.399	0.341	0.343	0.342	0.364	0.378	0.338	0.373	0.322	0.347	0.326	0.325	0.323	0.325	0.313	0.317	0.335
4	0.311	0.444	0.356	0.343	0.343	0.343	0.378	0.341	0.373	0.324	0.328	0.656	0.320	0.326	0.616	0.322	0.367	0.369
5	0.343	0.343	0.343	0.314	0.329	0.337	0.378	0.338	0.939	0.333	0.939	0.551	0.333	0.343	0.325	0.356	0.343	0.336
6	0.343	0.499	0.566	0.378	0.343	0.343	0.378	0.338	0.373	0.325	0.340	0.329	0.331	0.342	0.347	0.340	0.341	0.939
7	0.338	0.344	0.344	0.351	0.343	0.400	0.378	0.338	0.397	0.335	0.316	0.326	0.326	0.332	0.330	0.339	0.381	0.939
8	0.343	0.373	0.413	0.343	0.343	0.343	0.378	0.335	0.939	0.335	0.337	0.479	0.321	0.343	0.347	0.355	0.366	0.352
9	0.343	0.338	0.315	0.408	0.343	0.357	0.378	0.343	0.373	0.335	0.315	0.749	0.353	0.340	0.344	0.368	0.364	0.333
10	0.343	0.341	0.363	0.347	0.340	0.343	0.378	0.343	0.373	0.311	0.373	0.311	0.324	0.334	0.325	0.373	0.343	0.359
1HLN	Resilient Back-Propagation									Scaled Conjugate Gradient								
	L+L	L+T	L+P	T+T	T+L	T+P	P+P	P+L	P+T	L+L	L+T	L+P	T+T	T+L	T+P	P+P	P+L	P+T
1	0.314	0.316	0.321	0.319	0.311	0.337	0.326	0.318	0.330	0.326	0.311	0.332	0.342	0.324	0.325	0.318	0.319	0.317
2	0.330	0.372	0.312	0.324	0.329	0.355	0.316	0.328	0.326	0.328	0.323	0.317	0.328	0.330	0.327	0.322	0.343	0.332
3	0.337	0.346	0.324	0.340	0.317	0.329	0.331	0.323	0.318	0.339	0.376	0.331	0.321	0.323	0.329	0.328	0.315	0.328
4	0.323	0.339	0.336	0.361	0.327	0.339	0.317	0.316	0.318	0.331	0.304	0.331	0.334	0.322	0.361	0.319	0.324	0.313
5	0.320	0.379	0.343	0.330	0.328	0.340	0.346	0.321	0.334	0.334	0.331	0.341	0.335	0.324	0.327	0.325	0.323	0.337
6	0.321	0.351	0.328	0.354	0.313	0.330	0.322	0.319	0.318	0.326	0.347	0.320	0.330	0.338	0.333	0.330	0.343	0.313
7	0.316	0.352	0.321	0.332	0.315	0.341	0.337	0.318	0.343	0.326	0.348	0.328	0.320	0.328	0.318	0.334	0.341	0.326
8	0.313	0.327	0.442	0.307	0.343	0.336	0.345	0.326	0.340	0.328	0.378	0.353	0.330	0.336	0.306	0.314	0.326	0.329
9	0.322	0.376	0.309	0.347	0.321	0.352	0.336	0.322	0.338	0.324	0.327	0.328	0.317	0.321	0.354	0.323	0.341	0.333
10	0.300	0.323	0.333	0.331	0.325	0.357	0.310	0.322	0.335	0.330	0.311	0.300	0.351	0.317	0.380	0.333	0.326	0.330

Table 6.4 Trip (3) Scaled RMSE of 1-HL with NHLN nodes in the hidden layer for all activation functions probability combinations with all four training algorithms

1HLN	Levenberg-Marquardt									BFGS Quasi Newton								
	L+L	L+T	L+P	T+T	T+L	T+P	P+P	P+L	P+T	L+L	L+T	L+P	T+T	T+L	T+P	P+P	P+L	P+T
1	0.321	0.268	0.272	0.272	0.272	0.289	0.268	0.221	0.296	0.184	0.368	0.468	0.492	0.368	0.154	0.486	0.361	0.395
2	0.635	0.368	0.616	0.616	0.361	0.742	0.269	0.221	0.296	0.684	0.174	0.490	0.478	0.491	0.486	0.352	0.361	0.261
3	0.562	0.785	0.534	0.534	0.537	0.732	0.273	0.221	0.298	0.406	0.476	0.458	0.781	0.455	0.614	0.285	0.361	0.322
4	0.356	0.531	1.000	1.000	0.725	0.607	0.269	0.221	0.296	0.610	0.693	0.616	0.249	0.775	0.674	0.372	0.232	0.358
5	0.757	0.704	1.000	1.000	0.858	0.750	0.269	0.253	0.296	0.505	0.700	0.435	0.488	0.587	0.520	0.340	0.361	0.932
6	0.686	0.930	0.818	0.818	0.884	1.000	0.269	0.221	0.296	0.361	0.741	0.504	0.619	0.562	0.249	0.312	0.361	0.437
7	0.573	0.713	1.000	1.000	0.822	1.000	0.269	0.361	0.296	0.573	0.572	0.468	0.561	0.459	1.000	0.304	0.259	0.932
8	0.887	0.931	1.000	1.000	0.860	1.000	0.270	0.221	0.296	0.612	0.774	0.580	0.659	0.406	0.523	0.346	0.361	0.932
9	0.743	0.900	0.837	0.837	0.790	1.000	0.269	0.221	0.299	0.578	0.562	0.727	0.611	0.778	0.429	0.337	0.245	0.344
10	0.648	0.932	1.000	1.000	0.680	1.000	0.269	0.221	0.296	0.449	0.574	0.412	0.640	0.515	1.000	0.318	0.224	0.429
1HLN	Resilient Back-Propagation									Scaled Conjugate Gradient								
	L+L	L+T	L+P	T+T	T+L	T+P	P+P	P+L	P+T	L+L	L+T	L+P	T+T	T+L	T+P	P+P	P+L	P+T
1	0.558	0.439	0.499	0.524	0.539	0.525	0.464	0.703	0.553	0.559	0.932	0.558	0.567	0.368	0.543	0.241	0.330	0.285
2	0.764	0.572	0.614	0.560	0.355	0.719	0.481	0.462	0.584	0.548	0.256	0.939	0.711	0.219	0.318	0.321	0.160	0.353
3	0.653	0.458	0.581	0.465	0.494	0.564	0.301	0.559	0.450	0.509	0.330	0.674	0.702	0.561	0.541	0.255	0.246	0.413
4	0.505	0.604	0.559	0.548	0.505	0.448	0.581	0.544	0.472	0.190	0.326	0.461	0.536	0.599	0.339	0.319	0.213	0.424
5	0.595	0.619	0.593	0.485	0.355	0.725	0.432	0.458	0.600	0.585	0.431	0.310	0.691	0.467	0.555	0.250	0.341	0.461
6	0.565	0.702	0.485	0.488	0.394	0.722	0.461	0.447	0.593	0.462	0.603	0.722	0.592	0.408	0.646	0.240	0.186	0.320
7	0.602	0.542	0.641	0.635	0.537	0.653	0.797	0.490	0.498	0.646	0.932	0.877	0.773	0.666	0.602	0.316	0.215	0.330
8	0.711	0.512	0.549	0.611	0.781	0.759	0.427	0.737	0.531	0.513	0.477	0.804	0.615	0.465	0.895	0.420	0.269	0.317
9	0.479	0.647	0.601	0.574	0.633	0.645	0.736	0.636	0.486	0.549	0.387	0.667	0.437	0.600	0.966	0.354	0.393	0.400
10	0.631	0.489	0.553	0.647	0.702	0.620	0.334	0.574	0.517	0.584	0.555	0.979	0.509	0.442	0.371	0.323	0.173	0.324

Table 6.5 Trip (4) Scaled RMSE of 1-HL with NHLN nodes in the hidden layer for all activation functions probability combinations with all four training algorithms

IHLN	Levenberg-Marquardt									BFGS Quasi Newton								
	L+L	L+T	L+P	T+T	T+L	T+P	P+P	P+L	P+T	L+L	L+T	L+P	T+T	T+L	T+P	P+P	P+L	P+T
1	0.301	0.262	0.286	0.242	0.259	0.262	0.300	0.262	0.322	0.171	0.153	0.206	0.274	0.274	0.176	0.172	0.262	0.172
2	0.352	0.261	0.211	0.262	0.161	0.197	0.300	0.262	0.297	0.274	0.142	0.255	0.147	0.254	0.274	0.282	0.206	0.337
3	0.260	0.262	0.242	0.211	0.339	0.266	0.300	0.262	0.322	0.262	0.133	0.210	0.122	0.254	0.166	0.325	0.167	0.253
4	0.243	0.193	0.143	0.261	0.262	0.113	0.301	0.262	0.297	0.136	0.195	0.165	0.254	0.165	0.143	0.333	0.262	0.965
5	0.272	0.121	0.142	0.219	0.249	0.177	0.300	0.262	0.297	0.212	0.133	0.148	0.124	0.227	0.274	0.320	0.202	0.315
6	0.269	0.375	0.504	0.141	0.167	1.000	0.300	0.262	0.319	0.092	0.148	0.294	0.147	0.125	0.225	0.293	0.169	0.221
7	0.284	0.153	0.154	0.295	0.283	0.232	0.300	0.262	0.297	0.104	0.164	0.205	0.139	0.092	0.126	0.320	0.231	0.325
8	0.262	0.392	0.273	0.136	0.262	1.000	0.300	0.262	0.297	0.127	0.200	0.138	0.144	0.106	0.155	0.345	0.156	0.339
9	0.171	0.473	0.351	0.258	0.147	0.672	0.300	0.262	0.297	0.152	0.130	0.151	0.182	0.158	0.145	0.314	0.262	0.965
10	0.188	0.270	1.000	0.318	0.262	0.179	0.300	0.262	0.297	0.187	0.115	0.205	0.122	0.099	0.122	0.330	0.262	0.965
IHLN	Resilient Back-Propagation									Scaled Conjugate Gradient								
	L+L	L+T	L+P	T+T	T+L	T+P	P+P	P+L	P+T	L+L	L+T	L+P	T+T	T+L	T+P	P+P	P+L	P+T
1	0.142	0.208	0.155	0.199	0.254	0.205	0.168	0.137	0.186	0.274	0.215	0.202	0.149	0.274	0.144	0.154	0.147	0.185
2	0.134	0.143	0.159	0.177	0.206	0.149	0.173	0.187	0.168	0.215	0.220	0.156	0.145	0.206	0.155	0.180	0.137	0.177
3	0.121	0.152	0.209	0.137	0.129	0.143	0.191	0.145	0.168	0.274	0.145	0.129	0.205	0.143	0.124	0.184	0.169	0.178
4	0.133	0.153	0.136	0.186	0.142	0.126	0.205	0.138	0.178	0.131	0.177	0.130	0.148	0.144	0.136	0.186	0.182	0.187
5	0.130	0.135	0.153	0.212	0.122	0.156	0.189	0.120	0.170	0.119	0.116	0.141	0.173	0.149	0.159	0.193	0.140	0.182
6	0.124	0.130	0.132	0.189	0.110	0.119	0.163	0.144	0.167	0.116	0.114	0.135	0.161	0.119	0.153	0.153	0.262	0.192
7	0.110	0.130	0.148	0.161	0.146	0.218	0.152	0.155	0.240	0.093	0.137	0.157	0.126	0.135	0.192	0.170	0.153	0.184
8	0.143	0.161	0.139	0.139	0.136	0.129	0.258	0.154	0.183	0.148	0.179	0.144	0.151	0.131	0.145	0.151	0.164	0.152
9	0.198	0.188	0.166	0.143	0.144	0.142	0.212	0.130	0.163	0.090	0.127	0.172	0.156	0.134	0.153	0.161	0.149	0.202
10	0.137	0.127	0.110	0.154	0.102	0.146	0.153	0.149	0.191	0.156	0.196	0.124	0.169	0.194	0.179	0.189	0.141	0.189

Table 6.6 Trip (5) Scaled RMSE of 1-HL with NHLN nodes in the hidden layer for all activation functions probability combinations with all four training algorithms

1HLN	Levenberg-Marquardt									BFGS Quasi Newton								
	L+L	L+T	L+P	T+T	T+L	T+P	P+P	P+L	P+T	L+L	L+T	L+P	T+T	T+L	T+P	P+P	P+L	P+T
1	0.464	0.596	0.613	0.471	0.594	0.611	0.595	0.675	0.600	0.447	0.558	0.531	0.418	0.464	0.455	0.560	0.468	0.524
2	0.503	0.595	0.617	0.598	0.603	1.000	0.595	0.654	0.600	0.538	0.524	0.480	0.562	0.464	0.451	0.559	0.503	0.571
3	0.503	0.670	0.589	0.555	0.627	0.675	0.595	0.665	0.600	0.461	0.448	0.830	0.469	0.521	0.450	0.577	0.503	0.520
4	0.503	0.543	0.556	0.618	0.630	1.000	0.599	0.613	0.600	0.471	0.411	0.462	0.537	0.460	0.417	0.521	0.503	0.549
5	0.592	0.514	0.588	0.670	0.587	0.404	0.604	0.640	0.600	0.462	0.408	0.486	0.481	0.471	0.464	0.537	0.503	0.864
6	0.503	0.481	0.591	0.502	0.583	0.516	0.595	0.654	0.600	0.458	0.494	0.534	0.507	0.513	0.470	0.541	0.503	0.864
7	0.503	0.671	0.605	0.574	0.648	0.549	0.595	0.584	0.600	0.477	0.429	0.530	0.494	0.512	0.457	0.591	0.453	0.525
8	0.503	0.748	1.000	0.506	0.659	0.456	0.595	0.663	0.600	0.561	0.441	0.608	0.538	0.480	0.459	0.590	0.503	0.573
9	0.507	0.411	0.740	0.629	0.570	1.000	0.595	0.589	0.864	0.602	0.465	0.468	0.616	0.464	0.564	0.589	0.573	0.583
10	0.546	0.512	0.506	0.625	0.606	1.000	0.595	0.662	0.600	0.503	0.547	0.646	0.547	0.459	0.593	0.579	0.482	0.864
1HLN	Resilient Back-Propagation									Scaled Conjugate Gradient								
	L+L	L+T	L+P	T+T	T+L	T+P	P+P	P+L	P+T	L+L	L+T	L+P	T+T	T+L	T+P	P+P	P+L	P+T
1	0.440	0.406	0.464	0.466	0.469	0.499	0.414	0.463	0.429	0.464	0.463	0.420	0.443	0.464	0.429	0.435	0.428	0.534
2	0.435	0.492	0.447	0.454	0.416	0.489	0.403	0.454	0.409	0.464	0.464	0.437	0.451	0.495	0.433	0.494	0.447	0.521
3	0.371	0.446	0.536	0.427	0.439	0.492	0.415	0.462	0.414	0.459	0.459	0.459	0.464	0.558	0.420	0.520	0.503	0.448
4	0.439	0.457	0.449	0.458	0.444	0.566	0.425	0.472	0.431	0.503	0.462	0.463	0.475	0.504	0.486	0.420	0.436	0.510
5	0.482	0.428	0.442	0.424	0.461	0.401	0.436	0.471	0.417	0.463	0.422	0.537	0.448	0.472	0.425	0.535	0.464	0.538
6	0.467	0.500	0.523	0.418	0.559	0.429	0.410	0.464	0.419	0.503	0.506	0.469	0.446	0.443	0.464	0.460	0.444	0.529
7	0.456	0.482	0.448	0.440	0.460	0.501	0.396	0.473	0.422	0.490	0.446	0.445	0.479	0.466	0.446	0.485	0.455	0.463
8	0.416	0.491	0.487	0.478	0.527	0.433	0.418	0.467	0.419	0.471	0.480	0.469	0.522	0.468	0.471	0.429	0.503	0.444
9	0.447	0.542	0.418	0.464	0.449	0.463	0.476	0.465	0.409	0.491	0.480	0.513	0.459	0.522	0.467	0.416	0.446	0.459
10	0.474	0.414	0.526	0.439	0.565	0.573	0.431	0.467	0.437	0.469	0.467	0.497	0.491	0.476	0.463	0.480	0.467	0.458

Table 6.7 Trip (6) Scaled RMSE of 1-HL with NHLN nodes in the hidden layer for all activation functions probability combinations with all four training algorithms

1HLN	Levenberg-Marquardt									BFGS Quasi Newton								
	L+L	L+T	L+P	T+T	T+L	T+P	P+P	P+L	P+T	L+L	L+T	L+P	T+T	T+L	T+P	P+P	P+L	P+T
1	0.345	0.324	0.342	0.342	0.324	0.342	1.000	0.345	0.939	0.326	0.324	0.326	0.374	0.326	0.301	0.289	0.294	1.000
2	0.279	0.391	0.348	0.417	0.345	0.342	1.000	0.345	0.838	0.324	0.287	0.342	0.405	0.328	0.324	1.000	0.420	0.939
3	0.345	0.417	0.472	0.939	0.345	0.345	1.000	0.345	0.838	0.405	0.403	0.402	0.839	0.326	1.000	1.000	0.346	0.826
4	0.345	0.345	0.477	0.416	0.345	1.000	1.000	0.345	0.829	0.346	0.340	0.466	0.808	0.326	1.000	1.000	0.345	0.831
5	0.345	0.399	1.000	0.420	0.340	1.000	1.000	0.345	0.838	0.346	0.477	0.588	0.413	0.346	0.416	1.000	0.345	0.838
6	0.345	0.833	1.000	0.407	0.345	1.000	1.000	0.345	0.835	0.345	0.725	1.000	0.286	0.345	0.911	1.000	0.345	0.839
7	0.415	0.388	1.000	0.436	0.347	1.000	1.000	0.345	0.838	0.345	0.464	1.000	0.486	0.346	1.000	1.000	0.345	0.939
8	0.345	0.358	0.813	0.477	0.349	1.000	1.000	0.345	0.838	0.326	0.462	1.000	0.417	0.346	1.000	1.000	0.346	0.935
9	0.346	0.373	1.000	0.477	0.346	1.000	1.000	0.345	0.838	0.345	0.284	1.000	0.429	0.345	1.000	1.000	0.345	0.833
10	0.415	0.671	1.000	0.358	0.270	1.000	1.000	0.345	0.838	0.345	0.840	1.000	0.484	0.346	1.000	1.000	0.345	0.829
1HLN	Resilient Back-Propagation									Scaled Conjugate Gradient								
	L+L	L+T	L+P	T+T	T+L	T+P	P+P	P+L	P+T	L+L	L+T	L+P	T+T	T+L	T+P	P+P	P+L	P+T
1	0.340	0.384	0.438	0.409	0.343	0.711	0.920	0.416	0.713	0.389	0.454	0.323	0.805	0.417	0.353	0.292	0.346	0.336
2	0.352	0.386	0.644	0.464	0.326	0.326	0.847	0.414	0.820	0.398	0.473	0.326	0.360	0.298	0.370	0.339	0.352	0.694
3	0.346	0.333	0.437	0.379	0.374	0.265	0.430	0.413	0.554	0.324	0.614	0.462	0.410	0.270	0.284	1.000	0.337	1.000
4	0.413	0.366	0.518	0.347	0.332	0.419	0.716	0.380	0.733	0.345	0.565	0.356	0.389	0.346	0.659	0.792	0.347	0.756
5	0.329	0.280	0.282	0.515	0.311	0.579	0.867	0.397	0.382	0.350	0.745	0.603	0.473	0.336	0.439	1.000	0.357	0.734
6	0.465	0.570	0.475	0.337	0.413	0.839	0.677	0.346	0.368	0.407	0.325	0.342	0.294	0.321	0.316	0.577	0.345	0.826
7	0.356	0.446	0.338	0.268	0.279	0.580	1.000	0.389	0.635	0.346	0.462	0.843	0.394	0.398	1.000	0.901	0.347	0.767
8	0.374	0.429	0.757	0.399	0.416	0.346	0.375	0.410	0.535	0.319	0.353	0.469	0.398	0.350	0.753	0.853	0.349	0.576
9	0.378	0.467	0.677	0.374	0.293	1.000	0.965	0.312	0.798	0.292	0.470	0.393	0.397	0.340	0.614	0.593	0.345	0.481
10	0.339	0.422	0.449	0.327	0.345	1.000	0.685	0.347	0.266	0.331	0.571	0.484	0.739	0.275	0.515	0.751	0.345	0.364

Table 6.8 Trip (7) Scaled RMSE of 1-HL with NHLN nodes in the hidden layer for all activation functions probability combinations with all four training algorithms

1HLN	Levenberg-Marquardt									BFGS Quasi Newton								
	L+L	L+T	L+P	T+T	T+L	T+P	P+P	P+L	P+T	L+L	L+T	L+P	T+T	T+L	T+P	P+P	P+L	P+T
1	0.331	0.328	0.434	0.328	0.335	0.333	0.378	0.338	0.373	0.324	0.340	0.333	0.331	0.324	0.324	0.323	0.387	0.317
2	0.343	0.342	0.323	0.340	0.343	0.343	0.378	0.343	0.939	0.342	0.333	0.325	0.339	0.333	0.325	0.332	0.360	0.319
3	0.343	0.399	0.341	0.343	0.342	0.364	0.378	0.338	0.373	0.322	0.347	0.326	0.325	0.323	0.325	0.313	0.317	0.335
4	0.311	0.444	0.356	0.343	0.343	0.343	0.378	0.341	0.373	0.324	0.328	0.656	0.320	0.326	0.616	0.322	0.367	0.369
5	0.343	0.343	0.343	0.314	0.329	0.337	0.378	0.338	0.939	0.333	0.939	0.551	0.333	0.343	0.325	0.356	0.343	0.336
6	0.343	0.499	0.566	0.378	0.343	0.343	0.378	0.338	0.373	0.325	0.340	0.329	0.331	0.342	0.347	0.340	0.341	0.939
7	0.338	0.344	0.344	0.351	0.343	0.400	0.378	0.338	0.397	0.335	0.316	0.326	0.326	0.332	0.330	0.339	0.381	0.939
8	0.343	0.373	0.413	0.343	0.343	0.343	0.378	0.335	0.939	0.335	0.337	0.479	0.321	0.343	0.347	0.355	0.366	0.352
9	0.343	0.338	0.315	0.408	0.343	0.357	0.378	0.343	0.373	0.335	0.315	0.749	0.353	0.340	0.344	0.368	0.364	0.333
10	0.343	0.341	0.363	0.347	0.340	0.343	0.378	0.343	0.373	0.311	0.373	0.311	0.324	0.334	0.325	0.373	0.343	0.359
1HLN	Resilient Back-Propagation									Scaled Conjugate Gradient								
	L+L	L+T	L+P	T+T	T+L	T+P	P+P	P+L	P+T	L+L	L+T	L+P	T+T	T+L	T+P	P+P	P+L	P+T
1	0.314	0.316	0.321	0.319	0.311	0.337	0.326	0.318	0.330	0.326	0.311	0.332	0.342	0.324	0.325	0.318	0.319	0.317
2	0.330	0.372	0.312	0.324	0.329	0.355	0.316	0.328	0.326	0.328	0.323	0.317	0.328	0.330	0.327	0.322	0.343	0.332
3	0.337	0.346	0.324	0.340	0.317	0.329	0.331	0.323	0.318	0.339	0.376	0.331	0.321	0.323	0.329	0.328	0.315	0.328
4	0.323	0.339	0.336	0.361	0.327	0.339	0.317	0.316	0.318	0.331	0.304	0.331	0.334	0.322	0.361	0.319	0.324	0.313
5	0.320	0.379	0.343	0.330	0.328	0.340	0.346	0.321	0.334	0.334	0.331	0.341	0.335	0.324	0.327	0.325	0.323	0.337
6	0.321	0.351	0.328	0.354	0.313	0.330	0.322	0.319	0.318	0.326	0.347	0.320	0.330	0.338	0.333	0.330	0.343	0.313
7	0.316	0.352	0.321	0.332	0.315	0.341	0.337	0.318	0.343	0.326	0.348	0.328	0.320	0.328	0.318	0.334	0.341	0.326
8	0.313	0.327	0.442	0.307	0.343	0.336	0.345	0.326	0.340	0.328	0.378	0.353	0.330	0.336	0.306	0.314	0.326	0.329
9	0.322	0.376	0.309	0.347	0.321	0.352	0.336	0.322	0.338	0.324	0.327	0.328	0.317	0.321	0.354	0.323	0.341	0.333
10	0.300	0.323	0.333	0.331	0.325	0.357	0.310	0.322	0.335	0.330	0.311	0.300	0.351	0.317	0.380	0.333	0.326	0.330

The best RMSE of each training algorithm is highlighted in bold, while the overall best RMSE is also underlined. In most cases of different numbers of nodes in the hidden layer, the “Resilient Back-Propagation” and “Scaled Conjugate Gradient” outperforms the other back-propagation algorithms (with the exception of trip 3). In general, the NN performance, based on RMSE values get worse as:

“Scaled Conjugate Gradient” → “BFGS Quasi Newton” → “Levenberg-Marquardt”

While, based on the generalized suitability point of view as:

“Resilient back-propagation” → “Scaled Conjugate Gradient” → “BFGS Quasi Newton”

The analysis of preliminary results showed that the “Scaled Conjugate Gradient” training algorithm gave a smaller error than the other three training algorithms for trip 4 among all boiler trips considered for this study. The best NN topology combination of 1HL for all boiler trips is therefore as illustrated in Table (6.9).

Table 6.9 The best ANN topologies combination of 1HL for all boiler operation trips

Trip	NHL	RMSE	Architecture	Activation Function	Training Algorithm
1	1HL	0.433	6HL1	L+L	Scaled Conjugate Gradient
2	1HL	0.300	10HL1	L+L	Resilient back-propagation
3	1HL	0.154	1HL1	T+P	BFGS Quasi Newton
4	1HL	0.090	9HL1	L+L	Scaled Conjugate Gradient
5	1HL	0.371	3HL1	L+L	Resilient Back-Propagation
6	1HL	0.265	3HL1	T+P	Resilient Back-Propagation
7	1HL	0.300	10HL1	L+L	Resilient Back-Propagation

6.2.1.2 Training Results of 2HL

Tables (6.10 through 6.23) show the RMSE results of several two hidden layers NN topologies for all boiler trips. Each table has two sections, one for each of the four multidimensional minimization training algorithms is considered. In each section the minimum RMSE achieved by the corresponding training algorithm is in bold. In addition, in each table the minimum of these two RMSE is underlined. The underlined RMSE of each table corresponds to the minimum error value achieved by the specific training algorithm for that trip.

The NN preliminary training results of the 2HL showed that the linear summation function for the input node, the logistic activation function for the hidden node and the output node outperformed the hyperbolic tangent activation function in most cases with the exception of trip 7. More specifically, the performance achieved by all activation function probability combinations was found to be proportional to the NN input value history.

The comparison showed that the Levenberg-Marquardt training algorithm gave a smaller error value than the other three training algorithms for trips 4 and 7 respectively. For trips 3 and 5, the smaller error value achieved by the BFGS Quasi Newton training algorithm and the Resilient Back-Propagation outperformed the other three training algorithms for trip 2. Also, it can be noticed that the Scaled Conjugate Gradient gave the best NN combination with a minimum error value for trips 1 and 6.

Table 6.10 Scaled RMSE of 2-HL structure (with N1 and N2 in each layer) using Levenberg-Marquardt and Resilient Back-Propagation training algorithms for trip (1)

T+P+T		Levenberg-Marquardt									
N1	N2	1	2	3	4	5	6	7	8	9	10
1		0.501	0.511	0.494	0.516	0.491	0.477	0.516	0.516	0.509	0.515
2		0.535	0.537	0.537	0.491	0.516	0.524	0.566	0.537	0.716	0.502
3		0.495	0.641	0.513	0.536	0.555	0.474	0.687	0.557	0.484	0.478
4		0.741	0.505	0.650	0.464	0.565	0.496	0.481	0.486	0.482	0.522
5		0.459	0.531	0.480	0.530	0.578	0.523	0.511	0.440	0.495	0.468
6		0.466	0.494	0.475	0.595	0.773	0.503	0.721	0.651	0.886	0.472
7		0.544	0.480	0.514	0.650	0.622	0.616	0.520	0.707	0.637	0.487
8		0.756	0.765	0.719	0.844	0.429	0.615	0.844	0.492	0.522	0.526
9		0.498	0.640	0.694	0.624	0.596	0.476	0.493	1.005	0.447	0.575
10		0.495	0.902	0.458	0.470	0.524	0.562	0.684	0.653	0.527	0.510
T+T+L		Resilient Back-Propagation									
N1	N2	1	2	3	4	5	6	7	8	9	10
1		0.524	0.533	0.535	0.531	0.529	0.513	0.506	0.529	0.537	0.534
2		0.512	0.527	0.533	0.513	0.536	0.532	0.536	0.536	0.531	0.534
3		0.513	0.512	0.535	0.536	0.535	0.532	0.522	0.537	0.529	0.539
4		0.513	0.533	0.531	0.536	0.519	0.536	0.536	0.536	0.537	0.537
5		0.536	0.535	0.524	0.533	0.533	0.536	0.536	0.536	0.528	0.514
6		0.537	0.512	0.522	0.530	0.535	0.537	0.506	0.448	0.536	0.528
7		0.536	0.536	0.535	0.537	0.536	0.529	0.534	0.496	0.483	0.537
8		0.537	0.533	0.510	0.537	0.536	0.487	0.519	0.532	0.473	0.535
9		0.531	0.537	0.534	0.535	0.446	0.528	0.537	0.534	0.536	0.537
10		0.537	0.533	0.533	0.536	0.535	0.532	0.531	0.537	0.537	0.508

Table 6.11 Scaled RMSE of 2-HL structure (with N1 and N2 in each layer) using Scaled Conjugate Gradient and BFGS Quasi Newton training algorithms for trip (1)

P+T+L		Scaled Conjugate Gradient									
N1	N2	1	2	3	4	5	6	7	8	9	10
1		0.513	0.544	0.507	0.505	0.525	0.519	0.530	0.514	0.527	0.465
2		0.529	0.535	0.513	0.528	0.507	0.532	0.546	0.439	0.459	0.518
3		0.513	0.513	0.474	0.525	0.579	0.526	0.460	0.497	0.527	0.508
4		0.452	0.533	0.537	0.523	0.508	0.528	0.513	0.534	0.515	0.522
5		0.513	0.504	0.515	0.513	0.513	0.537	0.534	0.524	0.503	0.506
6		0.527	0.513	0.463	0.467	0.525	0.525	0.475	0.515	0.454	0.496
7		0.513	0.535	0.515	0.536	0.529	0.529	0.503	0.510	0.435	0.448
8		0.513	0.517	0.471	0.491	0.528	0.472	0.502	0.455	0.531	0.498
9		0.513	0.522	0.534	0.514	0.528	0.531	0.531	0.531	0.535	0.517
10		0.513	0.460	0.535	0.531	0.475	0.533	0.510	0.507	0.531	0.515
T+T+T		BFGS Quasi Newton									
N1	N2	1	2	3	4	5	6	7	8	9	10
1		0.534	0.508	0.537	0.457	0.872	0.610	0.750	0.884	0.533	0.538
2		0.535	0.464	0.536	0.513	0.838	0.561	0.452	0.451	0.530	0.462
3		0.525	0.531	0.526	0.487	0.460	0.533	0.494	0.535	0.496	0.491
4		0.465	0.466	0.492	0.520	0.468	0.471	0.505	0.530	0.542	0.458
5		0.479	0.435	0.536	0.521	0.530	0.536	0.486	0.472	0.470	0.551
6		0.501	0.467	0.489	0.537	0.562	0.556	0.467	0.446	0.487	0.537
7		0.610	0.537	0.464	0.468	0.554	0.506	0.595	0.619	0.539	0.515
8		0.535	0.463	0.551	0.508	0.517	0.496	0.481	0.508	0.516	0.490
9		0.493	0.475	0.504	0.474	0.587	0.542	0.473	0.483	0.519	0.532
10		0.462	0.486	0.515	0.654	0.463	0.465	0.583	0.524	0.467	0.528

Table 6.12 Scaled RMSE of 2-HL structure (with N1 and N2 in each layer) using Levenberg-Marquardt and Resilient Back-Propagation training algorithms for trip (2)

T+L+L		Levenberg-Marquardt									
N1	N2	1	2	3	4	5	6	7	8	9	10
1		0.341	0.337	0.340	0.323	0.327	0.343	0.337	0.324	0.342	0.359
2		0.330	0.343	0.343	0.343	0.332	0.343	0.343	0.343	0.343	0.343
3		0.335	0.342	0.335	0.330	0.330	0.343	0.341	0.345	0.343	0.343
4		0.317	0.343	0.336	0.343	0.343	0.343	0.340	0.343	0.343	0.343
5		0.343	0.343	0.360	0.327	0.337	0.343	0.343	0.343	0.343	0.328
6		0.331	0.346	0.339	0.343	0.318	0.337	0.343	0.354	0.343	0.343
7		0.340	0.343	0.343	0.377	0.343	0.343	0.337	0.326	0.354	0.343
8		0.399	0.343	0.312	0.357	0.343	0.343	0.343	0.329	0.343	0.343
9		0.297	0.329	0.343	0.343	0.307	0.343	0.343	0.343	0.343	0.336
10		0.343	0.343	0.329	0.332	0.333	0.335	0.336	0.326	0.343	0.343
L+T+L		Resilient Back-Propagation									
N1	N2	1	2	3	4	5	6	7	8	9	10
1		0.324	0.320	0.319	0.338	0.327	0.328	0.316	0.315	0.330	0.325
2		0.320	0.321	0.315	0.337	0.331	0.315	0.330	0.326	0.323	0.292
3		0.302	0.330	0.334	0.321	0.328	0.315	0.320	0.327	0.327	0.292
4		0.323	0.328	0.315	0.311	0.314	0.322	0.330	0.322	0.317	0.334
5		0.323	0.318	0.328	0.305	0.333	0.327	0.330	0.321	0.326	0.326
6		0.335	0.301	0.327	0.336	0.339	0.306	0.339	0.332	0.331	0.327
7		0.326	0.343	0.332	0.333	0.334	0.340	0.324	0.323	0.332	0.340
8		0.331	0.319	0.328	0.325	0.323	0.315	0.316	0.340	0.321	0.316
9		0.316	0.338	0.328	0.335	0.325	0.336	0.329	0.336	0.341	0.313
10		0.330	0.316	0.339	0.332	0.343	0.338	0.328	0.310	0.340	0.334

Table 6.13 Scaled RMSE of 2-HL structure (with N1 and N2 in each layer) using Scaled Conjugate Gradient and BFGS Quasi Newton training algorithms for trip (2)

L+T+L		Scaled Conjugate Gradient									
N1	N2	1	2	3	4	5	6	7	8	9	10
1		0.310	0.340	0.335	0.323	0.323	0.320	0.319	0.324	0.320	0.318
2		0.327	0.323	0.332	0.324	0.337	0.330	0.335	0.322	0.340	0.329
3		0.322	0.340	0.331	0.323	0.326	0.330	0.333	0.322	0.332	0.317
4		0.325	0.325	0.323	0.323	0.324	0.338	0.313	0.317	0.313	0.317
5		0.325	0.318	0.337	0.325	0.322	0.325	0.319	0.331	0.323	0.334
6		0.316	0.324	0.320	0.315	0.343	0.323	0.331	0.311	0.328	0.326
7		0.325	0.331	0.299	0.332	0.318	0.321	0.325	0.320	0.338	0.325
8		0.327	0.326	0.328	0.306	0.329	0.327	0.324	0.294	0.326	0.336
9		0.324	0.326	0.322	0.329	0.322	0.337	0.323	0.326	0.338	0.337
10		0.325	0.322	0.330	0.334	0.311	0.330	0.311	0.321	0.308	0.313
T+T+T		BFGS Quasi Newton									
N1	N2	1	2	3	4	5	6	7	8	9	10
1		0.324	0.331	0.324	0.324	0.319	0.322	0.294	0.325	0.383	0.326
2		0.340	0.333	0.309	0.336	0.324	0.332	0.345	0.324	0.352	0.331
3		0.328	0.325	0.341	0.325	0.330	0.331	0.335	0.326	0.324	0.391
4		0.325	0.331	0.325	0.337	0.323	0.328	0.334	0.349	0.338	0.339
5		0.322	0.319	0.332	0.358	0.319	0.342	0.330	0.343	0.333	0.348
6		0.325	0.332	0.339	0.333	0.327	0.328	0.325	0.318	0.333	0.341
7		0.332	0.366	0.334	0.338	0.305	0.342	0.329	0.338	0.325	0.339
8		0.342	0.324	0.328	0.343	0.341	0.333	0.325	0.324	0.331	0.356
9		0.332	0.323	0.337	0.307	0.337	0.336	0.361	0.342	0.345	0.345
10		0.327	0.338	0.307	0.330	0.318	0.328	0.375	0.340	0.380	0.343

Table 6.14 Scaled RMSE of 2-HL structure (with N1 and N2 in each layer) using Levenberg-Marquardt and Resilient Back-Propagation training algorithms for trip (3)

T+P+L		Levenberg-Marquardt									
N1	N2	1	2	3	4	5	6	7	8	9	10
1		0.241	0.588	0.703	0.283	0.368	0.686	0.696	0.576	0.327	0.244
2		0.530	0.751	0.809	0.136	0.784	0.723	0.604	0.665	0.361	0.738
3		0.787	0.920	0.617	0.796	0.721	0.305	0.896	0.764	0.633	0.537
4		0.247	0.784	0.701	0.891	0.361	0.685	0.357	0.884	0.797	0.460
5		0.387	0.539	0.711	0.658	0.361	0.376	0.717	0.669	0.666	0.780
6		0.552	0.361	0.932	0.361	0.685	0.570	0.804	0.576	0.627	0.454
7		0.475	0.759	0.735	0.932	0.329	0.419	0.477	0.908	0.812	0.925
8		0.922	0.932	0.361	0.663	0.932	0.868	0.667	0.354	0.671	0.721
9		0.680	0.621	0.784	0.844	0.604	0.581	0.830	0.777	0.599	0.579
10		0.834	0.789	0.931	0.622	0.361	0.467	0.382	0.882	0.749	0.887
P+T+L		Resilient Back-Propagation									
N1	N2	1	2	3	4	5	6	7	8	9	10
1		0.420	0.689	0.615	0.614	0.511	0.439	0.368	0.368	0.312	0.371
2		0.576	0.439	0.191	0.478	0.497	0.468	0.638	0.517	0.554	0.512
3		0.611	0.466	0.606	0.486	0.332	0.517	0.459	0.550	0.599	0.510
4		0.475	0.365	0.588	0.665	0.569	0.557	0.624	0.477	0.726	0.479
5		0.577	0.548	0.656	0.564	0.646	0.577	0.702	0.697	0.728	0.436
6		0.494	0.531	0.578	0.547	0.498	0.474	0.771	0.495	0.644	0.432
7		0.355	0.523	0.531	0.600	0.458	0.558	0.551	0.528	0.760	0.601
8		0.414	0.491	0.552	0.513	0.437	0.438	0.543	0.692	0.573	0.552
9		0.433	0.587	0.478	0.659	0.607	0.434	0.592	0.660	0.540	0.513
10		0.605	0.651	0.677	0.556	0.486	0.477	0.462	0.626	0.748	0.479

Table 6.15 Scaled RMSE of 2-HL structure (with N1 and N2 in each layer) using Scaled Conjugate Gradient and BFGS Quasi Newton training algorithms for trip (3)

P+P+L		Scaled Conjugate Gradient									
N1	N2	1	2	3	4	5	6	7	8	9	10
1		0.325	0.414	0.342	0.248	0.515	0.301	0.155	0.396	0.594	0.506
2		0.248	0.192	0.253	0.213	0.379	0.336	0.239	0.267	0.258	0.198
3		0.186	0.329	0.218	0.220	0.306	0.286	0.194	0.361	0.184	0.347
4		0.210	0.225	0.192	0.194	0.477	0.266	0.442	0.369	0.361	0.245
5		0.309	0.201	0.251	0.299	0.377	0.236	0.206	0.278	0.210	0.408
6		0.205	0.348	0.234	0.486	0.293	0.209	0.321	0.216	0.183	0.216
7		0.399	0.301	0.230	0.239	0.932	0.192	0.361	0.207	0.932	0.263
8		0.280	0.284	0.932	0.516	0.208	0.239	0.243	0.187	0.932	0.344
9		0.361	0.356	0.237	0.932	0.399	0.224	0.361	0.279	0.238	0.231
10		0.184	0.344	0.222	0.146	0.193	0.361	0.241	0.413	0.270	0.191
P+T+L		BFGS Quasi Newton									
N1	N2	1	2	3	4	5	6	7	8	9	10
1		0.244	0.570	0.368	0.368	0.529	0.808	0.368	0.368	0.368	0.368
2		0.368	0.361	0.118	0.163	0.449	0.249	0.737	0.533	0.368	0.510
3		0.368	0.368	0.361	0.422	0.361	0.564	0.789	0.544	0.454	0.579
4		0.267	0.522	0.692	0.932	0.644	0.626	0.694	0.512	0.395	0.932
5		0.368	0.251	0.625	0.368	0.819	0.493	0.457	0.534	0.237	0.815
6		0.577	0.361	0.463	0.368	0.425	0.721	0.664	0.376	0.685	0.722
7		0.368	0.906	0.236	0.562	0.566	0.631	0.611	0.515	0.365	0.490
8		0.291	0.472	0.346	0.473	0.516	0.162	0.725	0.624	0.275	0.581
9		0.368	0.270	0.296	0.605	0.374	0.430	0.789	0.742	0.388	0.907
10		0.368	0.623	0.571	0.368	0.374	0.410	0.606	0.598	0.463	0.573

Table 6.16 Scaled RMSE of 2-HL structure (with N1 and N2 in each layer) using Levenberg-Marquardt and Resilient Back-Propagation training algorithms for trip (4)

L+L+L		Levenberg-Marquardt									
N1	N2	1	2	3	4	5	6	7	8	9	10
1		0.219	0.295	0.281	0.142	0.241	0.262	0.146	0.327	0.262	0.144
2		0.201	0.274	0.262	0.252	0.294	0.263	0.262	0.262	0.171	0.262
3		0.254	0.296	0.289	0.237	0.207	0.198	0.149	0.099	0.093	0.214
4		0.219	0.254	0.228	0.207	0.262	0.196	0.194	0.255	0.233	0.106
5		0.262	0.262	0.177	0.262	0.211	0.184	0.174	0.191	0.233	0.152
6		0.261	0.071	0.101	0.174	0.235	0.120	0.262	0.169	0.228	0.262
7		0.213	0.301	0.108	0.262	0.241	0.262	0.130	0.246	0.228	0.210
8		0.285	0.167	0.241	0.199	0.236	0.165	0.256	0.079	0.173	0.111
9		0.254	0.128	0.201	0.114	0.262	0.262	0.262	0.244	0.222	0.209
10		0.274	0.242	0.259	0.207	0.262	0.245	0.122	0.262	0.252	0.114
P+L+L		Resilient Back-Propagation									
N1	N2	1	2	3	4	5	6	7	8	9	10
1		0.146	0.191	0.187	0.200	0.231	0.151	0.184	0.208	0.209	0.261
2		0.142	0.162	0.148	0.158	0.200	0.159	0.225	0.153	0.109	0.113
3		0.254	0.145	0.111	0.201	0.130	0.136	0.176	0.143	0.120	0.165
4		0.191	0.139	0.152	0.173	0.111	0.124	0.167	0.126	0.099	0.131
5		0.154	0.151	0.127	0.274	0.132	0.197	0.098	0.097	0.131	0.137
6		0.143	0.141	0.112	0.144	0.125	0.119	0.120	0.130	0.109	0.139
7		0.274	0.254	0.255	0.159	0.106	0.131	0.095	0.111	0.111	0.132
8		0.254	0.161	0.131	0.124	0.141	0.092	0.140	0.106	0.164	0.143
9		0.143	0.148	0.196	0.136	0.115	0.104	0.126	0.079	0.103	0.151
10		0.274	0.184	0.239	0.118	0.187	0.094	0.117	0.127	0.094	0.107

Table 6.17 Scaled RMSE of 2-HL structure (with N1 and N2 in each layer) using Scaled Conjugate Gradient and BFGS Quasi Newton training algorithms for trip (4)

L+T+L		Scaled Conjugate Gradient									
N1	N2	1	2	3	4	5	6	7	8	9	10
1		0.221	0.274	0.274	0.154	0.228	0.158	0.234	0.159	0.207	0.201
2		0.213	0.136	0.274	0.230	0.231	0.218	0.229	0.254	0.103	0.248
3		0.138	0.163	0.238	0.102	0.086	0.143	0.131	0.202	0.101	0.223
4		0.216	0.203	0.124	0.119	0.104	0.131	0.108	0.122	0.134	0.091
5		0.253	0.168	0.093	0.142	0.152	0.153	0.143	0.146	0.155	0.081
6		0.127	0.133	0.274	0.120	0.159	0.201	0.212	0.237	0.108	0.097
7		0.113	0.134	0.127	0.106	0.146	0.092	0.214	0.120	0.088	0.262
8		0.253	0.113	0.147	0.165	0.159	0.104	0.170	0.188	0.158	0.262
9		0.274	0.098	0.149	0.099	0.147	0.111	0.128	0.098	0.180	0.100
10		0.128	0.157	0.149	0.124	0.262	0.101	0.135	0.262	0.262	0.155
P+T+L		BFGS Quasi Newton									
N1	N2	1	2	3	4	5	6	7	8	9	10
1		0.213	0.274	0.274	0.274	0.274	0.274	0.274	0.181	0.128	0.265
2		0.262	0.262	0.171	0.211	0.199	0.262	0.274	0.191	0.274	0.141
3		0.274	0.274	0.303	0.202	0.274	0.227	0.201	0.259	0.145	0.079
4		0.274	0.262	0.254	0.178	0.123	0.313	0.162	0.225	0.092	0.137
5		0.239	0.274	0.274	0.254	0.135	0.254	0.173	0.255	0.237	0.252
6		0.262	0.142	0.274	0.093	0.228	0.130	0.298	0.198	0.146	0.115
7		0.274	0.176	0.262	0.254	0.255	0.117	0.173	0.203	0.201	0.092
8		0.255	0.187	0.257	0.246	0.208	0.166	0.155	0.092	0.144	0.240
9		0.274	0.274	0.142	0.149	0.115	0.306	0.169	0.167	0.225	0.206
10		0.274	0.143	0.305	0.221	0.254	0.101	0.166	0.252	0.108	0.120

Table 6.18 Scaled RMSE of 2-HL structure (with N1 and N2 in each layer) using Levenberg-Marquardt and Resilient Back-Propagation training algorithms for trip (5)

T+L+T		Levenberg-Marquardt									
N1	N2	1	2	3	4	5	6	7	8	9	10
1		0.597	0.593	0.651	0.518	0.548	0.446	0.448	0.612	0.583	0.586
2		0.518	0.537	0.630	0.597	0.569	0.593	0.573	0.571	0.608	0.864
3		0.578	0.614	0.550	0.616	0.581	0.466	0.565	0.672	0.583	0.621
4		0.532	0.430	0.621	0.573	0.524	0.556	0.864	0.528	0.584	0.393
5		0.582	0.529	0.557	0.610	0.576	0.533	0.433	0.583	0.565	0.526
6		0.528	0.554	0.560	0.565	0.610	0.565	0.497	0.579	0.586	0.519
7		0.563	0.434	0.572	0.577	0.602	0.536	0.544	0.614	0.469	0.607
8		0.543	0.565	0.569	0.583	0.539	0.561	0.572	0.880	0.547	0.534
9		0.563	0.579	0.546	0.604	0.528	0.506	0.604	0.523	0.481	0.557
10		0.545	0.568	0.552	0.593	0.536	0.573	0.547	0.601	0.576	0.579
T+L+P		Resilient Back-Propagation									
N1	N2	1	2	3	4	5	6	7	8	9	10
1		0.428	0.414	0.464	0.456	0.449	0.312	0.464	0.451	0.464	0.444
2		0.451	0.425	0.450	0.437	0.498	0.448	0.426	0.409	0.449	0.422
3		0.464	0.435	0.471	0.460	0.416	0.456	0.491	0.420	0.448	0.431
4		0.459	0.464	0.438	0.477	0.406	0.463	0.458	0.449	0.433	0.421
5		0.417	0.424	0.453	0.484	0.452	0.429	0.432	0.446	0.467	0.489
6		0.495	0.455	0.475	0.434	0.497	0.483	0.458	0.444	0.480	0.478
7		0.438	0.425	0.442	0.447	0.474	0.539	0.496	0.496	0.448	0.420
8		0.429	0.419	0.511	0.505	0.484	0.570	0.468	0.480	0.544	0.467
9		0.486	0.433	0.492	0.450	0.456	0.438	0.500	0.486	0.490	0.456
10		0.469	0.536	0.430	0.470	0.496	0.438	0.472	0.489	0.487	0.479

Table 6.19 Scaled RMSE of 2-HL structure (with N1 and N2 in each layer) using Scaled Conjugate Gradient and BFGS Quasi Newton training algorithms for trip (5)

P+T+L		Scaled Conjugate Gradient									
N1	N2	1	2	3	4	5	6	7	8	9	10
1		0.464	0.464	0.361	0.453	0.464	0.464	0.464	0.464	0.503	0.503
2		0.464	0.464	0.449	0.444	0.485	0.406	0.437	0.464	0.428	0.423
3		0.464	0.464	0.410	0.426	0.463	0.464	0.459	0.447	0.453	0.469
4		0.464	0.464	0.464	0.433	0.450	0.402	0.435	0.427	0.431	0.439
5		0.447	0.464	0.429	0.464	0.444	0.439	0.481	0.438	0.477	0.454
6		0.464	0.430	0.444	0.445	0.453	0.434	0.413	0.448	0.440	0.471
7		0.464	0.460	0.464	0.438	0.452	0.449	0.444	0.449	0.442	0.436
8		0.464	0.485	0.464	0.427	0.448	0.444	0.444	0.454	0.454	0.455
9		0.442	0.503	0.436	0.427	0.448	0.464	0.437	0.422	0.439	0.430
10		0.421	0.452	0.473	0.434	0.439	0.446	0.459	0.434	0.429	0.427
P+L+L		BFGS Quasi Newton									
N1	N2	1	2	3	4	5	6	7	8	9	10
1		0.464	0.464	0.464	0.464	0.503	0.464	0.464	0.464	0.464	0.464
2		0.462	0.428	0.503	0.464	0.464	0.464	0.464	0.466	0.464	0.503
3		0.464	0.464	0.419	0.464	0.503	0.477	0.426	0.424	0.503	0.464
4		0.462	0.503	0.428	0.464	0.462	0.471	0.462	0.462	0.358	0.503
5		0.503	0.464	0.446	0.426	0.448	0.480	0.485	0.503	0.464	0.493
6		0.464	0.503	0.432	0.503	0.503	0.419	0.449	0.475	0.433	0.499
7		0.503	0.464	0.464	0.445	0.503	0.464	0.453	0.465	0.519	0.530
8		0.464	0.451	0.451	0.442	0.503	0.447	0.483	0.501	0.424	0.473
9		0.503	0.503	0.503	0.457	0.484	0.451	0.421	0.486	0.443	0.458
10		0.503	0.462	0.455	0.451	0.456	0.456	0.503	0.503	0.466	0.449

Table 6.20 Scaled RMSE of 2-HL structure (with N1 and N2 in each layer) using Levenberg-Marquardt and Resilient Back-Propagation training algorithms for trip (6)

L+P+T		Levenberg-Marquardt									
N1	N2	1	2	3	4	5	6	7	8	9	10
1		0.324	0.342	0.320	0.342	0.341	0.336	0.340	0.326	0.340	0.341
2		0.366	0.421	0.338	0.347	0.348	0.398	0.326	0.347	0.440	0.836
3		0.939	0.407	0.426	0.341	0.477	0.403	0.313	0.477	0.832	0.811
4		0.416	0.387	0.430	0.475	0.459	0.477	0.390	0.422	0.419	0.475
5		0.477	0.680	0.418	0.529	0.379	0.838	0.391	0.405	0.340	0.374
6		0.361	0.486	0.475	0.488	0.400	0.412	0.533	0.507	0.471	0.385
7		0.478	0.420	0.832	0.488	0.477	0.364	0.477	0.444	0.421	0.531
8		0.717	0.477	0.423	0.416	0.397	0.477	0.398	0.477	0.344	0.242
9		0.477	0.399	0.516	0.477	0.510	0.836	0.939	0.828	0.476	0.477
10		0.939	0.939	0.792	0.408	0.808	0.471	0.479	0.477	0.921	0.477
L+L+L		Resilient Back-Propagation									
N1	N2	1	2	3	4	5	6	7	8	9	10
1		0.440	0.338	0.426	0.247	0.477	0.248	0.358	0.361	0.317	0.438
2		0.480	0.323	0.326	0.267	0.478	0.468	0.460	0.441	0.417	0.398
3		0.361	0.323	0.342	0.367	0.330	0.365	0.383	0.383	0.339	0.346
4		0.405	0.399	0.363	0.410	0.335	0.406	0.405	0.410	0.336	0.364
5		0.357	0.351	0.366	0.335	0.309	0.272	0.347	0.313	0.287	0.349
6		0.386	0.251	0.413	0.303	0.411	0.269	0.340	0.429	0.340	0.307
7		0.460	0.346	0.345	0.411	0.283	0.413	0.411	0.315	0.463	0.330
8		0.366	0.407	0.384	0.403	0.398	0.354	0.386	0.463	0.429	0.292
9		0.424	0.382	0.341	0.347	0.451	0.328	0.390	0.345	0.341	0.456
10		0.345	0.318	0.346	0.358	0.342	0.362	0.284	0.393	0.410	0.415

Table 6.21 Scaled RMSE of 2-HL structure (with N1 and N2 in each layer) using Scaled Conjugate Gradient and BFGS Quasi Newton training algorithms for trip (6)

L+L+L		Scaled Conjugate Gradient									
N1	N2	1	2	3	4	5	6	7	8	9	10
1		0.404	0.333	0.394	0.277	0.439	0.374	0.345	0.333	0.462	0.330
2		0.392	0.356	0.279	0.334	0.269	0.325	0.413	0.456	0.402	0.285
3		0.343	0.336	0.276	0.366	0.416	0.401	0.229	0.365	0.279	0.298
4		0.390	0.430	0.416	0.345	0.326	0.347	0.465	0.429	0.287	0.472
5		0.327	0.348	0.353	0.414	0.299	0.409	0.324	0.416	0.321	0.443
6		0.363	0.392	0.347	0.324	0.381	0.289	0.339	0.332	0.399	0.289
7		0.467	0.423	0.327	0.237	0.409	0.296	0.321	0.416	0.272	0.306
8		0.335	0.376	0.391	0.318	0.298	0.317	0.396	0.329	0.348	0.408
9		0.392	0.310	0.307	0.429	0.391	0.287	0.365	0.283	0.413	0.415
10		0.267	0.390	0.345	0.412	0.339	0.343	0.363	0.382	0.309	0.412
L+T+L		BFGS Quasi Newton									
N1	N2	1	2	3	4	5	6	7	8	9	10
1		0.325	0.277	0.324	0.325	0.326	0.389	0.332	0.324	0.423	0.346
2		0.324	0.326	0.267	0.457	0.399	0.479	0.345	0.350	0.326	0.374
3		0.346	0.307	0.326	0.346	0.359	0.345	0.346	0.331	0.333	0.414
4		0.345	0.330	0.416	0.345	0.337	0.325	0.346	0.343	0.268	0.335
5		0.406	0.297	0.346	0.345	0.347	0.414	0.436	0.417	0.345	0.274
6		0.325	0.324	0.326	0.346	0.369	0.391	0.418	0.416	0.324	0.347
7		0.422	0.477	0.417	0.252	0.328	0.343	0.318	0.340	0.346	0.345
8		0.324	0.399	0.346	0.416	0.416	0.345	0.347	0.440	0.345	0.343
9		0.395	0.394	0.417	0.346	0.347	0.345	0.346	0.347	0.330	0.333
10		0.478	0.416	0.325	0.416	0.378	0.416	0.457	0.378	0.354	0.347

Table 6.22 Scaled RMSE of 2-HL structure (with N1 and N2 in each layer) using Levenberg-Marquardt and Resilient Back-Propagation training algorithms for trip (7)

T+T+T		Levenberg-Marquardt									
N1	N2	1	2	3	4	5	6	7	8	9	10
1		0.553	0.493	0.699	0.640	0.631	0.740	0.768	0.644	0.768	0.629
2		0.704	0.668	0.768	0.768	0.666	0.672	0.768	0.941	0.762	0.667
3		0.646	0.653	1.000	0.716	0.768	0.708	0.725	1.000	0.736	0.768
4		0.728	1.000	0.666	0.755	0.674	1.000	0.665	0.879	0.630	0.658
5		0.663	0.599	0.782	0.768	0.765	0.856	0.767	0.672	1.000	1.000
6		0.536	0.636	1.000	0.757	0.783	0.634	0.801	1.000	1.000	1.000
7		0.611	0.663	0.993	1.000	0.805	0.673	1.000	1.000	1.000	0.814
8		0.672	0.652	0.670	0.654	0.734	0.770	1.000	0.671	0.762	0.830
9		0.713	0.688	0.763	1.000	0.607	1.000	0.748	1.000	0.673	1.000
10		0.728	0.656	1.000	1.000	0.825	0.622	1.000	0.727	1.000	1.000
L+L+P		Resilient Back-Propagation									
N1	N2	1	2	3	4	5	6	7	8	9	10
1		0.627	0.638	1.000	0.556	0.629	0.832	1.000	1.000	0.508	0.781
2		0.903	1.000	0.629	0.755	0.676	1.000	0.561	0.606	1.000	0.596
3		0.607	0.711	0.627	0.636	0.712	0.740	0.532	0.902	0.782	1.000
4		0.634	0.608	0.996	0.683	0.672	0.812	0.657	0.590	0.546	0.582
5		0.541	0.970	0.630	0.533	0.854	0.645	0.785	0.995	0.615	0.589
6		0.845	0.834	0.720	0.789	0.728	0.615	0.619	0.875	0.732	0.715
7		0.733	0.619	0.918	0.645	0.674	0.701	0.726	0.508	0.587	0.827
8		0.618	0.490	0.821	0.814	1.000	1.000	0.692	0.602	0.718	1.000
9		0.604	0.807	0.617	0.646	0.542	0.828	0.652	0.569	0.841	1.000
10		0.626	0.545	0.590	0.881	0.627	0.864	0.608	0.732	0.772	0.743

Table 6.23 Scaled RMSE of 2-HL structure (with N1 and N2 in each layer) using Scaled Conjugate Gradient and BFGS Quasi Newton training algorithms for trip (7)

T+P+P		Scaled Conjugate Gradient									
N1	N2	1	2	3	4	5	6	7	8	9	10
1		1.000	1.000	0.597	1.000	0.716	0.562	0.753	0.618	0.892	0.902
2		0.969	1.000	0.580	1.000	1.000	0.744	0.881	0.561	0.641	0.929
3		1.000	1.000	1.000	1.000	1.000	0.902	1.000	1.000	1.000	1.000
4		0.674	0.761	0.798	1.000	0.576	1.000	1.000	1.000	0.595	1.000
5		1.000	0.908	1.000	1.000	1.000	1.000	0.501	0.928	0.738	0.689
6		1.000	0.562	0.824	1.000	0.666	1.000	1.000	0.831	0.894	0.773
7		1.000	1.000	0.624	0.914	1.000	1.000	0.849	1.000	1.000	0.948
8		1.000	0.697	0.649	0.758	0.729	0.735	0.483	0.584	0.757	0.486
9		1.000	1.000	0.705	1.000	1.000	0.665	1.000	1.000	0.935	1.000
10		0.744	1.000	0.685	1.000	1.000	0.815	0.766	0.590	0.698	1.000
P+P+P		BFGS Quasi Newton									
N1	N2	1	2	3	4	5	6	7	8	9	10
1		0.525	0.634	0.500	0.645	0.583	1.000	0.584	0.578	0.485	0.654
2		0.948	0.697	0.887	0.741	1.000	1.000	0.998	0.627	0.771	1.000
3		1.000	0.965	0.750	0.964	1.000	1.000	1.000	0.837	1.000	0.649
4		1.000	1.000	1.000	0.922	1.000	1.000	1.000	0.508	1.000	1.000
5		0.612	1.000	0.812	1.000	1.000	1.000	1.000	1.000	1.000	1.000
6		0.570	0.701	1.000	1.000	1.000	1.000	1.000	1.000	1.000	1.000
7		0.899	1.000	1.000	1.000	1.000	1.000	1.000	1.000	1.000	1.000
8		1.000	1.000	1.000	1.000	1.000	1.000	1.000	1.000	1.000	1.000
9		1.000	1.000	1.000	1.000	1.000	1.000	1.000	1.000	1.000	1.000
10		1.000	1.000	1.000	1.000	1.000	1.000	1.000	1.000	1.000	1.000

It can be concluded that the exploration of the most fitting training algorithm among the four multidimensional minimization training algorithms for all boiler trips was quite difficult. For more details refer to Table (6.24).

Table 6.24 The best ANN topology combination of a 2HL for all boiler operation trips

Trip	RMSE	Architecture	Activation Function	Training Algorithm
1	0.434	7HL1-9HL2	P+T+L	Scaled Conjugate Gradient
2	0.292	3HL1-10HL2	L+T+L	Resilient Back-Propagation
3	0.118	2HL1-3HL2	P+T+L	BFGS Quasi Newton
4	0.071	6HL1-2HL2	L+L+L	Levenberg-Marquardt
5	0.358	4HL1-9HL2	P+L+L	BFGS Quasi Newton
6	0.229	3HL1-7HL2	L+L+L	Scaled Conjugate Gradient
7	0.483	1HL1-2HL2	T+T+T	Levenberg-Marquardt

It should be highlighted that in all of the combinations of activation functions, the last one is a logistic activation function with exception of trip 7. The reason behind this is that the output of this function is limited between 0 and 1, which indeed suites the normalized input (0 Min. to 1 Max.).

Table (6.25) shows the overall best performance (optimal RMSE) in the preliminary training exploration for both 1HL and 2HL architectures for all boiler trips. It can be seen that the logistic activation function for the output node performed better than the other two activation functions in most training cases.

Table 6.25 The best ANN topology combination for both the 1HL and the 2HL for all boiler operation trips

Trip	NHL	RMSE	Architecture	Activation Function	Training Algorithm
1	1HL	0.433	6HL1	L+L	Scaled Conjugate Gradient
2	2HL	0.292	3HL1-10HL2	L+T+L	Resilient Back-Propagation
3	2HL	0.118	2HL1-3HL2	P+T+L	BFGS Quasi Newton
4	2HL	0.071	6HL1-2HL2	L+L+L	Levenberg-Marquardt
5	2HL	0.358	4HL1-9HL2	P+L+L	BFGS Quasi Newton
6	2HL	0.229	3HL1-7HL2	L+L+L	Scaled Conjugate Gradient
7	1HL	0.300	10HL1	L+L	Resilient Back-Propagation

6.2.2 IMS-I Validation Process Results

This section presents the basic validation result process of the proposed IMS-I for boiler trips. Eight validation real data sets were constructed for this proposes. The first seven sets contained faulty real data and were used to validate how rapidly the proposed IMS-I detects the fault. The last set contained only normal operation real data and was used to validate the performance of the system during normal boiler operation. Details of the validation real data sets are shown in Table (6.26).

Table 6.26 Description of basic validation data sets for IMS-I

Data Set	Fault Status	Starting Date/Time	End Date/Time	No of Intervals	Interval that Fault Was Introduced
1	Trip 1	02.05.2008 12:52:00	02.05.2008 19:22:00	392	225
2	Trip 2	05.06.2008 01:56:00	05.06.2008 06:29:00	275	251
3	Trip 3	06.06.2008 7:23:00	06.06.2008 12:54:00	333	17
4	Trip 4	19.12.2008 21:19:00	20.12.2008 01:03:00	326	50
5	Trip 5	30.01.2009 03:39:00	30.01.2009 08:31:00	293	118
6	Trip 6	05.05.2009 10:20:00	05.05.2009 16:22:00	364	239
7	Trip 7	31.05.2009 20;24:00	31.05.2009 23:59:00	216	38
8	Normal	06.07.2008 06:05:00	06.07.2008 12:00:00	358	–

The proposed IMS-I was trained to come up with an output of “zero” during normal boiler operation and “one” during faulty boiler operation. The system predicated an output range of values from “zero” to “1”, therefore, some thresholds were to be applied in order to decide, below, which NN output value a normal boiler operation is assumed; and, above, which NN output value a fault boiler operation is detected. Due to alarm boundaries of the selected boiler operation variables, the NN output lower and upper thresholds were fixed at 0.4 and 0.5 correspondingly.

Thus, if the NN output was within the range of these two values, the system could assume that neither normal nor faulty operation occurs. The lower threshold is used

for shifting from faulty to normal boiler operation and the upper threshold is used for shifting from normal to faulty boiler operation.

6.2.2.1 IMS-I Validation Results of Trip 1

Figure (6.1) shows the IMS-I output on the first real data set. The time step is a one minute interval. Trip (1) represents the “boiler water wall tube leak” trip. The total data sampling interval is of the 392nd minute before the shutdown instance. The faulty operation is introduced in the 225th interval. The fault was detected by the intelligent system within the 220th interval. The system output is 0.95, which is considered as a strong fault indication (close to one).

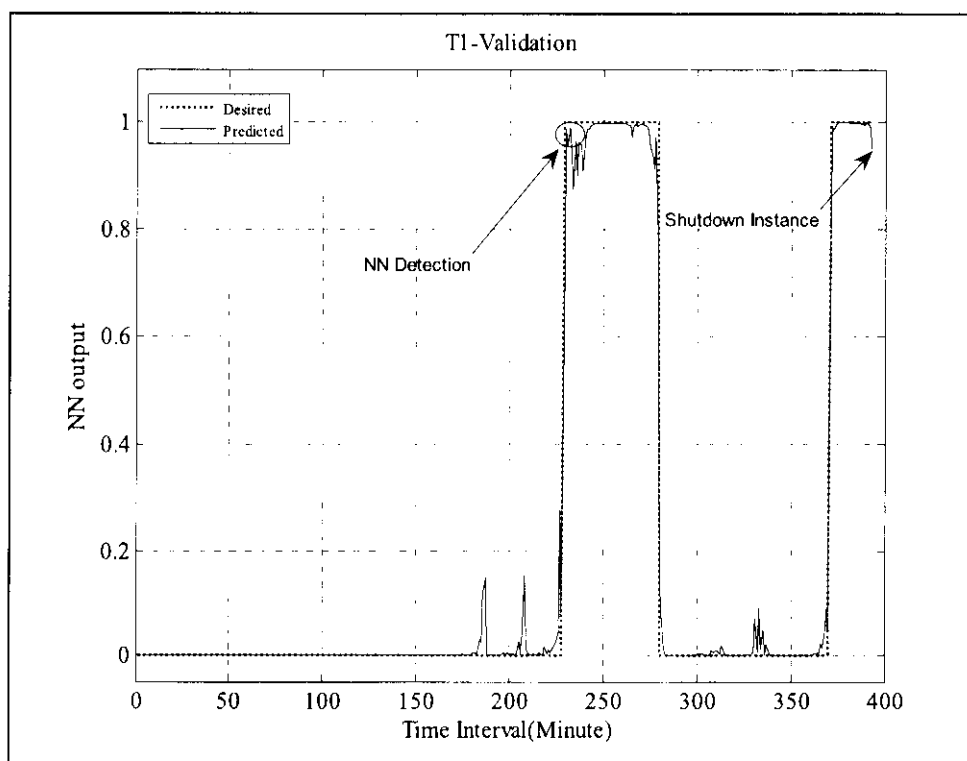


Figure 6.1 IMS-I outputs for trip (1)

It can be seen from the plot that even though the fault is detected, there are several significant intervals that the system output returned to the normal boiler operation value (below normal operation value 0.4). This happened once during the main boiler faulty operation and it also happened towards the end of the specific fault (after the

276th interval) where that was fault about to disappear. Thus, the boiler operation is returned to normal again.

6.2.2.2 IMS-I Validation Results of Trip 2

In Figure (6.2), the IMS-I response to the corresponding data set of trip (2) is presented. This trip is denoted as a “low temperature superheater” trip. The total data sampling interval is at the 275th minute before the shutdown instance. The data started with a normal boiler operation and the faulty operation is introduced in the 251st interval. The intelligent system detects the fault within the 235th interval (which is 16 minutes before the plant monitoring system). The IMS-I output is 0.57, which is considered as a weak fault indication (close to the threshold range).

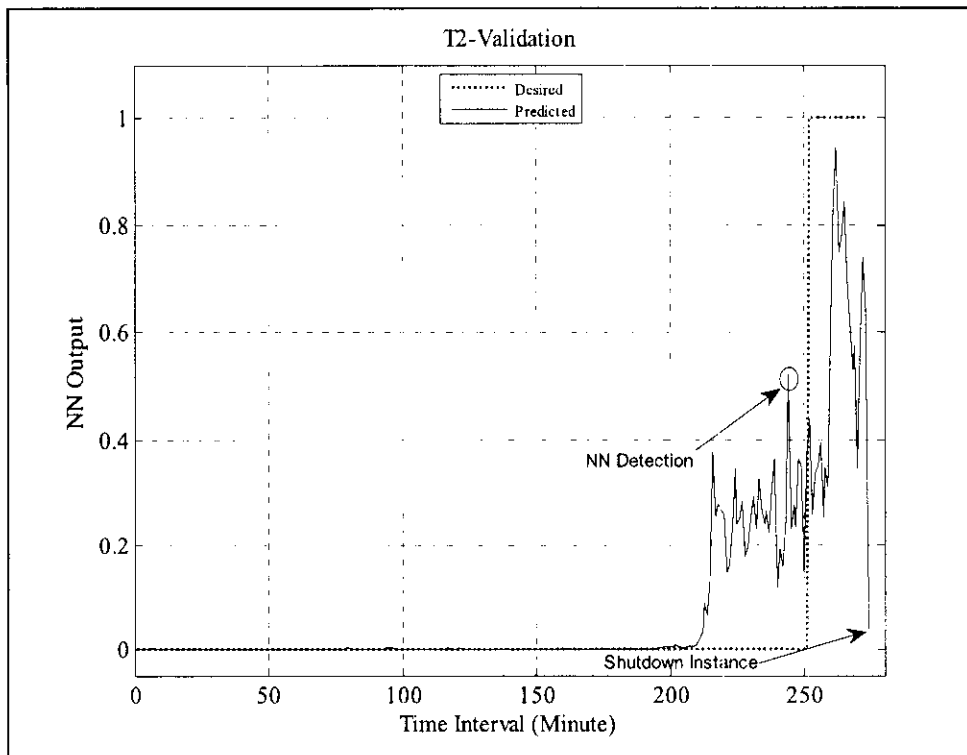


Figure 6.2 IMS-I outputs for trip (2)

6.2.2.3 IMS-I Validation Results of Trip 3

Figure (6.3) shows the IMS-I result outputs classified under “boiler drum level low” trip. The total data sampling interval is at the 334th minute before the shutdown

instance. The fault was introduced in the 17th interval. The proposed IMS-I detects the fault just 10 intervals before the plant monitoring system with an output value of 0.65. The IMS-I output drops below 0.5 (normal boiler operation) five minutes after the occurrence of the fault and stays in that region for several more intervals.

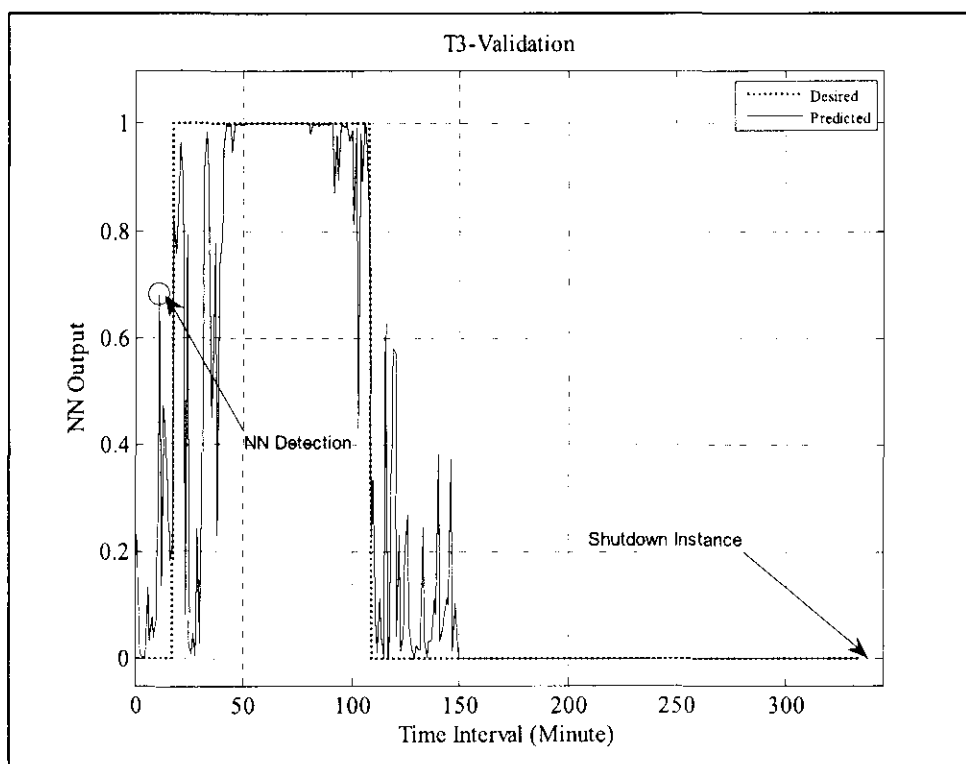


Figure 6.3 IMS-I outputs for trip (3)

6.2.2.4 IMS-I Validation Results of Trip 4

This trip, as trip (3), is also referred to as a “boiler drum level low” trip. But it happened in another plant unit. Figure (6.4) shows the proposed IMS-I output via the time interval for the corresponding real data set. The total data sampling interval is at the 327th minute before the shutdown instance. The fault was introduced in the 50th interval. It is clear here that the proposed IMS-I successfully captured the fault, even from the 40th step, the system gives a strong indication that a fault has occurred with an output value of 0.65. It should be mentioned, that even after the fault has been detected, it is not an important issue if the intelligent system fails to continuously detect it. The important indicator for the fault detection is the rapidness of detection.

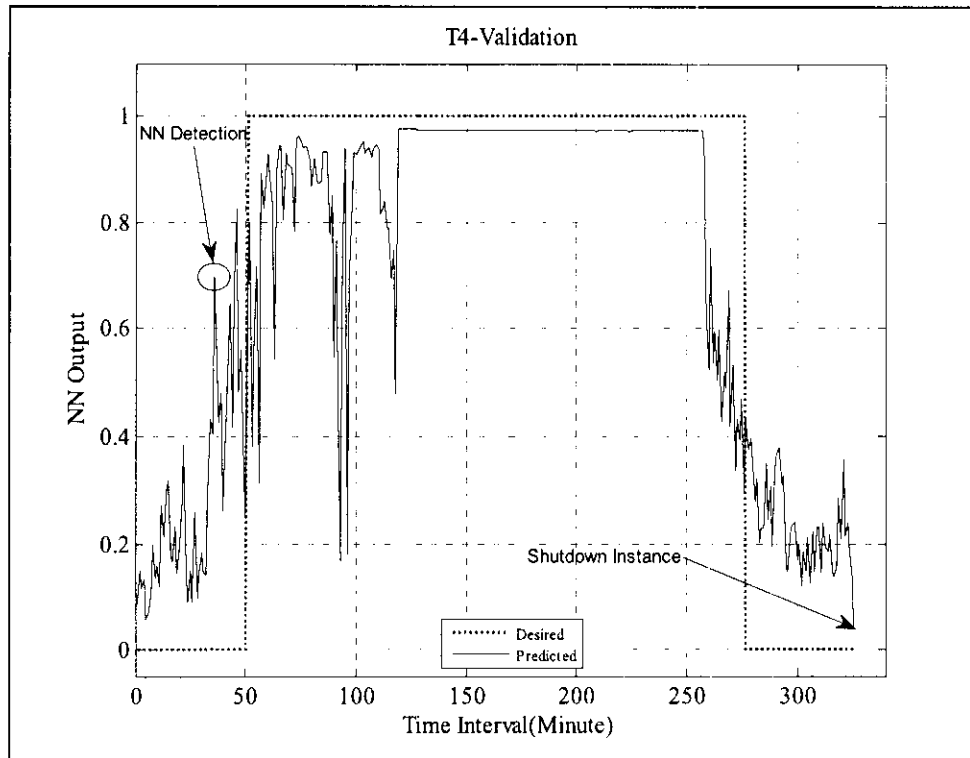


Figure 6.4 IMS-I outputs for trip (4)

6.2.2.5 IMS-I Validation Results of Trip 5

In Figure (6.5) the proposed intelligent system output during the fifth real data set for the “boiler feed pump” trip is shown. The total data sampling interval is at the 293rd minute before the shutdown instance. As in the case of trip (2), the data started with a normal boiler operation and the faulty operation is introduced in the 118th interval. It can be seen in the same figure, that the IMS-I detects the fault at the same time as the plant monitoring system interval (118th step) with an output of 0.53.

The proposed intelligent system output becomes high enough with a value of 0.96, which is considered as a very strong indication and during the occurrence of fault; the system output drops suddenly before the fault has started to vanish. As mentioned earlier, that sudden drop is not considered as a network disadvantage; however, the important factor for fault detection is the rapidness of detection.

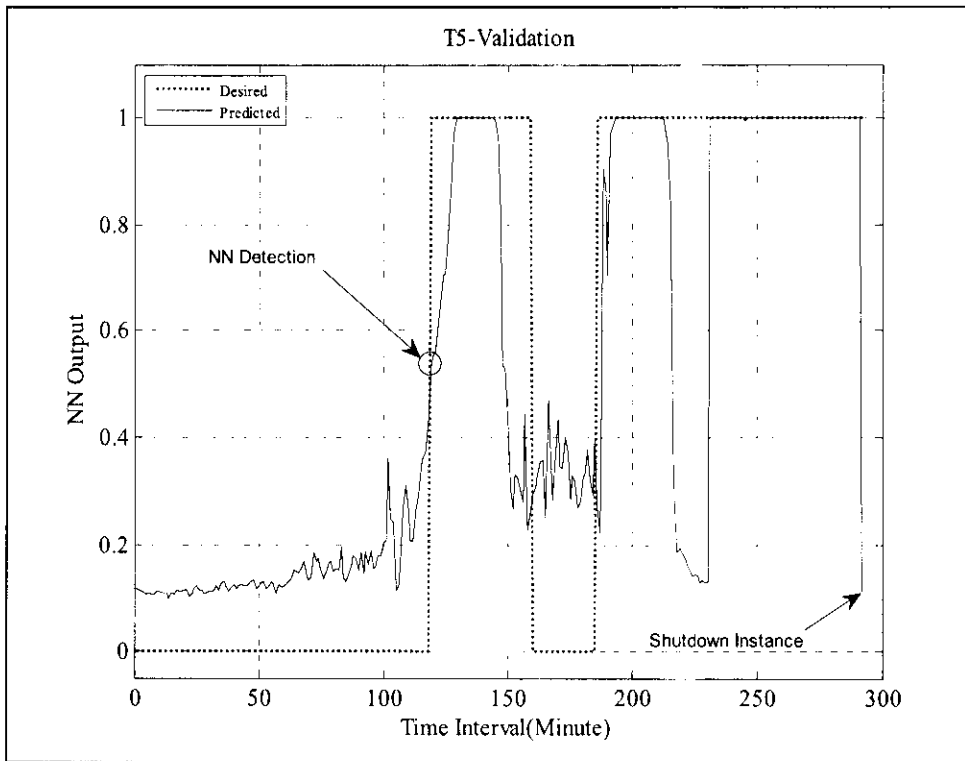


Figure 6.5 IMS-I outputs for trip (5)

6.2.2.6 IMS-I Validation Results of Trip 6

The proposed intelligent system output during the sixth real data set is shown in Figure (6.6). For a “boiler drum high level high” trip, the total data sampling interval is at the 365th minute before the shutdown instance. The boiler data started with a normal operation and the fault was introduced at the 239th interval. The faulty operation was detected by the intelligent system within 5 steps before the fault was introduced by the plant monitoring system with an IMS-I output value of 0.71. The intelligent system output value was also considered as a strong indication that the boiler operation was not normal, with higher values toward the end of the fault.

6.2.2.7 IMS-I Validation Results of Trip 7

Figure (6.7) shows the IMS-I output through the seventh real data set for a “high temperature superheater” trip. The total data sampling interval is at the 217th minute before the shutdown instance. From the graph, it can be observed that even though the

fault is detected by the intelligent system; there are several intervals that the system output returned to the normal operation limit. That occurred twice during the main period of the specific fault and it also took place towards the end of the fault (after interval 78). The rather periodical oscillation of the NN output values are caused by the nature of the sensor or actuator fault. This kind of fault was reproduced by adding a periodically changing noise to the reading of boiler water wall tube sensors and actuators. The system was extremely fast in detecting the fault within 15 intervals (23 minutes before the plant monitoring system). The IMS-I output value was 0.78. With that output value, it's considered as a strong indicator of the faulty boiler operation existence.

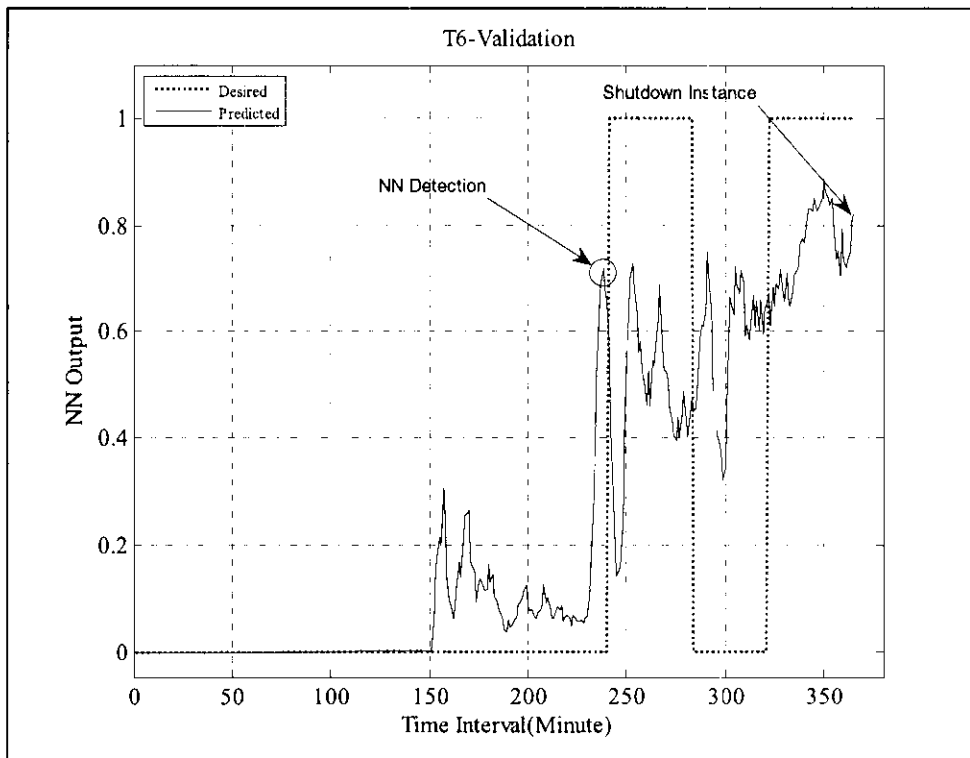


Figure 6.6 IMS-I outputs for trip (6)

6.2.2.8 IMS-I Validation Results of Normal Operation

Finally, the last real data set contains only normal boiler operation data and it was used to check the proposed intelligent system ability to continuously recognize normal boiler operation. The IMS-I output is shown in Figure (6.8). The plot shows

that the system output values are close to “zero” for almost the whole operating period.

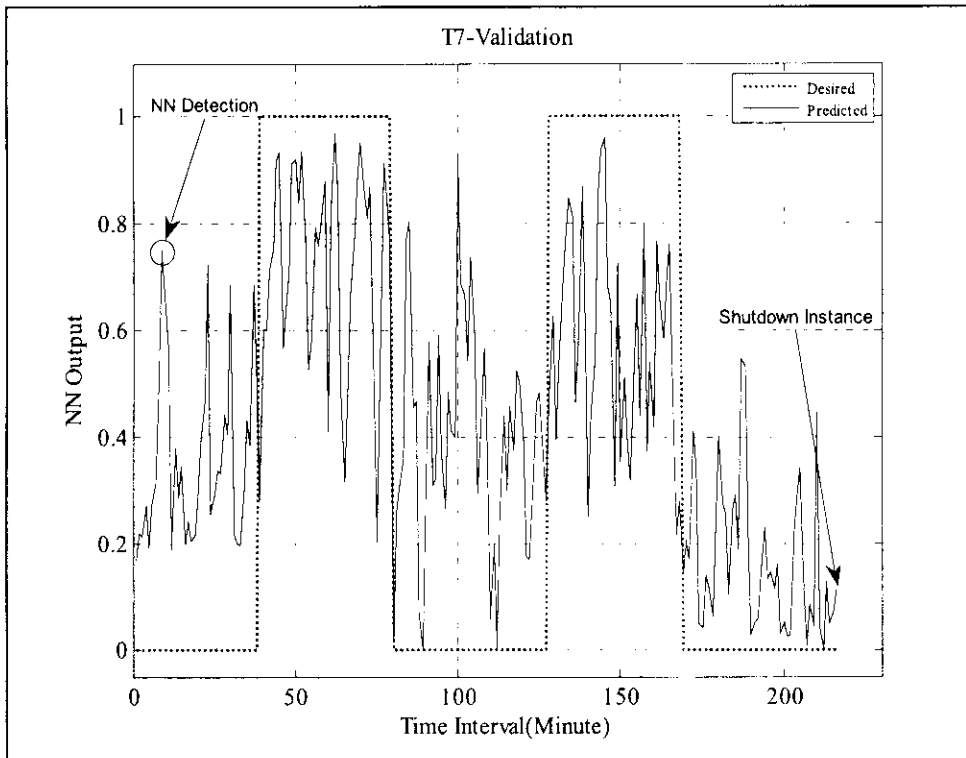


Figure 6.7 IMS-I outputs for trip (7)

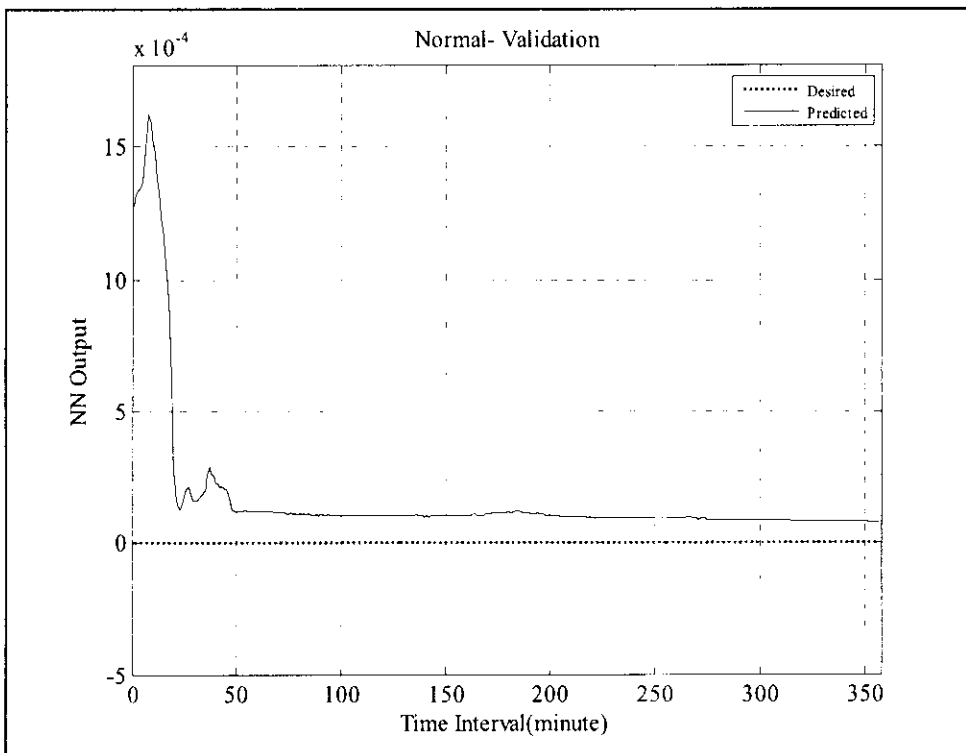


Figure 6.8 IMS-I outputs for Normal operation

In brief, the proposed IMS-I here was capable of detecting the specific thermal power plant trip within a period of around 20 minutes before or at the same time as the trip occurrence. This time period is considered satisfactory.

6.3 Application of IMS-II

NN topologies and boiler operation variables optimization are extremely important issues and many related studies are presented. Here, an intelligent solution “Genetic Algorithm (GA)” for the IMS-II. To date, GAs have become a popular optimization method as they often succeed in finding the best optimization in contrast to the most common optimization algorithms.

As described in chapter 4, the main NN topologies and boiler operation variables to be optimized are presented by a chromosome whereby NN topologies and boiler operation variables are encoded in a binary string. In this work, the initial population of the GA is randomly generated, except for one chromosome, which was set to use all NN topologies and boiler operation variables. The subsequent work is to evaluate the chromosomes generated by previous operations by the fitness function, while the design of the fitness function is a crucial point of using the GA, which determines what a GA should optimize. The evaluation of the fitness starts with the encoding of the chromosomes into neural networks. Then, the ANNs are trained and validated. It should be mentioned here that the same real boiler training and validation data sets which have been used to train and validate the IMS-I were used again to train and validate the IMS-II.

In addition, the other aspect in an evolutionary system (GA) is the way of encoding the several possible phenotypes of the NN topologies and boiler operation variables into specific genotypes. The basic GAs parameters that should be explored are:

- i. The probability of crossover (P_c),
- ii. The population size (P_z),
- iii. The probability of mutation (P_m),
- iv. And the number of generations (G_n).

Where the G_n : is a number of trials which had to be carried out to try to explore the best possible combination.

6.3.1 Determination of Crossover Probability

An important issue in this hybrid system is the determination of the best values of P_c and P_m ; these GA system trials were made with a P_z of 46 bit strings. The most common crossover type, one point crossover, was adopted. Corresponding to trips (1) to (7), Figures (6.9 through 6.15) show the (RMSE) results achieved by the hybrid IMS as a function of the probability of crossover for three different values of the probability of mutation (P_m), 0.01, 0.05 and 0.1. The best hybrid IMS performance was achieved with P_c values as below:

Trip:	T1	T2	T3	T4	T5	T6	T7
P_c :	0.6	0.95	0.8	0.8	0.9	0.9	0.95

The comparison showed that the probability of a mutation with the value of 0.05 outperformed the other two in most cases with expectation for trip 5 with a P_m value of 0.1. The usual range of the explored basic GA parameter values for the probability of a crossover range from 0.6 to 0.95 and for the probability of a mutation from 0.01 to 0.1 [94]. For more details refer to Table (6.27).

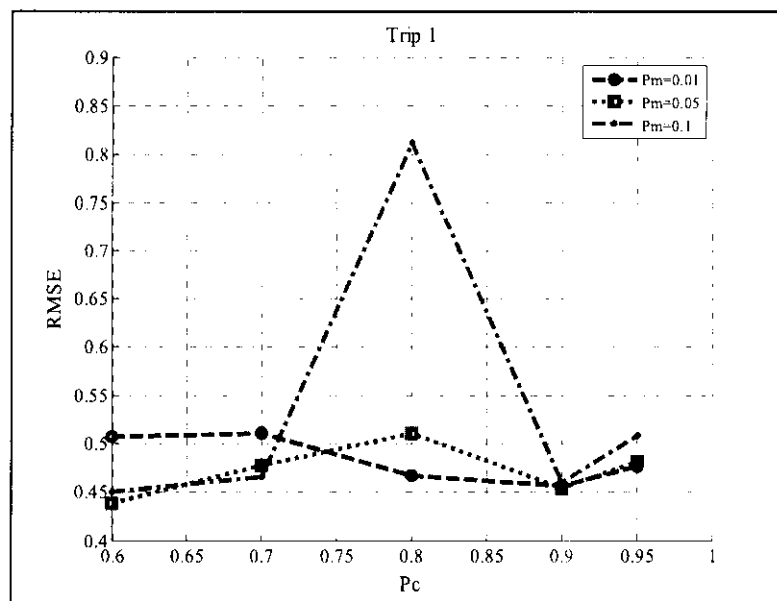


Figure 6.9 Performance of the IMS-II using several probabilities of crossover and mutation for trip (1)

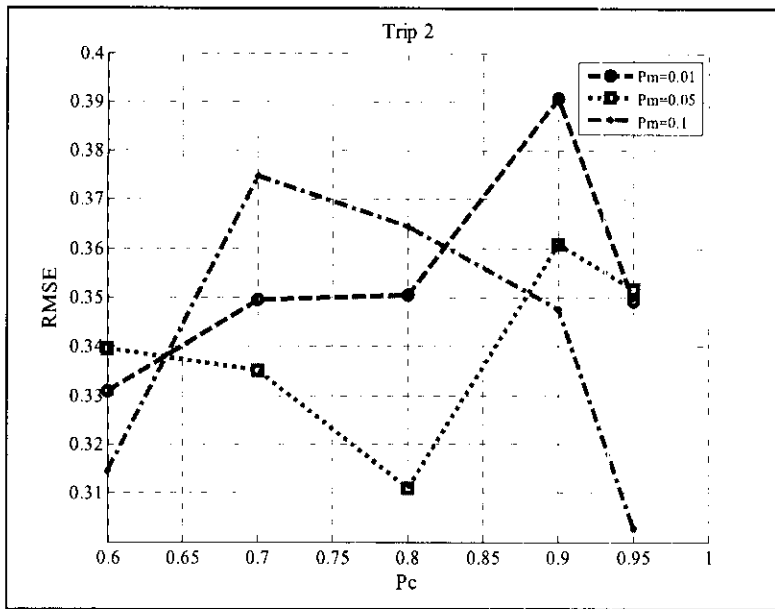


Figure 6.10 Performance of the IMS-II using several probabilities of crossover and mutation for trip (2)

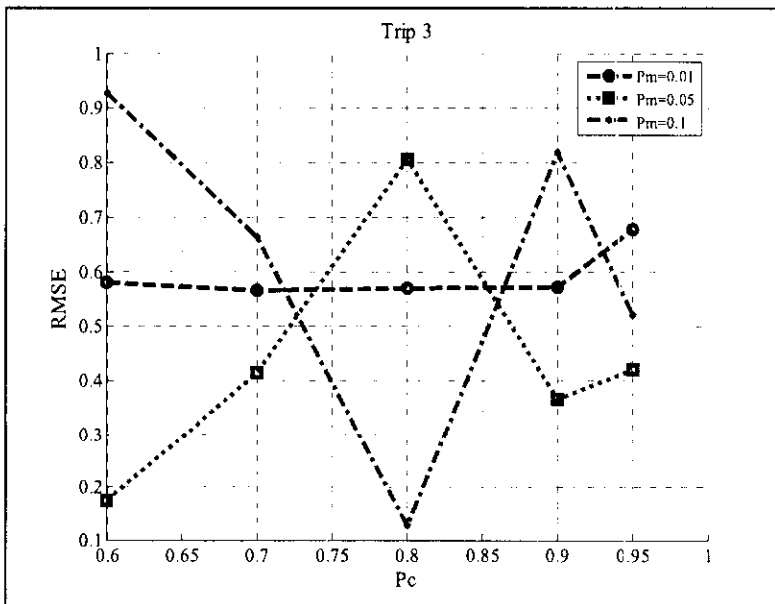


Figure 6.11 Performance of the IMS-II using several probabilities of crossover and mutation for trip (3)

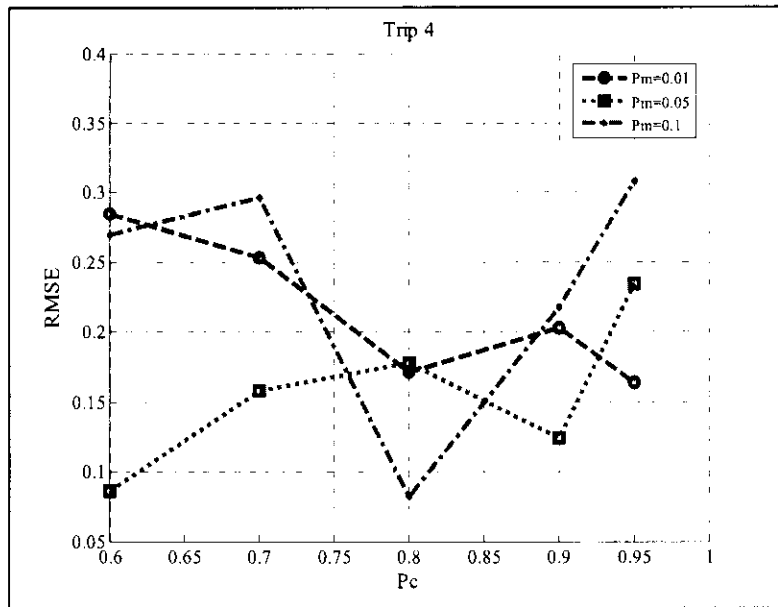


Figure 6.12 Performance of the IMS-II using several probabilities of crossover and mutation for trip (4)

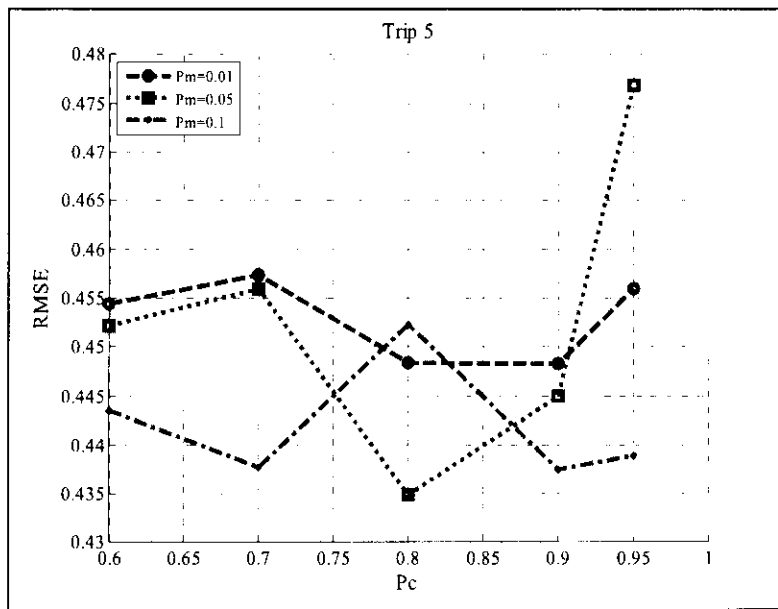


Figure 6.13 Performance of the IMS-II using several probabilities of crossover and mutation for trip (5)

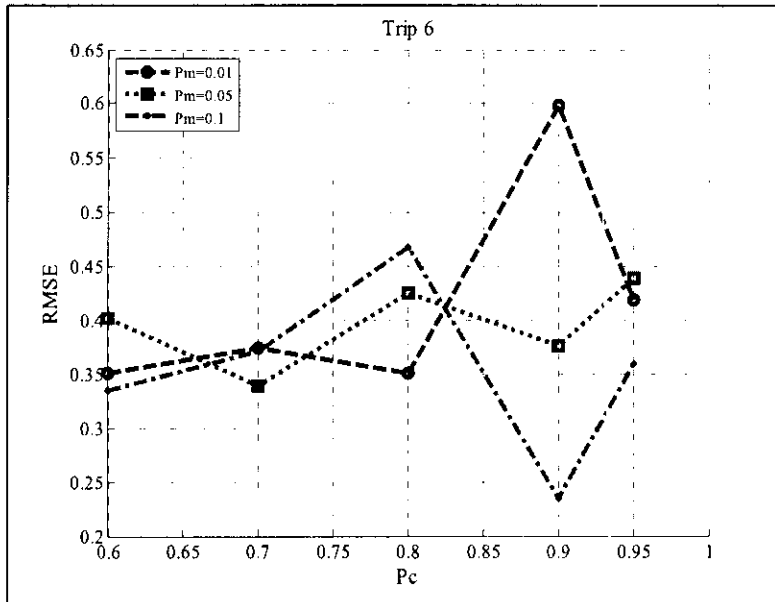


Figure 6.14 Performance of the IMS-II using several probabilities of crossover and mutation for trip (6)

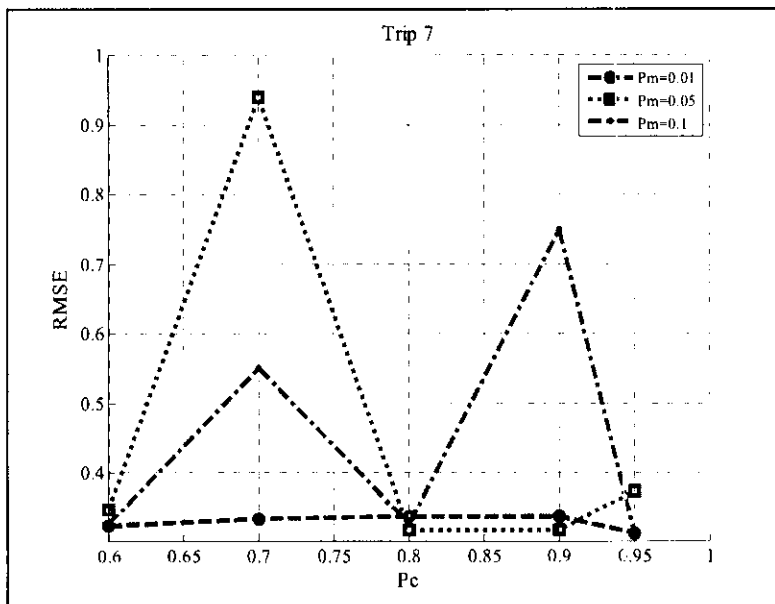


Figure 6.15 Performance of the IMS-II using several probabilities of crossover and mutation for trip (7)

Table 6.27 Several probabilities of crossover and mutation for GA System for seven trips

		T1 Scaled Conjugate Gradient			T2 Resilient Back- Propagation			T3 BFGS Quasi Newton			T4 Levenberg- Marquardt		
		1HL-L+L			2HL-L+ T+L			2HL-P+T+L			2HL-L+L+L		
		P _{M1}	P _{M2}	P _{M3}	P _{M1}	P _{M2}	P _{M3}	P _{M1}	P _{M2}	P _{M3}	P _{M1}	P _{M2}	P _{M3}
P _{C1}	0.6	0.507	0.451	0.458	0.331	0.315	0.368	0.580	0.927	0.591	0.284	0.270	0.117
P _{C2}	0.7	0.510	0.466	0.469	0.350	0.375	0.322	0.565	0.662	0.447	0.253	0.296	0.235
P _{C3}	0.8	0.466	0.811	0.496	0.350	0.364	0.383	0.569	0.127	0.695	0.171	0.082	0.307
P _{C4}	0.9	0.456	0.460	0.524	0.391	0.348	0.410	0.572	0.818	0.353	0.203	0.217	0.175
P _{C5}	0.95	0.476	0.508	0.516	0.349	0.303	0.386	0.678	0.521	0.658	0.164	0.308	0.305
		T5 BFGS Quasi Newton			T6 Scaled Conjugate Gradient			T7 Resilient Back-Propagation					
		2HL- P+L+L			2HL-L+L+L			1HL-L+L					
		P _{M1}	P _{M2}	P _{M3}	P _{M1}	P _{M2}	P _{M3}	P _{M1}		P _{M2}		P _{M3}	
P _{C1}	0.6	0.454	0.444	0.435	0.351	0.334	0.316	0.322		0.326		0.323	
P _{C2}	0.7	0.457	0.438	0.434	0.374	0.371	0.386	0.333		0.551		0.343	
P _{C3}	0.8	0.448	0.452	0.457	0.351	0.468	0.402	0.335		0.326		0.332	
P _{C4}	0.9	0.448	0.437	0.419	0.598	0.235	0.300	0.335		0.749		0.340	
P _{C5}	0.95	0.456	0.439	0.449	0.419	0.359	0.381	0.311		0.311		0.334	

6.3.2 Determination of Population Size

The investigations of the most appropriate size of population (P_z) were limited to population size L to $2*L$, where L is the length of the bit strings [95]. Therefore, population sizes between 46 and 92 were explored. Figures (6.16 through 6.22) show the best hybrid system performance for all seven boiler trips using two different values of generation numbers (15 and 30). It can be concluded from the results that the best performance was achieved with P_z as bellow:

Trip:	T1	T2	T3	T4	T5	T6	T7
P_z :	76	56	66	46	66	56	46

The results after 15 generations were better, with exception of trip 2 and trip 3 cases (within 30 generations). For more information refer to Table (6.28).

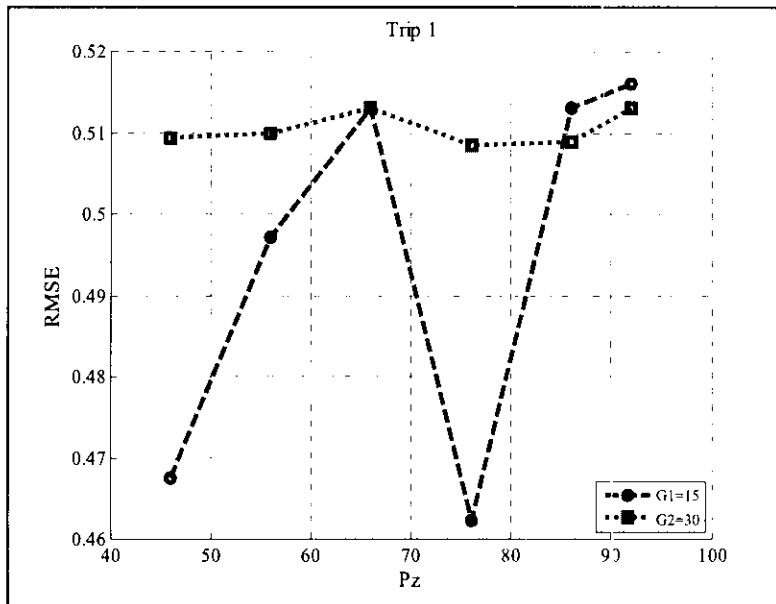


Figure 6.16 Performance of the IMS-II using two population size candidates for trip (1)

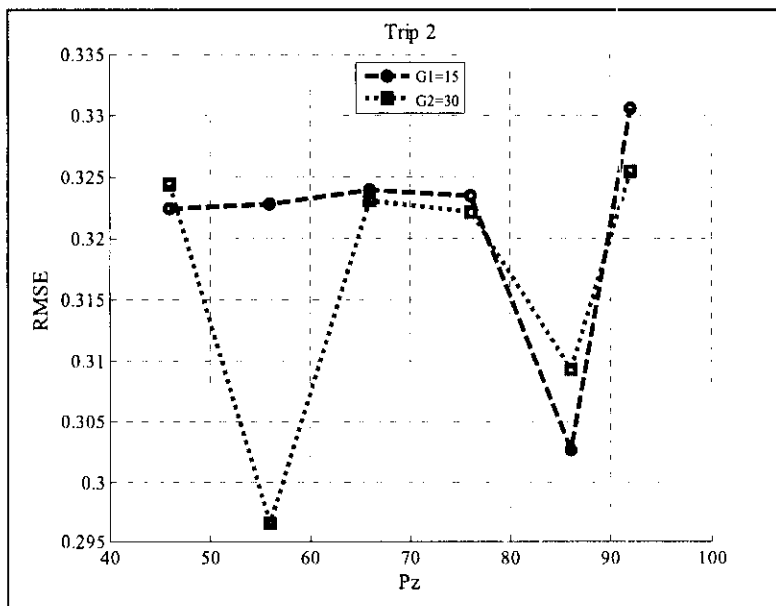


Figure 6.17 Performance of the IMS-II using two population size candidates for trip (2)

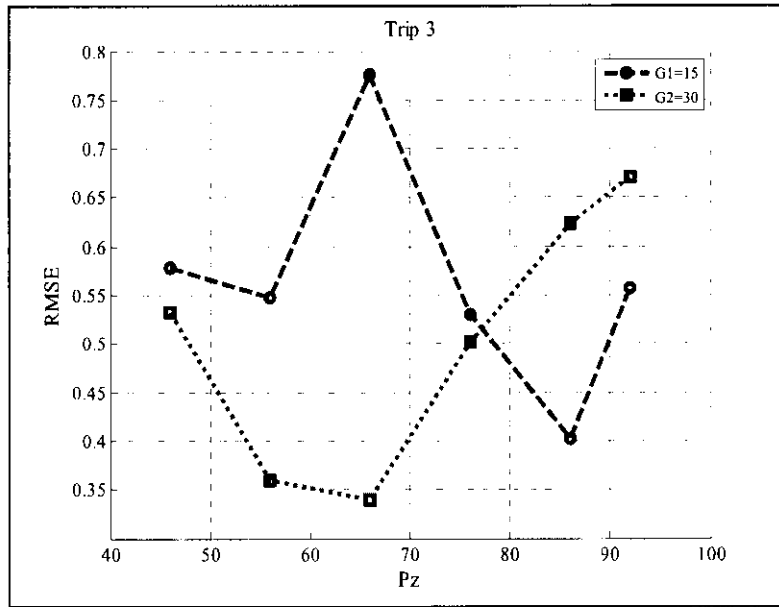


Figure 6.18 Performance of the IMS-II using two population size candidates for trip (3)

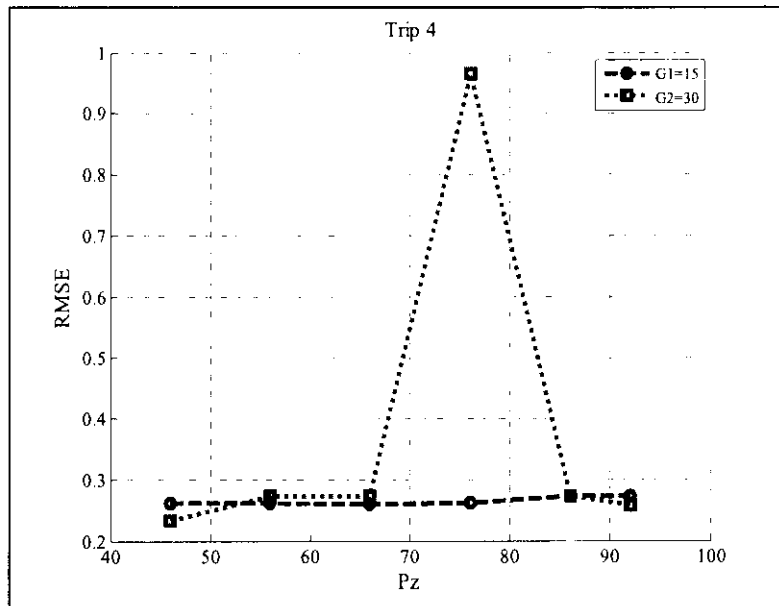


Figure 6.19 Performance of the IMS-II using two population size candidates for trip (4)

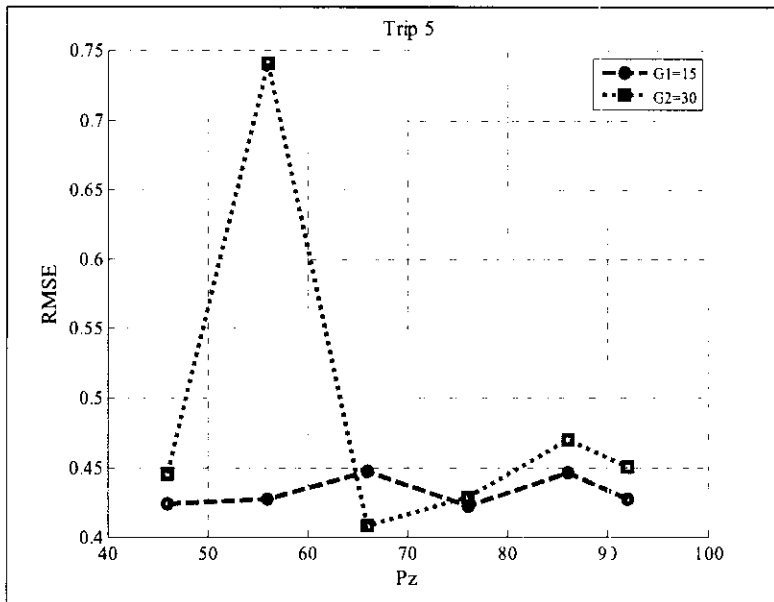


Figure 6.20 Performance of the IMS-II using two population size candidates for trip (5)

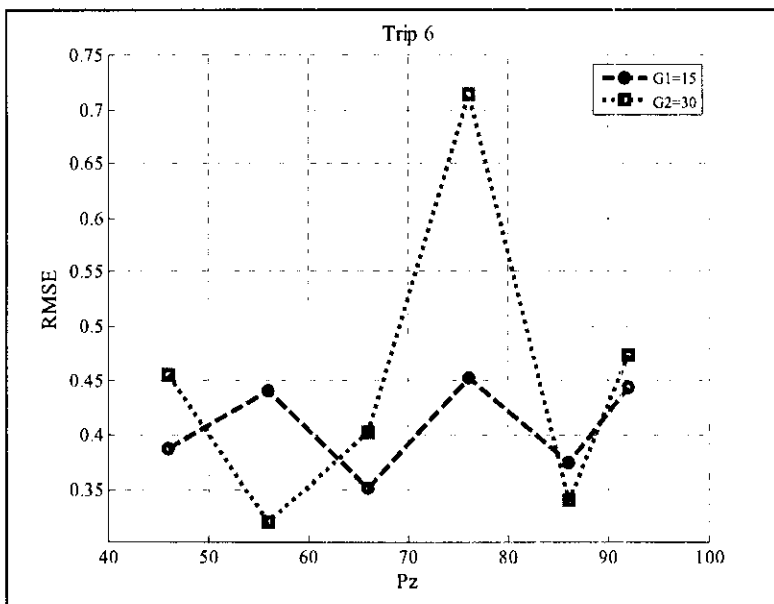


Figure 6.21 Performance of the IMS-II using two population size candidates for trip (6)

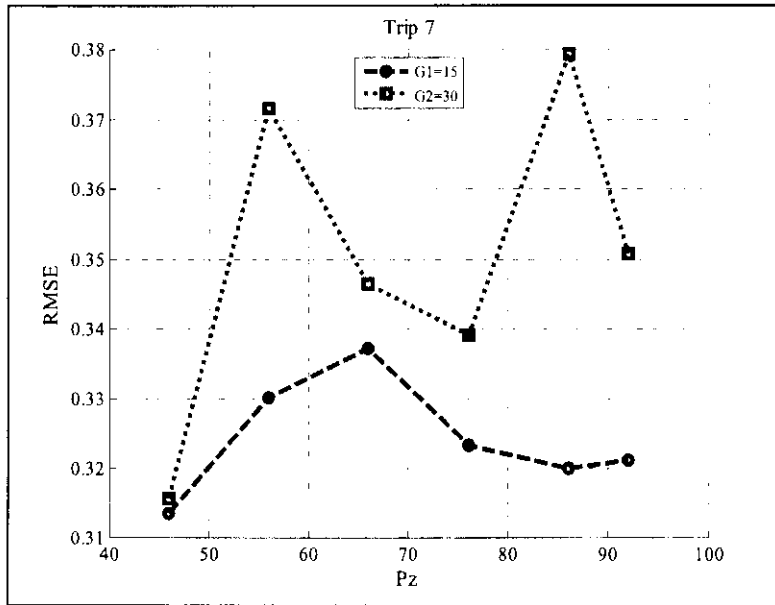


Figure 6.22 Performance of the IMS-II using two population size candidates for trip (7)

Table 6.28 Several population sizes for two values generations

		T1 Scaled Conjugate Gradient		T2 Resilient Back-Propagation		T3 BFGS Quasi Newton		T4 Levenberg-Marquardt	
		1HL-L+L		2HL-L+ T+L		2HL-P+T+L		2HL-L+L+L	
		G ₁	G ₂	G ₁	G ₂	G ₁	G ₂	G ₁	G ₂
P _{z1}	46	0.468	0.509	0.323	0.324	0.578	0.532	0.232	0.262
P _{z2}	56	0.497	0.510	0.323	0.297	0.548	0.359	0.274	0.262
P _{z3}	66	0.513	0.513	0.324	0.323	0.776	0.340	0.274	0.260
P _{z4}	76	0.462	0.509	0.323	0.322	0.530	0.501	0.965	0.261
P _{z5}	86	0.513	0.509	0.303	0.309	0.403	0.623	0.274	0.274
P _{z6}	92	0.516	0.513	0.331	0.325	0.557	0.671	0.258	0.274
		T5 BFGS Quasi Newton		T6 Scaled Conjugate Gradient		T7 Resilient Back-Propagation			
		2HL-P+L+L		2HL-L+L+L		1HL-L+L			
		G ₁	G ₂	G ₁	G ₂	G ₁		G ₂	
P _{z1}	46	0.446	0.425	0.454	0.387	0.314		0.316	
P _{z2}	56	0.742	0.428	0.319	0.440	0.330		0.372	
P _{z3}	66	0.409	0.447	0.402	0.351	0.337		0.346	
P _{z4}	76	0.43	0.422	0.714	0.452	0.323		0.339	
P _{z5}	86	0.47	0.447	0.339	0.374	0.320		0.379	
P _{z6}	92	0.451	0.428	0.473	0.443	0.321		0.351	

For all boiler operation trips, the best RMSEs found after each generation during the best run of the IMS-II are shown in Figures (6.23 through 6.29). Generally, one can see that the performance of the population improves due to the evolutionary selection process of the algorithm. For more information refer to Table (6.29).

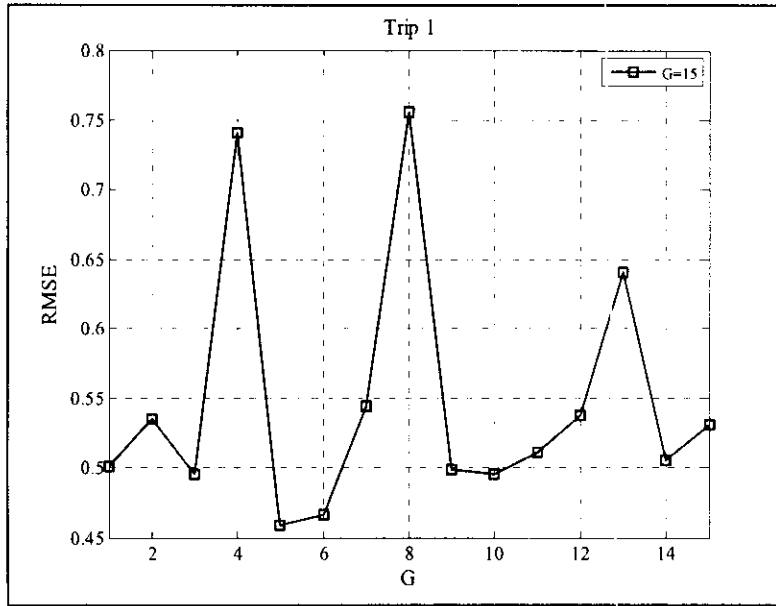


Figure 6.23 Best RMSE obtained during the best IMS-II run for trip (1)

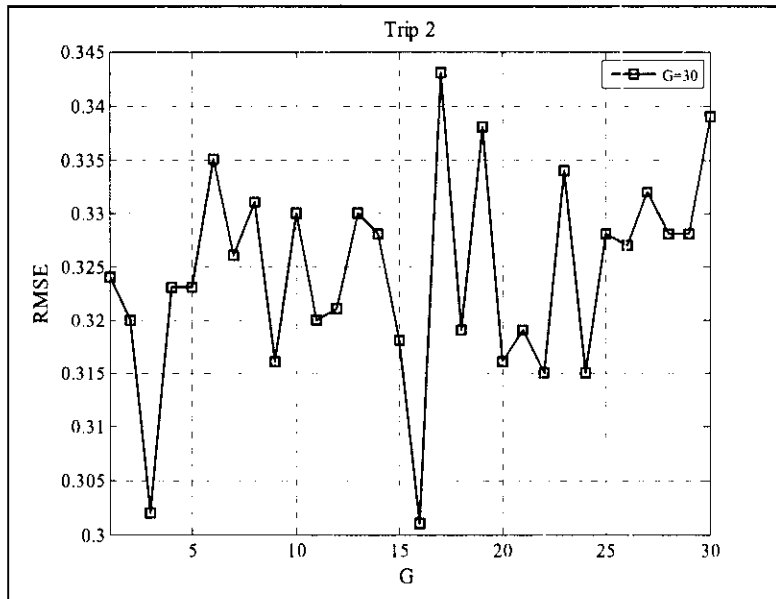


Figure 6.24 Best RMSE obtained during the best IMS-II run for trip (2)

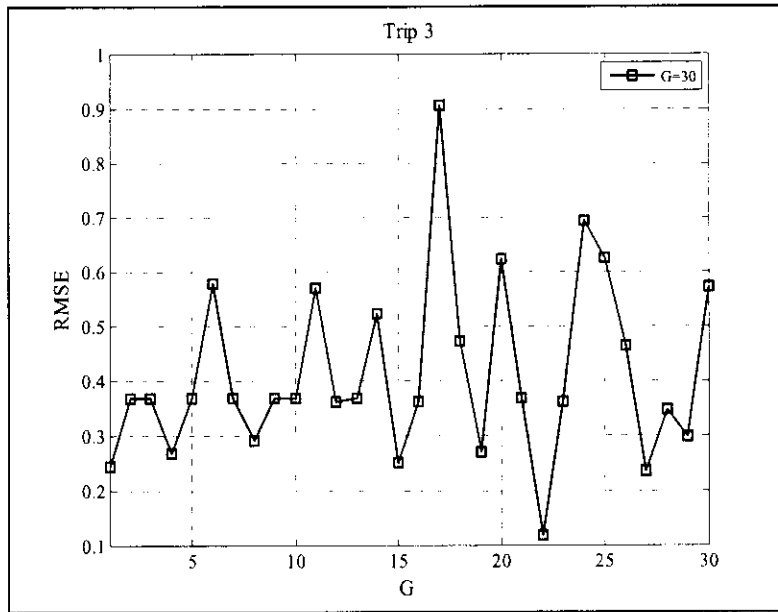


Figure 6.25 Best RMSE obtained during the best IMS-II run for trip (3)

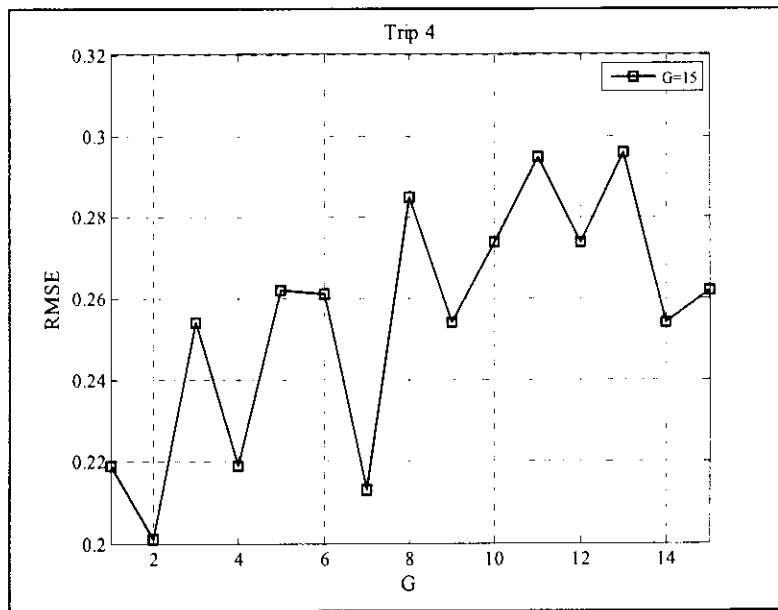


Figure 6.26 Best RMSE obtained during the best IMS-II run for trip (4)

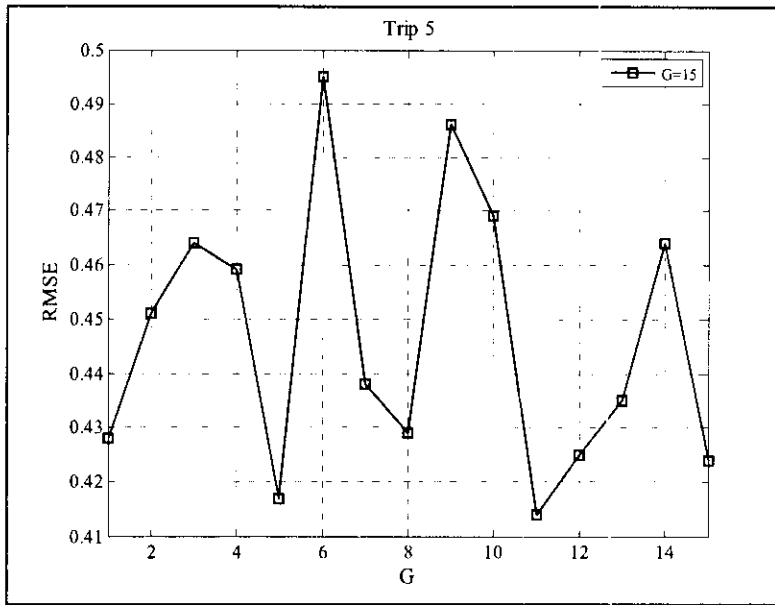


Figure 6.27 Best RMSE obtained during the best IMS-II run for trip (5)

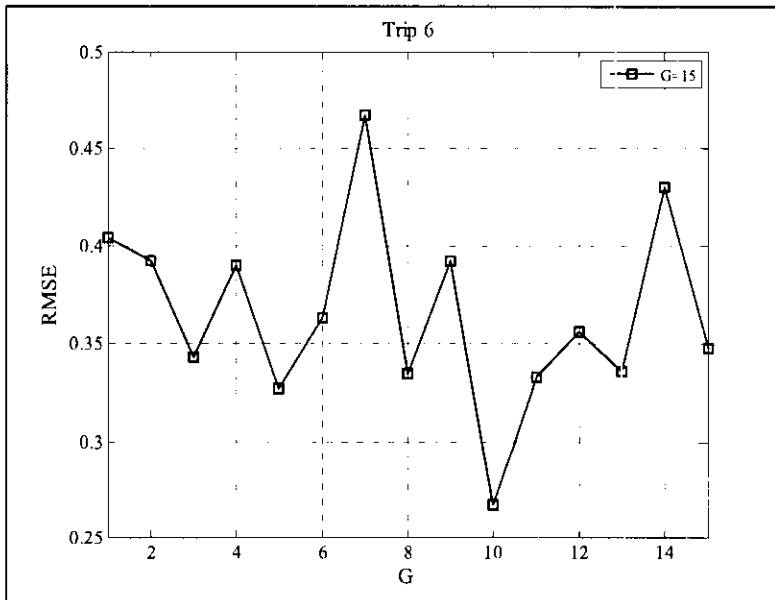


Figure 6.28 Best RMSE obtained during the best IMS-II run for trip (6)

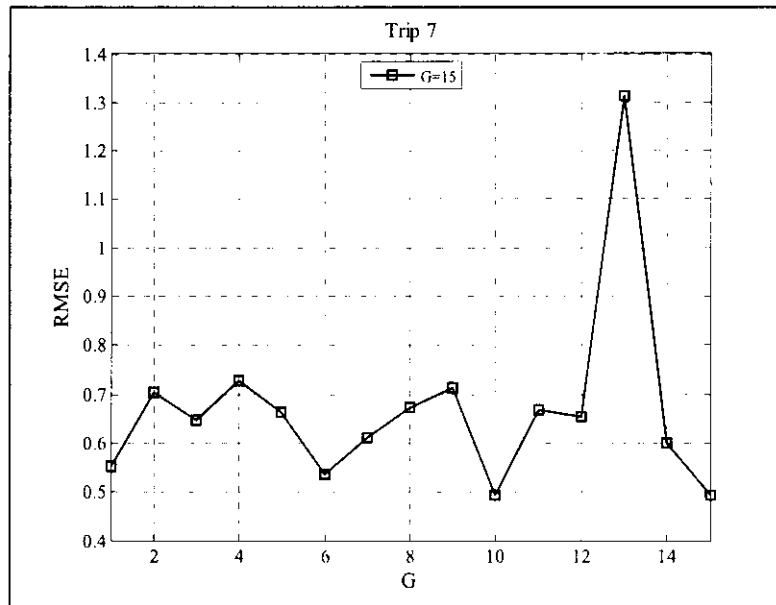


Figure 6.29 Best RMSE obtained during the best IMS-II run for trip (7)

Table 6.29 Best RMSE found during the best GA run for seven boiler trips

	T1	LM	T2	Rprop	T3	BFGS	T4	LM	T5	Rprop	T5	SCG	T7	Rprop
Generation	1HL (L+L)		2HL (L+T+L)		2HL (P+T+L)		2HL (L+L+L)		2HL (P+L+L)		2HL (L+L+L)		1HL (L+L)	
G ₁	0.501		0.324		0.244		0.219		0.428		0.404		0.553	
G ₂	0.535		0.320		0.368		0.201		0.451		0.392		0.704	
G ₃	0.495		0.302		0.368		0.254		0.464		0.343		0.646	
G ₄	0.741		0.323		0.267		0.219		0.459		0.390		0.728	
G ₅	0.459		0.323		0.368		0.262		0.417		0.327		0.663	
G ₆	0.466		0.335		0.577		0.261		0.495		0.363		0.536	
G ₇	0.544		0.326		0.368		0.213		0.438		0.467		0.611	
G ₈	0.756		0.331		0.291		0.285		0.429		0.335		0.672	
G ₉	0.498		0.316		0.368		0.254		0.486		0.392		0.713	
G ₁₀	0.495		0.330		0.368		0.274		0.469		0.267		0.493	
G ₁₁	0.511		0.320		0.570		0.295		0.414		0.333		0.668	
G ₁₂	0.537		0.321		0.361		0.274		0.425		0.356		0.653	
G ₁₃	0.641		0.330		0.368		0.296		0.435		0.336		1.313	
G ₁₄	0.505		0.328		0.522		0.254		0.464		0.430		0.599	
G ₁₅	0.531		0.318		0.251		0.262		0.424		0.348		0.493	
G ₁₆			0.301		0.361									
G ₁₇			0.343		0.906									
G ₁₈			0.319		0.472									
G ₁₉			0.338		0.270									
G ₂₀			0.316		0.623									
G ₂₁			0.319		0.368									
G ₂₂			0.315		0.118									
G ₂₃			0.334		0.361									
G ₂₄			0.315		0.692									
G ₂₅			0.328		0.625									
G ₂₆			0.327		0.463									
G ₂₇			0.332		0.236									
G ₂₈			0.328		0.346									
G ₂₉			0.328		0.296									
G ₃₀			0.339		0.571									

6.3.3 IMS-II Result Analysis

In IMS-II, the GA selection process of a bit string may or may not be selected as a parent for the next generation based on the overall performance of the bit string. The GA fitness function may have different forms for different optimization techniques. The GA fitness function was defined in chapter four to guide the search for the best combination of NN topology combinations and the most effective boiler operation variables. The GA fitness function should be designed to select fewer boiler operation variables by penalizing the selection which chooses more than necessary variables or the best NN topology while making the training error smaller for a fixed number of IMS-II training iterations.

6.3.3.1 Analysis of Trip 1 Results

The best GA search selections for each generation for a boiler water wall tube leak trip was actually found at generation 10 with the following individual's bit string of [001001011011101111100010000000111100010000000],(see Table A-1, Appendix A), which is interpreted as a 2HL with 9 and 3 neurons in the first and second hidden layers respectively, linear summation in the first hidden and output layer neurons, logistic function in the second hidden layer neurons trained with Resilient Back-Propagation training algorithm, 12 selected variables as ANN inputs. This best selection gave a value of RMSE = 0.456. Table (6.30) summarizes the best selection interpretation where "HSG." is the abbreviation of "hybrid system generation". It can be seen from that table, that the 2nd and the 3rd best GA optimization process selections, with slightly worse performance, were generation 15 and 9. For these results, two hidden layer architecture seemed to outperform in general the one hidden layer ones. Also, global optimal selections during the GA search for these generations were operation variables 2 and 10.

Table 6.30 Best GA selection interpretations for trip (1)

T1	RMSE	Selected Input Variables	No. of Inputs	ANN Topologies		
HSG.	Fitness			Training Algorithm	Architecture	Activation Function
G1	0.512541	V[1,4,6,7,9,10,12,13]	8	SCG	6HL1-2HL2	L+L+T
G2	0.510131	V[1,2,7,10,11,12]	6	BFGS	4HL1-4HL2	L+P+T
G3	0.534745	V[1,3,7,10]	4	Rprop	10HL1	L+P
G4	0.489741	V[1,2,3,4,5,6,10]	7	BFGS	3HL1-5HL2	L+T+T
G5	0.485571	V[1,2,3,4,7,10,11,12]	8	BFGS	3HL1-10HL2	L+P+P
G6	0.510384	V[2,7,10]	3	LM	7HL1-4HL2	L+P+L
G7	0.536561	V[2,3,4,5,9]	5	SCG	3HL1-2HL2	T+T+P
G8	0.564870	V[17,20,22,23,24,25,26,27,29,30]	10	BFGS	4HL1-10HL2	T+P+T
G9	0.474437	V[2,7,10,17,18,23,26,27,28]	9	LM	2HL1-7HL2	P+T+T
G10	0.456288	V[1,2,3,4,5,6,10,18,19,20,21,25]	12	Rprop	9HL1-3HL2	P+L+P
G11	0.530030	V[16,17,18,21,24,25,26]	7	LM	6HL1-8HL2	P+P+P
G12	0.486163	V[1,2,23,25,26,27,28,30,31]	9	Rprop	3HL1-8HL2	P+T+P
G13	0.523695	V[1,4,5,6,7,9,10,12,29]	9	SCG	2HL1-9HL2	T+T+T
G14	0.523899	V[11,12,13,14,15,16,19,20,23,31,32]	11	SCG	2HL1-4HL2	T+P+L
G15	0.471608	V[2,4,7,10]	4	LM	4HL1-5HL2	L+T+L

6.3.3.2 Analysis of Trip 2 Results

For the low temperature superheater trip, the best GA optimization solution was formed at generation 30. The following string represents that best optimal solution, [11011101011011010000010010000000000000000000000000], (see Table A-2, Appendix A), which is interpreted as a 2HL with 7 and 4 nodes in the first and second hidden layer respectively, logistic activation function in input and output nodes, linear summation activation function for hidden nodes trained with the Levenberg-Marquardt training algorithm and three selected boiler operation variables as ANN inputs.

This best optimal solution gave a smaller error with a value of 0.300. The interpretations of the best optimal solutions for each generation in the GA search are given in Table (6.31).

Table 6.31 Best GA selection interpretations for trip (2)

T2	RMSE	Selected Input Variables	No.of Inputs	ANN Topologies		
				Training Algorithm	Architecture	Activation Function
G1	0.330945	V[1,2,7,10,11,12]	6	BFGS	4HL1-4HL2	L+P+T
G2	0.343152	V[1,2,3,4,5,6,10,17,18,19,20,21,25]	13	Rprop	9HL1-3HL2	P+L+P
G3	0.343152	V[1,2,23,25,26,27,28,30,31]	9	Rprop	3HL1-8HL2	P+T+P
G4	0.311258	V[17,20,22,23,24,25,26,28,29]	9	BFGS	4HL1-10HL2	T+P+T
G5	0.343152	V[2,7,10]	3	LM	7HL1-4HL2	L+P+L
G6	0.343152	V[2,7,10,16,17,23,26,27,28]	9	LM	2HL1-7HL2	P+T+T
G7	0.337884	V[1,2,3,4,5,6,10]	7	BFGS	3HL1-5HL2	L+T+T
G8	0.343150	V[11,12,13,14,15,16,19,20,23,31,32]	11	SCG	2HL1-4HL2	T+P+L
G9	0.343152	V[2,3,4,5,9]	5	SCG	3HL1-2HL2	T+T+P
G10	0.343152	V[2,4,7,10]	4	LM	4HL1-5HL2	L+T+L
G11	0.323658	V[1,2,3,4,7,10,11,12]	8	BFGS	3HL1-10HL2	L+L+P
G12	0.341953	V[2,4,5,6,7,9,10,12,29]	9	SCG	2HL1-9HL2	T+T+T
G13	0.322375	V[16,17,18,21,24,25,26]	7	LM	6HL1-8HL2	P+P+P
G14	0.323532	V[1,3,7,10]	4	Rprop	10HL1	L+P
G15	0.332782	V[1,4,6,7,8,9,10,12,13]	9	SCG	6HL1-2HL2	L+L+T
G16	0.325263	V[16,17,18,21,24,27,28]	7	LM	6HL1-8HL2	P+P+P
G17	0.335066	V[1,2,3,4,5,7,11]	7	BFGS	3HL1-5HL2	L+T+T
G18	0.335068	V[2,7,10,16,17,23,26,29,30]	9	LM	2HL1-7HL2	P+T+T
G19	0.335140	V[2,4,8,11]	4	LM	4HL1-5HL2	L+T+L
G20	0.311030	V[1,2,3,4,5,6,10,17,18,19,20,22,26]	13	Rprop	9HL1-3HL2	P+L+P
G21	0.313608	V[2,4,5,6,7,9,10,13,30]	9	SCG	2HL1-9HL2	T+T+T
G22	0.330046	V[17,20,22,23,24,25,26,30,31]	9	BFGS	4HL1-10HL2	T+P+T
G23	0.337142	V[1,2,7,10,13,14]	6	BFGS	4HL1-4HL2	L+P+T
G24	0.323244	V[1,2,11,12,13,14,15,16,19,20,23]	11	SCG	2HL1-4HL2	T+P+L
G25	0.319979	V[1,2,3,4,7,10,13,14]	8	BFGS	3HL1-10HL2	L+L+P
G26	0.321165	V[2,3,4,6,10]	5	SCG	3HL1-2HL2	T+T+P
G27	0.316047	V[1,3,8,11]	4	Rprop	10HL1	L+P
G28	0.312531	V[1,2,,4,5,23,25,26,27,28]	9	Rprop	3HL1-8HL2	P+T+P
G29	0.322184	V[1,4,6,7,8,9,10,14,15]	9	SCG	6HL1-2HL2	L+L+T
G30	0.300041	V[2,8,11]	3	LM	7HL1-4HL2	L+P+L

The 2nd and the 3rd best optimal solutions, with slightly worse performance, were generation 20 and 4. Two hidden layer networks seemed to outperform in general the one hidden layer ones. Interestingly, the trade-off between the number of selected variables and the network error is not always true. No additional variables have been added into the global optimal selection to form the best selection.

6.3.3.3 Analysis of Trip 3 Results

Table (6.32) illustrates the interpretation of the best selections for a boiler drum level low trip. Among 30 generations, the best GA search selection was found at generation 11.

Table 6.32 Best GA selection interpretations for trip (3)

T3	RMSE	Selected Input Variables	No. of Inputs	ANN Topologies		
HSG.	Fitness			Training Algorithm	Architecture	Activation Function
G1	0.320848	V[1,2,23,25,26,27,28,30,31]	9	Rprop	3HL1-8HL2	P+T+P
G2	0.634648	V[16,17,18,21,24,25,26]	7	LM	6HL1-8HL2	P+P+P
G3	0.561774	V[2,4,7,10]	4	LM	4HL1-5HL2	L+T+L
G4	0.356231	V[16,17,18,21,24,27,28]	7	LM	6HL1-8HL2	P+P+P
G5	0.756969	V[1,3,7,10]	4	Rprop	10HL1	L+P
G6	0.686279	V[11,12,13,14,15,16,19,20,23,31,32]	11	SCG	2HL1-4HL2	T+P+L
G7	0.572845	V[1,2,3,4,7,10,11,12]	8	BFGS	3HL1-10HL2	L+L+P
G8	0.887247	V[1,2,3,4,7,10,13,14]	8	BFGS	3HL1-10HL2	L+L+P
G9	0.742736	V[1,4,6,7,8,9,10,12,13]	9	SCG	6HL1-2HL2	L+L+T
G10	0.647519	V[1,4,6,7,8,9,10,14,15]	9	SCG	6HL1-2HL2	L+L+T
G11	0.183808	V[1,3,9,12]	4	Rprop	10HL1	L+P
G12	0.684241	V[2,3,4,5,9]	5	SCG	3HL1-2HL2	T+T+P
G13	0.406363	V[2,7,10]	3	LM	7HL1-4HL2	L+P+L
G14	0.609929	V[17,20,22,23,24,25,26,28,29]	9	BFGS	4HL1-10HL2	T+P+T
G15	0.504909	V[1,2,3,4,5,6,10]	7	BFGS	3HL1-5HL2	L+T+T
G16	0.361325	V[2,4,9,12]	4	LM	4HL1-5HL2	L+T+L
G17	0.573284	V[1,2,3,4,5,8,12]	7	BFGS	3HL1-5HL2	L+T+T
G18	0.611913	V[17,20,22,23,24,25,26,30,31]	9	BFGS	4HL1-10HL2	T+P+T
G19	0.578195	V[2,3,4,7,11]	5	SCG	3HL1-2HL2	T+T+P
G20	0.448989	V[2,7,10,16,17,23,26,27,28]	9	LM	2HL1-7HL2	P+T+T
G21	0.557859	V[2,7,10,16,17,23,26,29,30]	9	LM	2HL1-7HL2	P+T+T
G22	0.764343	V[1,2,11,12,13,14,15,16,19,20,23]	11	SCG	2HL1-4HL2	T+P+L
G23	0.652641	V[2,4,5,6,7,9,10,12,29]	9	SCG	2HL1-9HL2	T+T+T
G24	0.504517	V[1,2,3,4,5,6,10,17,18,19,20,21,25]	13	Rprop	9HL1-3HL2	P+L+P
G25	0.594946	V[1,2,3,4,7,10,11,12]	8	BFGS	3HL1-10HL2	L+L+P
G26	0.564571	V[1,2,3,4,7,10,13,14]	8	BFGS	3HL1-10HL2	L+L+P
G27	0.601809	V[1,2,3,4,5,6,10,17,18,19,20,23,27]	13	Rprop	9HL1-3HL2	P+L+P
G28	0.711433	V[1,2,3,23,25,26,27,28,32]	9	Rprop	3HL1-8HL2	P+T+P
G29	0.479057	V[2,9,12]	3	LM	7HL1-4HL2	L+P+L
G30	0.630544	V[2,4,5,6,7,9,10,14,31]	9	SCG	2HL1-9HL2	T+T+T

The interpretations of the best GA selection bits string, [000001010001101010000010000000000000000000], (see Table A-3, Appendix A), are: 1HL network with 10 neurons in the hidden layer, logistic function in hidden neurons and linear summation activation function in output neurons trained with a Resilient Back-Propagation training algorithm and four selected variables as ANN inputs.

This best string gave a value of RMSE = 0.183. From the Best GA selection interpretation table, the 2nd and the 3rd best GA optimization process selections, with slightly worse performance, were generations 1 and 4. From these results, it can be

concluded that there was no general architecture and optimal selection during the GA search for these generations.

6.3.3.4 Analysis of Trip 4 Results

For each generation, the optimal selection of a GA optimization process for a boiler drum level low trip was essentially explored at generation 14 with the optimal string of [1000101111001111111100010000000000000000000000], (see Table A-4, Appendix A), which is interpreted as a 2HL with 3 and 5 neurons in the first and second hidden layers respectively, logistic function in the first hidden layer neurons, hyperbolic tangent activation function in the second hidden layer neurons and output layer neurons which were trained with a BFGS Quasi Newton training algorithm, and seven boiler operation variables were selected as ANN inputs. This best selection gave a value of RMSE = 0.135.

Table (6.33) shows the list of the best selections interpretation. The 2nd and the 3rd best GA search selections, with slightly worse performance, were generation 11 and 9. The comparison of these best generation results showed that the two hidden layer architecture seemed to outperform in general the one hidden layer ones. Also, there was no global optimal selection during the GA search for these generations.

Table 6.33 Best GA selection interpretations for trip (4)

T4	RMSE	Selected Input Variables	No.of Inputs	ANN Topologies		
	Fitness			Training Algorithm	Architecture	Activation Function
G1	0.300613	V[11,12,13,14,15,16,19,20,23,31,32]	11	SCG	2HL1-4HL2	T+P+L
G2	0.352365	V[1,4,6,7,8,9,10,12,13]	9	SCG	6HL1-2HL2	L+L+T
G3	0.259901	V[2,4,7,10]	4	LM	4HL1-5HL2	L+T+L
G4	0.243125	V[1,4,6,7,8,9,10,12,13,25,26]	11	SCG	6HL1-2HL2	L+L+T
G5	0.271718	V[2,7,10]	3	LM	7HL1-4HL2	L+P+L
G6	0.268666	V[1,2,23,25,26,27,28,30,31]	9	Rprop	3HL1-8HL2	P+T+P
G7	0.283586	V[17,20,22,23,24,25,26,28,29]	9	BFGS	4HL1-10HL2	T+P+T
G8	0.262282	V[1,3,7,10]	4	Rprop	10HL1	L+P
G9	0.170900	V[1,2,7,10,11,12]	6	BFGS	4HL1-4HL2	L+P+T
G10	0.187712	V[2,3,4,5,9]	5	SCG	3HL1-2HL2	T+T+P
G11	0.170509	V[16,17,18,21,24,25,26]	7	LM	6HL1-8HL2	P+P+P
G12	0.273633	V[1,2,7,10,21,23,24]	7	Rprop	10HL1	L+P
G13	0.262282	V[1,2,7,10,11,12, 25,27,31,32]	10	BFGS	4HL1-4HL2	L+P+T
G14	0.135982	V[1,2,3,4,5,6,9]	7	BFGS	3HL1-5HL2	L+T+T
G15	0.211557	V[1,2,16,17,18,21,24,25,26]	7	LM	6HL1-8HL2	P+P+P

6.3.3.5 Analysis of Trip 5 Results

The best GA search selections for each generation for a boiler feed pump trip was actually found at generation 11 with the following individual's bit string of [0100100110111100100010011100001000011001000000], (see Table A-5, Appendix A), which is interpreted as a 2HL with 2 and 10 neurons in the first and second hidden layers respectively, a linear summation in the first hidden layer, logistic function in the second hidden layer neurons and output layer neurons which were trained with a Scaled Conjugate Gradient training algorithm, and nine selected variables as ANN inputs. This best selection gave a value of RMSE = 0.447. Table (6.34) summarizes the best selections interpretation. It can be seen from that table, that the 2nd and the 3rd best GA optimization process selections, with slightly worse performance, were generation 13 and 15. For these results, two hidden layer architecture seemed to outperform in general the one hidden layer ones. Also, global optimal selections during the GA search for these generations were operation variables (3, 7, 11 and 12).

Table 6.34 Best GA selection interpretations for trip (5)

T5	RMSE	Selected Input Variables	No.of Inputs	ANN Topologies		
	Fitness			Training Algorithm	Architecture	Activation Function
G1	0.463750	V[1,2,7,10,16,19,21,25,27]	9	SCG	10HL1-4HL2	T+L+P
G2	0.502983	V[6,7,8,9,10,12,13,23,26]	9	LM	9HL1-8HL2	P+T+L
G3	0.502681	V[1,2,3,7,10,11,12,16,17,20]	10	BFGS	4HL1	P+T
G4	0.502983	V[2,3,4,7,10,11,12]	7	Rprop	2HL1-6HL2	L+L+L
G5	0.592105	V[4,7,10]	3	BFGS	9HL1-4HL2	P+P+T
G6	0.502983	V[7,10,11,12,31]	5	BFGS	5HL1-7HL2	T+L+L
G7	0.503142	V[7,10]	2	BFGS	4HL1-6HL2	L+T+P
G8	0.502983	V[3,4,7,10,11,12,18,20,25]	9	Rprop	8HL1-7HL2	P+L+T
G9	0.506503	V[4,5,7,11,12,13,19,29,30,31]	10	BFGS	10HL1	L+T
G10	0.546013	V[1,4,7,10,20,25]	6	BFGS	2HL1	T+L
G11	0.447213	V[3,7,10,11,12,17,22,23,26]	9	SCG	2HL1-10HL2	P+L+L
G12	0.537946	V[2,3,4,5,6,10,17,21,27,31]	10	SCG	6HL1-9HL2	T+L+T
G13	0.461338	V[1,3,4,7,11,12,13,18,25]	9	BFGS	10HL1-9HL2	L+P+P
G14	0.471404	V[2,4,7,10,11,12]	6	Rprop	4HL1-9HL2	T+P+P
G15	0.462237	V[3,5,7,11,12,13]	6	SCG	3HL1-9HL2	T+T+L

6.3.3.6 Analysis of Trip 6 Results

Table (6.35) illustrates the interpretation of the best selections for a boiler drum level high trip. Among 15 generations, the best GA search selection was found at generation 2. The interpretations of the best GA selection bit string of

[1001000011010100000001001000000000000000000000]. (see Table A-6, Appendix A), are 2HL with 4 and 6 neurons in the first and second hidden layers respectively, a logistic activation function in the first hidden layer, hyperbolic tangent activation function in the second hidden layer neurons and linear summation in the output layer neurons which were trained with a BFGS Quasi Newton training algorithm, and two selected variables as ANN inputs.

Table 6.35 Best GA selection interpretations for trip (6)

T6	RMSE	Selected Input Variables	No.of Inputs	ANN Topologies		
				Training Algorithm	Architecture	Activation Function
G1	0.345222	V[1,4,7,10,21,26]	6	BFGS	2HL1	T+L
G2	0.279432	V[8,11]	2	BFGS	4HL1-6HL2	L+T+P
G3	0.345352	V[3,7,10,11,12,17,22,24,27]	9	SCG	2HL1-10HL2	P+L+L
G4	0.345458	V[1,2,3,7,10,11,12,16,18,21]	10	BFGS	4HL1	P+T
G5	0.345222	V[6,7,8,9,10,12,13,24,27]	9	LM	9HL1-8HL2	P+T+L
G6	0.345352	V[7,10,11,13,32]	5	BFGS	5HL1-7HL2	T+L+L
G7	0.414909	V[3,5,7,11,14,15]	6	SCG	3HL1-9HL2	T+T+L
G8	0.345370	V[1,3,4,7,11,12,13,19,26]	9	BFGS	10HL1-9HL2	L+P+P
G9	0.345639	V[3,4,7,10,11,12,18,21,26]	9	Rprop	8HL1-7HL2	P+L+T
G10	0.415308	V[2,4,7,10,13,14]	6	Rprop	4HL1-9HL2	T+P+P
G11	0.325963	V[2,3,4,7,10,13,14]	7	Rprop	2HL1-6HL2	L+L+L
G12	0.324384	V[1,2,7,10,16,19,21,26,28]	9	SCG	10HL1-4HL2	T+L+P
G13	0.404811	V[2,3,4,5,6,10,17,21,28,32]	10	SCG	6HL1-9HL2	T+L+T
G14	0.345777	V[1,4,5,7,11,12,13,19,29,32]	10	BFGS	10HL1	L+T
G15	0.346405	V[4,7,10]	3	BFGS	9HL1-4HL2	P+P+T

This best string gave a value of RMSE = 0.279. From the best GA selection interpretation table, the 2nd and the 3rd best GA optimization process selections, with slightly worse performance, were generations 12 and 11. From these results, two hidden layer architecture seemed to outperform in general the one hidden layer ones. Moreover, there was no global optimal selection during the GA searches for these generations.

6.3.3.7 Analysis of Trip 7 Results

For a high temperature superheater trip, the best GA optimization solution was formed at generation 4. The following string represents that best optimal solution, [10010101100110100000100110010000000000000000000], (see Table A-7, Appendix A), which is interpreted as a 2HL with 5 and 7 nodes in the first and second hidden layers respectively, a hyperbolic tangent activation function in the first hidden layer

nodes, a logistic activation function for the second hidden layer nodes which were trained with BFGS Quasi Newton, and five selected boiler operation variables as ANN inputs.

This best optimal solution gave a smaller error with a value of 0.311. The interpretations for the best optimal solutions for each generation in the GA search are given in Table (6.36). The 2nd and the 3rd best optimal solutions, with a slightly worse performance, were generation 13 and 14. The two hidden layer network seemed to outperform in general the one hidden layer ones. As well, the global optimal selections during the GA search for these generations were operation variables 7 and 11.

Table 6.36 Best GA selection interpretations for trip (7)

T7	RMSE	Selected Input Variables	No.of Inputs	ANN Topologies		
HSG.	Fitness			Training Algorithm	Architecture	Activation Function
G1	0.330945	V[1,2,7,10,16,19,21,28,29]	9	SCG	10HL1-4HL2	T+L+P
G2	0.343152	V[4,9,12]	3	BFGS	9HL1-4HL2	P+P+T
G3	0.343152	V[1,2,3,4,5,6,10,17,21,29]	10	SCG	6HL1-9HL2	T+L+T
G4	0.311258	V[2,7,10,11,12,14]	5	BFGS	5HL1-7HL2	T+L+L
G5	0.343152	V[3,7,10,11,12,17,22,25,28]	9	SCG	2HL1-10HL2	P+L+L
G6	0.343152	V[6,7,8,9,10,12,13,25,27]	9	LM	9HL1-8HL2	P+T+L
G7	0.337884	V[1,4,7,10,22,27]	6	BFGS	2HL1	T+L
G8	0.343150	V[1,4,5,7,11,12,13,19,29,32]	10	BFGS	10HL1	L+T
G9	0.343152	V[2,4,7,10,13,14]	6	Rprop	4HL1-9HL2	T+P+P
G10	0.343152	V[9,12]	2	BFGS	4HL1-6HL2	L+T+P
G11	0.323658	V[1,3,4,7,11,12,13,20,27]	9	BFGS	10HL1-9HL2	L+P+P
G12	0.341953	V[3,4,7,10,11,12,18,22,27]	9	Rprop	8HL1-7HL2	P+L+T
G13	0.322375	V[3,5,7,11,14,15]	6	SCG	3HL1-9HL2	T+T+L
G14	0.323532	V[1,2,3,7,10,11,12,16,19,22]	10	BFGS	4HL1	P+L
G15	0.332782	V[2,3,4,7,10,13,15]	7	Rprop	2HL1-6HL2	L+L+L

Table (6.37) shows the best GA search selections for all of the boiler operation trips. It can be observed that the two hidden layers network outperformed the one hidden layer network in most cases with the exception of the trip 3 case. In general, the IMS-II gave a smaller error value of less than 0.5. Moreover, few numbers of selected operation variables as ANN inputs were explored. Also, it seemed that the BFGS Quasi Newton and Resilient Back-Propagation training algorithms did better than the other two training algorithms in most cases.

Table 6.37 Best GA selection interpretations for all boiler operation trips

Trip	HSG.	RMSE	Selected input variables	No. of Inputs	ANN Topologies		
		Fitness			Training Algorithm	Architecture	Activation Function
1	G10	0.456288	V[1,2,3,4,5,6,10,18,19,20,21,25]	12	Rprop	9HL1-3HL2	P+L+P
2	G30	0.300041	V[2,8,11]	3	LM	7HL1-4HL2	L+P+L
3	G11	0.183808	V[1,3,9,12]	4	Rprop	10HL1	L+P
4	G14	0.135982	V[1,2,3,4,5,6,9]	7	BFGS	3HL1-5HL2	L+T+T
5	G11	0.447213	V[3,7,10,11,12,17,22,23,26]	9	SCG	2HL1-10HL2	P+L+L
6	G2	0.279432	V[8,11]	2	BFGS	4HL1-6HL2	L+T+P
7	G4	0.311258	V[2,7,10,11,12,14]	5	BFGS	5HL1-7HL2	T+L+L

6.4 IMS-II Performance

The validation process is repeated again on the IMS-I. But this time using the optimal obtained results from the IMS-II. The same real boiler validation data sets which have been used to validate how rapidly the IMS-I detects the fault were used. These validation data sets are described in Table (6.19).

The same decision support approach as adopted in the IMS-I (refer to section 6.2.2) was used in order to make a decision whether a fault has been indicated or not. In addition, the decision support approach was used here in order to evaluate the intelligent system initially.

Consequently, the IMS-I output values above 0.5 indicate a faulty boiler operation; output values below 0.4 indicate a normal boiler operation and the output values in the threshold range [0.4-0.5] indicate the previously known condition of the system output.

6.4.1 IMS-II Validation Results of Trip 1

Figure (6.30) shows the IMS-II output on the first validation data set. The time step is a “one” minute interval. The “boiler water wall tube leak” trip was introduced in the 225th interval. The fault was detected by the intelligent system within the 223th interval. The system output is 0.65, which is considered as a strong fault indication (close to one). The comparison of the validation results before and after using the IMS-II outcomes shows that the first validation process outperformed the second one

based on the rapid fault detection. Hence, the interval time difference was 3 minutes only.

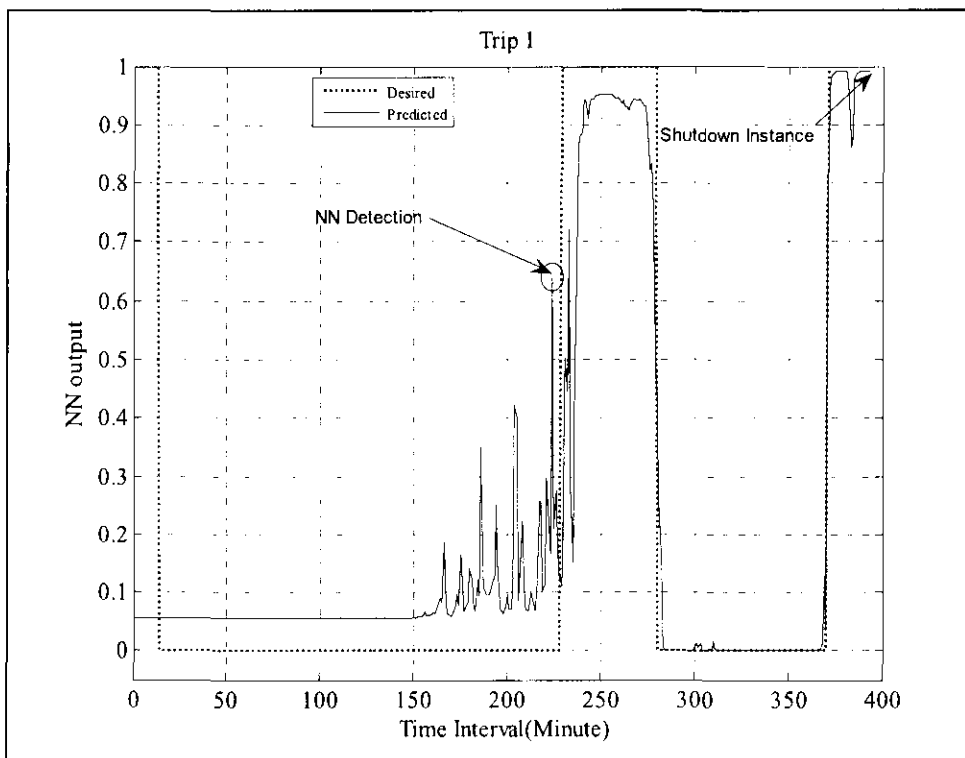


Figure 6.30 IMS-I output during the first validation real data set (T1)

6.4.2 IMS-II Validation Results of Trip 2

In Figure (6.31) the system response in the second validation data set is presented. This real set contains a “low temperature superheater” trip. The data started with a normal boiler operation and the faulty operation is introduced in the 225th interval. It is clear that the IMS-I detected the fault within the 225th interval (at the same time as the plant control system); the system output is 9.1, which is considered a very strong fault indication (close to one). The comparison of the validation results before and after using the IMS-II outcomes shows that the first validation process outperformed the second one based on the rapid fault detection. Hence, the interval time difference was 16 minutes.

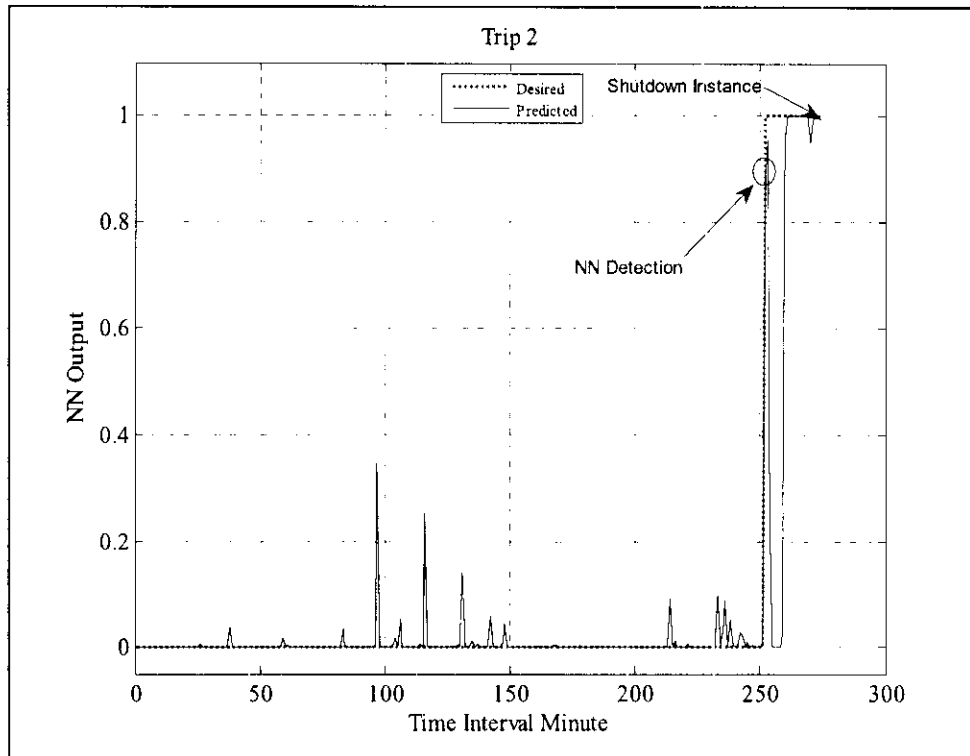


Figure 6.31 IMS-I output during the first validation real data set (T2)

6.4.3 IMS-II Validation Results of Trip 3

Figure (6.32) shows the specific period of the third validation data set for a “boiler drum level low” trip, where the fault was introduced in the 17th interval. The IMS-I takes a few steps before the boiler control system to indicate a possible fault (15th interval) with a model output value of 0.55, while the system output drops below 0.5 (normal boiler operation) 5 minutes after the occurrence of the fault and stays in that region for a few more intervals. The comparison of the validation results before and after using the IMS-II outcomes shows that the first validation process outperformed the second one based on the rapid fault detection. Hence, the interval time difference was 8 minutes only.

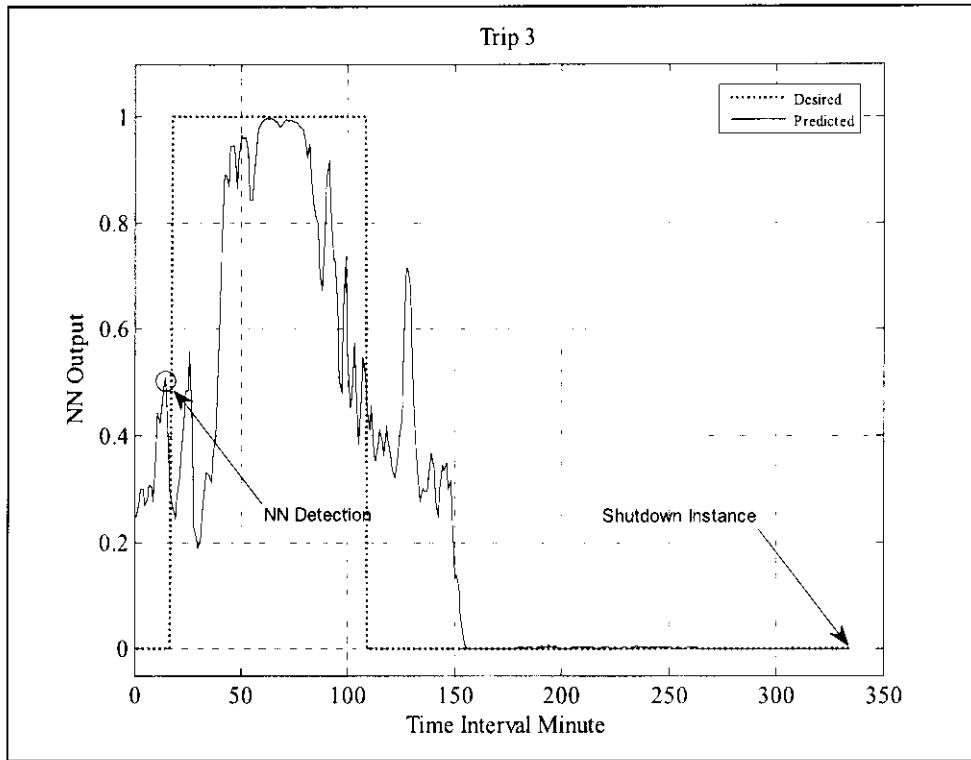


Figure 6.32 IMS-I output during the first validation real data set (T3)

6.4.4 IMS-II Validation Results of Trip 4

These can be better seen in Figure (6.33), where the proposed IMS-I outputs are shown for the entire validation data set for a “boiler drum level low” trip also, but in a different unit. The fault was introduced in the 50th interval. It is clear here that this kind of fault is detected very fast by the intelligent system, even from the 10th step, the system gives a weak indication that a fault has occurred with an output value of 0.55. Therefore, after the fault has been detected, it is not an important issue if the IMS-I fails to continuously detect it. The validation results before and after using the IMS-II outcomes shows that the second validation process outperformed the first one based on the rapid fault detection. Hence, the interval time difference was 30 minutes.

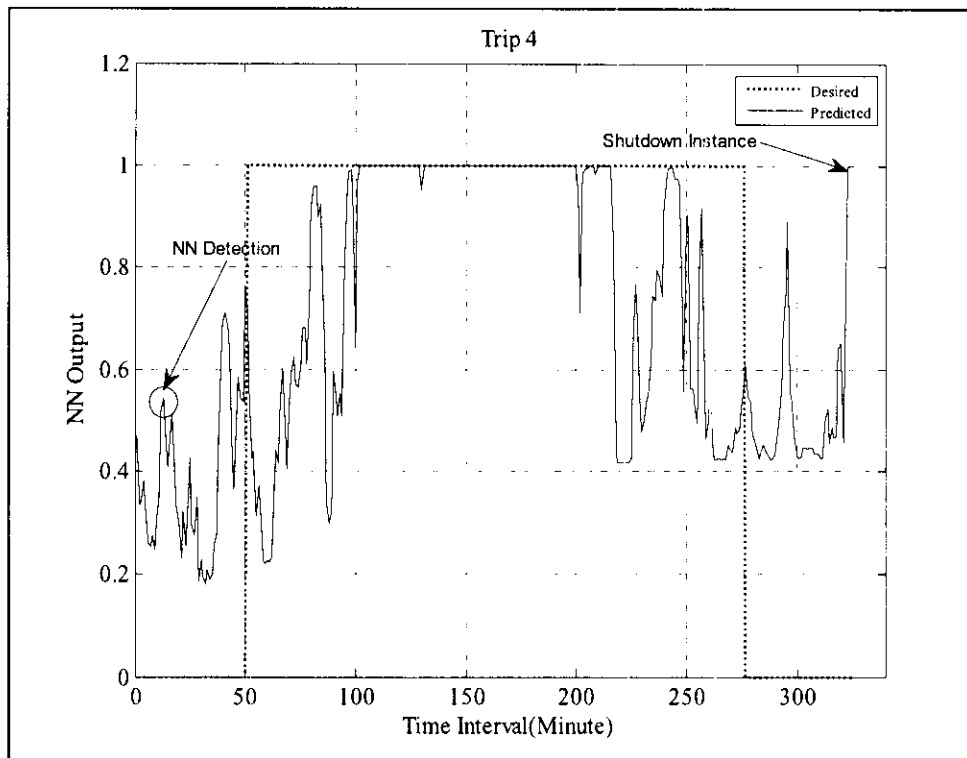


Figure 6.33 IMS-I output during the first validation real data set (T4)

6.4.5 IMS-II Validation Results of Trip 5

In Figure (6.34) the IMS-I output during the fifth validation data set for the “boiler feed pump” trip is shown. As in the case of the second real data set, the data started with a normal boiler operation and the faulty operation is introduced in the 118th interval. It can be seen in the figure, that the proposed system detects the fault two steps before the plant control system interval (116th step).

The intelligent system output becomes high enough at 0.61, which is considered as a strong indication of the fault and during the occurrence of the fault; the system output drops suddenly before the fault has started to vanish. As mentioned earlier, that sudden drop is not considered as a network disadvantage; however, the important factor for fault detection is the rapidness of detection. The validation results before and after using the IMS-II outcomes shows that the second validation process outperformed than first one based on the rapid fault detection. Hence, the interval time difference was 2 minutes only.

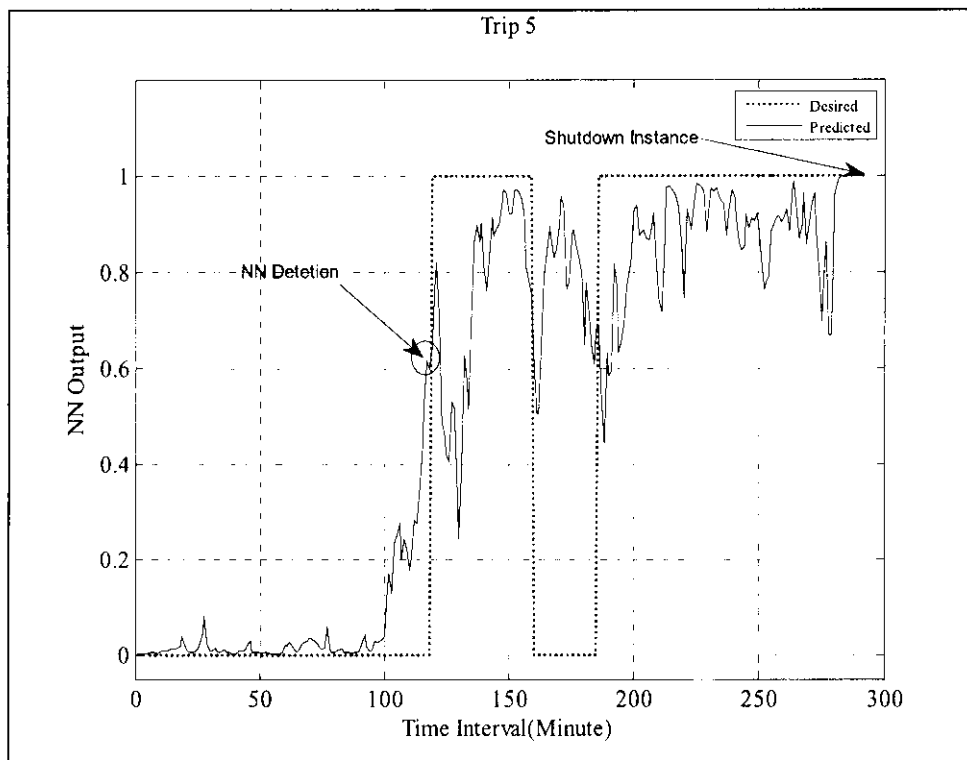


Figure 6.34 IMS-I output during the first validation real data set (T5)

6.4.6 IMS-II Validation Results of Trip 6

The IMS-I output during the sixth validation data set is shown in Figure (6.35). The boiler data started with a normal operation and the “boiler drum level high” trip was introduced at the 239th interval. It is clear that the intelligent system detected the fault within the 155th interval (84 steps before the plant monitoring system) with a system output value of 0.78. The proposed IMS-I output value was also considered as a strong indication that the boiler operation was not normal with higher values toward the end of the fault.

The comparison of validation results before and after using the IMS-II outcomes shows that the second validation process outperformed the first one based on the rapid fault detection. Hence, the interval time difference was 84 minutes. It considers such a high difference in the detection time instance needs more effort to study the nature of the influencing operation variables of the plant.

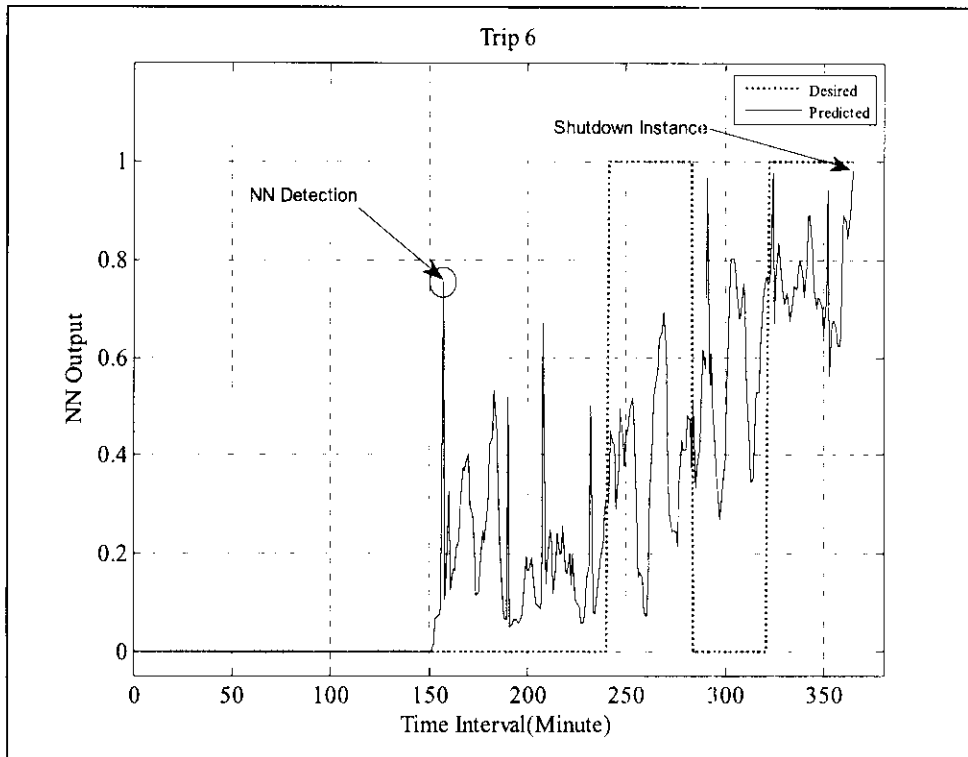


Figure 6.35 IMS-I output during the first validation real data set (T6)

6.4.7 IMS-II Validation Results of Trip 7

Figure (6.36) shows the IMS-I output through the seventh validation data set for a “high temperature superheater” trip. From the graph, it can be observed that even though the fault is detected by the intelligent system, there are several intervals where the system output returned to the normal operation limit. That occurred twice during the main period of the specific fault and it also took place towards the end of the fault (after interval 78). The system was extremely fast in detecting the fault within 5 intervals (35 minutes before the plant monitoring system). The IMS-I output value was 0.62. With that output value it’s considered as a strong indicator of the faulty boiler operation existence. The validation results before and after using the IMS-II outcomes shows that the second validation process did better than the first one based on the rapid fault detection. Thus, the difference in detection time instance was 12 minutes.

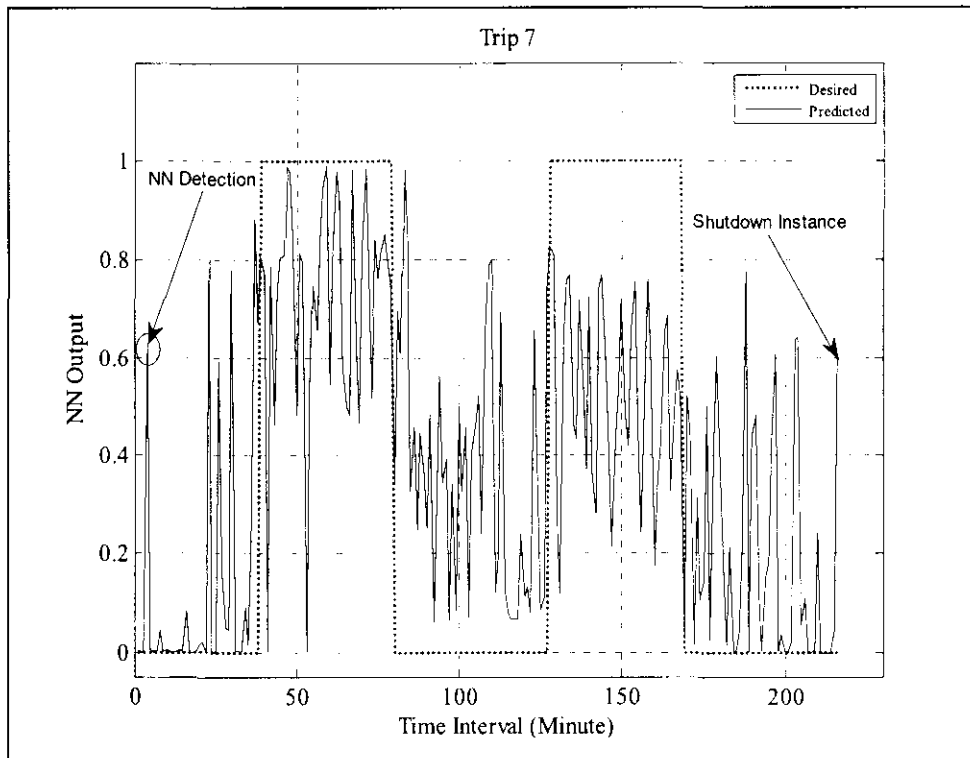


Figure 6.36 IMS-I output during the first validation real data set (T7)

6.5 Comparison between IMS-I and IMS-II Performances

The proposed IMS-I was capable of detecting the specific boiler operation trips before the fault occurrence with exception of trip 2 (at the same time as the plant control system), with slight differences from the first proposed system and it's considered satisfactory.

Based on the previous section results, it is obvious that the IMS-II was capable of finding an optimal solution that provided satisfactory accuracy in the NN training and validation processes. The IMS-II was proposed in order to optimize and automate the procedure of selection of the optimal combination of NN topologies and boiler operation variables for a specific boiler trip.

The most commonly used technique for that purpose is a pure NN. It was clear that the general problem space under investigation is infinite. The problem space can be radically diminished after some limitations on the selection of the available NN topologies and the number of the most influential boiler operation variables as NN inputs. A pure NN technique in this kind of problem covers limited portions of them.

It can be noticed from the literature, that for some cases the pure NN technique may be “profitable”, while for some others it may be “unprofitable”. However, when the problem space is enormous, the probabilities of being profitable decrease radically. But, the luck of the pure NN technique to be successful increases with the use of experience and achievable knowledge by the user who performs the technique [14-19].

In this work, the problem space consisted of 2^{46} possible combinations. If one also considers that each combination has to be trained several times with different initial conditions, then it’s clear that an exhaustive search becomes almost impractical and the pure NN technique becomes quite ambiguous. A sophisticated optimization technique merged with an NN technique as a hybrid intelligent system, is able to explore vast spaces of the considered problem in a computationally intelligent way so that the processing power is radical to an exhaustive search and the problem results are more probable to be an optimal solution than the result of a pure NN technique.

After all of these, it can be concluded that a direct comparison of results achieved by IMS-II and by IMS-I cannot lead to a complete decision on which the best system is, but it can give an insight into the successful degree of the IMS-II. Therefore, a preliminary training process was performed using a pure NN in order to find the optimal NN topology.

The search explorations were essentially focused on 1HL and 2HL architectures. Detailed results that were obtained by the IMS-I, together with the ones achieved by the IMS-II, are shown in Table (6.38).

Table 6.38 Optimal solution given by the IMS-I and IMS-II

T	RMSE	IMS-I			RMSE	IMS-II		
		ANN Topologies				ANN Topologies		
		Architecture	Activation Function	Training Algorithm		Architecture	Activation Function	Training Algorithm
1	0.0642	6HL1	L+L	SCG	0.2029	9HL1-3HL2	P+L+P	Rprop
2	0.1414	3HL1-10HL2	L+T+L	Rprop	0.1387	7HL1-4HL2	L+P+L	LM
3	0.2752	2HL1-3HL2	P+T+L	BFGS	0.2564	10HL1	L+P	Rprop
4	0.3597	6HL1-2HL2	L+L+L	LM	0.2599	3HL1-5HL2	L+T+T	BFGS
5	0.3571	4HL1-9HL2	P+L+L	BFGS	0.2835	2HL1-10HL2	P+L+L	SCG
6	0.337	3HL1-7HL2	L+L+L	SCG	0.3367	4HL1-6HL2	L+T+P	BFGS
7	0.4247	10HL1	L+L	Rprop	0.3794	5HL1-7HL2	T+L+L	BFGS

Table (6.38) shows that the IMS-II did slightly better than the IMS-I in most boiler trips with exception of trip 1. The two hidden layer network seemed to outperform in general the one hidden layer ones. Also, it seemed that the BFGS Quasi Newton and Resilient Back-Propagation training algorithms outperformed the other two training algorithms in most cases.

The logistic activation function and linear summation in the first hidden and output layer nodes outperformed other activation functions in most cases. A slightly lower RMAE was observed in the second system which reveals that the IMS-II performed better than the IMS-I. Only for the first trip of the hybrid system does it give a worse performance than the performance of the IMS-I (higher error).

Concerning trip (1), it is the opinion of the researcher to extend the work on the tube leakage fault, where its nature is different than the other boiler trips. It is not subjected to sensing and measurable variables in contrast to the other trips, where the related variables were measurable.

The global optimal selections by a plant control system and a hybrid IMS system are given in Table (6.39). From this table; it's clear that the IMS-II succeeded in finding the most effective boiler operation with expectation of trip 6.

Table 6.39 The most effective boiler variables by plant control system and IMS-II

Effective boiler operation variables		
Trip	Plant control system	IMS-II
1	V[5,8,9,11,14,17,18,20,22,23,24,25,26,27,29]	V[1,2,3,4,5,6,10,18,19,20,21,25]
2	V[3,4,5,9,11,12,20,21,31]	V[2,8,11]
3	V[1,2,3,13,19,24]	V[1,3,9,12]
4	V[5,8,23,25,26,27,28]	V[1,2,3,4,5,6,9]
5	V[1,2,3,13,15,19,20,21,22,23,24,29,31]	V[3,7,10,11,12,17,22,23,26]
6	V[1,3,4,6,12,13,15,18,19,30]	V[8,11]
7	V[2,4,14,19,21]	V[2,7,10,11,12,14]

6.6 Actions on Detecting the MNJTTP Boilers Trips

After the detection of the faulty boiler operation and identification of the specific trip(s), taking a certain remedial action is possible and a more appropriate approach. The corrective action might come in many different forms. It is fairly possible, and evidently a simple remedy, to read just some control component so as to restore a satisfactory operation. On the other hand, the fault has to be pinpointed so that a replaceable component or sub-system can be introduced.

The former course of action has many similarities with the concept of adaptive control. In fact, tracing a fault back to its real cause is not essential since the interaction of different components is likely to cause different faults that can be traced back to many alternate sources.

When a failure or incipient failure, has been detected, it is considerably possible to come up with substitute measurements to reduce downtime. Substitute measurements involve the determination of the missing measurements mainly from general energy and mass balances. The provision for substitute measurements is, in fact, equivalent to providing stand-by or redundant instruments in the process of a failure, but without incurring any extra costs except computer cost [2].

If an operator detects a malfunction, he generally manipulates the process control system in order to place the automatic loop on manual control. Similarly, with a computer control, a supervisory program can prevent control action from being taken based on incorrect information by closing paths in the redundancy network which include the faulty equipment, and divert the information flow through a path known to be functioning correctly [2].

This function can be easily implemented as a simple computer program, there by improving plant availability in the face of instrument or equipment failure. In either case, when the fault is detected, distinguishing whether the trouble is in the plant or in the detectors is an important decision that should be made. Second, a decision has to be made to determine whether the fault is fatal or just temporary. A real failure might call for an urgent plant shutdown, whereas, if the trouble resides in the measuring

instruments, the plant continues running, but the operators will be alarmed about the anomalies.

Tables (6.40 through 6.46) illustrate the necessary actions that should be taken by the MNJTTP operator to take appropriate corrective action. These tables have been built based on the proposed IMS-II results. The shaded table fields represent the global influential boiler variables to the plant monitoring system and the proposed IMS-II.

Table 6.40 Necessary actions for trip (1)

Investigations	Possible Causes	Actions To Be Taken		
High Alarm	Failure In Measurements	Ask The Instrumentation Specialist For Investigations And Take The Appropriate Corrective Action		
		Sensors	Actuators	
Boiler Water Wall Tube Leak-Unit 1	TOTAL COMBINED STEAM FLOW		JMJG_U1_HAC01CF501X5V	
	FEED WATER FLOW		JMJG_U1_HAC61CF501X5V	
	BOILER DRUM PRESSURE	JMJG_U1_HAD01CP501AXV1		
		JMJG_U1_HAD01CP501BXV1		
		JMJG_U1_HAD01CP501CXV1		
		JMJG_U1_HAD01CP501X3V		
	SH STEAM PRESSURE	JMJG_U1_HAH92CP501X3V		
	SH STEAM TEMPERATURE	JMJG_U1_HAH92CT501X3V		
	ECONOMISER INLET TEMPERATURE	JMJG_U1_HAC01CT501X3V		
		JMJG_U1_HAC01CT501XV1		
		JMJG_U1_HAC01CT502XV1		
		JMJG_U1_HAC01CT503XV1		
	HT S/HTR I/L HDR MET TEMP	JMJG_U1_HAH91CT551XV1		
		JMJG_U1_HAH91CT552XV1		
		JMJG_U1_HAH91CT553XV1		
		JMJG_U1_HAH91CT554XV1		
		JMJG_U1_HAH91CT601XV1		
		JMJG_U1_HAH91CT602XV1		
	ECONOMISER O/L TEMP	JMJG_U1_HAC21CT501XV1		
		JMJG_U1_HAC22CT501XV1		
	FEEDWATER FLOW TX	JMJG_U1_HAC61CF501AXV1		
		JMJG_U1_HAC61CF501BXV1		
		JMJG_U1_HAC61CF501CXV1		
		JMJG_U1_HAC61CF501X3V		
	BOILER CIRC PMP1 DIFF PRESS	JMJG_U1_HAG01CP501XV1		
		JMJG_U1_HAG01CP502XV1		
	BOILER CIRC PUMP2 DIFF PRESS	JMJG_U1_HAG02CP501XV1		
		JMJG_U1_HAG02CP502XV1		
	LT S/HTR RW EXCH MET TEMP	JMJG_U1_HAH39CT511XV1		
		JMJG_U1_HAH39CT512XV1		

Table 6.41 Necessary actions for trip (2)

Investigations	Possible Causes	Actions To Be Taken		
High Alarm	Failure In Measurements	Ask The Instrumentation Specialist For Investigations And Take The Appropriate Corrective Action		
		Sensors	Actuators	
Low Temperature Super Heater Unit 3	FEED WATER FLOW		JMJG_U3_HAC61CF501X5V	
	HT S/HTR EXCH MET TEMP	JMJG_U3_HAH90CT511XV1		
		JMJG_U3_HAH90CT512XV1		
		JMJG_U3_HAH90CT513XV1		
		JMJG_U3_HAH90CT514XV1		
		JMJG_U3_HAH90CT511XV1		
		JMJG_U3_HAH90CT512XV1		
		JMJG_U3_HAH90CT513XV1		
	FINAL S/HTR O/L TEMPERATURE	JMJG_U3_HAH92CT501XV1		
		JMJG_U3_HAH92CT502XV1		
		JMJG_U3_HAH92CT503XV1		
		JMJG_U3_HAH93CT501XV1		
		JMJG_U3_HAH93CT502XV1		
		JMJG_U3_HAH93CT503XV1		
		JMJG_U3_HAH93CT501X3V		

Table 6.42 Necessary actions for trip (3)

Investigations	Possible Causes	Actions To Be Taken	
High Alarm	Failure In Measurements	Ask The Instrumentation Specialist For Investigations And Take The Appropriate Corrective Action	
		Sensors	Actuators
Boiler Drum Level Low Unit 3	TOTAL COMBINED STEAM FLOW		JMJG_U3_HAC01CF501X5V
	BOILER DRUM PRESSURE	JMJG_U3_HAD01CP501AXV1	
		JMJG_U3_HAD01CP501BXV1	
		JMJG_U3_HAD01CP501CXV1	
		JMJG_U3_HAD01CP501X3V	
	IT S/HTR EXCH MET TEMP	JMJG_U3_HAH90CT515XV1	
		JMJG_U3_HAH90CT516XV1	
		JMJG_U3_HAH90CT517XV1	
		JMJG_U3_HAH90CT518XV1	
	FINAL S/HTR O/L TEMPERATURE	JMJG_U3_HAH92CT501XV1	
		JMJG_U3_HAH92CT502XV1	
		JMJG_U3_HAH92CT503XV1	
		JMJG_U3_HAH93CT501XV1	
		JMJG_U3_HAH93CT502XV1	
		JMJG_U3_HAH93CT503XV1	
		JMJG_U3_HAH93CT501X3V	

Table 6.43 Necessary actions for trip (4)

Investigations	Possible Causes	Actions To Be Taken		
High Alarm	Failure In Measurements	Ask The Instrumentation Specialist For Investigations And Take The Appropriate Corrective Action		
		Sensors	Actuators	
Boiler Drum Level Low -Unit 2	TOTAL COMBINED STEAM FLOW		JMJG_U2_HAC01CF501X5V	
	FEED WATER FLOW		JMJG_U2_HAC61CF501X5V	
	BOILER DRUM PRESSURE	JMJG_U2_HAD01CP501AXV1		
		JMJG_U2_HAD01CP501BXV1		
		JMJG_U2_HAD01CP501CXV1		
		JMJG_U2_HAD01CP501X3V		
	SH STEAM PRESSURE	JMJG_U2_HAH92CP501X3V		
	SH STEAM TEMPERATURE	JMJG_U2_HAH92CT501X3V		
	ECONOMISER INLET TEMPERATURE	JMJG_U2_HAC01CT501X3V		
		JMJG_U2_HAC01CT501XV1		
		JMJG_U2_HAC01CT502XV1		
		JMJG_U2_HAC01CT503XV1		
	IT S/HTR EXCH MET TEMP	JMJG_U2_HAH90CT515XV1		
		JMJG_U2_HAH90CT516XV1		
		JMJG_U2_HAH90CT517XV1		
		JMJG_U2_HAH90CT518XV1		

Table 6.44 Necessary actions for trip (5)

Investigations	Possible Causes	Actions To Be Taken	
High Alarm	Failure In Measurements	Ask The Instrumentation Specialist For Investigations And Take The Appropriate Corrective Action	
		Sensors	Actuators
Boiler Feed Pump -Unit 2	BOILER DRUM PRESSURE	JMJG_U2_HAD01CP501AXV1	
		JMJG_U2_HAD01CP501BXV1	
		JMJG_U2_HAD01CP501CXV1	
		JMJG_U2_HAD01CP501X3V	
	ECONOMISER INLET TEMPERATURE	JMJG_U2_HAJ61CT501AXV1	
		JMJG_U2_HAJ61CT501BXV1	
		JMJG_U2_HAJ62CT501AXV1	
		JMJG_U2_HAJ62CT501BXV1	
	HT S/HTR I/L HDR MET TEMP	JMJG_U2_HAH91CT551XV1	
		JMJG_U2_HAH91CT552XV1	
		JMJG_U2_HAH91CT553XV1	
		JMJG_U2_HAH91CT554XV1	
		JMJG_U2_HAH91CT601XV1	
		JMJG_U2_HAH91CT602XV1	
	FINAL S/HTR O/L TEMPERATURE	JMJG_U2_HAH92CT501XV1	
		JMJG_U2_HAH92CT502XV1	
		JMJG_U2_HAH92CT503XV1	
		JMJG_U2_HAH93CT501XV1	
		JMJG_U2_HAH93CT502XV1	
		JMJG_U2_HAH93CT503XV1	
		JMJG_U2_HAH93CT501X3V	
	S/HTR STEAM PRESS TX (CONTROL)		JMJG_U2_HAH93CP501XV1
			JMJG_U2_HAH93CP502XV1
			JMJG_U2_HAH93CP503XV1
			JMJG_U2_HAH92CP501XV1
			JMJG_U2_HAH92CP502XV1
			JMJG_U2_HAH92CP503XV1
			JMJG_U2_HAH92CP501X3V
			JMJG_U2_HAH93CP501X3V
	DRUM LEVEL COMPENSATED (FROM PROTECTION)	JMJG_U2_HAD01CL651X5V	
	LT S/HTR LW O/L BFR D/SHTR	JMJG_U2_HAH37CT501XV1	
	LT S/HTR RW O/L BFR D/SHTR	JMJG_U2_HAH38CT501XV1	
	IT S/HTR EXCH MET TEMP	JMJG_U2_HAH80CT511XV1	
JMJG_U2_HAH80CT512XV1			
JMJG_U2_HAH80CT513XV1			
JMJG_U2_HAH80CT514XV1			
JMJG_U2_HAH80CT515XV1			
JMJG_U2_HAH80CT516XV1			

Table 6.45 Necessary actions for trip (6)

Investigations	Possible Causes	Actions To Be Taken	
High Alarm	Failure In Measurements	Ask The Instrumentation Specialist For Investigations And Take The Appropriate Corrective Action	
		Sensors	Actuators
Boiler Drum Level High Unit 2	HT S/HTR EXCH MET TEMP	JMIG_U2_HAH90CT511XV1	
		JMIG_U2_HAH90CT512XV1	
		JMIG_U2_HAH90CT513XV1	
		JMIG_U2_HAH90CT514XV1	
	FINAL S/HTR O/L TEMPERATURE	JMIG_U2_HAH92CT501XV1	
		JMIG_U2_HAH92CT502XV1	
		JMIG_U2_HAH92CT503XV1	
		JMIG_U2_HAH93CT501XV1	
		JMIG_U2_HAH93CT502XV1	
		JMIG_U2_HAH93CT503XV1	
		JMIG_U2_HAH93CT501X3V	

Table 6.46 Necessary actions for trip (7)

Investigations	Possible Causes	Actions To Be Taken	
High Alarm	Failure In Measurements	Ask The Instrumentation Specialist For Investigations And Take The Appropriate Corrective Action	
		Sensors	Actuators
High Temperature Super-heater -Unit 1	FEED WATER FLOW		JMJG_U1_HAC61CF501X5V
	ECONOMISER INLET TEMPERATURE	JMJG_U1_HAJ61CT501AXV1	
		JMJG_U1_HAJ61CT501BXV1	
		JMJG_U1_HAJ62CT501AXV1	
		JMJG_U1_HAJ62CT501BXV1	
	HT S/HTR I/L HDR MET TEMP	JMJG_U1_HAH91CT551XV1	
		JMJG_U1_HAH91CT552XV1	
		JMJG_U1_HAH91CT553XV1	
		JMJG_U1_HAH91CT554XV1	
		JMJG_U1_HAH91CT601XV1	
		JMJG_U1_HAH91CT602XV1	
	FINAL S/HTR O/L TEMPERATURE	JMJG_U1_HAH92CT501XV1	
		JMJG_U1_HAH92CT502XV1	
		JMJG_U1_HAH92CT503XV1	
		JMJG_U1_HAH93CT501XV1	
		JMJG_U1_HAH93CT502XV1	
		JMJG_U1_HAH93CT503XV1	
		JMJG_U1_HAH93CT501X3V	
	S/HTR STEAM PRESS TX (CONTROL)		JMJG_U1_HAH93CP501XV1
			JMJG_U1_HAH93CP502XV1
			JMJG_U1_HAH93CP503XV1
			JMJG_U1_HAH92CP501XV1
			JMJG_U1_HAH92CP502XV1
			JMJG_U1_HAH92CP503XV1
			JMJG_U1_HAH92CP501X3V
			JMJG_U1_HAH93CP501X3V
	FEEDWATER CONTROL POSITON S/U VALVE		JMJG_U1_HAC01CG123CXV1

6.7 Summary

The two systems were coded in MATLAB environment. The results of the proposed IMSs (training and validation) together with some additional information about the IMSs' performance were presented. Consequently, the achieved results from the proposed systems were led to some complete decision on which was the best system but it gave an insight into the successful degree of the IMS-II. The overall performance and adaptability of the proposed IMSs were discussed. Slightly lower root mean square error was observed in the second system which reveals that the IMS-II performed better than IMS-I. The discussion focused on determining the best NN topologies combination together with the most influence boiler operation variables for each trip. Furthermore, an 'action to be taken' guide was proposed and presented to assist the plant operator to avoid or reduce the trip occurrence. The proposed intelligent systems could be applied on-line as a reliable controller of thermal power plant boiler.

CHAPTER 7

CONCLUSIONS AND FUTURE WORKS

7.1 Introduction

Motivated by the need for an “early boiler trips” detection system to maintain normal and safe operational conditions, two artificial intelligent monitoring systems (IMSS) specialized in boiler trips diagnosis were proposed in this work. The IMS-I represents the use of a pure artificial neural network technique (Pure ANN). The IMS-II was a hybrid intelligent system which merges Genetic Algorithms and Artificial Neural Networks as a hybrid intelligent system (ANN+GA).

The processes of training and validation of the two systems have been performed using real boiler operational data captured from the plant integration acquisition (PIA) system of the MNJ coal-fired power plant. Seven boiler trips were considered as follows: boiler water wall tube leak trip (T1), low temperature superheater trip (T2), boiler drum water low level trip (occurred twice in different identical boiler units, T3, T4), boiler feed pump trip (5), boiler drum water high level trip (T6), and high temperature superheater trip (T7).

An integrated plant data preparation framework for seven boiler trips with related operational variables has been proposed for the IMSSs data analysis. The MLP feed-forward NN methodology has been adopted as a major computational intelligent tool in both systems. The main advantage of this computational tool is that no mathematical model for boiler trip detection was needed.

In order to achieve the overall objectives of the research, four implemental phases have been proposed and executed in the order below:

- i. Plant data preparation phase.
- ii. Development of IMS-I (Pure ANN) phase.
- iii. Development of IMS-II (ANN+GA) phase.
- iv. Analysis and development of advisory guide phase.

7.2 Contributions of the Research

The main contributions of the present work presented in this thesis could be summarized in the following order:

1. Adoption of real data for training and validation

The reviewed literature addresses that a few relevant approaches have been conducted using real site data. The majority of the literature works (which were applied mostly in nuclear power plants) are based on mathematically simulated data, which is inappropriate for decision making. In this work, real plant data containing normal and faulty boiler operation patterns from the MNJ coal-fired power plant have been identified, captured, manipulated and used to train and validate the established codes.

2. Integrated data preparation framework for (IMSS)

No standard data preparation framework for IMSSs so far has been suggested. Following the envisaged importance of plant data preparation, a framework for seven boiler trips with thirty-two operational variables has been proposed to train, validate and analyze the IMSSs. The integrated plant data scheme consisted of three stages:

- i. Data pre-analysis stage, in which boiler operational variables were identified and collected for each specific boiler trip.
- ii. Data preprocessing stage, in which noisy and non-number data was filtered and normalized between one and zero.

- iii. Data post-analysis stage, in which data was segmented into two sub groups for each trip, NN targets were identified and the behaviors of the influencing boiler operation variables were analyzed.

The data preparation framework presented in this research was much broader than other proposed frameworks and it is aimed at filling up a gap in the literature.

3. Development of MATLAB codes for IMSs

The proposed IMSs were coded in MATLAB software. The first code permits training and validation of the IMS-I. The second code was structured to permit optimization, training and validation of the IMS-II. The hybrid system is capable of performing optimal selection of main NN topology combinations and boiler operation variables.

4. Development of IMS-II for thermal power plant boiler

After the investigation of various main ANN topology combinations, a new technique has been introduced in the IMS-II which couples the ANN with the GA into a hybrid to explore the final architecture of the hybrid intelligent system. In addition, the IMS-II has been adopted to select the most influential variables from hundreds of boiler operation variables. This technique replaces the trial and error of the pure NN approach and overcomes the difficulties in human intervention which are commonly used in the ANN training.

7.3 Critique of the Work

The two IMSs presented in this work were proposed to guide the search for an optimal NN topology combinations and boiler operational variables selection. However, there are some limitations in the current proposed IMSs which require further efforts to enhance their capability.

The first limitation is on the pure NN training algorithm. The back-propagation NN is probably the best known and the most commonly used among the current types of ANN training algorithms. This network is an outgrowth of perceptrons, with the addition of hidden layers and the use of the *Generalized Delta Rule* for learning. The

principle disadvantage of the back-propagation is the processing speed (computational time) at which the learning converges or learns. The elementary back-propagation topology was manipulated in many ways to bias this algorithm to converge faster.

The second limitation is on the GAs. GAs can be trapped in local minima if initial population is not good enough and it requires some general a priori knowledge or intuition about the proposed system. The degree of the GA success is based on its full automation for the combinational problems. More specifically, it incorporates some user experience about the system problem.

The other limitation is the number of the effective operational variables. The boiler operation variables selection is extremely an important issue. In the present work, thirty-two boiler operation variables have been selected for the proposed IMS-I based on the plant operator experience. Such decision requires further searches and investigations to improve the IMSs performance by identify, more specifically, the most influential variables on each boiler trip.

7.4 Conclusions of IMSs

Since different results were gained from the two proposed IMSs, the conclusions would be segregated to present the findings from each system, separately:

7.4.1 The IMS-I Conclusions

- i. The feed forward NN methodology was capable of exploring the most suitable NN topology combination for each trip, involving: type of multidimensional minimization training algorithms, type of activation function, the number of neurons for each hidden layer and the number of hidden layers based on the NN performance indicator (RMSE).
- ii. The one Hidden Layer NN structure (1HL) and two Hidden Layer NN structure (2HL) were applied for each trip. No general trend of the HL selection was gained. The 1HL produced better detection, in cases of trip1 and trip 7, while 2HL performed better for all other trips.

- iii. The Levenberg-Marquardt training algorithm provided a smaller error value compared to the other three training algorithms for trip 4 and trip 7. For trip 3 and trip 5, the smallest error value was achieved by the BFGS Quasi Newton training algorithm. The Resilient Back-Propagation outperformed the other three training algorithms for trip 2. The Scaled Conjugate Gradient gave the best NN topology combination with a minimum error value for trip 1 and trip 6.
- iv. The logistic activation function for the output node performed better than the other two activation functions in most cases.
- v. All the seven boiler trips considered in this study were detected by the proposed pure system before or at the same time as the plant control system, so that the IMS-I can be applied on-line as a reliable monitoring system of the operation of a thermal power plant boiler.

7.4.2 The IMS-II Conclusions

- i. Encoding and optimization process of a GA was successfully applied to select the best NN topology and boiler operation variables combination problems such as the decision of what are the optimal NN topology combination and the most effective boiler operation variable for a specific trip.
- ii. In most cases, the IMS-II should be preferable, mostly due to its automated methodology, compared to the IMS-I based on the properties of optimization.
- iii. Slightly better trip detection performance was observed in the IMS-II compared with the IMS-I. Only for the first trip of the hybrid system was it retarded in detecting compared with IMS-I. The reason behind this is that the tube leakage case is more likely to be a breakdown fault than a measurable boiler trip.
- iv. In most cases, the IMS-II results could give useful information about the specific trip and insight for further, more flexible methodology of the IMS-I.

7.5 Recommendations and Future Works

- i. The heuristic optimization method of genetic algorithms can be used to explore the optimal learning rate, NN connections weight, coefficient of momentum, number of NN iterations and partial connections.
- ii. There was some confusion about the boiler wall tube leak trip (trip1) diagnosis. In order to overcome this kind of confusion, trip one should be considered as a break down. More operational variables need to be sampled in order to distinguish this type of break down, which is not an operational variable; e.g. corrosion, acid attack, graphitization... etc.
- iii. To approach the actual thermal power plant application, many boiler trips have to be monitored, which requires more real data from the plant to train and validate the IMSs.
- iv. The IMSs could be coupled with a “safety variables display” control system in order to assist the plant operator in monitoring the plant operating conditions.
- v. The effectiveness of the intelligent monitoring systems reported here relayed strongly on two resources of information. The first resource was the domain knowledge of boiler trips. The second resource was the boiler operational measurements for each specific boiler trip. Complete and detailed measurements will increase the results reliability of the intelligent monitoring systems. Therefore, addition of any measurement will enhance the performance of these intelligent monitoring systems. Analytical process development of intelligent monitoring systems for cost and benefits evaluation with utilizing additional measurements would be worth more for guiding future applications.
- vi. The plant operators’ experience, whose knowledge will be elicited, should be educated on the basics of methods that are adopted in the intelligent monitoring systems. This would be more helpful for them to judge the level of their knowledge and to provide the domain knowledge consequently.
- vii. Maintaining the knowledge bases is recommended in thermal power plants concerning the boiler operation before and during the actual execution of the proposed IMSs performance.

- viii. A comprehensive intelligent trip detection interface should be designed in order to provide the analyzed performance status and advisory results from the IMSs to the user at the thermal power plant. Clear and efficient display of the IMSs results adds extra reliability to the trip detection system.
- ix. Two issues should be taken into account; the first is the history of the trips and the performance status in the detection domain. The second is the information about the plant maintenance schedule (the time left until the beginning or end of a scheduled maintenance).
- x. The present work provides intelligent trip detection for future thermal power plants. Therefore, its application in currently operating thermal power plant is recommended.
- xi. Repeatability of the training and validation by different segregation criteria of the real data will provide important recommendations to the AIS researchers to train and validate their systems.

REFERENCES

- [1] L. H. Chiang, E. Russell and R. D. Braatz, *Fault Detection and Diagnosis in Industrial Systems*. Springer Verlag, 2001.
- [2] D. M. Himmelblau, *Fault Detection and Diagnosis in Chemical and Petrochemical Processes*. Elsevier Amsterdam, 1978.
- [3] R. N. Claek, "Instrument Fault Detection," *Aerospace and Electronic Systems*, IEEE Transactions on, vol. AES-14, pp. 456-465, 1978.
- [4] F. Finch and M. Kramer, "Narrowing diagnostic focus using functional decomposition," *AIChE J.*, vol. 34, pp. 25-36, 1988.
- [5] R. Patton, P. M. Frank and R. Clark, *Issues of Fault Diagnosis for Dynamic Systems*. Springer Verlag, 2000.
- [6] J. Korbicz, J. M. Koscielny and Z. Kowalczyk, *Fault Diagnosis: Models, Artificial Intelligence, Applications*. Springer Verlag, 2004.
- [7] K. P. Ferentinos, "Neural network fault detection and diagnosis in deep-trough hydroponic systems," *Ph.d Thesis*, 2002.
- [8] A. Konar, *Artificial Intelligence and Soft Computing: Behavioral and Cognitive Modeling of the Human Brain*. CRC, 2000.
- [9] M. Arbib, *The Metaphorical Brain 2 Neural Networks and Beyond*, John Wiley & Sons, New Yourk, 1989.
- [10] M. Caudill and C. Butler, *Understanding Neural Networks; Computer Explorations*. MIT Press Cambridge, MA, USA, 1992.

- [11] Z. Guo, "Nuclear power plant fault diagnostics and thermal performance studies using neural networks and genetic algorithms", Ph.d Thesis, University of Tennessee, 1992.
- [12] J. Holland, *Adaptation in natural and artificial systems: an introductory analysis with applications to biology, control and artificial intelligence*, Ann Arbor, MI, 1975.
- [13] D. E. Goldberg, *Genetic Algorithms in Search, Optimization, and Machine Learning*. Addison-wesley Reading Menlo Park, 1989.
- [14] X. Sun, T. Chen and H. J. Marquez, "Boiler leak detection using a system identification technique," *Ind Eng Chem Res*, vol. 41, pp. 5447-5454, 2002.
- [15] X. Sun, H. J. Marquez, T. Chen and M. Riaz, "An improved PCA method with application to boiler leak detection," *ISA Trans.*, vol. 44, pp. 379-397, 2005.
- [16] J. Smrekar, D. Pandit, M. Fast, M. Assadi and S. De, "Prediction of power output of a coal-fired power plant by artificial neural network," *Neural Computing & Applications*, vol. 19, pp. 1-16, 2010.
- [17] A. Jankowska, "Approach to Early Boiler Tube Leak Detection with Artificial Neural Networks," *Recent Advances in Mechatronics*, pp. 57-61, 2007.
- [18] P. Yang and S. S. Liu, "Fault diagnosis for boilers in thermal power plant by data mining," in *Control, Automation, Robotics and Vision Conference, ICARCV 2004 8th*, pp. 2176-2180, 2004.
- [19] A. Kusiak and A. Burns, "Mining temporal data: A coal-fired boiler case study," in *Knowledge-Based Intelligent Information and Engineering Systems*, pp. 953-958, 2005.
- [20] A. G. Parlos, "Incipient fault detection and identification in process systems using accelerated neural network learning," *Nucl Technol*, vol. 105, pp. 145-161, 1994.
- [21] T. Sorsa, H. N. Koivo and H. Koivisto, "Neural networks in process fault diagnosis," *IEEE Trans. Syst. Man Cybern.*, vol. 21, pp. 815-825, 1991.

- [22] A. A. Hopgood, *Intelligent Systems for Engineers and Scientists*. CRC, 2001.
- [23] J. Bernard and T. Washio, *Expert Systems Applications within the Nuclear Industry*. La Grange Park, IL (United States); American Nuclear Society, 1989.
- [24] S. L. Fulton and C. O. Pepe, "An introduction to model-based reasoning." *AI EXPERT.*, vol. 5, pp. 48-55, 1990.
- [25] M. Negnevitsky, *Artificial Intelligence: A Guide to Intelligent Systems*. Addison-Wesley Longman, 2005.
- [26] C. Nikolopoulos, *Expert Systems: Introduction to First and Second Generation and Hybrid Knowledge Based Systems*. CRC, 1997.
- [27] V. Palade, C. D. Bocaniala and L. C. Jain, *Computational Intelligence in Fault Diagnosis (Advanced Information and Knowledge Processing)*. Springer-Verlag New York, Inc. Secaucus, NJ, USA, 2006.
- [28] M. W. Golay and B. Yildiz, "Development of a hybrid intelligent system for on-line real-time monitoring of nuclear power plant operations," Ph.d Thesis, Massachusetts, Institute of Technology, 2003.
- [29] D. Flynn, *Thermal Power Plant Simulation and Control*. Inst of Engineering & Technology, 2003.
- [30] R. E. Uhrig and L. H. Tsoukalas, "Soft computing technologies in nuclear engineering applications," *Prog. Nuclear Energy*, vol. 34, pp. 13-75, 1999.
- [31] K. Kim, T. Aljundi and E. Bartlett, *Nuclear Power Plant Fault-Diagnosis using Artificial Neural Networks*, 1992.
- [32] G. Guglielmi, T. Parisini and G. Rossi, "Keynote paper: Fault diagnosis and neural networks: A power plant application," *Control Eng. Pract.*, vol. 3, pp. 601-620, 5, 1995.
- [33] S. Simani and C. Fantuzzi, "Fault diagnosis in power plant using neural networks," *Inf. Sci.*, vol. 127, pp. 125-136, 2000.

- [34] A. Babar and H. Kushwaha, "Symptom based diagnostic system for nuclear power plant operations using artificial neural networks," *Reliability Engineering and System Safety*, vol. 82, pp. 33-40, 2003.
- [35] H. Bae, S. P. Chun and S. Kim, "Predictive fault detection and diagnosis of nuclear power plant using the two-step neural network models," *Advances in Neural Networks-ISNN 2006*, pp. 420-425, 2006.
- [36] L. M. Romeo and R. Garetta, "Neural network for evaluating boiler behavior," *Appl. Therm. Eng.*, vol. 26, pp. 1530-1536, 10, 2006.
- [37] H. Rusinowski and W. Stanek, "Neural modelling of steam boilers," *Energy Conversion and Management*, vol. 48, pp. 2802-2809, 11, 2007.
- [38] S. De, M. Kaiadi, M. Fast and M. Assadi, "Development of an artificial neural network model for the steam process of a coal biomass cofired combined heat and power (CHP) plant in Sweden," *Energy*, vol. 32, pp. 2099-2109, 11, 2007.
- [39] K. Mo, S. J. Lee and P. H. Seong, "A dynamic neural network aggregation model for transient diagnosis in nuclear power plants," *Prog. Nuclear Energy*, vol. 49, pp. 262-272, 4, 2007.
- [40] Enping Zhang, Huifen Zhang and Bicui Xue, "Application of integrated neural network based on information combination for fault diagnosis in steam turbine generator," *International Conference on Condition Monitoring and Diagnosis, CMD 2008*, pp. 1293-1297, 2008.
- [41] T. Santosh, A. Srivastava, V. Sanyasi Rao, A. Ghosh and H. Kushwaha, "Diagnostic system for identification of accident scenarios in nuclear power plants using artificial neural networks," *Reliab. Eng. Syst. Saf.*, vol. 94, pp. 759-762, 2009.
- [42] M. Fast, M. Assadi and S. De, "Development and multi-utility of an ANN model for an industrial gas turbine," *Appl. Energy*, vol. 86, pp. 9-17, 1, 2009.
- [43] M. Fast and T. Palmé, "Application of artificial neural networks to the condition monitoring and diagnosis of a combined heat and power plant," *Energy*, vol. 35, pp. 1114-1120, 2, 2010.

- [44] J. Smrekar, M. Assadi, M. Fast, I. Kuštrin and S. De, "Development of artificial neural network model for a coal-fired boiler using real plant data," *Energy*, vol. 34, pp. 144-152, 2, 2009.
- [45] Z. Guo and R. E. Uhrig, "Using genetic algorithms to select inputs for neural networks," *International Workshop on Combinations of Genetic Algorithms and Neural Networks, COGANN-92*, pp. 223-234, 1992.
- [46] J. W. Hines, D. W. Miller and B. K. Hajek, "Hybrid approach for detecting and isolating faults in nuclear power plant interacting systems," *Nucl Technol*, vol. 115, pp. 342-358, 1996.
- [47] Keehoon Kim and E. B. Bartlett, "Nuclear power plant fault diagnosis using neural networks with error estimation by series association," *Nuclear Science, IEEE Transactions on*, vol. 43, pp. 2373-2388, 1996.
- [48] M. B. Hadjiski, N. G. Christova and P. P. Groumpos, "Design of hybrid models for complex systems," *Department of Automation in Industry, University of Chemical Technology and Metallurgy, Ennate*, 2001.
- [49] S. A. Kalogirou, "Applications of artificial neural-networks for energy systems," *Appl. Energy*, vol. 67, pp. 17-35, 9, 2000.
- [50] A. Volponi, H. DePold, R. Ganguli and C. Daguang, "The use of Kalman filter and neural network methodologies in gas turbine performance diagnostics: a comparative study," *Journal of Engineering for Gas Turbines and Power*, vol. 125, pp. 917, 2003.
- [51] Z. Yangping, Z. Bingquan and W. DongXin, "Application of genetic algorithms to fault diagnosis in nuclear power plants," *Reliab. Eng. Syst. Saf.*, vol. 67, pp. 153-160, 2, 2000.
- [52] Bilge Yildiz, Michael W.golay, Kenneth P. Maynard, Maamar Maghraoui "Development of a hybrid intelligent system for one-line monitoring of nuclear power plant", 6th International conference on Probabilistic Safety Assessment and Management (PSAM6), San Juan, Puerto Rico, USA, 23-28 June, 2002.

[53] Man Gyun Na, Sun Ho Shin, Sun Mi Lee, Dong Won Jung, Soong Pyung Kim, Ji Hwan Jeong and Byung Chul Lee, "Prediction of major transient scenarios for severe accidents of nuclear power plants," *Nuclear Science, IEEE Transactions on*, vol. 51, pp. 313-321, 2004.

[54] Shing Chiang Tan and Chee Peng Lim, "Application of an adaptive neural network with symbolic rule extraction to fault detection and diagnosis in a power generation plant," *Energy Conversion, IEEE Transactions on*, vol. 19, pp. 369-377, 2004.

[55] M. J. Embrechts and S. Benedek, "Hybrid identification of nuclear power plant transients with artificial neural networks," *Industrial Electronics, IEEE Transactions on*, vol. 51, pp. 686-693, 2004.

[56] K. P. Ferentinos, "Biological engineering applications of feedforward neural networks designed and parameterized by genetic algorithms," *Neural Networks*, vol. 18, pp. 934-950, 2005.

[57] Zhiguang Tian, Huifen Zhang and Youbo Wang, "Failure diagnosis of steam turbine-generator set based on genetic algorithm and BBP network," *Sixth International Conference on Intelligent Systems Design and Applications, ISDA '06.*, pp. 930-935, 2006.

[58] X. Shi, C. Xie and Y. Wang, "Nuclear power plant fault diagnosis based on genetic-RBF neural network," *Journal of Marine Science and Application*, vol. 5, pp. 57-62, 2006.

[59] H. Rusinowski and W. Stanek, "Hybrid model of steam boiler," *Energy*, vol. 35, pp. 1107-1113, 2, 2010.

[60] O. Ahmed, M. Nordin, S. Sulaiman and W. Fatimah, "Study of Genetic Algorithm to Fully-automate the Design and Training of Artificial Neural Network," *IJCSNS*, vol. 9, pp. 217, 2009.

[61] R.M. Hristev , *Artificial Neural Network*.1997.

[62] R. P. Lippmann, "An introduction to computing with neural nets," *ARIEL*, vol.

209, pp. 115.245, 1987.

[63] J. M. Zurada, Introduction to Artificial Neural Systems St. Paul: West, 1992.

[64] Dass, S.K., Neural Network and Fuzzy Logic. New Delhi: Shree Publishers & Distributors,2006 .

[65] A. Browne, Neural Network Analysis, Architectures, and Applications. Taylor & Francis, 1997.

[66] N. K. Kasabov, Foundations of Neural Networks, Fuzzy Systems, and Knowledge Engineering. The MIT Press, 1996.

[67] R. Vaidyanathan, "Process fault detection and diagnosis using neural networks," Ph.d Thesis, ETD Collection for Purdue University, 1991.

[68] R. L. Harvey, Neural Network Principles. Prentice-Hall, Inc. Upper Saddle River, NJ, USA, 1994.

[69] M. Nørgaard, O. Ravn, N. K. Poulsen and L. K. Hansen, Neural Networks for Modelling and Control of Dynamic Systems: A Practitioner's Handbook. Springer Verlag, 2000.

[70] J. Srinivas and M.Ananda Rao, Neural Networks: Algorithms and Applications Alpha Science International, 2003.

[71] J. P. M. de Sá, Applied Statistics: Using SPSS, STATISTICA, and MATLAB. Springer Verlag, 2003.

[72] A. Van Rooij, R. Johnson and L. Jain, Neural Network Training using Genetic Algorithms. World Scientific Publishing Co., Inc. River Edge, NJ, USA, 1996.

[73] M. Mitchell, An Introduction to Genetic Algorithms. The MIT press, 1998.

[74] S. Sivanandam and S. Deepa, Introduction to Genetic Algorithms. Springer Verlag, 2007.

[75] J. R. Koza, Genetic Programming: On the Programming of Computers by Means

of Natural Selection. The MIT press, 1992.

[76] K. F. Man, K. S. Tang and S. Kwong, Genetic Algorithms: Concepts and Designs. Springer Verlag, 1999.

[77] MathWorks, Genetic Algorithm and Direct Search Toolbox User's Guide for use with MATLAB, version 1, 2004.

[78] D. A. Sofge, "Using genetic algorithm based variable selection to improve neural network models for real-world systems," in Proceedings of the 2002 International Conference on Machine Learning & Applications, 2002.

[79] S. Mok, C. Kwong and W. Lau, "A hybrid neural network and genetic algorithm approach to the determination of initial process parameters for injection moulding," The International Journal of Advanced Manufacturing Technology, vol. 18, pp. 404-409, 2001.

[80] Ramalingam, K. K., A Course on Power Plant Engineering. Chennai, India: Scitech Publications (India), 2007.

[81] P. Nag, Power Plant Engineering. Tata McGraw-Hill, 2002.

[82] Lean Yu, Shouyang Wang and K. K. Lai, "An integrated data preparation scheme for neural network data analysis," Knowledge and Data Engineering, IEEE Transactions on, vol. 18, pp. 217-230, 2006.

[83] R. Roiger and M. W. Geatz, Data Mining: A Tutorial-Based Primer. Addison Wesley Boston, 2003.

[84] L. Fortuna, S. Graziani, A. Rizzo and M. G. Xibilia, Soft Sensors for Monitoring and Control of Industrial Processes. Springer Verlag, 2007.

[85] H. Lee, K. Chen and I. Jiang, "A neural network classifier with disjunctive fuzzy information," Neural Networks, vol. 11, pp. 1113-1125, 8, 1998.

[86] E. J. Rzepoluck, Neural Network Data Analysis using Simulnet. Springer Verlag, 1998.

- [87] G. Purushothaman and N. B. Karayiannis, "Quantum neural networks (QNN's): Inherently fuzzy feedforward neural networks," *IEEE Trans. Neural Networks*, vol. 8, pp. 679-693, 1997.
- [88] S. Ishii and M. Sato, "Constrained neural approaches to quadratic assignment problems," *Neural Networks*, vol. 11, pp. 1073-1082, 8, 1998.
- [89] A. Gupta and S. M. Lam, "Weight decay backpropagation for noisy data," *Neural Networks*, vol. 11, pp. 1127-1138, 8, 1998.
- [90] A. K. Jain, Jianchang Mao and K. M. Mohiuddin, "Artificial neural networks: a tutorial," *Computer*, vol. 29, pp. 31-44, 1996.
- [91] H. Demuth and M. Beale, *Neural network toolbox, MathWorks Version*, vol. 4, 2001.
- [92] E. Davalo, *Neural Networks, MACHILIN Edition*, 1991.
- [93] G. F. Miller, P. M. Todd and S. U. Hegde, "Designing neural networks using genetic algorithms," in *Proceedings of the Third International Conference on Genetic Algorithms*, pp. 384, 1989.
- [94] D. B. Fogel, "An introduction to simulated evolutionary optimization," *Neural Networks, IEEE Transactions on*, vol. 5, pp. 3-14, 1994.
- [95] C. R. Reeves, *Modern Heuristic Techniques for Combinatorial Problems*. John Wiley & Sons, Inc. New York, NY, USA, 1993.

PUBLICATIONS

- [1] **Al-Naimi, Firas Basim Ismail** and AL-Kayiem, H.H., “Hybrid Neural Networks and Genetic Algorithm for Fault Detection and Diagnosis of a Plant”, Proceedings of National Postgraduate Conference (NPC2008) University Technology PETRONAS, Malaysia, pp.50, 31 march, 2008.
- [2] **Al-Naimi, Firas Basim Ismail** and AL-Kayiem, H.H., “Hybrid Intelligent Systems for Boiler Fault Detection and Diagnosis”, Proceedings of National Postgraduate Conference (NPC2009) University Technology PETRONAS, Malaysia, pp.80, from 25 to 26 March, 2009.
- [3] **Al-Naimi, Firas Basim Ismail** and AL-Kayiem, H.H., “Multidimensional Minimization Training Algorithms for steam boiler drum level trip using Artificial Intelligence Monitoring system”. Proceedings of 3rd International Conference on Intelligent and Advanced Systems (ICIAS), Malaysia, pp.29, from 14 - 17 June 2010.
- [4] **Al-Naimi, Firas Basim Ismail** and AL-Kayiem, H.H., “Artificial Intelligence system for steam boiler diagnosis based on superheater monitoring”, Proceedings of 2nd International Conference on Plant Equipment and Reliability (ICPER2010), Malaysia, pp.52 from 15 to 17 June 2010.
- [5] **Al-Naimi, Firas Basim Ismail** and AL-Kayiem, H.H., “Multidimensional Minimization Training Algorithms for Steam Boiler High Temperature Superheater Trip using Artificial Intelligence Monitoring System”, 11th International Conference on Control, Automation, Robotics and Vision (ICARCV), Singapore, (Accepted on 3rd July,2010).

[6] **Al-Naimi, Firas Basim Ismail** and AL-Kayiem, H.H., “Artificial Intelligence system for steam boiler diagnosis based on superheater monitoring”, Journal of Applied Sciences, Malaysia, (Accepted on 2nd August, 2010 for publication).

[7] **Al-Naimi, Firas Basim Ismail** and AL-Kayiem, H.H., “Multidimensional Minimization Training Algorithms for steam boiler drum level trip using Artificial Intelligence Monitoring system”, Journal of IEEE Malaysia, (Accepted on 17th June, 2010 for publication).

Table A-5: Binary representation of NN topologies for trip (5)

T5	Bit Sequence																																																		
	TA		Architecture							AF					Boiler Operation Variables																																				
G	1	2	3	4	5	6	7	8	9	0	1	2	3	4	5	6	7	8	9	0	1	2	3	4	5	6	7	8	9	0	1	2	3	4	5	6															
1	0	1	1	0	1	0	1	0	1	0	0	1	0	1	0	1	1	0	0	0	1	0	0	1	0	0	0	0	0	1	0	0	1	0	1	0	0	0	1	0	1	0	0	0	0						
2	1	1	1	0	1	0	0	0	0	0	1	0	1	1	0	0	0	0	0	1	1	1	1	1	0	1	1	0	0	0	0	0	0	0	0	0	0	0	0	1	0	0	1	0	0	0	0	0			
3	1	0	0	0	0	0	1	0	0	0	1	0	0	1	1	1	1	0	0	0	1	0	0	1	1	1	0	0	0	1	1	0	0	1	0	0	0	0	0	0	0	0	0	0	0	0	0	0	0		
4	0	0	0	0	0	1	1	1	1	1	1	0	0	0	0	1	1	1	0	0	1	0	0	1	1	1	0	0	0	0	0	0	0	0	0	0	0	0	0	0	0	0	0	0	0	0	0	0	0		
5	1	0	1	0	0	1	1	0	0	1	0	0	0	0	0	0	0	1	0	0	1	0	0	1	0	0	0	0	0	0	0	0	0	0	0	0	0	0	0	0	0	0	0	0	0	0	0	0	0		
6	1	0	0	1	0	1	0	1	1	0	0	1	1	0	0	0	0	0	0	0	1	0	0	1	1	1	0	0	0	0	0	0	0	0	0	0	0	0	0	0	0	0	0	0	0	0	0	0	1	0	
7	1	0	0	1	0	0	0	0	1	1	0	1	0	1	0	0	0	0	0	0	1	0	0	1	0	0	0	0	0	0	0	0	0	0	0	0	0	0	0	0	0	0	0	0	0	0	0	0	0	0	
8	0	0	1	0	0	0	1	1	0	0	1	1	0	1	0	0	1	1	0	0	1	0	0	1	1	1	0	0	0	0	0	1	0	1	0	0	0	0	0	1	0	0	0	0	0	0	0	0	0	0	
9	1	0	0	0	0	1	0	1	0	0	0	1	0	1	0	0	0	1	1	0	1	0	0	0	1	1	1	0	0	0	0	0	0	0	1	0	0	0	0	0	0	0	0	0	0	0	1	1	1	0	
10	1	0	0	0	0	0	0	1	0	0	0	0	1	0	1	0	0	1	0	0	1	0	0	1	0	0	0	0	0	0	0	0	0	0	0	0	0	0	0	0	0	0	0	0	0	0	0	0	0	0	
11	0	1	0	0	1	0	0	1	1	0	1	1	1	1	0	0	1	0	0	0	1	0	0	1	1	1	0	0	0	0	1	0	0	0	0	0	0	0	0	0	0	0	0	0	0	0	0	0	0	0	
12	0	1	0	1	1	0	1	1	0	0	0	1	0	0	0	1	1	1	1	1	0	0	0	1	0	0	0	0	0	0	1	0	0	0	0	0	0	0	0	0	0	0	0	0	0	0	0	0	0	0	0
13	1	0	1	0	1	1	0	1	0	1	1	0	1	0	1	0	1	1	0	0	1	0	0	0	1	1	1	0	0	0	0	1	0	0	0	0	0	0	0	0	0	0	0	0	0	0	0	0	0	0	0
14	0	0	0	1	0	0	1	0	0	0	1	0	0	0	0	1	0	1	0	0	1	0	0	1	1	1	0	0	0	0	0	0	0	0	0	0	0	0	0	0	0	0	0	0	0	0	0	0	0	0	0
15	0	1	0	0	1	1	0	1	1	0	0	0	1	0	0	0	1	0	1	0	1	0	0	0	1	1	1	0	0	0	0	0	0	0	0	0	0	0	0	0	0	0	0	0	0	0	0	0	0	0	0

Table A-7: Binary representation of NN topologies for trip (7)

T7	Bit Sequence																																																		
	TA		Architecture							AF					Boiler Operation Variables																																				
G	1	2	3	4	5	6	7	8	9	0	1	2	3	4	5	6	7	8	9	0	1	2	3	4	5	6	7	8	9	0	1	2	3	4	5	6	7	8	9	0	1	2	3	4	5	6					
1	0	1	1	0	1	0	1	0	1	0	0	1	0	1	0	1	1	0	0	0	1	0	0	1	0	0	0	0	0	1	0	0	1	0	1	0	0	0	0	0	0	0	1	1	0	0	0				
2	1	0	1	0	0	1	1	0	0	1	0	0	0	0	0	0	0	1	0	0	0	0	1	0	0	1	0	0	0	0	0	0	0	0	0	0	0	0	0	0	0	0	0	0	0	0	0	0	0		
3	0	1	0	1	1	0	1	1	0	0	0	1	0	0	1	1	1	1	1	1	0	0	0	1	0	0	0	0	0	0	1	0	0	0	1	0	0	0	0	0	0	0	0	0	0	0	1	0	0	0	
4	1	0	0	1	0	1	0	1	1	0	0	1	1	0	1	0	0	0	0	0	1	0	0	1	1	0	0	1	0	0	0	0	0	0	0	0	0	0	0	0	0	0	0	0	0	0	0	0	0	0	
5	0	1	0	0	1	0	0	1	1	0	1	1	1	1	0	0	1	0	0	0	1	0	0	1	1	1	0	0	0	0	1	0	0	0	0	1	0	0	0	0	1	0	0	1	0	0	1	0	0	0	
6	1	1	1	0	1	0	0	0	0	0	1	0	1	1	0	0	0	0	0	1	1	1	1	1	0	1	1	0	0	0	0	0	0	0	0	0	0	0	0	0	0	0	0	1	0	0	1	0	0	0	
7	1	0	0	0	0	0	0	1	0	0	0	0	1	0	1	0	0	1	0	0	1	0	0	1	0	0	0	0	0	0	0	0	0	0	0	0	0	0	0	1	0	0	0	0	1	0	0	0	0		
8	1	0	0	0	0	1	0	1	0	0	0	1	0	1	1	0	0	1	0	0	0	1	1	1	0	0	0	0	0	0	0	0	0	0	1	0	0	0	0	0	0	0	0	0	0	0	0	1	0	0	1
9	0	0	0	1	0	0	1	0	0	0	1	0	0	0	0	1	0	1	0	0	1	0	0	1	0	0	1	1	0	0	0	0	0	0	0	0	0	0	0	0	0	0	0	0	0	0	0	0	0	0	
10	1	0	0	1	0	0	0	0	1	1	0	1	0	1	0	0	0	0	0	0	0	0	0	1	0	0	1	0	0	0	0	0	0	0	0	0	0	0	0	0	0	0	0	0	0	0	0	0	0	0	
11	1	0	1	0	1	1	0	1	0	1	1	0	1	0	1	0	1	1	0	0	1	0	0	0	1	1	1	0	0	0	0	0	0	0	0	0	0	0	0	0	0	0	0	0	0	0	0	0	0	0	
12	0	0	1	0	0	0	1	1	0	0	1	1	0	1	0	0	1	1	0	0	1	0	0	1	1	1	0	0	0	0	0	0	0	0	0	0	0	0	0	0	0	0	0	0	0	0	0	0	0	0	0
13	0	1	0	0	1	1	0	1	1	0	0	0	1	0	0	0	1	0	1	0	1	0	0	0	1	0	0	1	1	0	0	0	0	0	0	0	0	0	0	0	0	0	0	0	0	0	0	0	0	0	0
14	1	0	0	0	0	0	1	0	0	0	1	0	0	1	1	1	1	0	0	0	1	0	0	1	1	1	0	0	0	1	0	0	1	0	0	1	0	0	1	0	0	0	0	0	0	0	0	0	0	0	0
15	0	0	0	0	0	1	1	1	1	1	1	0	0	0	0	1	1	1	1	0	0	1	0	0	1	0	0	1	0	0	1	0	0	0	0	0	0	0	0	0	0	0	0	0	0	0	0	0	0	0	0

APPENDIX B: IMS-I and IMS-II Codes

The proposed codes for IMS-I and IMS-II are found in the attached CD. Table B-1 shows the attached CD contain.

Table B-1 Proposed codes name for IMS-I and IMS-II

Code No.	IMS-I Codes	Code No.	IMS-II Codes
1	Rprop Training Algorithm-1HL	9	GATrain Function
2	Rprop Training Algorithm-2HL	10	GA Function
3	BFG Training Algorithm-1HL	11	Decoding Function
4	BFG Training Algorithm-2HL	12	NNTrain Function
5	LM Training Algorithm-1HL	13	Fitness Function
6	LM Training Algorithm-2HL	14	Selection Function
7	SCG Training Algorithm-1HL	15	Crossover Function
8	SCG Training Algorithm-2HL	16	Mutation Function